REPORT DOCUMENTATION PAGE			Form Approved OMB No. 0704-0188

Public reporting burden for this collection of information is estimated to average 1 hour per response, including the time for reviewing instructions, searching existing data sources, gathering and maintaining the data needed, and completing and reviewing the collection of information. Send comments regarding this burden estimate or any other aspect of this collection of information, including suggestions for reducing this burden, to Washington Headquarters Services, Directorate for Information Operations and Reports, 1215 Jefferson Davis Highway, Suite 1204, Arlington, VA 22202-4302, and to the Office of Management and Budget, Paperwork Reduction Project (0704-0188), Washington, DC 20503.

1. AGENCY USE ONLY (Leave Blank)	2. REPORT DATE May 8, 1997	3. REPORT TYPE AND DATES COVERED Final Report for period of 9/1/92 - 12/31/96	
4. TITLE AND SUBTITLE Constitutive Modeling of Metal Matrix Composites Under Cyclic Loading			5. FUNDING NUMBERS AFOSR Grant No. F49620-93-1-0097DEF AFOSR Grant No. F49620-92-J-0463 AFOSR TR 97 0485
6. AUTHORS Dr. George Z. Voyiadjis Dr. Rainer Echle			
7. PERFORMING ORGANIZATION NAME(S) AND ADDRESS(ES) Department of Civil and Environmental Engineering Louisiana State University Baton Rouge LA 70803			8. PERFORMING ORGANIZATION REPORT NUMBER
9. SPONSORING / MONITORING AGENCY NAME(S) AND ADDRESS(ES) AFOSR/PKA 110 Duncan Avenue, Room B115 Bolling Air Force Base DC 20332 NA			10. SPONSORING / MONITORING AGENCY REPORT NUMBER
11. SUPPLEMENTARY NOTES			

12a. DISTRIBUTION / AVAILABILITY STATEMENT Approved for public release; distribution unlimited.	12b. DISTRIBUTION CODE

13. ABSTRACT (Maximum 200 words)

A micro-mechanical cyclic/fatigue damage model is developed for metal matrix composites. The model is based on thermodynamical principles within the framework of continuum damage mechanics and employs physical principles of damage behavior in metal matrix composites. A micro-mechanical approach is used in the sense that the overall material behavior is predicted by modeling the material behavior of the individual constituents. The Mori-Tanaka method is employed as a homogenization procedure. Individual anisotropic damage variables in the form of second order tensors are used for each of the constituents to allow for the modeling of appropriate damage and failure mechanisms in the composite. Individual damage initiation and evolution equations are developed for each constituent where physical principles of the damage mechanisms observed in experiments are considered. Damage mechanisms such as debonding and delamination are represented through individual damage tensors. The overall damage in the composite is obtained based on the individual damage tensors by means of the employed homogenization procedure. The elasto-plastic constitutive equations incorporate the influence of damage through the definition of the so-called damage effect tensors. A numerical implementation of the model is used to simulate cyclic/fatigue damage in metal matrix composites. Comparison of the results from the numerical simulations with experimental data show good agreement and substantiate the capabilities of the model.

14. SUBJECT TERMS fatigue, damage, micromechanics, metal matrix composites			15. NUMBER OF PAGES 81
			16. PRICE CODE
17. SECURITY CLASSIFICATION OF REPORT UNCLASSIFIED	18. SECURITY CLASSIFICATION OF THIS PAGE UNCLASSIFIED	19. SECURITY CLASSIFICATION OF ABSTRACT UNCLASSIFIED	20. LIMITATION OF ABSTRACT

DTIC QUALITY INSPECTED 3

Constitutive Modeling of Metal Matrix Composites Under Cyclic Loading

Final Report

Submitted to the

Air Force Office of Sponsored Research

Submitted by

Dr. George Z. Voyiadjis
Boyd Professor and Principal Investigator

Dr. Rainer Echle
Research Associate

Department of Civil and Environmental Engineering
Louisiana State University
Baton Rouge LA 70803

19971003 018

May 1997

DTIC QUALITY INSPECTED 3

Table of Contents

Constitutive Modeling of Metal Matrix Composites Under Cyclic Loading

Principal Investigator: Dr. George Z. Voyiadjis
Department of Civil and Environmental Engineering
Louisiana State University
Baton Rouge LA 70803

OVERVIEW:

The objectives of this project are:
1. Formulation of a constitutive model for the analysis of fatigue damage in metal matrix composites
2. Development of a finite element program in which the developed fatigue damage model will be integrated
3. Involvement and training of graduate students in this advanced research in the area of fatigue damage of metal matrix composites

The appendix contains copies of scientific articles which are representative of the publications written during the course of this project.

SUMMARY OF ACCOMPLISHMENTS:

The research accomplished during the project phase is described below in three major categories:
I.   Theoretical formulation of the cyclic and fatigue damage model
II. Numerical Implementation of the model into a finite element code
III. Extent of the involvement and participation of graduate students
This is followed by a listing of the publications written during the course of this project, including books, refereed journal articles, conference proceedings and presentations.

I.   Theoretical Formulation:

The theoretical formulation is based on the effective stress concept, and incorporates the damage-plasticity theory for composite materials using a micromechanical approach. In the micromechanical approach the damage phenomenon due to applied cyclic/fatigue loading is considered at the constituent level. For this purpose a homogenization technique in the form of the Mori-Tanaka method is employed in order to allow for the distribution of the external applied loading to the

individual constituents by means of the so-called stress and strain concentration tensors. The material behavior is then modeled at the constituent level based on the distributed loading. Elasto-plastic deformations as well as damage initiation and evolution processes are considered in the constituents individually. For this purpose individual constitutive equations to model the elasto-plastic behavior of and the damage evolution process in the constituents are established for each of the constituents. The damage evolution process includes the modeling of damage initiation and damage propagation up to final failure for which a specific failure criterion is applied. Through the use of the employed homogenization technique the overall composite material behavior, damage state and damage evolution is predicted based on the material behavior and damage evolution in the constituents.

The developed micromechanical cyclic/fatigue damage model is based on a consistent formulation in the framework of continuum mechanics and on thermodynamical principles. The formulation for the damage evolution includes also the physical aspects of fatigue damage in metal matrix composites. Through the use of individual damage variables in the form of second order tensors for the constituents it is possible to model anisotropic damage development and anisotropic damage evolution in the constituents. Furthermore, the micromechanical approach allows to model different damage and failure modes in the composite material based on the failure in the individual constituent. Hence composite failure modes such as overload failure due to matrix cracking or fiber cracking, depending on the type of composite, maybe modeled. Furthermore the introduction of an additional second order damage tensor for the fiber-matrix interface allows for the modeling of damage and failure modes due to debonding as well.

II.   Numerical Implementation:

The cyclic/fatigue damage constitutive model is implemented numerically and used to simulate damage development and evolution in metal matrix composites. Numerical problems encountered during the implementation and testing phase, such as numerical instabilities, divergence problems, have been addressed and appropriate measures to resolve them have been taken and included. Appropriate necessary material and model parameters are established based on available experimental results. The numerical implementation is used to simulate various loading cases for metal matrix composite specimen, and the results are then compared with the results from the experimental investigations. Comparison of the results from the numerical simulations with those from experiments show good agreement (see sample publications in the appendix) and substantiate the capabilities of the model.

III.   **Publications, Presentations and Organization of Symposia:**

A.   **Books**

1.   Voyiadjis, G. Z., and Allen, D. H., editors, Studies in Applied Mechanics, Vol. 44, Damage and Interfacial Debonding in Composites, 275 p., Elsevier, Amsterdam, 1996.

2.   Voyiadjis, G. Z., and Ju, J. W., editors, Studies in Applied Mechanics, Vol. 41, Inelasticity and Micromechanics of Metal Matrix Composites, 351 p., Elsevier, Amsterdam, 1994.

3.   Voyiadjis, G. Z., Bank, L. C., and Jacobs, L. J., editors, Studies in Applied Mechanics, Vol. 35, Mechanics of Materials and Structures, 436 p., Elsevier, Amsterdam, 1994.

4.   Voyiadjis, G. Z., editor, Studies in Applied Mechanics, Vol. 34, Damage in Composite Materials, 286 p., Elsevier, Amsterdam, 1993.

B.   **Refereed Journal Articles**

1.   Voyiadjis, G. Z., and Zolochevsky, A., "Creep Theory for Transversely Isotropic Solids Sustaining Unilateral Damage," Mechanics Research Communications Journal, 7 manuscript pages (in review).

2.   Voyiadjis, G. Z., and Echle, R., "High Cycle Fatigue Damage Evolution in Uni-Directional Metal Matrix Composites Using a Micro-Mechanical Approach," Mechanics of Materials Journal, 37 manuscript pages (in review).

3.   Park, T., and Voyiadjis, G. Z., "Kinematic Description of Damage," Journal of Applied Mechanics, ASME, 15 manuscript pages (in review).

4.   Voyiadjis, G. Z., and Kattan, P. I., "Equivalence of the Overall and Local Approaches to Damage in Metal Matrix Composites", International Journal of Plasticity, 24 manuscript pages (in review).

5.   Shi, G., and Voyiadjis, G. Z., "A New Free Energy for Plastic Damage Analysis," Mechanics Research Communications Journal, 7 manuscript pages (in press).

6.   Venson, A. R., and Voyiadjis, G. Z., "Damage Quantification in Metal Matrix Composites," Journal of Experimental Mechanics, 41 manuscript pages (in review).

7.   Voyiadjis, G. Z., and Deliktas, B., "Damage in MMCs Using the GCM: Theoretical Formulation," Journal of Composites Engineering, Part B, 42 manuscript pages (in press).

8.   Voyiadjis, G. Z., and Thiagarajan, G., "Micro and Macro Anisotropic Cyclic Damage-Plasticity Models for MMC's," International Journal of Engineering Science, 29 manuscript pages (in press).

9.   Voyiadjis, G. Z., and Park, T., "Anisotropic Damage Effect Tensors for the Symmetrization of the Effective Stress Tensor," Journal of Applied Mechanics, ASME, Vol. 64, 1997, pp. 106-110.

10. Voyiadjis, G. Z., and Park, T., "Local and Interfacial Damage Analysis of Metal Matrix Composites Using the Finite Element Method," Journal of Engineering Fracture Mechanics, Vol. 56, No. 4, 1997, pp. 483-511.

11. Park, T., and Voyiadjis, G. Z., "Damage Analysis and Elasto-Plastic Behavior of Metal Matrix Composites Using the Finite Element Method," Journal of Engineering Fracture Mechanics, Vol. 56, No. 5, 1997, pp. 623-646.

12. Voyiadjis, G. Z., and Kattan, P. I., "On the Symmetrization of the Effective Stress Tensor in Continuum Damage Mechanics," Journal of the Mechanical Behavior of Materials, Vol. 7, No. 2, 1996, pp. 139-165.

13. Voyiadjis, G. Z., and Park, T., "Anisotropic Damage for the Characterization of the Onset of Macro-Crack Initiation in Metals," International Journal of Damage Mechanics, Vol. 5, No. 1, 1996, pp. 68-92.

14. Voyiadjis, G. Z., and Park, T., "Stress and Strain Concentration Tensors for Damaged Fibrous Composites," Journal of the Mechanical Behavior Materials, Vol. 7, No. 2, 1996, pp. 119-138.

15. Voyiadjis, G. Z., and Zakaria Guelzim, "A Coupled Incremental Damage and Plasticity Theory for Metal Matrix Composites," Journal of the Mechanical Behavior of Materials, Vol. 6, No. 3, 1996, pp. 193-219.

16. Voyiadjis, G. Z., and Thiagarajan, G., "A Cyclic Anisotropic Plasticity Model for Metal Matrix Composites," International Journal of Plasticity, Vol. 12, No. 1, 1996, pp. 69-91.

17. Kattan, P. I., and Voyiadjis, G. Z., "Damage-Plasticity in a Uniaxially-Loaded Composite Lamina: Overall Analysis," International Journal of Solids and Structures, Vol. 33, No. 4, February 1996, pp. 555-576.

18. Voyiadjis, G. Z., and Thiagarajan, G., "An Anisotropic Yield Surface Model for Directionally Reinforced Metal Matrix Composites," International Journal of Plasticity, Vol. 11, No. 8, 1995, pp. 867-894.

19. Voyiadjis, G. Z., Venson, A. R., and Kattan, P. I., "Experimental Determination of Damage Parameters in Uniaxially-Loaded Metal Matrix Composites Using the Overall Approach," International Journal of Plasticity, Vol. 11, No. 8, 1995, pp. 895-926.

20. Voyiadjis, G. Z., and Park, T., "Anisotropic Damage of Fiber Reinforced MMC Using an Overall Damage Analysis," Journal of Engineering Mechanics, ASCE, Vol. 121, No. 11, 1995, pp. 1209-1217.

21. Voyiadjis, G. Z., and Venson, A. R., "Experimental Damage Investigation of a SiC-Ti Aluminide Metal Matrix Composite," International Journal of Damage Mechanics, Vol. 4, No. 4, October 1995, pp. 338-361.

22. Voyiadjis, G. Z., and Park T., "Local and Interfacial Damage Analysis of Metal Matrix Composites, " International Journal of Engineering Science, Vol. 33, No. 11, 1995, pp. 1595-1621.

23. Kattan, P. I., and Voyiadjis, G. Z., "Overall Damage and Elasto-Plastic Deformation in Fibrous Metal Matrix Composites," International Journal of Plasticity, Vol. 9, No. 8, 1993, pp. 931-949.

24. Voyiadjis, G. Z., and Kattan, P. I., "Damage of Fiber-Reinforced Composite Materials with Micromechanical Characterization," International Journal of Solids and Structures, Vol. 30, No. 20, 1993, pp. 2757-2778.

25. Voyiadjis, G. Z., and Kattan, P. I., "Local Approach to Damage in Elasto-Plastic Metal Matrix Composites," International Journal of Damage Mechanics, Vol. 2, No. 1, 1993, pp. 92-114.

26. Kattan, P. I., and Voyiadjis, G. Z., "A Plasticity-Damage Theory for Large Deformation of Solids, Part II: Applications to Finite Simple Shear," International Journal of Engineering Science, Vol. 31, No. 1, 1993, pp. 183-199.

27. Kattan, P. I., and Voyiadjis, G. Z., "Micromechanical Modeling of Damage in Uniaxially Loaded Unidirectional Fiber-Reinforced Composite Laminae," International Journal of Solids and Structures, Vol. 30, No. 1, 1993, pp. 19-36.

C.   Refereed Proceedings

1. Voyiadjis, G. Z., Echle, R., "A Micro-Mechanical Fatigue Damage Model for Uni-Directional Metal Matrix Composites," Applications of Continuum Damage Mechanics to Fatigue and Fracture, STP 1315, ASTM, 1997, 31 manuscript pages (in press).

2. Echle, R., and Voyiadjis, G. Z., "Fatigue Damage Evolution in Uni-Directional Metal Matrix Composites Using a Micro-Mechanical Damage Model," 8th Annual International Energy Week Conference & Exhibition, Energy Engineering I, Vol. III, Composite Materials Design & Analysis, ASME Publishing Company, 1997, pp. 152-159.

3. Thiagarajan G., and Voyiadjis, G. Z., "A Damage Cyclic Plasticity Model for MMC'S Using a Micromechanical Model," 8th Annual International Energy Week Conference & Exhibition, Energy Engineering I, Vol. III, Composite Materials Design & Analysis, ASME Publishing Company, 1997, pp. 145-151.

4. Voyiadjis, G. Z., and Park, T., "Elasto-Plastic Stress and Strain Concentration Tensors for Damaged Fibrous Composites," Studies in Applied Mechanics, Vol. 44, Damage and Interfacial Debonding in Composites, edited by G. Z. Voyiadjis and D. H. Allen, Elsevier Publishing Company, 1996, pp. 81-106.

5. Voyiadjis, G. Z., and Thiagarajan, G., "A Damage Cyclic Plasticity Model for Metal Matrix Composites," Studies in Applied Mechanics, Vol. 44, Damage and Interfacial Debonding in Composites, edited by G. Z. Voyiadjis and D. H. Allen, Elsevier Publishing Company, 1996, pp. 107-132.

6. Voyiadjis, G. Z., and Guelzim, Z., "Incremental Damage Theory for Metal Matrix Composites," Contemporary Research in Engineering Science, edited by R. C. Batra, 1995, pp. 576-592.

7. Voyiadjis, G. Z., and Park, T., "Finite Element Analysis of Damage and Elasto-Plastic Behavior of Metal Matrix Composites," Computational Mechanics, Vol. 1, edited by S. N. Atluri, G. Yagawa and T. A. Cruse, Springer Publishing Company, 1995, pp. 1205-1210.

5

8. Voyiadjis, G. Z., and Thiagarajan, G., "A Damage Cyclic Plasticity Model for Metal Matrix Composites," Constitutive laws: Experiments and Numerical Implementation, edited by A. M. Rajendran and R. C. Batra, a publication of International Center for Numerical Methods in Engineering (CIMNE), 1995, pp. 159-170.

9. Voyiadjis, G. Z., and Thiagarajan, G., "A Cyclic Plasticity Model for Metal Matrix Composites," Computational Mechanics, Vol. 2, edited by S. N. Atluri, G. Yagawa and T. A. Cruse, Springer Publishing Company, 1995, pp. 1739-1744.

10. Voyiadjis, G. Z., and Venson, A. R., "Finite Element Implementation of the Overall Approach to Damage in Metal Matrix Composites," Engineering Mechanics, Proceedings of 10th Conference, Vol. 1, edited by Stein Sture, Engineering Mechanics Division of the ASCE, 1995, pp. 389-392.

11. Voyiadjis, G. Z., and Kattan, P. I., "Micromechanical Modeling of Damage and Plasticity in Continuously Reinforced MMCs," Studies in Applied Mechanics, Vol. 41, Inelasticity and Micromechanics of Metal Matrix Composites, edited by G. Z. Voyiadjis and J. W. Ju, Elsevier Publishing Company, 1994, pp.307-345.

12. Voyiadjis, G. Z., and Thiagarajan, G., "A Cyclic Plasticity Model for Metal Matrix Composites Using an Anisotropic Yield Surface," Studies in Applied Mechanics, Vol. 41, Inelasticity and Micromechanics of Metal Matrix Composites, edited by G. Z. Voyiadjis and J. W. Ju, Elsevier Publishing Company, 1994, pp.51-81.

13. Voyiadjis, G. Z., and Park, T., "Interfacial and Local Damage Analysis in Metal Matrix Composites," Damage Mechanics in Composites, 1994, edited by D.H. Allen, and J.W. Ju, ASME, AMD-Vol. 185, 1994, pp. 87-108.

14. Voyiadjis, G. Z., and Kattan, P. I., "Coupling of Damage and Viscoplasticity for Large Deformation of Metals," Large Plastic Deformations: Fundamental Aspects and Applications to Metal Forming, edited by C. Teodosiu, J. L. Raphanel, and F. Sidoroff, A. A. Balkema Publishing Company, 1993, pp. 345-352.

15. Voyiadjis, G. Z., Kattan, P. I., and Venson, A. R., "Evaluation of a Damage Tensor for Metal Matrix Composites," Direction des Etudes et Recherches d' Electricite de France: MECAMAT 93, International Seminar on Micromechanics of Materials, Vol. 84, 1993, pp. 406-417.

16. Voyiadjis, G. Z., and Kattan, P. I., "Micromechanical Characterization of Damage-Plasticity in Metal Matrix Composites," Studies in Applied Mechanics, Vol. 34, Damage in Composite Materials, edited by G. Z. Voyiadjis, Elsevier Publishing Company, 1993, pp. 67-102.

D.   Technical Reports

1. Voyiadjis, G. Z., Kattan, P. I., Venson, A. R., Park, T., and Thiagarajan, G., "Constitutive Modeling of Metal Matrix Composites Under Cyclic Loads - Second Annual Report (1993-94), F49620-93-1-0097DEF and F49620-92-J-0463," Air Force Office of Scientific Research, Washington, D.C., September 1994, 155 pages.

2. Voyiadjis, G. Z., Kattan, P. I., and Venson, A. R., "Constitutive Modeling and Finite Element Analysis of Fatigue Damage in Metal Matrix Composites - First Annual Report (1992-93), F49620-93-1-0097DEF and F49620-92-J-0463," Air Force Office of Scientific Research, Washington, D.C., October 1993, 130 pages.

3. Voyiadjis, G. Z., Kattan, P. I., Venson, A. R., and Park, T., "Anisotropic Damage Mechanics Modeling in Metal Matrix Composites - Final Report, AFOSR-90-0227 DEF," Air Force Office of Scientific Research, Washington, D.C., May 1993, 141 pages.

4. Voyiadjis, G. Z., Kattan, P. I., and Venson, A., "Anisotropic Damage Mechanics Modeling in Metal Matrix Composites - Second Annual Report (1991-92), AFOSR-90-0227 DEF," Air Force Office of Scientific Research, Washington, D.C., May 1992, 104 pages.

E. Papers presented in conferences and invited lectures

1. Voyiadjis, G. Z., and Echle, R., "Fatigue Damage in Metal Matrix Composites." Invited lecture presented in the "Symposium on Failure Mechanisms and Mechanisms-Based Modeling in High Temperature Composites," of the 1996 ASME, International Mechanical Engineering Congress and Exposition, Atlanta, Georgia, November 1996.

2. Voyiadjis, G. Z., and Echle, R., "A Micro-Mechanical Fatigue Damage Model for Uni-Directional Metal Matrix Composites."Invited lecture presented in the "High Temperature Fatigue in MMCs Symposium," of the 33rd Annual Technical Meeting of the Society of Engineering Science, Arizona State University, Tempe, Arizona, October 1996.

3. Voyiadjis, G. Z., and Park, T., "Quantification of Different Types of Damage in Constituents of MMC Laminates." Invited lecture presented at the "Prager Symposium" of the 33rd Annual Technical Meeting of the Society of Engineering Science, Arizona State University, Tempe, Arizona, October 1996.

4. Voyiadjis, G. Z., and Park, T., "The Kinematics of Damage in Metal Matrix Composites." Invited lecture presented at the First Euroconference and U.S. Workshop on Material Instabilities in Deformation and Fracture, Porto Carras, Chalkidiki, Greece, September 1996.

5. Echle, R., and Voyiadjis, G. Z., "A Micro-Mechanical Fatigue Damage Approach for Metal Matrix Composites." Presented at the "Third International Conference on Composites Engineering, ICCE/3, New Orleans, Louisiana, July 1996.

6. Voyiadjis, G. Z., and Deliktas, B., "Local Damage using the Generalized Cell Method in MMCs." Invited lecture presented at the "Third International Conference on Composites Engineering," ICCE/3, New Orleans, Louisiana, July 1996.

7. Park, T., and Voyiadjis, G. Z., "Interfacial Damage in Metal Matrix Composites." Presented at the "Third International Conference on Composites Engineering," ICCE/3, New Orleans, Louisiana, July 1996.

8. Thiagarajan, G., and Voyiadjis, G. Z., "In-Situ Modeling of Titanium Based Matrix in Metal-Matrix Composites Subjected to Cyclic Loading." Presented at the "Third International Conference on Composites Engineering," ICCE/3, New Orleans, Louisiana, July 1996.

9.   Voyiadjis, G. Z., and Deliktas, B., "Damage in Metal Matrix Composites Using the Generalized Cells Method." Presented at the 1996 ASME Mechanics and Materials Conference, Baltimore, Maryland, June 1996.

10.   Voyiadjis, G. Z., and Echle, R., "Fatigue Model for Damage in Metal Matrix Composites." Invited lecture presented in the Symposium on "Application of Continuum Damage Mechanics to Fatigue and Fracture," at the ASTM Conference, Orlando, Florida, May 1996.

11.   Voyiadjis, G. Z., and Park, T., "Effect of Damage Due to Delamination on the Flexural Stiffness of Laminated Composite Plates." Invited lecture presented at the Symposium on "Damage and Interfacial Debonding in Composites," at the 32nd Annual Technical Meeting of the Society of Engineering Science, New Orleans, Louisiana, October 1995.

12.   Thiagarajan, G., and Voyiadjis, G. Z., "Cyclic Damage with Cyclic Plasticity in Metal Matrix Composites." Lecture presented at the 32nd Annual Technical Meeting of the Society of Engineering Science, New Orleans, Louisiana, October 1995.

13.   Voyiadjis, G. Z., and Guelzim, Z., "Incremental Damage Theory for Metal Matrix Composites." Invited lecture presented at the "Eringen Medal Symposium: S. Atluri," at the 32nd Annual Technical Meeting of the Society of Engineering Science, New Orleans, Louisiana, October 1995.

14.   Park, T., and Voyiadjis, G. Z., "Analysis of Interfacial and Local Damage in Metal Matrix Composites using the FE Method." Lecture presented at the 32nd Annual Technical Meeting of the Society of Engineering Science, New Orleans, Louisiana, October 1995.

15.   Thiagarajan, G., and Voyiadjis, G. Z., "Cyclic Plasticity with Damage in Metal Matrix Composites." Lecture presented at the Symposium on "Micromechanics of Fibers or Composites," at the Second International Conference on Composites Engineering, New Orleans, Louisiana, August 1995.

16.   Voyiadjis, G. Z., and Rainer, E., "Fatigue Damage in Metal Matrix Composites." Invited lecture presented at the Symposium on "Fatigue of Composites," at the Second International Conference on Composites Engineering, New Orleans, Louisiana, August 1995.

17.   Park, T., and Voyiadjis, G. Z., "Stress and Strain Concentration Tensors for Interfacial Damage." Lecture presented at the Symposium on "Micromechanics of Fibers or Composites," at the Second International Conference on Composites Engineering, New Orleans, Louisiana, August 1995.

18.   Venson, A. R., and Voyiadjis, G. Z., "Experimental Determination of Damage in Titanium Aluminide with Silicon Carbide Fibers." Lecture presented at the Symposium on "Metal Matrix Composites," at the Second International Conference on Composites Engineering, New Orleans, Louisiana, August 1995.

19.   Voyiadjis, G. Z., and Thiagarajan, G., "A Cyclic Plasticity Model for Metal Matrix Composites." Invited lecture presented at the Symposium on "Recent Advances in Constitutive Laws for Engineering Materials," at the International Conference on Computational Engineering Science (ICES-95), Mauna Lani, Hawaii, August 1995.

20. Voyiadjis, G. Z., and Park, T., "Finite Element Analysis of Damage and Elasto-Plastic Behavior of Metal Matrix Composites." Invited lecture presented at the Symposium on "Inelastic Deformation, Damage and Life Analysis," at the International Conference on Computational Engineering Science (ICES-95), Mauna Lani, Hawaii, August 1995.

21. Voyiadjis, G. Z., and Thiagarajan, G., "A Damage Cyclic Plasticity Model for Metal Matrix Composites." Invited lecture presented at the Symposium on "Micromechanics and Constitutive Modeling of Composite Materials," at the ASME joint Applied Mechanics and Materials Summer Conference AMD-MD '95, Los Angeles, California, June 1995.

22. Voyiadjis, G. Z., and Park, T., "Finite Element Analysis of Interfacial and Local Damage in Metal Matrix Composites." Invited lecture presented at the Symposium on "Recent Advances in Damage Mechanics," at the ASME joint Applied Mechanics and Materials Summer Conference AMD-MD '95, Los Angeles, California, June 1995.

23. Voyiadjis, G. Z., Park, T., and Venson, A. R., "Finite Element Implementation of the Overall Approach to Damage in Metal Matrix Composites." Invited lecture presented at the Symposium on "Damage Mechanics in Engineering Materials," at the 10th ASCE Engineering Mechanics Conference, Boulder, Colorado, May 1995.

24. Voyiadjis, G. Z., "Damage in Materials." Invited lecture presented at Louisiana State University, Saturday Science at LSU Seminar Series, Baton Rouge, Louisiana, December 1994.

25. Voyiadjis, G. Z., and Park, T., "Interfacial and Local Damage Analysis of Metal Matrix Composites." Invited lecture presented at the Symposium on "Damage Mechanics in Composites," at the ME '94, The International Mechanical Engineering Congress and Exposition, Chicago, Illinois, November 1994.

26. Voyiadjis, G. Z., "Constitutive Modeling of Plasticity with Damage in Metal Matrix Composites." Invited lecture presented at the National Science Foundation Workshop on Mechanics and Processing of Advanced Engineering Materials - II, Atlanta, Georgia, October, 1994.

27. Voyiadjis, G. Z., Venson, A.R., and Kattan, P.I. "Damage Approaches to Unidirectional Elastoplastic Laminas Under Uniaxial Tension." Invited lecture presented at the 31st Annual Technical Meeting of the Society of Engineering Science, College Station, Texas, October 1994.

28. Voyiadjis, G. Z., and Kattan, P. I., "Damage and Plastic Deformation in a Uniaxially Loaded Thin Composite Ply." Invited lecture presented at the First International Conference on Composites Engineering, New Orleans, Louisiana, August 1994.

29. Voyiadjis, G. Z., and Kattan, P. I., "Micromechanical Modeling of Damage and Plasticity in Continuously Reinforced Metal Matrix Composites." Invited lecture presented at the 12th U.S. National Congress of Applied Mechanics, Seattle, Washington, June 1994.

30. Voyiadjis, G. Z., "Damage Accumulation in Metal Matrix Composites." Invited lecture presented at the National Science Foundation Workshop on "Processing and Constitutive Modeling of Advanced Engineered Materials - I," Washington State University, Pullman, Washington, October 1993.

31. Voyiadjis, G. Z., "Damage in Metal Matrix Composites." Invited lecture presented in the Department of Mechanical Engineering, University of Delaware, Newark, Delaware, October 1993.

32. Voyiadjis, G. Z., Venson, A. R., and Kattan, P. I., "Damage Mechanism in Metal Matrix Composite Plates." Invited lecture presented at the Army Research Office Workshop on Dynamic Response of Composite Structures, New Orleans, Louisiana, August 1993.

33. Voyiadjis, G. Z., Kattan, P. I., and Venson, A. R., "Evaluation of a Damage Tensor for Metal Matrix Composites." Presented at the MECAMAT '93, International Seminar on Micromechanics of Materials, Fontainebleau, France, July 1993.

34. Voyiadjis, G. Z., and Sivakumar, S. M., "Cyclic Plasticity and Ratchetting." Presented at the MEET'N'93, First SES-ASME-ASCE Joint Meeting on Mechanics, Bieniek Symposium on Mechanics of Materials and Structures, Charlottesville, VA, June 1993.

35. Voyiadjis, G. Z., and Kattan, P. I., "Damage and Inelastic Deformation of SiC/Ti-Aluminide Composites." Invited lecture presented at the MEET'N'93, First SES-ASME-ASCE Joint Meeting on Mechanics, Symposium on Inelastic Micromechanics in SiC/Ti Composites, Charlottesville, VA, June 1993.

F.   Symposia organized by Dr. G. Z. Voyiadjis:

1. Co-Organizer and Co-Chairman of three sessions of the Symposium on "Failure Predictions in Dynamic Environments," to be held in the 1997 ASME, IMECE, Dallas, Texas, November 1997.

2. Co-Organizer and Co-Chairman of eleven sessions of the Symposium on "Damage Mechanics in Engineering Materials," to be held in the Joint ASME/ASCE/SES Mechanics Conference, Northwestern University, Evanston, Illinois, June/July 1997.

3. Organizer and Chairman of the Symposium on "High Temperature Fatigue in Metal Matrix Composites," held in the Society of Engineering Science 33rd Annual Technical Meeting, Arizona State University, Tempe, Arizona, October 1996.

4. Co-Organizer and Co-Chairman of four sessions of the Symposium on "Damage and Interfacial Debonding in Composites," held in the 32nd Society of Engineering Science Meeting, New Orleans, Louisiana, October/November 1995.

5. On the Organizing Committee of the 32nd Annual Technical Meeting of the Society of Engineering Science, New Orleans, Louisiana, October 29 - November 1, 1995.

6. Co-Organizer and Co-Chairman of four sessions of the Symposium on "Micromechanics of Fibers or Composites," held in the 2nd International Conference on Composites Engineering, New Orleans, Louisiana, August 1995.

7. Co-Organizer and Co-Chairman of four sessions of the Symposium on "Fatigue of Composites," to be held in the 2nd International Conference on Composites Engineering, New Orleans, Louisiana, August 1995.

8. Co-Organizer and Co-Chairman of five sessions of the Symposium on "Inelasticity and Micromechanics of Metal Matrix Composites," held in the Twelfth U.S. National Congress of Applied Mechanics, Seattle, Washington, June/July 1994.

9. Panel Member of the session on "Damage Accumulation and Life Prediction in Metal Matrix Composites," of the National Science Foundation Workshop on "Processing and Constitutive Modeling of Advanced Engineered Materials," Washington State University, Pullman, Washington, October 1993.

10. Co-Organizer and Co-Chairman of four sessions of the <u>Maciej P. Bieniek Symposium</u> on "Mechanics of Materials and Structures," held in the MEET'N'93, First Joint ASCE-ASME-SES Mechanics Conference, University of Virginia, Charlottesville, Virginia, June 1993.

Ph.D. Students Completed:

1. Rainer Echle: A Micro - Mechanical Fatigue Damage Model for Uni - Directional Metal Matrix Composites; May 1997, LSU.

2. Ganesh Thiagarajan: A Cyclic Plasticity/Damage Model for Metal Matrix Composites; May 1996, LSU. Currently: Instructor, Department of Civil and Environmental Engineering, Louisiana State University, Baton Rouge, Louisiana.

3. A. R. Venson: Experimental Macro and Microstructural Characterization of Damage for Metal Matrix Composites; December 1994, LSU. Currently: Assistant Professor, Department of Civil Engineering, University of Southwestern Louisiana, Lafayette, Louisiana.

4. Taehyo Park: Finite Element Analysis of Damage and Elastic-Plastic Behavior of Metal Matrix Composites; December 1994, LSU. Currently: Research Associate, Department of Civil and Environmental Engineering, Louisiana State University, Baton Rouge, Louisiana

M.Sc. Students Completed:

1. Babur Deliktas: Damage in Metal Matrix Composite Using the Generalized Cells Model; May 1996, LSU.

APPENDIX

The following copies of scientific papers are representative of the publications written during the course of this project.

Pergamon

0749-6419(95)00045-3

A CYCLIC ANISOTROPIC-PLASTICITY MODEL FOR METAL MATRIX COMPOSITES

George Z. Voyiadjis and Ganesh Thiagarajan

Department of Civil Engineering, Louisiana State University, Baton Rouge, LA-70803, U.S.A.

Abstract—Based on a six parameter general anisotropic yield surface proposed earlier by Voyiadjis and Thiagarajan (An Anisotropic Yield Surface Model for Directionally Reinforced Metal Matrix Composites, *Int. J. Plasticity* [1995]), a cyclic plasticity model to model the behavior of directionally reinforced metal matrix composite, has been proposed here. Apart from being able to model different initial yielding behavior along different stress directions, a number of features have been incorporated into the plasticity model. They include the usage of a proposed non-associative flow rule, kinematic hardening rule of Phillips type, a modified form of the bounding surface model for modelling the cyclic behavior, and the usage of a proposed form for evaluating the plastic modulus for anisotropic materials. Previous experimental data have been used for the evaluation of the yield surface parameters as well as those for the determination of the plastic modulus. The stress–strain results generated from the model have then been compared with those from the experiments. The behavior of the model under certain simulated cyclic loading situations has also been presented.

I. INTRODUCTION

This paper focuses upon the treatment of a metal matrix composite (MMC) as a continuum and is an extension of the work presented earlier by the authors (Vojiadjis & Thiagarajan [1995]) wherein an anisotropic yield surface has been proposed with application to continuous directionally reinforced metal matrix composites. The yield surface proposed earlier has been correlated to the experimental observations of Dvorak *et al.* [1988] and Nigam *et al.* [1993]. A model is proposed herein to account for the material behavior of MMC which is transversely isotropic and subjected to cyclic, proportional and non-proportional loadings. The cyclic plasticity model for the anisotropic material is based on a modification of the bounding surface model proposed by Dafalias and Popov [1976] for the case of isotropic materials.

It is also observed that the plastic strains that develop in an MMC are non-associative in nature. To account for this, a non-associative flow rule is proposed here, based on definitions of the yield and a complimentary yield function, termed as "constrained yield function." Also a suitable kinematic hardening rule is adopted here.

Based on the above observations the elastoplastic stiffness matrix is derived for the cyclic plasticity model. This model has been implemented in a computer program to generate the stress–strain curves under different loading conditions. These curves have been generated along loading paths followed by Nigam *et al.* [1993]. Plastic strains are obtained and compared to those documented by Dvorak *et al.* [1988] and Nigam *et al.*

69

[1993]. Other simulated loading conditions are applied to the proposed model and results are presented here, to demonstrate the versatility of the model under various loading conditions.

II. PROPOSED YIELD SURFACE

Voyiadjis and Thiagarajan [1995] proposed an anisotropic yield surface for continuous fiber reinforced metal matrix composites, using a fourth order anisotropic yield tensor $\bar{M}$. Two coordinate systems are used, namely the local coordinate system and the global coordinate system (Fig. 1). In the local coordinate system, the coordinate axes coincide with the three principal axes of material anisotropy. The orientation of the fiber is defined in the global coordinate system. The loading is also defined with respect to the global coordinate system.

The proposed yield function in the local coordinate axes is of the form shown below.

$$\bar{M}_{ijkl}\bar{\sigma}_{ij}\bar{\sigma}_{kl} - 1 = 0 \tag{1}$$

where $\bar{\sigma}_{ij}$ is the overall state of stress in this system. $\bar{M}$ is the fourth order anisotropic yield tensor expressed as a function of two second order tensors a_{ij} and b_{ij} as follows:

$$\bar{M} = \bar{M}(a, b) \tag{2}$$

The expression for $\bar{M}$ is given as,

$$\bar{M}_{ijkl} = A(a_{ij}a_{kl}) + B(a_{ik}a_{jl}) + C(a_{il}a_{jk}) + D(b_{ij}b_{kl}) \tag{3}$$

where A, B, C and D are constants and a_{ij} and b_{ij} are functions of the six strength parameters k_i ($i = 1, ..., 6$). Three of these parameters are directly related to the axial strengths and the other three are shear strength parameters. They are used to define yielding for an anisotropic material. These parameters are measured and determined along the principal axes of anisotropy. a_{ij} and b_{ij} are given as follows:

$$a_{ij} = \begin{bmatrix} k_1 & 0 & 0 \\ 0 & k_2 & 0 \\ 0 & 0 & k_3 \end{bmatrix} \tag{4}$$

$$b_{ij} = \begin{bmatrix} 0 & k_4 & k_5 \\ k_4 & 0 & k_6 \\ k_5 & k_6 & 0 \end{bmatrix}. \tag{5}$$

Substituting (3) into (1) we can express the yield equation in the local coordinate axes in component form as follows:

$$
\begin{aligned}
(A + B + C)&(k_1^2\bar{\sigma}_{11}^2 + k_2^2\bar{\sigma}_{22}^2 + k_3^2\bar{\sigma}_{33}^2) \\
+ (2A)&(k_1k_2\bar{\sigma}_{11}\bar{\sigma}_{22} + k_1k_3\bar{\sigma}_{11}\bar{\sigma}_{33} + k_2k_3\bar{\sigma}_{22}\bar{\sigma}_{33}) \\
+ (2(B + C)k_1k_2 + 4Dk_4^2)&\bar{\sigma}_{12}^2 + (2(B + C)k_1k_3 + 4Dk_5^2)\bar{\sigma}_{13}^2 \\
+ (2(B + C)k_2k_3 &+ 4Dk_6^2)\bar{\sigma}_{23}^2 = 0.
\end{aligned} \tag{6}
$$

The constants A, B, C and D are not material parameters. The possible choices of combinations of these values are outlined by Voyiadjis and Thiagarajan [1995]. The values of these constants chosen here for this implementation are $A = \frac{-1}{9}$, $B = C = \frac{1}{6}$ and $D = \frac{1}{6}$. These values reduce the above equation to the following form.

$$F = \frac{2}{9}(k_1^2 \bar{\sigma}_{11}^2 + k_2^2 \bar{\sigma}_{22}^2 + k_3^2 \bar{\sigma}_{33}^2)$$
$$- \frac{2}{9}(k_1 k_2 \bar{\sigma}_{11} \bar{\sigma}_{22} + k_2 k_3 \bar{\sigma}_{22} \bar{\sigma}_{33} + k_1 k_3 \bar{\sigma}_{11} \bar{\sigma}_{33}) \qquad (7)$$
$$+ \frac{2}{3}(k_1 k_2 + k_4^2)\bar{\sigma}_{12}^2 + \frac{2}{3}(k_1 k_3 + k_5^2)\bar{\sigma}_{13}^2 + \frac{2}{3}(k_2 k_3 + k_6^2)\bar{\sigma}_{23}^2 - 1.0.$$

One can also express the yield equation in the global axes of reference as follows:
$$\sigma_{ij} M_{ijkl} \sigma_{kl} - 1 = 0. \qquad (8)$$

The stresses are transformed from the global to the local axes of reference as follows
$$\bar{\sigma}_{ij} = d_{ip} \sigma_{pq} d_{qj} \qquad (9)$$

where d_{ij} are the coefficients of the orthogonal transformation matrix. Assuming that the fibers are aligned along the x-axis (1-direction) one can write,
$$d_{1j} = (\eta_1, \eta_2, \eta_3) \qquad (10)$$

where η_i, $(i = 1,2,3)$ are the direction cosines of the fiber in the global coordinate system. A lamina of any arbitrary orientation is derived by rotating the principal axes of anisotropy about the z-axis(3-direction) of the global axes of reference. Hence one obtains $d_{3j} = (0, 0, 1)$. The terms of d_{2j} can then be derived from the condition
$$d_{pi} d_{qi} = \delta_{pq}. \qquad (11)$$

Substituting for $\bar{\sigma}_{ij}$ in the yield (1) one obtains
$$\sigma_{pq} d_{ip} d_{jq} \bar{M}_{ijkl} d_{km} d_{ln} \sigma_{mn} - 1 = 0. \qquad (12)$$

From the above equation M_{ijkl} can be expressed as,
$$M_{ijkl} = \bar{M}_{pqrs} d_{ip} d_{jq} d_{kr} d_{ls}. \qquad (13)$$

Further details about the computation of the parameters, their reduction to certain well-known yield criteria and their comparison with the yield surfaces obtained from experimental evidence have been demonstrated in the paper by Voyiadjis and Thiagarajan [1995].

III. THEORETICAL DEVELOPMENT OF THE CONSTITUTIVE MODEL

The description of the elasto-plastic behavior of the metal matrix composite, when treated as a continuum is a complex task. The fact that MMC is transversely isotropic and the presence of continuous fibers with their respective constraints, necessitates the usage of anisotropic hardening and non-associative flow rules. The formulation proposed here is also intended to describe the behavior of MMC under cyclic loading conditions. The bounding surface model is adopted here to simulate the mechanical

behavior of the material. In this paper, the thrust is thus on transversely isotropic materials.

III.1. *Elastic behavior*

The elastic behavior of the composite material, treated as a homogeneous continuum with transversely isotropic properties has been defined Walpole [1969] and is used here. The linear constitutive relation is expressed as

$$\sigma_{ij} = C_{ijkl}\epsilon_{kl} \tag{14}$$

where **C** is the fourth order elastic stiffness tensor relating the symmetric second order tensors σ and ϵ of stress and strain, respectively. For a transversely isotropic material the fourth order elastic stiffness tensor is given as follows:

$$C_{ijkl} = Kt_{ij}t_{kl} + El_{ij}l_{kl} + 2m_t E^3_{ijkl} + 2p E^4_{ijkl} \tag{15}$$

where,

$$t_{ij} = m_{ij} + 2\nu l_{ij} \tag{16}$$

$$l_{ij} = \eta_i\eta_j \tag{17}$$

$$m_{ij} = \delta_{ij} - \eta_i\eta_j \tag{18}$$

$$E^3_{ijkl} = \frac{1}{2}[m_{ik}m_{jl} + m_{jk}m_{il} - m_{ij}m_{kl}] \tag{19}$$

$$E^4_{ijkl} = \frac{1}{2}[m_{ik}l_{jl} + m_{il}l_{jk} + m_{jl}l_{ik} + m_{jk}m_{il}] \tag{20}$$

and 'K' is the plane-strain bulk modulus, m_t is the transverse shear modulus, p is the axial shear modulus and E and ν are the Young's Modulus and Poisson ratio, respectively, when the material is loaded in the fiber direction. For a transversely isotropic material the plane-strain bulk modulus can be defined in terms of the other four elastic constants.

III.2. *Non-associative flow rule*

It has been well established by now that the determination of plastic strains, for any anisotropic material in general, and a MMC in particular must adopt a non-associative flow rule. Dvorak *et al.* [1988] and Nigam *et al.* [1993] have experimentally demonstrated this and have established that there is a tendency for the direction of plastic strains to be more inclined towards the shear direction in a combined transverse tension–shear loading situation. It has also been shown that there exists, to a large extent, plastic inextensibility along the fiber direction.

To account for the above factors, a plastic potential function is proposed here, the form of which is based on the proposed yield function. The nature of this potential function is explained below.

III.3. *Proposed potential function*

In order to determine the plastic strain increments ($\dot{\epsilon}''_{ij}$) use is made of a non-associative flow rule as outlined earlier such that,

$$\dot{\epsilon}''_{ij} = \dot{\Lambda}\frac{\partial G}{\partial \sigma_{ij}} \tag{21}$$

where G is the plastic potential function. The potential function is defined later as a function of the yield function and the constrained yield function. The constrained yield function is defined such that it satisfies the condition of plastic inextensibility along the direction defined by η. This is accomplished by defining a function g which is of the functional form of the yield function f. The function g is defined using the fourth order anisotropic yield tensor M and a constrained stress term r_{ij} such that,

$$g = r_{ij}M_{ijkl}r_{kl} - 1. \tag{22}$$

The constraint that is introduced in the stress term is that the plastic strain increment is independent of the component of stress along a specified direction (defined here by η_i). Following the procedure outlined by Spencer [1972] the constraint is incorporated into the stress term as follows:

$$r_{ij} = \sigma_{ij} - T\eta_i\eta_j \tag{23}$$

where $T\eta_i\eta_j$ is the reaction to an inextensibility constraint along the direction η. Taking the inner product on both sides of (23) with $\eta_i\eta_j$ one obtains,

$$r_{ij}\eta_i\eta_j = \sigma_{ij}\eta_i\eta_j - T\eta_i\eta_j\eta_i\eta_j. \tag{24}$$

One can impose the constraint is in the stress term r_{ij} as follows

$$r_{ij}\eta_i\eta_j = 0. \tag{25}$$

Substituting this constraint in (24) one obtains,

$$\sigma_{ij}\eta_i\eta_j = T\eta_i\eta_j\eta_i\eta_j \tag{26}$$

and using the condition $\eta_i\eta_j = 1$ it can be shown that

$$T = \sigma_{ij}\eta_i\eta_j. \tag{27}$$

Hence one can expand (23) as follows:

$$r_{ij} = \sigma_{ij} - (\sigma_{rs}\eta_r\eta_s)\eta_i\eta_j. \tag{28}$$

Using the yield function and the function g defined above, the potential function G can now be defined as follows,

$$G = \omega f + (1.0 - \omega)g, \quad 0 \leq \omega \leq 1.0. \tag{29}$$

In order to illustrate the capability of this potential function we consider the yield function in the $\sigma_{11} - \sigma_{12}$ space. Assuming that $\eta = (1,0,0)$ then f and g functions can be represented as shown in Fig. 2. Since $\eta = (1,0,0)$, this implies that the fiber is along the 1-direction and the stress along this direction σ_{11} does not influence yielding. Hence in Fig. 2 the yield function f represents yielding both axes whereas the constrained yield function g is parallel to the σ_{11}-axis, physically representing the requirement that σ_{11}

does not influence yielding. The unit normals to these functions, which are also shown in Fig. 2, can be expressed in tensor form as follows:

$$n_{ij}^f = \frac{\partial f}{\partial \sigma_{ij}} / \left\| \frac{\partial f}{\partial \sigma_{rs}} \right\| \tag{30}$$

$$n_{ij}^g = \frac{\partial g}{\partial \sigma_{ij}} / \left\| \frac{\partial g}{\partial \sigma_{rs}} \right\| \tag{31}$$

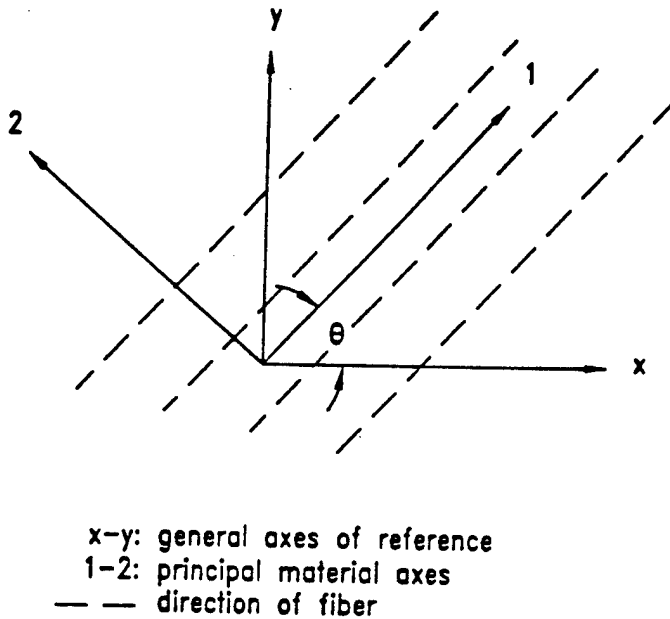where n_{ij}^f and n_{ij}^g represent the normality to the two surfaces represented by f and g.

x-y: general axes of reference
1-2: principal material axes
— — direction of fiber

Fig. 1. Local and global axes of reference for a single lamina.

⬭ Yield Surface 'f'

---- Constrained Yield Surface 'g'
with $\eta = (1,0,0)$
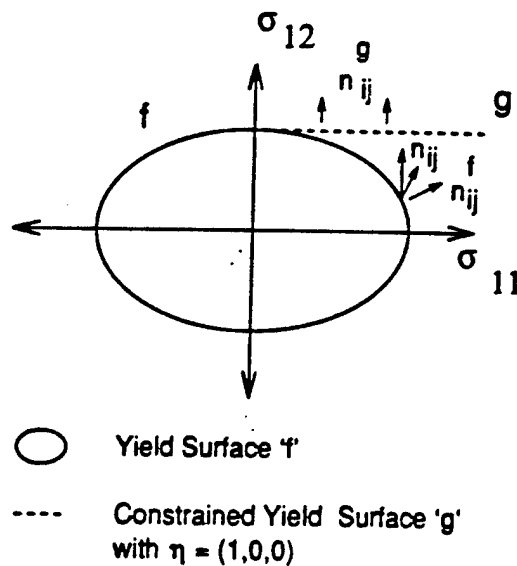
Fig. 2. Illustration of non-associative flow rule in $\sigma_{11} - \sigma_{12}$ space.

The non-associativity of the flow rule in built into the definition of the potential function through the factor ω. Based on the flow rule, one can define a second order tensor representing the direction of plastic strains as follows.

$$n_{ij} = \omega n^f_{ij} + (1.0 - \omega)n^g_{ij}. \tag{32}$$

The experimental evidence that the plastic strains are predominantly along the shear direction can be incorporated into the flow rule by using a value of ω in between 0.0 and 1.0. A value of $\omega = 1.0$ gives a purely associative flow rule. Using a value of $\omega = 0.0$ would result in the usage of only the function g in (21). For this case it can be easily shown that the plastic strains along the direction defined by η are zero. In the $\sigma_{11} - \sigma_{21}$ space in the local coordinate axes one thus obtains strains only along the shear direction.

The actual incremental plastic strain direction is observed to be different from both n^f_{ij} and n^g_{ij}. To simplify the issue, one can assume that this deviation is constant in any stress space or loading level and measure the angle of deviation as θ, then ω can be measured as follows. One can then express θ as follows

$$\cos(\theta) = n_{ij}n^f_{ij} \tag{33}$$

$$= [\omega n^f_{ij} + (1 - \omega)n^g_{ij}]n^f_{ij} \tag{34}$$

$$= \omega n^f_{ij}n^f_{ij} + (1 - \omega)n^g_{ij}n^f_{ij} \tag{35}$$

$$\cos(\theta) = \omega + (1 - \omega)n^g_{ij}n^f_{ij}. \tag{36}$$

By measuring θ at a defined loading level one can then derive the value of ω that would be appropriate.

Similarly for loading cases in the $\sigma_{22} - \sigma_{12}$ space, one can choose $\eta = (0,1,0)$ (although physically this does not represent the actual fiber direction). This enables one to control the direction of plastic strains in this space and hence one can incorporate the non-associativity of the flow rule in this stress-space. This is illustrated in Fig. 3.
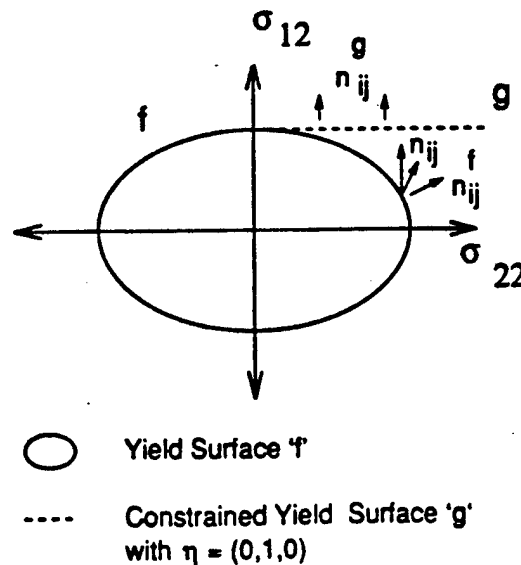

Fig. 3. Illustration of non-associative flow rule in $\sigma_{22} - \sigma_{12}$ space.

The factor ω can be adjusted to suit experimentally determined values of the plastic strain. Constraints in multiple directions can simultaneously be defined using one equation by appropriately modifying (23), details of which are not presented here. The plastic strains can then be expressed as follows,

$$\dot{\epsilon}_{ij}'' = \frac{<L>}{H} n_{ij}$$ (37)

$$= \frac{\dot{\sigma}}{H} n_{ij}$$ (38)

where $L = \dot{\sigma} = \dot{\sigma}_{ij} n_{ij}$ is the projection of the stress rate $\dot{\sigma}_{ij}$ on n_{ij} and $\dot{\sigma} > 0$ (for plastic loading after yielding). H is the plastic modulus. A detailed description of the determination of the plastic modulus for the anisotropic material is given later in this paper.

III.4. *Hardening rule*

To determine the shape and location of subsequent yield surfaces as loading/unloading progresses, the hardening parameter is introduced in the yield function. From the experimental data of Dvorak *et al.* [1988] it has been demonstrated that the predominant form of hardening is kinematic hardening. Also no significant distortion of the shape of the yield surface has been reported. Using these observations as the basis for formulating the hardening rule, it is proposed to use here a purely kinematic hardening rule of the Phillips type. It is assumed that there is no significant change in the size of the initial yield surface. Hence the effect of "proportional hardening"—which accounts for different expansion of the yield surface in different directions—is ignored. This hardening is accounted for by modifying the form of the yield surface as follows.

$$f = (\sigma_{ij} - \alpha_{ij}) M_{ijkl} (\sigma_{kl} - \alpha_{kl}) - 1.0 .$$ (39)

The evolution equation for the kinematic hardening rule based on the Phillips rule can be expressed as follows.

$$\dot{\alpha}_{ij} = \mu \dot{\sigma}_{ij}$$ (40)

The above equation can be rewritten in the following form as follows,

$$\dot{\alpha}_{ij} = \|\dot{\alpha}_{rs}\| l_{ij}$$ (41)

where

$$l_{ij} = d\sigma_{ij} / \|d\sigma_{rs}\|$$ (42)

defines the unit tensor along the direction of loading. The norm of $\dot{\alpha}_{ij}$, $\|\dot{\alpha}_{rs}\|$, is found from the consistency condition as follows.

$$\frac{\partial f}{\partial \sigma_{ij}} \dot{\sigma}_{ij} + \frac{\partial f}{\partial \alpha_{ij}} \dot{\alpha}_{ij} = 0 .$$ (43)

For finite increments of loading and rate independent plasticity the constitutive relationships can be obtained by first expressing Δf, for a constant M such that,

$$\Delta f = f(\sigma + \Delta\sigma, \alpha + \Delta\alpha) - f(\sigma, \alpha) = 0 .$$

Expanding the above equation one obtains

$$
\begin{aligned}
M_{ijkl}(\sigma_{ij} + \Delta\sigma_{ij} - \alpha_{ij} - \Delta\alpha_{ij})(\sigma_{kl} + \Delta\sigma_{kl} - \alpha_{kl} - \Delta\alpha_{kl}) \\
- M_{ijkl}(\sigma_{ij} - \alpha_{ij})(\sigma_{kl} - \alpha_{kl}) - 1 = 0 .
\end{aligned}
\tag{44}
$$

Substituting for $\Delta\alpha_{ij}$ from (41), as it is rate independent, it can be shown that $\|\Delta\alpha_{rs}\|$ can be solved from the quadratic equation

$$a\|\Delta\alpha_{rs}\|^2 - b\|\Delta\alpha_{rs}\| + c = 0 \tag{45}$$

where

$$
\begin{aligned}
b = M_{ijkl}(\sigma_{ij}l_{kl} + \sigma_{kl}l_{ij}) + M_{ijkl}(\Delta\sigma_{ij}l_{kl} + l_{ij}\Delta\sigma_{kl}) \\
+ M_{ijkl}(\alpha_{ij}l_{kl} + l_{ij}\alpha_{kl})
\end{aligned}
\tag{46}
$$

$$a = M_{ijkl}l_{ij}l_{kl} \tag{47}$$

$$
\begin{aligned}
c = M_{ijkl}(\sigma_{ij}\Delta\sigma_{kl} + \Delta\sigma_{ij}\sigma_{kl}) \\
+ M_{ijkl}(\Delta\sigma_{ij}\Delta\sigma_{kl}) - M_{ijkl}(\Delta\sigma_{ij}\alpha_{kl} + \alpha_{ij}\Delta\sigma_{kl}).
\end{aligned}
\tag{48}
$$

Once the magnitude of $\|\Delta\alpha_{rs}\|$ is found, then the evolution of backstress for the yield surface is obtained and updated as follows:

$$\alpha_{ij}^{\text{new}} = \alpha_{ij}^{\text{old}} + \Delta\alpha_{ij} . \tag{49}$$

IV. CYCLIC PLASTICITY MODEL

The proposed plasticity model is further developed to model the behavior of the composite material under cyclic loading situations. To model this behavior, a modified form of the bounding surface model is used. The determination of the plastic modulus H is the main aim of this section.

For initially isotropic materials the plastic modulus is usually expressed in functional form as

$$H = H^*[1 + g(\delta_{\text{in}}) \cdot f(\delta_{\text{in}}, \delta)] \tag{50}$$

where δ_{in} and δ are the proximity parameters and H^* is the asymptotic value of the plastic modulus. Various functional forms for $g(\delta)$ and $f(\delta_{in}, \delta)$ have been proposed by Dafalias and Popov [1976] and McDowell [1989]. Voyiadjis and Sivakumar [1991, 1994] had proposed a more general form for this expression as,

$$H = H^*[1 + g(\delta_{\text{in}}, \zeta) \cdot f(\delta_{\text{in}}, \delta)] \tag{51}$$

where the extra term ζ is a parameter introduced to blend the Phillips's deviatoric stress rate direction rule for the motion of yield surfaces, when the yield and the bounding

surfaces are away from each other and the Tseng-Lee [1983] rule for nesting of yield surfaces, when the two surfaces are closer to each other.

For isotropic materials, the functional form of the plastic modulus as defined by Dafalias and Popov [1976] is of the form

$$H = H^* + h\delta/(\delta_{in} - \delta) . \tag{52}$$

In the above equation, H^* is the asymptotic value of the plastic modulus, h is a positive shape parameter and δ_{in} is the initial value of the distance between the yield and the bounding surfaces when plastic behavior begins in the loading direction. For isotropic materials, the values of the three parameters H^*, h and δ_{in} would be the same, irrespective of the location of the current stress point on the yield surface, and for loading along any direction. This is not the case for anisotropic materials.

IV.1. Plastic modulus for initially anisotropic materials

Most of the models mentioned above have been developed for initially isotropic materials, although anisotropy is induced due to plastic strains subsequently. In such cases it is assumed that both H^* and δ_{in} remain the same along any direction (at any point on the yield surface). However for initially anisotropic or orthotropic materials the asymptotic value of the plastic modulus H^* need not, and in most cases will not, be the same for all points on the yield surface. For materials where we assume the behavior in tension and compression to be similar, it is reasonable to assume that at mirror image points of the yield surface, this asymptotic value of the plastic modulus is the same.

In Fig. 4, which shows the yield and the bounding surfaces in the $\sigma_{22} - \sigma_{12}$ stress space, points A and B are the location of the stress points for initial yielding for loading
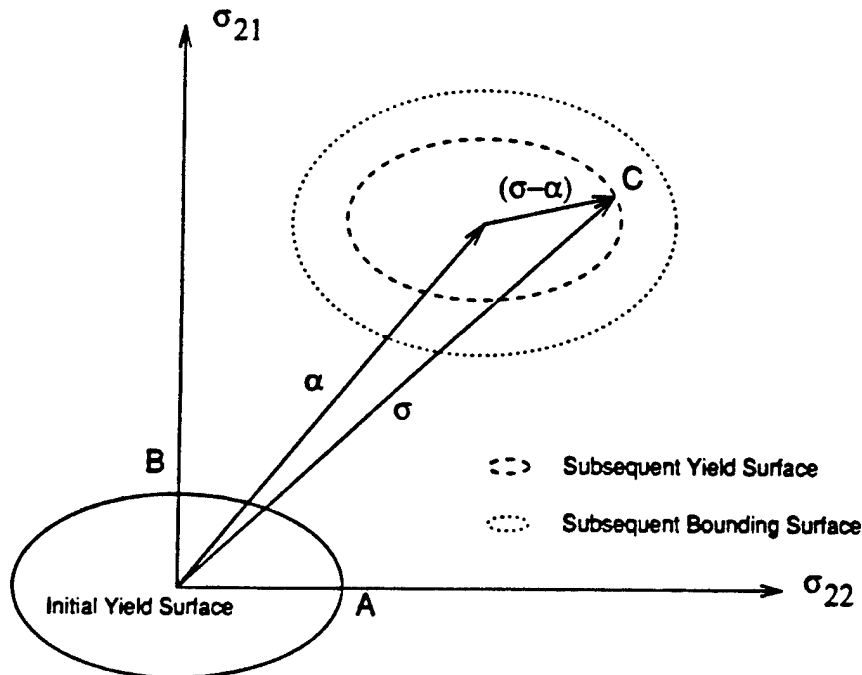

Fig. 4. Illustration to explain plastic modulus determination for an anisotropic material.

in the σ_{22} and σ_{12} respectively. From the two uniaxial stress–strain behaviors, it is observed that the plastic modulus and hence the values of the three parameters that are required to determine the plastic modulus, are different.

In order to incorporate the above phenomenon, a matrix/tensor form of H should be used to provide for a selection of the hardening parameters corresponding to the type of loading that the composite is subjected to. On the other hand the form of (51) that is adopted for the determination of the plastic modulus is scalar and has three parameters that are scalar in nature. In this paper the authors propose the following form for the determination of the parameters, while maintaining their scalar nature.

Consider the anisotropic yield surface proposed here in the $(\sigma_{22} - \sigma_{12})$ stress subspace. It can be represented as an ellipse as shown in Fig. 4. One can assume the general location of the yield surface as shown. The location of a general stress point σ when yielding has occurred—represented by point C in the figure—with respect to the center of the yield surface α, is represented by $(\sigma - \alpha)$. The distance of C from the center of the yield surface is then given by

$$\gamma = \sqrt{(\sigma_{ij} - \alpha_{ij})(\sigma_{ij} - \alpha_{ij})} \, . \tag{53}$$

A unit tensor along this direction can be written as

$$\Delta_{ij} = (\sigma_{ij} - \alpha_{ij})/\gamma \, . \tag{54}$$

As mentioned earlier the observed values of the parameters involved in the determination of the plastic modulus are different along different loading directions. This could be achieved by using the tensors in the form of second order tensors δ_{ij}^{in}, h_{ij} and H_{ij}^*. These are then converted to a scalar valued form by taking the inner product of these tensors with another second order tensor ρ_{ij} and representing the result as follows:

$$\tilde{H}^* = H_{ij}^* \rho_{ij} \tag{55}$$

$$\tilde{h} = h_{ij} \rho_{ij} \tag{56}$$

$$\tilde{\delta}^{in} = \delta_{ij}^{in} \rho_{ij} \, . \tag{57}$$

The expression for the plastic modulus can then be expressed as

$$H = \tilde{H}^* + \tilde{h}\delta/(\tilde{\delta}^{in} - \delta) \tag{58}$$

where δ is the distance between the stress point on the yield surface and the image point on the bounding surface, as explained later.

Two possible choices for ρ_{ij} are proposed here and the option of using either one would really depend on the observed physical behavior.

IV.1.1. *Choice of* $\rho_{ij} = \Delta_{ij}$. This choice of ρ_{ij} essentially states that the values of the parameters are dependent on the distance of the location of the stress point on the yield surface. This could be expressed as follows.
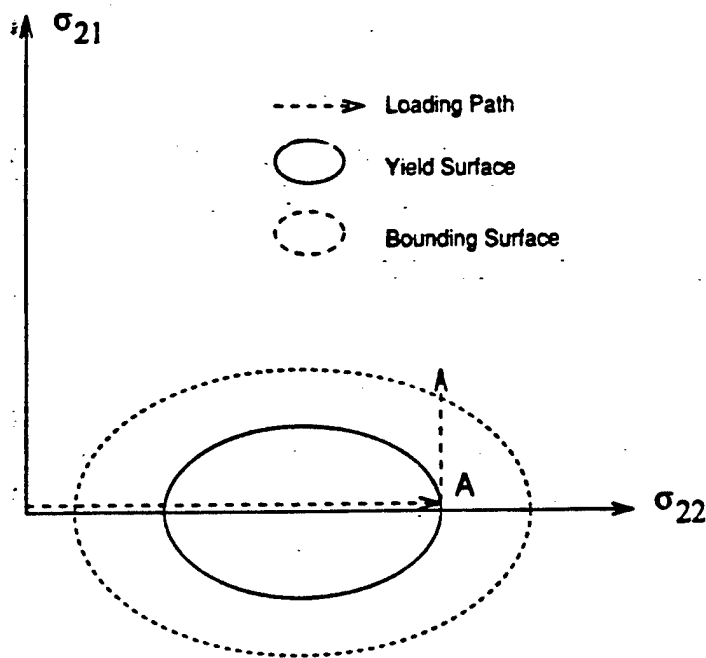
$$H = \hat{H}(\gamma) \, . \tag{59}$$

Fig. 5. Loading path to illustrate appropriateness of the choice of ρ_{ij}.

It ensures that the value of the parameters along the axial directions, assume the respective values. At intermediate points it is obtained through interpolation. Although these conditions are satisfied, sometimes this is not a very appropriate choice, especially under non-proportional loading. As shown in Fig. 5, if the composite is first loaded uniaxially along the σ_{22} direction into the plastic range, the only non-zero term of Δ_{ij} is $\Delta_{22} = 1.0$. This ensures that the three values of the parameters chosen are those corresponding to those for uniaxial loading along this direction. If the material is then loaded along the σ_{21} direction, the values of the parameters chosen would be close to the values that existed for the previous loading, since the subsequent location of the point on the yield surface is close to the previous point. However for loading along the shear direction it would be more reasonable for the parameters to assume those values corresponding to the shear direction. Hence this choice, which has been tried first in this model and found unsuitable for the above reason, might not be the best choice.

IV.1.2. *Choice of* $\rho_{ij} = l_{ij}$. Since l_{ij} is the unit tensor along the loading direction the choice of $\rho_{ij} = l_{ij}$ would essentially ensure that the values of the parameters chosen are dependent on the direction of loading. This choice is adopted here in the proposed model, since it has been found to be more suitable. Also this model is thus open for adoption of any other suitable choices.

IV.2. *Determination of bounding surface*

The initial bounding surface used here is an identical expansion of the initial yield surface. This is done by determining the y-intercept of the bound lines at the zero plastic strain level, in the stress–plastic strain curve. The bounding surface is expressed as

$$f^b(\sigma_{ij}^b, \beta_{ij}, \bar{a}_{ij}, \bar{b}_{ij}) = 0 \qquad (60)$$

where σ_{ij}^b is the image point on the bounding surface and β_{ij} is its center and

$$\bar{a}_{ij} = \begin{bmatrix} \bar{k}_1 & 0 & 0 \\ 0 & \bar{k}_2 & 0 \\ 0 & 0 & \bar{k}_3 \end{bmatrix} \qquad (61)$$

$$\bar{b}_{ij} = \begin{bmatrix} 0 & \bar{k}_4 & \bar{k}_5 \\ \bar{k}_4 & 0 & \bar{k}_6 \\ \bar{k}_5 & \bar{k}_6 & 0 \end{bmatrix} . \quad . \qquad (62)$$

The values of $\bar{k}_i(i = 1, \ldots, 6)$ are computed from experimental data along the respective axial directions. The initial yield and the initial bounding surfaces are assumed to be congruent. This is to ensure that the normals at the stress point on the yield surface and the image point on the bounding surface correspond to each other. For example, a uniaxial state of stress would correspond to the same uniaxial state of stress on the bounding surface.

The motion of the bounding surface is assumed to be dependent on the motion of yielding surface and constrained such that when the two surfaces intersect, they do so tangentially. This is ensured by finding the image point on the bounding surface from the state of stress on the yield surface, such that the normals to the two surfaces at the respective points are identical. Given the state of stress on the yield surface one can find the normal to it n_{ij}^f and using this value one can locate the image point on the bounding surface by solving a set of non-linear algebraic equations—using the Newton–Raphson technique. Since the normals to the two surfaces are the same, $n_{ij}^b = n_{ij}^f$. We can express n_{ij}^b in terms of the bounding surface parameters and image point stress values. It can be expressed in functional form as follows:

$$n_{ij}^b = \frac{\partial f^b}{\partial \sigma_{ij}^b} / \| \frac{\partial f^b}{\partial \sigma_{rs}^b} \| . \qquad (63)$$

All but one of the equations represented by n_{ij}^b which are non-linear functions of the image point of stress on the bounding surface, are used along with the bounding surface equation (which is also a non-linear function of stresses). All the equations for n_{ij}^b cannot be used because they are interrelated by the expression $n_{ij}^b n_{ij}^b = 1$.

IV.3. Backstress for the bounding surface

The evolution of the center of the bounding surface in the stress space as loading continues is related to the evolution of backstress for the yield surface as well as the relative distance between the stress point and the image point. As given in Dafalias and Popov [1976] it can be expressed as follows:

$$\dot{\beta}_{ij} = \dot{\alpha}_{ij} - \left(1 - \frac{H^*}{H}\right) \frac{\dot{\sigma}_{rs} n_{rs}}{\mu_{kl} n_{kl}} \mu_{ij} \qquad (64)$$

where

$$\mu_{ij} = (\sigma_{ij}^b - \sigma_{ij}) / \|\sigma_{rs}^b - \sigma_{rs}\| . \qquad (65)$$

Here we use a modified form as follows,

$$\dot{\beta}_{ij} = \dot{\alpha}_{ij} - \left(1 - \frac{\tilde{H}^*}{H}\right) \frac{\dot{\sigma}_{rs} n_{rs}^f}{\mu_{kl} n_{kl}^f} \mu_{ij}. \tag{66}$$

As the two surfaces touch each other $\mu_{ij} = 0$ and hence $\dot{\beta}_{ij} = \dot{\alpha}_{ij}$ for all subsequent loadings. From this increment, the total backstress for the bounding surface is then computed.

The controlling parameter δ in the determination of the plastic modulus H is then found from the formula

$$\delta = \sqrt{(\sigma_{rs}^b - \sigma_{rs})(\sigma_{rs}^b - \sigma_{rs})} . \tag{67}$$

V. ELASTO-PLASTIC STIFFNESS MATRIX

In order to determine the elasto-plastic matrix for the unidirectionally oriented MMC lamina, one has to incorporate all the procedures outlined above. Small deformations and rate independence of plastic strains are assumed. This allows one to use an additive decomposition of the incremental strain tensor $d\epsilon_{ij}$ such that,

$$d\epsilon_{ij} = d\epsilon_{ij}' + d\epsilon_{ij}'' \tag{68}$$

where $d\epsilon_{ij}'$ is the elastic part and $d\epsilon_{ij}''$ is the plastic part of the strain tensor. The incremental stress–strain relations can be expressed as follows:

$$d\sigma_{ij} = C_{ijkl} d\epsilon_{kl}' \tag{69}$$

$$= C_{ijkl}(d\epsilon_{kl} - d\epsilon_{kl}'') . \tag{70}$$

Using (38) for the plastic strain part we can write the above equation as follows:

$$d\sigma_{ij} = C_{ijkl}\left(d\epsilon_{kl} - \frac{d\sigma}{H} n_{kl}\right) . \tag{71}$$

Equation (71) may also be expressed as follows:

$$\dot{\sigma}_{ij} = C_{ijkl}\dot{\epsilon}_{kl} - C_{ijkl}n_{kl}\dot{\sigma}/H . \tag{72}$$

Taking the inner product of both sides with n_{ij} one obtains,

$$\dot{\sigma}_{ij}n_{ij} = C_{ijkl}n_{ij}\dot{\epsilon}_{kl} - C_{ijkl}n_{ij}n_{kl}\dot{\sigma}/H = \dot{\sigma} . \tag{73}$$

Or,

$$\dot{\sigma}\left(1 + \frac{C_{ijkl}n_{ij}n_{kl}}{H}\right) = C_{ijkl}n_{ij}\dot{\epsilon}_{kl} . \tag{74}$$

From the above equation one can express $\dot{\sigma}$ as follows:

$$\dot{\sigma} = \frac{C_{ijkl}n_{ij}\dot{\epsilon}_{kl}}{H + C_{ijkl}n_{ij}n_{kl}}H .$$

(75)

Hence the expression for plastic strains using (34) can be written explicitly as follows:

$$d\epsilon''_{ij} = \frac{C_{abcd}n_{ab}d\epsilon_{cd}}{H + C_{pqrs}n_{pq}n_{rs}}n_{ij} .$$

(76)

Substituting this in the equation for the incremental stress–strain relations one obtains,

$$d\sigma_{ij} = C_{ijkl}\left[d\epsilon_{kl} - \frac{C_{abcd}n_{ab}d\epsilon_{cd}}{H + C_{pqrs}n_{pq}n_{rs}}n_{kl}\right]$$

(77)

$$= C_{ijkl}d\epsilon_{kl} - \frac{C_{ijkl}C_{abcd}n_{ab}n_{kl}d\epsilon_{cd}}{H + C_{pqrs}n_{pq}n_{rs}} .$$

(78)

Interchanging the indices kl with cd in the second term of the above equation one obtains,

$$d\sigma_{ij} = C_{ijkl}d\epsilon_{kl} - \frac{C_{ijcd}C_{abkl}n_{ab}n_{cd}d\epsilon_{kl}}{H + C_{pqrs}n_{pq}n_{rs}}$$

(79)

or,

$$d\sigma_{ij} = D^{EP}_{ijkl}d\epsilon_{kl}$$

(80)

where D^{EP}_{ijkl} is the elasto-plastic stiffness of the material and is expressed as follows:

$$D^{EP}_{ijkl} = C_{ijkl} - \frac{C_{ijcd}n_{cd}C_{abkl}n_{ab}}{H + C_{pqrs}n_{pq}n_{rs}} .$$

(81)

VI. NUMERICAL SIMULATION FOR GENERATING STRESS–STRAIN CURVES

The above model has been built into a computer program MC-PLAST, for the generation of stress–strain curves. Input includes the elastic constants of the material, the initial yield and bounding surface parameters, the values of the plastic modulus constants and the non-associativity parameter ω. This program also reads in a sequence of loading in incremental form to be applied and outputs stresses, strains and plastic strains at the end of each increment.

In order to exhibit the validity of the proposed model, the model here is compared with results obtained from the experimental data of Dvorak et al. [1988] and Nigam et al. [1993]. The parameters and constants have been determined from these experimental data. The experiments had been done using boron–aluminum tubular composite specimen having unidirectional lamina. The fibers are aligned along the direction of the axis of the tube.

Under plane stress conditions, the component form of the yield surface (7) reduces to the following form:

$$\left(\frac{2}{9}\right)(k_1^2\bar{\sigma}_{11}^2 + k_2^2\bar{\sigma}_{22}^2) - \left(\frac{2}{9}\right)(k_1 k_2 \bar{\sigma}_{11}\bar{\sigma}_{22})$$
$$+ \left(\frac{2}{3}\right)(k_1 k_2 + k_4^2)\bar{\sigma}_{12}^2 - 1 = 0 \ . \tag{82}$$

From the experimental data the following values of yield stresses have been taken. $\sigma_{11}^Y = 160.0$ MPa, $\sigma_{22}^Y = 45.0$ MPa and $\sigma_{12}^Y = 25.0$ MPa. Using these data the following values of k_1, k_2 and k_4 for the initial yield surface have been computed as $k_1 = 0.0133$, $k_2 = 0.0471$, $k_4 = 0.0421$.

A number of loading situations—both actual and simulated—are presented here in order to show the validity and the stability of the model.

VI.1. *Experimental comparison and discussions*

The loading path shown in Table 1 that has been used by Nigam *et al.* [1993] has been used for comparison. From the data they had presented in the paper, the following values for the bounding surface have been evaluated. $\sigma_{11}^b = 196.0$ MPa, $\sigma_{22}^b = 91.5$ MPa and $\sigma_{21}^b = 34.0$ MPa. This results in computed values of the initial bounding surface parameters of $\bar{k}_1 = 0.0108$, $\bar{k}_2 = 0.0232$ and $\bar{k}_4 = 0.0323$. The values for k_3, k_5 and k_6 are not needed here and have been taken to be zero. However in order to make the initial yield and bounding surface congruent, a value of $k_1 = 0.0065$ is chosen and k_4 is modified to $k_4 = 0.0338$. This does not effect the outcome of results of this model because this modification affects the plastic behavior of the composite in the fiber direction. However for the MMC, since a relatively high value of the yield stress in the fiber direction is observed, it ensures relatively plastic inextensibility in the fiber direction.

Table 1. Actual experimental loading sequence (and modelled) in $\sigma_{22} - \sigma_{12}$ (Nigam *et al.* [1993])

Point	σ_{22} (MPa)	σ_{12} (MPa)
0	0.00	0.00
1	18.00	0.00
2	109.20	0.00
3	1.20	0.00
4	43.00	0.00
5	70.00	41.20
6	70.00	33.60
7	1.00	20.50
8	70.00	33.60
9	34.10	28.00
10	1.50	−19.00
11	8.00	−9.50
12	38.10	−9.40
13	66.60	36.00
14	62.00	29.75
15	35.00	29.60
16	6.50	−14.43
17	8.00	−9.50
18	38.00	−9.50

The computation of the plastic modulus constants is the next step in this process, i.e. the evaluation of and H^*_{ij} and h_{ij}. Different values of these constants are evaluated from experimental results of the uniaxial stress–plastic strain curves along different stress
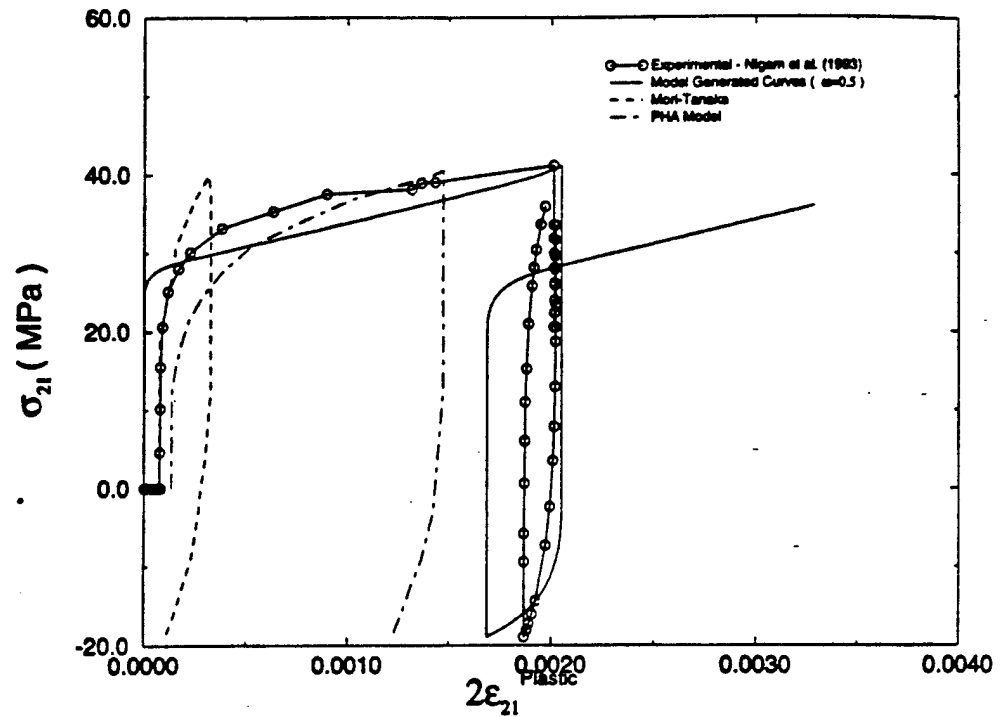

Fig. 6. Shear stress–plastic shear strain curve comparison of experimental and model generated results, using non-associative flow rule.
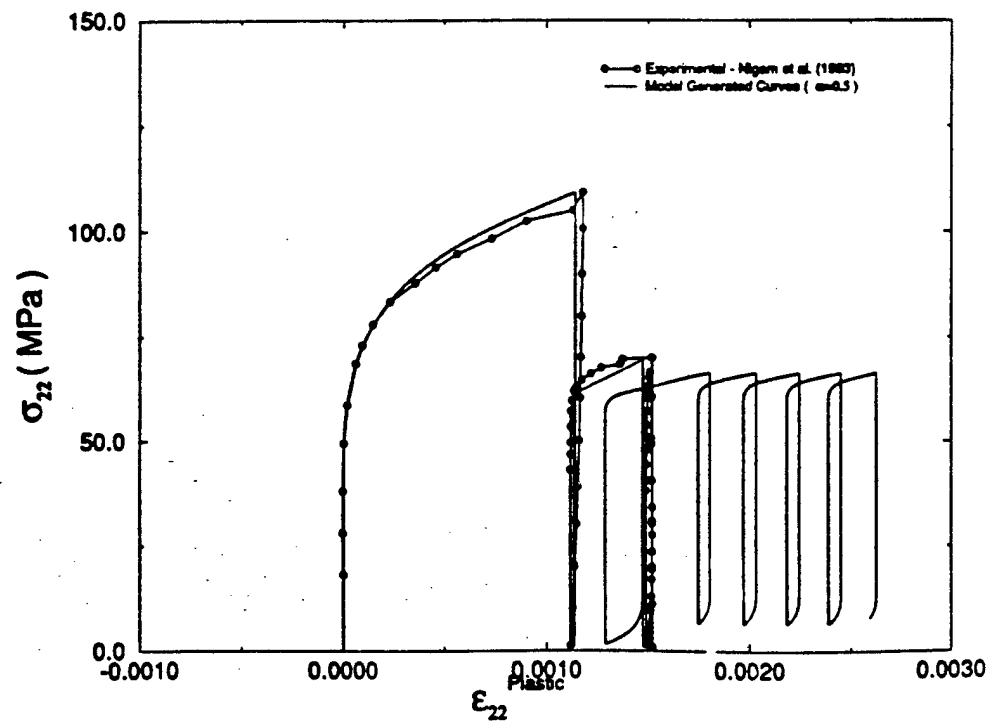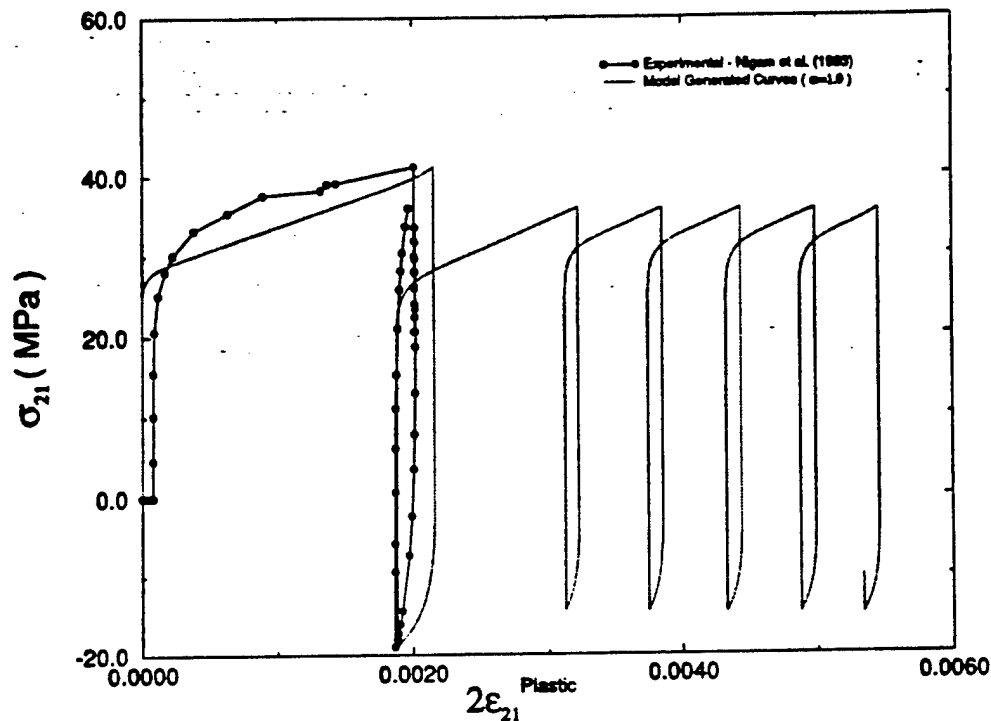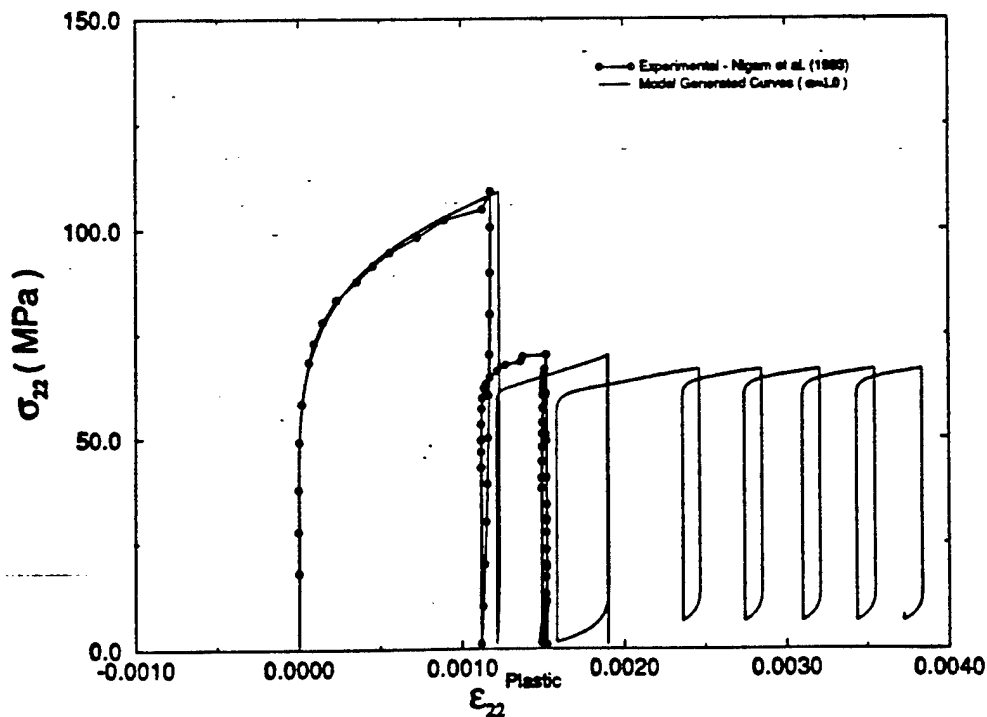

Fig. 7. Transverse stress–plastic strain curve comparison for experimental and model generated results, using non-associative flow rule.

directions. The values of these constants have been evaluated as follows. $H_{11}^* = 1,600,$ 000 MPa, $H_{22}^* = 12,000$ MPa and $H_{12}^* = 6000$ MPa and the values of the other parameter h_{ij} are $h_{11} = 9,650,000$, $h_{22} = 90,000$ and $h_{21} = 40,000$ MPa, respectively. The other values of this tensor are assumed to be zero.

Fig. 8. Shear stress–plastic shear strain curve comparison of experimental and model generated results, using associative flow rule.

Fig. 9. Transverse stress–plastic strain curve comparison for experimental and model generated results, using associative flow rule.

In order to incorporate the non-associativity of the flow rule that has been built into the model, the value of ω has been chosen, by trial and error, as $\omega = 0.5$.

Figure 7 shows the comparison between the experimentally obtained and model-generated $\sigma_{22} - \epsilon_{22}''$ curve and Fig. 6 shows the same for $\sigma_{21} - 2\epsilon_{12}''$. From the comparison of the experimental results of Dvorak *et al.* [1988] and Nigam *et al.* [1993] and the model generated stress–strain curves, a reasonably good correlation is observed. In Figs 6 and 7 the prediction of plastic strains for the case of uniaxial loading and unloading in the σ_{22} direction (loading path 1–2, 2–3) is good. For reloading along a multi-axial path 4–5, where load is applied simultaneously along the σ_{22} and σ_{21} directions, the model has been able to successfully predict the onset of yielding, which in the authors' opinion is a very significant fact, and the total magnitude of plastic strains reasonably well.

The tendency for ratchetting to occur for cyclic loading, for five cycles of loading path 12–13–14–15–16–17 has also been observed. But the tendency to stabilize has been different for the experimental and model predicted results. This is because a drastic degradation of elastic behavior has been observed in the experimental results. For the results of the experimental behavior the readers are referred to the paper by Nigam *et al.* [1993]. It has been unable to measure this degradation in elastic behavior and incorporate them in the model, where a constant elastic behavior is assumed throughout the entire loading sequence.

Another important feature that has been proposed here and used successfully is the non-associative flow rule for the prediction of plastic strains. In order to demonstrate that we must adopt a non-associative flow rule, the model is run with the same loading situation, but with $\omega = 1.0$, which results in the usage of an associated flow rule. Figures 8 and 9 show the comparison of model and experimental results for this case. For a pure associative flow rule ($\omega = 1.0$) it is seen that plastic strains ϵ_{22}'' have been overpredicted.
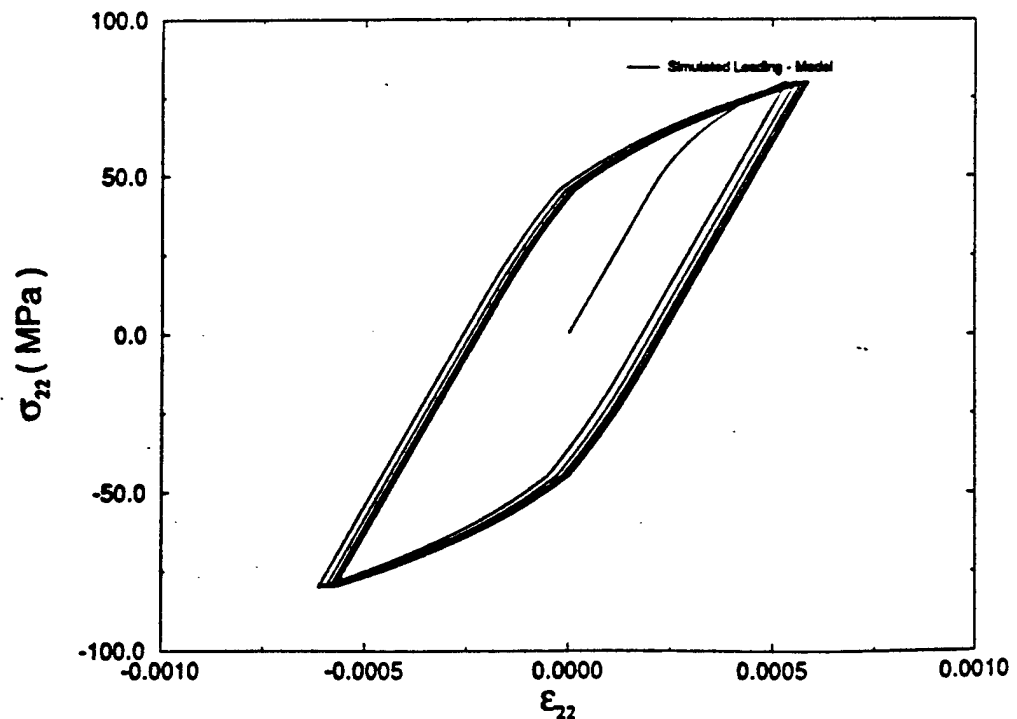

Fig. 10. Stress–plastic strain curve for simulated uniaxial cyclic loading of σ_{22} stress only.

A factor of $\omega = 0.5$ which incorporated non-associativity into the model has been successfully used to predict the plastic strains reasonably in this direction.

A number of simulated cyclic loading situations have been run on this model. They are uniaxial cyclic loading in the σ_{22} and σ_{12} directions and also radial cyclic loading in
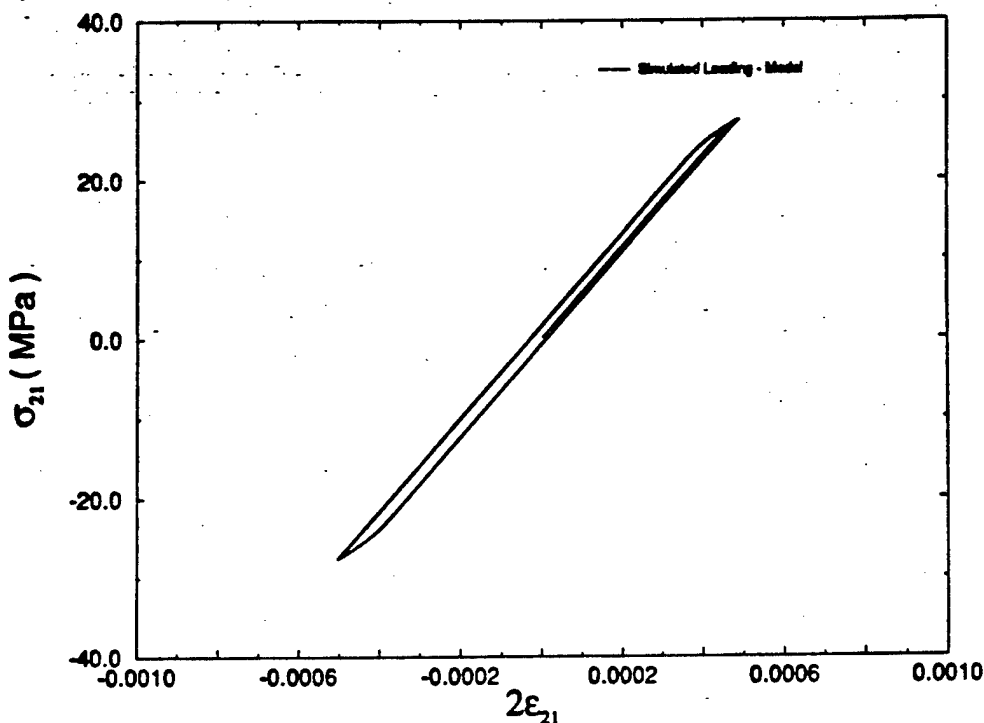
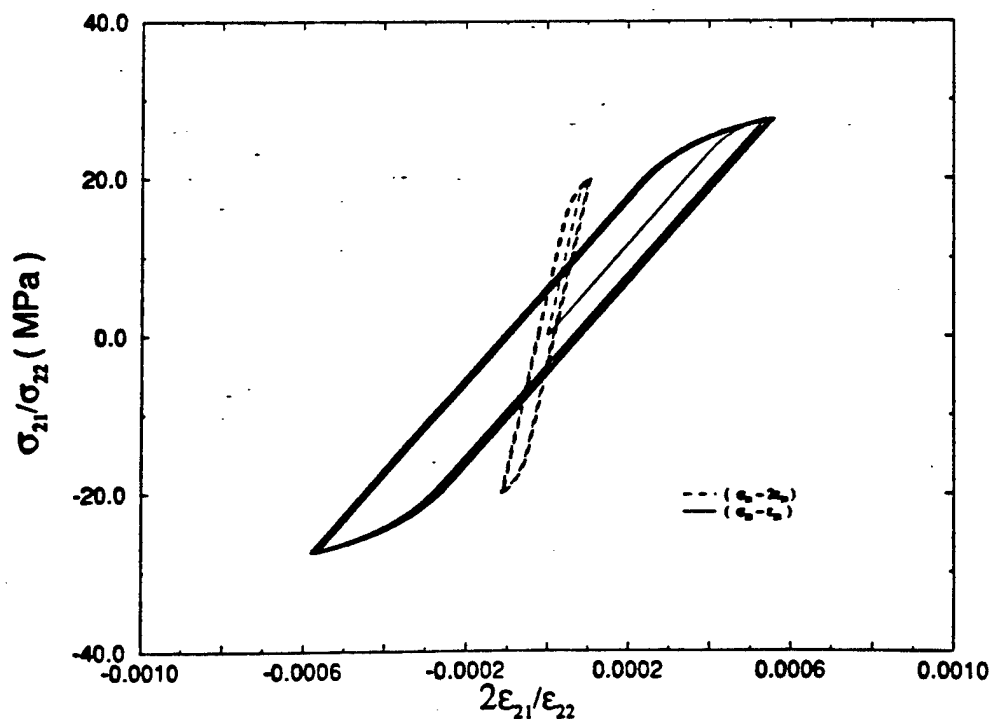Fig. 11. Stress–plastic strain curve for simulated uniaxial cyclic loading for shear stress only.

Fig. 12. Stress–plastic strain curve for simulated radial stress loading in $\sigma_{22} - \sigma_{21}$.

the $(\sigma_{22} - \sigma_{12})$ space. Figures 10 and 11 show the simulated model predicted response under uniaxial cyclic loading in the σ_{22} and σ_{21} directions, respectively. Ratchetting behavior under constant mean stress is observed. Figure 12 shows the same for radial cyclic loading in the $(\sigma_{22} - \sigma_{21})$ stress space. It is observed that the model is able to predict different behavior in different stress spaces during the loading process.

The model presented here will be used in the micromechanical damage model proposed by Voyiadjis and Kattan [1993]. The proposed model will be used to characterize the *in situ* behavior of the matrix within the fiber. This is being currently investigated by the authors.

VI.2. Comparison with other proposed models

The plastic strains predicted by the proposed model have also been compared with those predicted by two micromechanical models, namely the Periodic Hexagonal Array (PHA) model developed by Dvorak and Teply [1985] and the self-consistent scheme of Hill [1948, 1965] and Budiansky [1965] using the Mori–Tanaka [1973] averaging scheme for the evaluation of the concentration factors by Lagoudas *et al.* [1991]. The data for the self-consistent and the PHA model have been taken from the paper by Lagoudas *et al.* [1991].

This comparison has been made in Fig. 6, which shows the comparison of the shear stress–plastic shear strain curves generated by the models along with those from the experimental data. It is seen that while the Mori–Tanaka and the PHA model results underpredict the plastic strains, the proposed model using the non-associative flow rule comes closer in its prediction. In the transverse direction Fig. 7 the PHA and the proposed model predict the plastic strains fairly well whereas the Mori–Tanaka model underpredicts here also. The PHA and the Mori–Tanaka model results have not been shown here to avoid congestion.

VII. CONCLUSIONS

This proposed continuum model for the elasto-plastic behavior of an MMC has been able to successfully capture and model certain trends and characteristics that have been observed experimentally. Primarily they are, the usage of a proposed non-associative flow rule to predict plastic strains, incorporation of the fiber-direction plastic inextensibility criterion, the usage of a proposed criterion for evaluating the plastic modulus and its incorporation into the cyclic plasticity model. Comparison with experimental data has shown reasonably good correlation and certain simulated cyclic loading situations demonstrate ratchetting behavior. One feature that is observed in the experimental results, namely the degradation of elastic constants, has however not been incorporated here as it has been found to be very difficult to measure them.

REFERENCES

1948   Hill, R., "A Theory of the Yielding and Plastic Flow of Anisotropic Metals," Proc. Roy. Soc. London, A193, 281–297.

1951   Drucker, D.C., "A More Fundamental Approach to Plastic Stress–Strain Relations," Proc. First U.S. National Congress Applied Mech., ASME, New York, 487–491.

1954   Hershey, A.V., "The Plasticity of an Isotropic Aggregate of Anisotropic Face Centered Cubic Crystals," J. Appl. Mech. Trans. ASME, 21, 241.

1957   Smith, G. F. and Rivlin, R.S., "The Anisotropic Tensors," 25(3), 308–314.

1959   Drucker, D.C., "A Definition of Stable Inelastic Material," J. Appl. Mech. Trans. ASME, 26, 101.

1962   Hashin Z. and Shtrikman S., "A Variational Approach to the Theory of the Elastic Behavior of Polycrystals," J. Mech. Phys. Solids, 10, 343–352.

1965   Budiansky, B., "On the Elastic Moduli of Some Heterogeneous Materials," J. Mech. Phys. Solids, 13, 223–227.

1965   Hill, R., "Continuum micro-mechanics of elasto-plastic polycrystals," J. Mech. Phys. Solids, 13, 89–101.

1967   Mulhern, J.F., Rogers, T.G. and Spencer, A.J.M., "A Continuum Model for a Fiber Reinforced Plastic Material," Proc. Roy. Soc. London, A301, 473–492.

1969   Mulhern, J.F., Rogers, T.G. and Spencer, A.J.M., "A Continuum Theory of an Elastic–Plastic Fiber Reinforced Material," Proc. Roy. Soc. London, 7, 129–152.

1969   Walpole, L.J., "On the Overall Elastic Moduli of Composite Materials," J. Mech. Phys. Solids, 17, 235–251.

1970   Hutchinson, J.W., "Elastic–plastic Behavior of Polycrystalline Metals and Composites," Proc. Roy. Soc. London, A319, 247–272.

1971   Huang, W.C., "Plastic Behavior of Some Composite Materials," J. Composite Mater., 5, 320–338.

1971   Tsai, S.W. and Wu, E.M., J. Composite Mater., 5, 58.

1972   Spencer, A.J.M., "Deformations of Fiber-reinforced Materials," Clarendon Press, Oxford.

1973   Mori, T. and Tanaka, K., "Average Stress in the Matrix and Average Elastic Energy of Materials with Misfitting Inclusions," Acta Met., 21, 571–574.

1976   Dafalias, Y.F. and Popov, E.P., "Plastic Internal Variables Formalism of Cyclic Plasticity," J. Appl. Mech., 43, 645–651.

1979   Dvorak, G. J. and Bahei-El-Din, Y.A., "Elastic–Plastic Behavior of Fibrous Composites," J. Mech. Phys. Solids, 27, 51–72.

1983   Tseng, N.T. and Lee, G.C., "Simple Plasticity Theory of the Two-Surface Type," ASCE J. of Engg Mechanics, 109, 795–810.

1984   Eisenberg, M.A. and Yen, C.F., "The Anisotropic Deformation of Yield Surfaces," ASME J. Engng Mater. Technol., 106, 355–360.

1985   Dvorak, G.J. and Teply, J.L., Plasticity Today: Modelling, Methods, and Applications, Periodic Hexagonal Array Models for Plasticity Analysis of Composite Materials, p. 623. Elsevier, Amsterdam.

1987   Benveniste, Y., "A New Approach to the Application of Mori–Tanaka Theory in Composite Materials," Mechanics of Materials, 6, 147–157.

1987   Dvorak, G.J. and Bahei-El-Din, Y.A., "A Bimodal Plasticity Theory of Fibrous Composite Materials," Acta Mech., 69, 219–241.

1988   Dvorak, G.J., Bahei-El-Din, Y.A., Macheret, Y. and Liu C.H., "An Experimental Study of Elastic–Plastic Behavior of a Fibrous Boron-Aluminum Composite," J. Mech. Phys. Solids, 36, 655–687.

1988   Teply, J.L. and Dvorak, G.J., "Bounds on Overall Instantaneous Properties of Elastic–Plastic Composites," J. Mech. Phys. Solids, 36, 29–58.

1988   Dvorak, G.J. and Bahei-El-Din, Y.A., "Plasticity Analysis of Fibrous Composites," J. Appl. Mech., 49, 327–335.

1989   McDowell, D.L., "Evaluation of Intersection Conditions for Two Surface Plasticity Theory," International Journal of Plasticity, 5, 29–50.

1990   Voyiadjis, G.Z. and Foroozesh, M., "An Anisotropic Distortional Yield Model," ASME J. Appl. Mech., 57, 537–547.

1990   Weng, G.J. "The Overall Elastoplastic Stress-Strain Relations of Dual Phase Metals," J. Mech. Phys. of Solids, 38, 3419–441.

1990   Zhao, Y.H. and Weng, G.J., "Theory of Plasticity for a Class of Inclusion and Fiber-Reinforced Composites," Weng, G.J., Taya, M. and Abe, H. (eds), Micromechanics and Inhomogeneities: The Toshio Mura 65th Anniversary Volume. Springer, New York.

1991   Hansen, A.C., Blackketter, D.M. and Walrath, D.E., "An Invariant based Flow Rule for Orthotropic Plasticity applied to Composite Materials,": J. Appl. Mech., 58(4), 881–888.

1991   Lagoudas, D.C., Gavazzi, A.C. and Nigam, H., "Elastoplastic behavior of metal matrix composites based on incremental plasticity and the Mori-Tanaka averaging scheme," Comp. Mech., 8, 193–203.

1991   Voyiadjis, G.Z. and Sivakumar, S.M., "A Robust Kinematic Hardening for Cyclic Plasticity with Ratchetting Effects. Part I: Theoretical formulation," Acta Mech., 90, 105–123.

1992   Spencer, A.J.M., "Plasticity Theory for Fiber-reinforced Composites," J. Engng Math., 26, 107–118.

1993   Nigam, H., Dvorak, G.J. and Bahei-El-Din, Y.A., "An Experimental Investigation of Elastic–Plastic Behavior of a Fibrous Boron–Aluminum Composite. I. Matrix-Dominated Mode," Int. J. Plasticity, **10**, 23–48.

1993   Schmidt, R.J., Wang, D.Q. and Hansen, A.C., "Plasticity Model for Transversely Isotropic Materials," J. Engng Mech., **119**(4), 748–766.

1993   Voyiadjis, G.Z. and Kattan, P.I., "Local Approach to Damage in Elasto-Plastic Metal Matrix Composites," Int. J. Damage Mech. **2**(1), 92–114.

1994   Voyiadjis, G.Z. and Sivakumar, S.M., "A Robust Kinematic Hardening Rule for Cyclic Plasticity with Ratchetting Effects. Part II: Application to Nonproportional loading Cases," Acta Mech. **107**, 117–136.

1994   Voyiadjis, G.Z., Thiagarajan, G. and Petrakis, E., "Constitutive Modelling for Granular Media Using an Anisotropic Distortional Yield Model," Acta Mech., **110**, 151–171.

1995   Voyiadjis, G.Z. and Thiagarajan, G., "An Anisotropic Yield Surface Model for Directionally Reinforced Metal Matrix Composites," Int. J. Plasticity, **11**, 867–894.

AUTHORS' NAMES:

George Z. Voyiadjis[1] and Rainer Echle[2]

TITLE OF PAPER:

A Micro-Mechanical Fatigue Damage Model For Uni-Directional Metal Matrix Composites

AUTHORS' AFFILIATIONS:

[1] Boyd Professor, Department of Civil and Environmental Engineering, Louisiana State University, Baton Rouge LA 70803.

[2] Doctoral Student, Department of Civil and Environmental Engineering, Louisiana State University, Baton Rouge LA 70803.

ABSTRACT: Improvement in design and enhancement in performance of aerospace vehicles calls for the development of advanced materials capable of sustaining the arising loading conditions while maintaining their structural integrity. Special consideration has to be given to the behavior of such materials under fatigue loading conditions which are dominating the flight regime loads. A micro-mechanical fatigue damage model for uni-directional metal matrix composites is proposed. Damage evolution is considered at the constituent level through the application of the Mori-Tanaka averaging scheme. Individual damage criteria for the constituents are proposed and employed to define damage evolution equations for each of the constituents. Numerical results for high cycle fatigue loading are presented for variations in material and model parameters.

Introduction

With the increase in performance of aerospace vehicles design factors such as weight and material strength play an increased role in the design philosophies of such structures. Along with such drastic performance enhancements appropriate light weight materials need to be developed that are capable of performing under such conditions as those occurring during flight while retaining their structural integrity. Such candidate materials have been identified among the composite materials, especially in the area of metal matrix composites. Special consideration has been given to Titanium Matrix Composites (TMC) due to the fact that these materials maintain their excellent strength to density ratio even at elevated temperatures. This intrinsic material property has drawn attention from the turbine engine manufacturing industry for potential use of such materials in advanced aircraft turbine engines. The main reason for this success is attributed to the tremendous reduction in weight of the key engine components leading to a possible increase in engine performance and/or a reduced fuel consumption. Titanium matrix composites offer higher mechanical properties, better dimensional stability, and strength retention at elevated temperatures, such as those occurring in turbine engines, as compared to their monolithic counterparts. Nevertheless the use/employment of MMC's and TMC's still has major drawbacks. First, the production/manufacturing costs for such material are still high due to the special manufacturing processes involved. Second the employment of such materials in vital components of an aircraft or space vehicle, such as a turbine engine, requires a thorough understanding and control of the material behavior under extreme loading conditions such as those occurring during the regular service life of such vehicles. This calls for the development of material models which are capable of predicting real life behavior of such materials with a deterministic margin of risk. As of today the behavior of such MMC's and TMC's is not yet fully understood and appropriate material models still lack reliability and applicability as compared to those of their monolithic counterparts. Considerable experimental as well as theoretical research effort is put forward to better understand and analytically model metal matrix composites in order to provide a more efficient use of the tremendous potential contained in these new materials. In particular, the literature lacks a consistent and systematic approach to the analysis of cyclic damage (low-cycle / high-cycle fatigue) in high temperature metal matrix composites. It is this area which is addressed in this paper, especially the consistent development of a fatigue damage model for

uni-directional Metal Matrix Composites.

Cyclic/Fatigue Damage Models in the Literature

Reviewing the literature on the subject of fatigue in engineering materials reveals that the explanation of fatigue phenomena and the prediction of fatigue life have been the focus of immense research efforts for the last 50 years. The two major analytical approaches used are the phenomenological approach and the crack propagation approach. The former is concerned with lifetime prediction for complex loading histories using existing lifetime test data, mostly $S - N$ data for constant amplitude cyclic loading. The second approach is concerned with predicting the growth of a dominant crack due to cyclic load which is not the case for metal matrix composites.

Almost all of the known fatigue damage models for composite materials are based on the models developed for their isotropic counterparts (Owen and Howe 1972, Subramanyan 1976, Srivatsavan and Subramanyan 1978, Lemaitre and Plumtree 1979, Fong 1982, Hashin 1985, Hwang and Han 1986a,b, Whitworth 1990). Lack of theoretical knowledge and sufficient experimental tests on composite materials led to the application of known fatigue damage models to predict fatigue lifetime of such materials, despite the fact that the fatigue behavior of composite materials is quite different from that of isotropic materials, such as metals. With improvement in theoretical knowledge on composite materials and experimental equipment, a lot of studies have been conducted involving fatigue life and residual strength degradation, modulus degradation and residual life theories. However, it was soon recognized from the obtained models that the material structure of such composites has to be included in the development of fatigue damage models in order to arrive at more feasible and reliable models. Up to date there is no universal fatigue damage model based on the micro-structure of the composite material capable of predicting fatigue life time for general fatigue loading with reasonable reliability.

Arnold and Kruch (1991a,b) presented a phenomenological, isothermal transversely-isotropic differential continuum damage mechanics (CDM) model for fatigue of unidirectional composites. This model is based on the CDM fatigue models for isotropic materials developed at ONERA (Chaboche and Lesne 1988, Chaboche 1988a,b, 1987, Lesne and Savalle 1987, Lesne and Cailletaud 1987). They considered the metal matrix composite as a pseudo homogeneous material with locally definable characteristics. Such local characteristics have been considered in the form of a directional

tensor representing the fiber direction. Furthermore the concept of anisotropic failure surfaces has been introduced into the model based on deformation theories for high temperature metal matrix composites of Robinson et al. (1987) and Robinson and Duffy (1990). Despite the rigorous development the proposed model has two major drawbacks: (1) the expensive experimental setup and exhaustive experiments needed to obtain the material parameters used in the model equations, and (2) the employed scalar measure for the damage variable. Recently Wilt and Arnold (1994) presented a fatigue damage algorithm which employs the fatigue damage model developed by Arnold and Kruch (1991a,b). They implemented their algorithm into the commercial finite element code MARC and used it to analyze a cladded MMC ring. Results were presented on a qualitative basis since no experimental results are available.

Nicholas (1995) recently reviewed fatigue life time prediction models for TMC's which use fundamentally different approaches. His investigation showed that various models are based on a single parameter and have limited applicability. Two other models, a dominant damage model (Neu 1993) and a life fraction model, show applicability to various loading ranges, frequencies and temperature profiles. Neu (1993) pointed out that despite the fact that there exist several damage mechanisms it is possible to consider the most dominant ones for modeling and include the influence of others in those since their behavior might be similar. His model was able to match experimental data for isothermal and thermo-mechanical fatigue for low-cycle fatigue experiments. The life fraction models, which are based on the fact that fatigue damage accumulates simultaneously due to independent mechanisms, are able to model only specific composite layups for which their parameters have been calibrated. Various other fatigue investigations have been performed but their focus is on specific ply-stacking sequences of interest at the time of the investigations. In general it is found that even though micro-mechanical effects or mechanisms are considered and incorporated into the models there does not yet exist a true micro-mechanical fatigue damage model which considers the material behavior and damage evolution in the constituents individually. The following proposed micro-mechanical fatigue damage model is intended to exactly fill in this gap. It is considered as a first step along a consistent route to develop a universal micro-mechanical fatigue damage model capable of modeling various loading conditions including thermo-mechanical effects as well as environmental

effects which occur during the service life of dynamically loaded composite structures.

Damage Mechanics Applied to Composite Materials

Kachanov (1958) pioneered the idea of damage in the framework of continuum mechanics. For the case of isotropic damage and using the concept of effective stress, the damage variable is defined as a scalar in the following manner

$$\varphi = \frac{A - \bar{A}}{A} \tag{1}$$

where $\bar{A}$ is the effective (net) resisting area corresponding to the damaged area A. Using the hypothesis of elastic energy equivalence (Sidoroff 1980), the effective stress $\bar{\sigma}$ can be obtained from the above equation by equating the force acting on the hypothetical undamaged area with the force acting on the actual damaged area.

In a general state of deformation and damage, the scalar damage variable φ is replaced by a fourth-order damage effect tensor M which depends on a second-order damage tensor ϕ. In general, the effective stress tensor $\bar{\sigma}$ is obtained using the following relation

$$\bar{\sigma} = M : \sigma \tag{2}$$

where (:) indicates tensor contraction over two indices. The nature of the damage effect tensor M is discussed in the literature by Voyiadjis and Kattan (1992, 1993a).

In general the analysis of composite materials falls into two categories. The first category consists of all approaches that employ the continuum concept (Talreja 1987, Christensen 1990), where the composite system is treated as one continuum and the equations of anisotropic elasticity are used in the analysis. The second category encompasses all approaches that use micro-mechanical models together with averaging procedures and homogenization techniques (Poursatip et al. 1982, Dvorak and Bahei-El-Din 1982, 1987, Dvorak and Laws 1987, Dvorak et al. 1985) to describe the material behavior. In these models, the composite is considered to be composed of a number of individual phases for which local equations are formulated. Employing a suitable homogenization procedure then allows one to analyze the material behavior of the entire composite system based on the local analysis.

Dvorak and Bahei-El-Din (1982, 1987) employed an averaging technique to analyze the elasto-plastic behavior of fiber-reinforced composites. They considered elastic fibers with an elasto-plastic matrix. However, no attempt was made to introduce damage in the constitutive equations. Voyiadjis and Kattan (1993b), Voyiadjis et al. (1993), Voyiadjis and Kattan (1993c) introduced a consistent and systematic damage theory for metal matrix composites utilizing the micro-mechanical composite model of Dvorak and Bahei-El-Din (1987). They introduced two approaches, referred to in the literature as the overall and the local approach, which allow for a consistent incorporation of the damage phenomenon in a composite material system.

The overall approach (Kattan and Voyiadjis 1993) to damage in composite materials employs one single damage tensor to reflect all types of damage mechanisms that the composite undergoes like initiation, growth and coalescence of micro-voids and micro-cracks. Voyiadjis and Park (1995) improved the overall approach by including and adopting a general damage criteria for orthotropic materials by extending the formulation of Stumvoll and Swoboda (1993) to MMC's. In this improved model all damage types are considered but the model lacks the consideration of local (constituent) as well as interfacial damage effects. In contrary to the overall approach the local approach (Voyiadjis and Kattan 1993d) introduces two independent damage tensors, ϕ^m and ϕ^f, and hence two independent damage effect tensors, M^m and M^f, to reflect appropriate damage mechanisms in the matrix and fibers, respectively. It is this latter approach which is employed in the proposed micro-mechanical fatigue damage model.

Micro-Mechanical Fatigue Damage Model

Stress and Strain Concentration Tensors – In the derivation of the model, the concept of effective stress (Rabotnov 1968, Sidoroff 1980) is used. The effective stress is defined as the stress in a hypothetical state of deformation that is free of damage and is mechanically equivalent to the current state of deformation and damage. In a general state of deformation and damage, the effective Cauchy stress tensor $\bar{\sigma}$ is related to the current Cauchy stress tensor by the linear relation given as in equation (2). In the case of composite materials, similar constituent (local) stress relations hold

for the matrix and fiber stress tensors σ^m and σ^f, respectively.

$$\bar{\sigma}^m = M^m : \sigma^m \tag{3a}$$

$$\bar{\sigma}^f = M^f : \sigma^f \tag{3b}$$

where M^m and M^f are fourth-order local damage effect tensors for the matrix and fiber materials, respectively. The damage effect tensors M^m and M^f are dependent on second order damage variables ϕ^m and ϕ^f, respectively. These latter second order tensors quantify the crack density in the matrix and fibers, respectively (Voyiadjis and Venson 1995). The crack density tensors incorporate both, cracks in the fiber, matrix, as well as those due to fiber debonding. A complete discussion on these tensors is given in the work of Voyiadjis and Venson (1995).

In the proposed model the matrix is assumed to be elasto-plastic and the fibers are assumed to be elastic, continuous and aligned. Consequently, the undamaged (effective) incremental local (constituent) constitutive relations are given by:

$$d\bar{\sigma}^m = \bar{D}^m : d\bar{\varepsilon}^m \tag{4a}$$

$$d\bar{\sigma}^f = \bar{E}^f : d\bar{\varepsilon}^f \tag{4b}$$

The fourth-rank tensors $\bar{D}^m$ and $\bar{E}^f$ are the undamaged (effective) matrix elasto-plastic stiffness tensor and fiber elastic stiffness tensor, respectively. The incremental composite constitutive relation in the damaged state is expressed as follows

$$d\sigma = D : d\varepsilon \tag{5}$$

where $d\varepsilon$ is the incremental composite strain tensor.

In order to arrive at the local (constituent) relations, given by equations (4), a homogenization technique in the form of the Mori-Tanaka averaging scheme (Chen et al. 1992) is employed. Through the use of the so-called stress and strain concentration tensors, a relationship between the global applied effective composite stress, $\bar{\sigma}$, and the local effective stress in the constituents, $\bar{\sigma}^{(m,f)}$, is

obtained as follows

$$\bar{\sigma}^m = \bar{B}^m : \bar{\sigma} \tag{6a}$$

$$\bar{\sigma}^f = \bar{B}^f : \bar{\sigma} \tag{6b}$$

where $\bar{B}^f$ and $\bar{B}^m$ represent the effective stress concentration tensors connecting the local effective stresses with the global effective stresses. In the damaged configuration the following relations are obtained

$$\sigma^m = B^m : \sigma \tag{7a}$$

$$\sigma^f = B^f : \sigma \tag{7b}$$

Combining equations (2), (3), (6) and (7) one obtains the relation between the local stress concentration tensor and the local effective stress concentration tensor as follows

$$B^f = M^{-f} : \bar{B}^f : M \tag{8a}$$

$$B^m = M^{-m} : \bar{B}^m : M \tag{8b}$$

Similar relations may be obtained for the deformations in the effective (undamaged) configuration as follows

$$\bar{\varepsilon}^m = \bar{A}^m : \bar{\varepsilon} \tag{9a}$$

$$\bar{\varepsilon}^f = \bar{A}^f : \bar{\varepsilon} \tag{9b}$$

where $\bar{A}^f$ and $\bar{A}^m$ represent the effective strain concentration tensors connecting the local effective strains with the global effective strains. In the damaged configuration the relations are given by

$$\varepsilon^m = A^m : \varepsilon \tag{10a}$$

$$\varepsilon^f = A^f : \varepsilon \tag{10b}$$

and furthermore

$$A^f = M^f : \bar{A}^f : M^{-1} \tag{11a}$$

$$A^m = M^m : \bar{A}^m : M^{-1} \tag{11b}$$

Effective Volume Fractions – During the process of damage evolution in the material another phenomenon has to be considered. As damage progresses within each constituent the effective load resisting area/volume changes while the gross area/volume remains the same. Since the distribution of forces/stresses to the constituents depends directly on the area/volume intact to resist an applied force/stress there is a change in the allocation of the external applied force/stress to the constituents. This redistribution of force/stress due to progressing damage can be accounted for by defining the so-called effective volume fractions which are based on the updated damage variable during each load/stress increment. Expressions for the effective volume fractions are given as

$$\bar{c}^m = \frac{1 - \phi_{eq}^m}{(1 - \phi_{eq}^m) + (1 - \phi_{eq}^f)\frac{c_0^f}{c_0^m}} \tag{12}$$

and

$$\bar{c}^f = \frac{1 - \phi_{eq}^f}{(1 - \phi_{eq}^f) + (1 - \phi_{eq}^m)\frac{c_0^m}{c_0^f}} \tag{13}$$

where c_0^f and c_0^m are defined as the volume fractions for the fiber and matrix in the virgin material, respectively. The expressions for ϕ_{eq}^m and ϕ_{eq}^f are given as

$$\phi_{eq}^f = \frac{||\phi^f||_2}{||\phi_{crit}^f||_{L2}} \tag{14a}$$

$$\phi_{eq}^m = \frac{||\phi^m||_2}{||\phi_{crit}^m||_{L2}} \tag{14b}$$

with ϕ_{crit}^f and ϕ_{crit}^m defined as the critical damage tensors for the fibers and the matrix, respectively, and $|| \cdot ||_{L2}$ defined as the $L_2 - norm$ of the quantity enclosed in the vertical bars.

Proposed Micro-Mechanical Fatigue Damage Model – The proposed fatigue damage criterion g

is considered as a function of the applied stress σ, the damage parameter ϕ, the damage hardening parameter κ, and a tensor quantity γ, which is explained below. The equation for g is defined by:

$$g = \mathcal{F}^n - 1 \tag{15}$$

where $\mathcal{F}$ is defined as

$$\mathcal{F} = w_{ij}^{-1} w_{jk}^{-1} (Y_{kl} - \gamma_{kl})(Y_{li} - \gamma_{li}) \tag{16}$$

The term $(Y_{kl} - \gamma_{kl})$ represents the translation of the damage surface and therefore accounts for damage evolution during cyclic loading. The tensor Y represents the thermo-dynamical force conjugate to the damage variable ϕ and is defined as

$$Y_{ij} = \frac{1}{2} \left(\sigma_{cd} C_{abpq} M_{pqkl} \sigma_{kl} + \sigma_{pq} M_{uvpq} C_{uvab} \sigma_{cd} \right) \frac{\partial M_{abcd}}{\partial \phi_{ij}} \tag{17}$$

with $C_{ijkl} = E_{ijkl}^{-1}$, while the quantity γ can in principle be compared to the backstress in plasticity theory hence representing in this case the center of the damage surface in the thermo-dynamical conjugate force space Y. Its evolution equation is given as follows

$$\dot{\gamma}_{ij} = c\, \dot{\phi}_{ij} \tag{18}$$

similarly to the evolution equation for the backstress in plasticity. The tensor quantity w_{ij} accounts for the anisotropic expansion of the damage surface and is given as follows

$$w_{ij} = u_{ij} + V_{ij} \tag{19}$$

where the tensor u is defined as

$$u_{ij} = \lambda_{(i)}\, \eta_{(i)} \left(\frac{\kappa}{\lambda_{(i)}} \right)^{\xi_{(i)}} \delta_{ij} \qquad \text{(no sum on } i\text{)} \tag{20}$$

The tensor V_{ij} can be interpreted physically as the damage threshold tensor for the constituent

material considered, while κ represents the effect of damage hardening and is defined as follows

$$\kappa = \int_{\phi_1}^{\phi_2} Y : d\phi = \int_0^t Y : \dot{\phi}\, dt \tag{21}$$

Damage hardening is based on the increase in the initial damage threshold due to micro-hardening occurring at a very local material level (Chow and Lu 1989). The parameter γ_{ij} in equation (16) adds to this hardening behavior due to the movement of the damage surface in the direction of the evolution f damage. The remaining variables n, λ_i, η_i, ξ_i and c are material parameters to be determined for each individual constituent. Especially the form of the variable ξ_i will be discussed below in the numerical implementation.

Based on the thermo-dynamical principles a potential function for each constituent is defined as (Voyiadjis and Kattan 1993d)

$$\Omega = \Pi^p + \Pi^d - \dot{\Lambda}_1\, f - \dot{\Lambda}_2\, g \tag{22}$$

where Π^p, Π^d, f and g represent the dissipation energy due to plasticity, the dissipation energy due to damage, the plasticity yield surface for the constituent material considered, and the damage surface, respectively. For loading in the elastic regime (high cycle fatigue) the terms involving plastic dissipation energy are neglected. The term Π^d representing the dissipation energy due to damage is given as

$$\Pi^d = Y_{ij}\, \dot{\phi}_{ij} + \mathcal{K}\, \dot{\kappa} \tag{23}$$

Applying the theory of calculus of several variables to solve for the coefficients $\dot{\Lambda}_1$ and $\dot{\Lambda}_2$ yields

$$\frac{\partial \Omega}{\partial Y_{ij}} = 0 \tag{24}$$

from which an expression for the damage increment is obtained as follows

$$d\phi_{ij} = d\Lambda_2\, \frac{\partial g}{\partial Y_{ij}} \tag{25}$$

Hence $d\Lambda_2$ may be determined using the consistency condition

$$dg = \frac{\partial g}{\partial \sigma} : d\sigma + \frac{\partial g}{\partial \phi} : d\phi + \frac{\partial g}{\partial \kappa}d\kappa + \frac{\partial g}{\partial \gamma} : d\gamma = 0 \qquad (26)$$

Substitution of the appropriate terms (equations (18) and (21)) into equation (26) yields

$$dg = \frac{\partial g}{\partial \sigma} : d\sigma + \frac{\partial g}{\partial \phi} : d\phi + \frac{\partial g}{\partial \kappa}Y : d\phi - c\frac{\partial g}{\partial Y} : d\phi = 0 \qquad (27)$$

Replacing $d\phi$ with equation (25) an expression for $d\Lambda_2$ is obtained as follows

$$d\Lambda_2 = -\frac{\frac{\partial g}{\partial \sigma_{kl}}d\sigma_{kl}}{\left(\frac{\partial g}{\partial \phi_{ij}} + Y_{ij}\frac{\partial g}{\partial \kappa} - c\frac{\partial g}{\partial Y_{ij}}\right)\frac{\partial g}{\partial Y_{ij}}} \qquad (28)$$

Backsubstitution of equation (28) into equation (25) yields an expression for the damage increment for the appropriate constituent in terms of a given stress increment as

$$d\phi_{mn} = -\frac{\frac{\partial g}{\partial \sigma_{kl}}\frac{\partial g}{\partial Y_{mn}}d\sigma_{kl}}{\left(\frac{\partial g}{\partial \phi_{ij}} + Y_{ij}\frac{\partial g}{\partial \kappa} - c\frac{\partial g}{\partial Y_{ij}}\right)\frac{\partial g}{\partial Y_{ij}}} \qquad (29)$$

or

$$d\phi_{ij} = \Psi_{ijkl}\,d\sigma_{kl} \qquad (30)$$

where

$$\Psi_{ijkl} = -\frac{\frac{\partial g}{\partial Y_{ij}}\frac{\partial g}{\partial \sigma_{kl}}}{\left(\frac{\partial g}{\partial \phi_{rs}} + Y_{rs}\frac{\partial g}{\partial \kappa} - c\frac{\partial g}{\partial Y_{rs}}\right)\frac{\partial g}{\partial Y_{rs}}} \qquad (31)$$

and

$$Y_{rs} = \frac{1}{2}\left[\sigma_{cd}\,\bar{E}^{-1}_{abpq}\,M_{pqkl}\,\sigma_{kl} + \sigma_{pq}\,M_{uvpq}\,\bar{E}^{-1}_{uvab}\,\sigma_{cd}\right]\frac{\partial M_{abcd}}{\partial \phi_{rs}} \qquad (32)$$

$$\qquad (33)$$

As stated elsewhere (Stumvoll and Swoboda 1993) a damaging state in a constituent is given if for

any state the damage criterion is satisfied

$$g = 0 \tag{34}$$

for that specific constituent. In general four different loading states are possible

$$g < 0 \qquad \qquad \text{(non-damaging loading)} \tag{35}$$

$$g = 0 \qquad \frac{\partial g}{\partial Y_{ij}} dY_{ij} < 0 \qquad \text{(elastic unloading)} \tag{36}$$

$$g = 0 \qquad \frac{\partial g}{\partial Y_{ij}} dY_{ij} = 0 \qquad \text{(neutral unloading)} \tag{37}$$

$$g = 0 \qquad \frac{\partial g}{\partial Y_{ij}} dY_{ij} > 0 \qquad \text{(loading from damaging state)} \tag{38}$$

Using equation (29) the damage increment per fatigue cycle maybe obtained by integration over one stress cycle as

$$\frac{d\phi_{ij}}{dN} = \int_{\sigma_{min}}^{\sigma_{max}} \Psi_{ijkl} \, d\sigma_{kl} + \int_{\sigma_{max}}^{\sigma_{min}} \Psi_{ijkl} \, d\sigma_{kl} \tag{39}$$

where ψ_{ijkl} is given according to equation (31). The dependence of damage on the mean stress and the amplitude of the stress cycle is implicitly included through the integration of equation (39).

Return to the Damage Surface

In the numerical implementation of the model it appears that after calculating the damage increment $d\phi$ for the current stress increment $d\sigma$ and updating all the appropriate parameters depending on the damage variable ϕ, the damage surface is in general not satisfied. Therefore it is necessary to return the new image point to the damage surface by employing an appropriate return criteria.

At the beginning of the $(n+1)^{st}$ increment we assume that the damage surface g is satisfied

$$g^{(n)} \left(\sigma^{(n)}, \phi^{(n)}, \kappa^{(n)} \gamma^{(n)} \right) = 0 \tag{40}$$

Applying the stress increment $d\sigma$ (assuming a damage loading) will result in a damage increment $d\phi$ which will be used to update the values for κ and γ. Checking the damage surface (equation 15)

with the updated values for σ, ϕ, κ and γ will in general yield

$$g^{(n+1)}\left(\sigma^{(n+1)}, \phi^{(n+1)}, \kappa^{(n+1)}, \gamma^{(n+1)}\right) > 0 \tag{41}$$

where

$$\sigma^{(n+1)} = \sigma^{(n)} + d\sigma^{(n+1)} \tag{42}$$

$$\phi^{(n+1)} = \phi^{(n)} + d\phi^{(n+1)} \tag{43}$$

$$\kappa^{(n+1)} = \kappa^{(n)} + d\kappa^{(n+1)} \tag{44}$$

$$\gamma^{(n+1)} = \gamma^{(n)} + d\gamma^{(n+1)} \tag{45}$$

Using a *Taylor series* expansion of order one expands the left hand side of equation (41) to yield

$$
\begin{aligned}
g^{(n+1)} & \left(\sigma^{(n)} + d\sigma^{(n+1)}, \phi^{(n)} + d\phi^{(n+1)}, \kappa^{(n)} + d\kappa^{(n+1)}, \gamma^{(n)} + d\gamma^{(n+1)}\right) \\
& = g^{(n)}\left(\sigma^{(n)}, \phi^{(n)}, \kappa^{(n)}\gamma^{(n)}\right) + \left.\frac{\partial g}{\partial \sigma}\right|^{(n)} d\sigma^{(n+1)} + \left.\frac{\partial g}{\partial \phi}\right|^{(n)} d\phi^{(n+1)} \\
& + \left.\frac{\partial g}{\partial \kappa}\right|^{(n)} d\kappa^{(n+1)} + \left.\frac{\partial g}{\partial \gamma}\right|^{(n)} d\gamma^{(n+1)} > 0
\end{aligned}
\tag{46}
$$

Recalling the relationships in equation (18) and (21) relation (46) is given by

$$g^{(n+1)}\left(\sigma^{(n)} + d\sigma^{(n+1)}, \phi^{(n)} + d\phi^{(n+1)}, \kappa^{(n)} + Y^{(n)} : d\phi^{(n+1)}, \gamma^{(n)} + c\, d\phi^{(n+1)}\right) > 0 \tag{47}$$

The return to the damage surface, hence $g^{(n+1)} = 0$, is now achieved by adjusting the damage increment $d\phi$ using a linear coefficient α such that

$$g^{(n+1)}\left(\sigma^{(n)} + d\sigma^{(n+1)}, \phi^{(n)} + \alpha\, d\phi^{(n+1)}, \kappa^{(n)} + \alpha Y^{(n)} : d\phi^{(n+1)}, \gamma^{(n)} + \alpha\, c\, d\phi^{(n+1)}\right) = 0 \tag{48}$$

Substitution of the appropriate expressions for the derivatives in equation (48) as well as equation (21) and (18) and setting the left hand side equal to zero allows one to solve for the unknown

coefficient α such that

$$\alpha = -\frac{\left(g^{(n)} + \frac{\partial g}{\partial \sigma}\Big|^{(n)} d\sigma^{(n+1)}\right)}{\left(\frac{\partial g}{\partial \phi}\Big|^{(n)} + \frac{\partial g}{\partial \kappa}\Big|^{(n)} Y^{(n)} + \varsigma \frac{\partial g}{\partial \gamma}\Big|^{(n)}\right) d\phi^{(n+1)}} \tag{49}$$

Numerical Analysis

The above model is implemented into a numerical algorithm and used to investigate the fatigue damage evolution in the individual constituents of a uni-directionally fiber reinforced metal matrix composite. No assumption, except those implicitly included in the stress and strain concentration tensors based on the Mori-Tanaka averaging scheme (Chen et al. 1992) are made. The implementation is performed using a full 3-D modeling hence avoiding any assumptions to be made upon simplification of fourth order tensors to two-dimensional matrix representation. The Mori-Tanaka averaging scheme is implemented using the numerical algorithm according to Lagoudas et al. (1991). Only an elastic analysis is performed at this time. Since no experimental data is yet available a parametric study is conducted in order to demonstrate the influence of various parameters on the damage evolution in the constituents. The constituents are assumed to consist of an isotropic material. The material used in the analysis are given in Johnson et al. (1990) and are shown in Table 1. The fatigue loading is applied in the form of a sinusoidal uni-axial loading given as

$$\sigma_{ij} = \sigma_{ij,mean} + \sigma_{ij,A} \sin\left(\frac{\theta}{2\pi}\right) \tag{50}$$

where

$$\sigma_{11,mean} = 550\, MPa \qquad \text{and } \sigma_{ij,mean} = 0 \qquad \text{(for } i, j \neq 1)$$

$$\sigma_{11,A} = 450\, MPa \qquad \text{and } \sigma_{ij,A} = 0 \qquad \text{(for } i, j \neq 1)$$

For the numerical integration scheme an adaptive algorithm was implemented such that the stress

increments where taken as

$$\Delta\sigma_{ij} = \frac{\sigma_{ij,mean}}{25} \qquad \text{if } \sigma_{ij} < \sigma_{mean,ij} \quad \text{(non-damage state)}$$

$$\Delta\sigma_{ij} = 1\,MPa \qquad \text{if } \sigma_{ij} < \sigma_{mean,ij} \quad \text{(damage state)}$$

during the loading phase to the mean stress and

$$\Delta\sigma_{ij} = \left[\sin\left(\frac{\theta+\Delta\theta}{2\pi}\right) - \sin\left(\frac{\theta}{2\pi}\right)\right] * \sigma_{ij,A} \qquad \text{(during cyclic loading)}$$

with

$$\Delta\theta = \frac{\pi}{50} \qquad\qquad \text{(during a non-damaging state)}$$

$$\Delta\theta = \frac{\pi}{900} \qquad\qquad \text{(during a damaging state)}$$

for the cyclic loading phase. Here θ represents simply the phase angle during the cyclic loading. The above limit values were adopted based on a numerical investigation which yielded satisfactory behavior of the model using the above values.

The damage criterion is evaluated within each increment and a return criterion as described in equations (48) and (49) is applied if $|g^{(n+1)}| \geqq 10^{-3}$. Except at the very first incident of damage this criterion shows satisfactory performance during the application of the return criterion (equations (41) - (49)). The numerical noise at the initiation of damage has been investigated and it is found that a reduction in the step size for the stress increment reduces the numerical error appropriately to fall within the specified bounds. This phenomenon is not observed at any other time during the analysis (Figure 1). It is attributed to the point of discontinuity in the damage criterion at the wake of damage. The flexibility of the model is demonstrated through a parametric study based on variations in the parameters λ and ξ. For the parametric study the values of all the parameters except for one are kept constant in order to study the effect of a single parameter on the model as shown in Table 2. The parameters ξ' and ξ^m account for the variation in the damage evolution with respect to the number of cycles, especially the increase in the damage rate during the fatigue life of a material. The specific form of the parameters ξ' and ξ^m is obtained from experimental curves, such as those shown in Figures 4 and 5, where the fatigue damage in the material

is plotted versus the number of applied cycles. Since fatigue damage evolution for a specific stress ratio R is dependent on the applied mean stress as well as the stress amplitude, such experimental curves have to be obtained for different applied mean stresses and stress amplitudes. The damage ϕ in the material during the fatigue life maybe obtained by using the stiffness degradation or an equivalent method, such as sectioning and subsequent SEM evaluation of the specimens for damage quantification. Upon inspection of the obtained experimental curves it is observed that basically three different regions can be distinguished during the fatigue life of the material (Figures 4 and 5). These different regions pertain to the damage initiation phase (Phase I), the damage propagation phase (Phase II), and the failure phase (Phase III). A distinction for these regions maybe made by specifying bounds in the form of the number of cycles such as N_1 and N_2, as indicated in Figure 4. This is done in general by visual inspection using engineering judgment and physical intuition. Using these curves an evolution equation for ξ with respect to the number of cycles N, the applied mean stress σ_{mean} and the stress ratio R maybe established. For the current analysis, since no such experimental data are available, the following forms for the parameters ξ' and ξ^m in terms of N_1 and N_2 have been used and are given as

$$\xi_N^m = \frac{N_1^m - N}{N_1^m - 1} a^m + \left(1 - \frac{N_1^m - N}{N_1^m - 1}\right) b^m \qquad (1 \leq N \leq N_1^m) \tag{51}$$

$$\xi_N^m = \xi_0^m + \Delta\xi_1^m + \left(\frac{N - N_1^m}{N_2^m - N_1^m}\right) \Delta\xi_2^m \qquad (N_1^m < N \leq N_2^m) \tag{52}$$

$$\xi_N^m = \xi_0^m + \Delta\xi_1^m + \left(\frac{N - N_1^m}{N_2^m - N_1^m}\right)^2 \Delta\xi_2^m \qquad (N > N_2^m) \tag{53}$$

$$\xi_N' = \xi_0' + \left(\frac{N - 1}{N_2' - 1}\right) \Delta\xi_2' \qquad (1 < N \leq N_2') \tag{54}$$

$$\xi_N' = \xi_0' + \left(\frac{N - 1}{N_2' - 1}\right)^2 \Delta\xi_2' \qquad (N > N_2') \tag{55}$$

where

$$a^m = \xi_0^m + \sqrt[4]{\frac{N_1^m}{N}} \log\left(\frac{N}{N_1^m}\right) \Delta\xi_1^m \tag{56}$$

$$b^m = \xi_0^m + \Delta\xi_1^m + \left(\frac{N - N_1^m}{N_2^m - N_1^m}\right) \Delta\xi_2^m \tag{57}$$

The results for the parametric study in order to investigate the influence of the model parameter

ζ_0 on the damage evolution in the matrix are shown in Figure 3 with all other parameters kept constant. Varying the value of the parameter λ and keeping ζ_0 constant will result in the curves shown in Figure 2. Only the damage variable ϕ_{11} is shown since the other components of ϕ are equal to zero or their value is smaller by a magnitude of 100. The reference frames of the damage tensor and the material system are identical, hence "1" representing the fiber direction while "2" and "3" indicate the transverse directions. For clarification it should be emphasized that the plateaus exhibited in Figures 2 and 3 represent the unloading phase in the cyclic loading where no further damage occurs.

Two sample analyses of complete fatigue simulations have been conducted to show the capabilities of the developed model. The result of such an analysis for the damage evolution in the matrix, in the fiber and the overall composite is shown in Figure 6. Failure of the entire composite occurs due to fiber failure at about 116000 cycles for the case of $\sigma_{11,max} = 1000\,MPa$ and a stress ratio $R = 0.1$. In a second complete fatigue simulation failure occurs at about 217000 fatigue cycles for $\sigma_{11,max} = 940\,MPa$ and a stress ratio $R = 0.1$. The obtained fatigue life in the two cases is compared with experimental results for a uni-directional composite (Johnson 1989) as shown in Figure 7. The results show satisfactory agreement which establishes the potential of the proposed model.

Conclusions

A micro-mechanical damage model for fatigue loading based on thermo-dynamical principles is proposed. The model is applied to uni-directionally reinforced MMC's. Only elastic loading in the form of a uni-axial fatigue loading (in the fiber direction) is considered hence reflecting high cycle fatigue loading. Numerical results from the parametric study show the influence of various model parameters on the damage evolution in the constituents. A sample analysis for a complete fatigue simulation with final failure is shown.

References

M. J. Owen and R. J. Howe. The Accumulation of Damage in a Glass-reinforced Plastic under Tensile and Fatigue Loading. Journal of Physics, D:5:1637–1649, 1972.

S. Subramanyan. A Cumulative Damage Rule Based on the Knee Point of the *S-N*-Curve. Journal of Engineering Mechanics and Technology, pages 316–321, 1976.

P. Srivatsavan and S. Subramanyan. A Cumulative Damage Rule Based on Successive Reduction in Fatigue Limit. Journal of Engineering Mechanics and Technology, 100:212–214, 1978.

J. Lemaitre and A. Plumtree. Application of Damage Concepts to Predict Creep-Fatigue Failures. Journal of Engineering Mechanics and Technology, 101:284–292, 1979.

J. T. Fong. What is Fatigue Damage? In K. L. Reifsnider, editor, Damage in Composite Materials, pages 243–266. American Society for Testing and Materials, Philadelphia, PA, 1982.

Z. Hashin. Cumulative Damage Theory for Composite Materials, Residual Life and Residual Strength Methods. Composite Science and Technology, 23:1–19, 1985.

W. Hwang and K. S. Han. Cumulative Fatigue Damage Models and Multi-Stress Fatigue Life Prediction. Journal of Composite Materials, 20:125–153, 1986a.

W. Hwang and K. S. Han. Fatigue of Composites - Fatigue Modulus Concept and Life Prediction. Journal of Composite Materials, 20:154–165, 1986b.

H. A. Whitworth. Cumulative Damage in Composites. Transactions of the ASME, 112:358–361, 1990.

S. M. Arnold and S. Kruch. Differential Continuum Damage Mechanics Models for Creep and Fatigue of Unidirectional Metal Matrix Composites. Technical Memorandum 105213, NASA, 1991a.

S. M. Arnold and S. Kruch. A Differential CDM Model for Fatigue of Unidirectional Metal Matrix Composites. Technical Memorandum 105726, NASA, 1991b.

J. L. Chaboche and P. M. Lesne. A Non-Linear Continuous Fatigue Damage Model. Fatigue and Fracture of Engineering Materials and Structures, 11(1):1–17, 1988.

J.-L. Chaboche. Continuum Damage Mechanics: Part I - General Concepts. Journal Of Applied Mechanics, 55:59–64, 1988a.

J. L. Chaboche. Continuum Damage Mechanics: Part II - Damage Growth, Crack Initiation and Crack Growth. Journal of Applied Mechanics, 55:65–72, 1988b.

J. L. Chaboche. Fracture Mechanics and Damage Mechanics: Complementarity of Approaches. In Proceedings of the 4th International Conference on "NUMERICAL METHODS IN FRACTURE MECHANICS", pages 309–324, 1987.

P. M. Lesne and S. Savalle. A Differential Damage Rule with Microinitiation and Micropropagation. La Recherche Aérospatiale, 1987(2):33–47, 1987.

P.M. Lesne and G. Cailletaud. Creep-Fatigue Interaction under High Frequency Loading. Int. Conf. on Mechanical Behavior of Materials, Beijing, China, 1987.

D. N. Robinson, S. F. Duffy, and J. R. Ellis. A Viscoplastic Constitutive Theory for Metal Matrix Composites at High Temperature. pages 49–56, 1987.

D. N. Robinson and S. F. Duffy. Continuum Deformation Theory for High-Temperature Metallic Composites. Journal of Engineering Mechanics, 116(4):832–844, 1990.

T. E. Wilt and S. M. Arnold. A Coupled/Uncoupled Deformation and Fatigue Damage Algorithm Utilizing the Finite Element Method. NASA TM 106526, NASA, Lewis Research Center, Cleveland, OH, 1994.

T. Nicholas. Fatigue Life Prediction in Titanium Matrix Composites. Journal of Engineering Materials and Technology, 117:440–447, 1995.

R. W. Neu. A Mechanistic-Based Thermomechanical Fatigue Life Prediction Model For Metal Matrix Composites. Fatigue and Fracture of Engineering Materials and Structures, 16(8):811–828, 1993.

L. M. Kachanov. On the Creep Fracture Time. Izv. Akad. Nauk. USSR Otd. Tekh., 8:26–31, 1958.

F. Sidoroff. Description of Anisotropic Damage Application to Elasticity. In J. Hult and J. Lemaitre, editors, Physical Non-Linearities in Structural Analysis, IUTAM Series, pages 237–244. Springer-Verlag, 1980.

G. Z. Voyiadjis and P. I. Kattan. A Plasticity-Damage Theory for Large Deformation of Solids - I. Theoretical Formulation. International Journal of Engineering Science, 30(9):1089-1108, 1992.

G. Z. Voyiadjis and P. I. Kattan. A Plasticity-Damage Theory for Large Deformation of Solids - II. Applications to Finite Simple Shear. International Journal of Engineering Science, 31(1):183-199, 1993a.

R. Talreja. Fatigue of Composite Materials. Technomic Publishing Co., Lancaster, PA, 1987.

R. M. Christensen. Tensor Transformations and Failure Criteria for the Analysis of Fiber Composite Materials. Part II: Necessary and Sufficient Conditions for Laminate failure. Journal of Composite Materials, 24:796-800, 1990.

A. Poursatip, M. F. Ashby, and P. W. R. Beaumont. Damage Accumulation During Fatigue of Composites. In T. Hayashi, K. Kawata, and S. Umekawa, editors, Progress in Science and Engineering Composites, pages 693-700. 1982.

George J. Dvorak and Y. A. Bahei-El-Din. Plasticity Analysis of Fibrous Composites. Journal of Applied Mechanics, 49:327-335, 1982.

George J. Dvorak and Y. A. Bahei-El-Din. A Bimodal Plasticity Theory of Fibrous Composite Materials Theory. ACTA Mechanica, 69:219-241, 1987.

G. J. Dvorak and N. Laws. Analysis of Progressive Matrix Cracking in Composite Laminates - II. First Ply Failure. Journal of Composite Materials, 21:309-329, 1987.

G. J. Dvorak, N. Laws, and M. Hejazi. Analysis of Progressive Matrix Cracking in Composite Laminates - I. Thermoelastic Properties of a Ply with Cracks. Journal of Composite Materials, 19, 1985.

G. Z. Voyiadjis and P. I. Kattan. Damage of Fiber-Reinforced Composite Materials with Micromechanical Characterization. International Journal of Solids and Structures, 30(20):2757-2778, 1993b.

G. Z. Voyiadjis, P. I. Kattan, and A. R. Venson. Evolution of a Damage tensor for Metal Matrix Composites. In MECAMAT 93, International Seminar on Micromechanics of Materials, volume 84, pages 406–417, Moret-sur-Loing, France, 1993.

G. Z. Voyiadjis and P. I. Kattan. Micromechanical Characterization of Damage-Plasticity in Metal Matrix Composites. In G. Z. Voyiadjis, editor, Studies in Applied Mechanics, Vol. 34: Damage in Composite Materials, pages 67–102. 1993c.

P. I. Kattan and G. Z. Voyiadjis. Overall Damage and Elasto-Plastic Deformation in Fibrous Metal Matrix Composites. International Journal of Plasticity, 9:931–949, 1993.

G. Z. Voyiadjis and T. Park. Anisotropic Damage Of Fiber Reinforced MMC Using An Overall Damage Analysis. Journal of Engineering Mechanics, 121(11):1209–1217, 1995.

M. Stumvoll and G. Swoboda. Deformation Behavior of Ductile Solids Containing Anisotropic Damage. Journal of Engineering Mechanics, 119(7):169–192, 1993.

G. Z. Voyiadjis and P. I. Kattan. Local Approach to Damage in Elasto-Plastic Metal Matrix Composites. International Journal of Damage Mechanics, 2:92–114, 1993d.

Y. N. Rabotnov. Creep Rupture. In Proceedings of the XII International Congree on Applied Mechanics, pages 342–349. (Stanford-Springer, 1969), 1968.

G. Z. Voyiadjis and A. R. Venson. Experimental Damage Investigation of a SiC-Ti-Aluminide Metal Matrix Composite. International Journal of Damage Mechanics, 4(4):338–361, 1995.

T. Chen, George J. Dvorak, and Y. Benveniste. Mori-Tanaka Estimates of the Overall Elastic Moduli of Certain Composite Materials. Journal of Applied Mechanics, 59:539–546, 1992.

C. L. Chow and T. J. Lu. On Evolution Laws of Anisotropic Damage. Engineering Fracture Mechanics, 34(3):679–701, 1989.

D. C. Lagoudas, A. C. Gavazzi, and H. Nigam. Elastoplastic Behavior of Metal Matrix Composites Based on Incremental Plasticity and the Mori-Tanaka Averaging Scheme. Computational Mechanics, 8:193–203, 1991.

W. S. Johnson, S.J. Lubowinski, and A.L. Highsmith. Mechanical Characterization of Unnotched SCS_6/Ti-15-3 Metal Matrix Composites at Room Temperature. In J.M. Kennedy, H.H. Moeller, and W. S. Johnson, editors, <u>Thermal and Mechanical Behavior of Metal Matrix and Ceramic Matrix Composites</u>, ASTM STP 1080, pages 193–218. ASTM, Philadelphia, PA, 1990.

W. S. Johnson. Fatigue Testing and Damage Development in Continuous Fiber Reinforced Metal Matrix Composites. In W. S. Johnson, editor, <u>Metal Matrix Composites: Testing, Analysis and Failure Modes</u>, pages 194–221. 1989.

Table 1: Material properties used in the analysis

	$E\,(GPa)$	ν	$\sigma_u\,(MPa)$	$\sigma_y\,(MPa)$	c (in %)
Matrix $(Ti-15-3)$	92.4	0.35	933.6	689.5	67.5
Fiber $(SCS-6)$	400.0	0.25	N/A	N/A	32.5

Table 2: Model parameters used in the analysis

	$V\,(MPa)$	$\lambda\,(MPa)$	η	ξ	$c\,(MPa)$	n	Figure
Matrix $(Ti-15-3)$	0.1	80000	1.0	refer to Eqs. (51) - (57)	1.0	1.0	6
Fiber $(SCS-6)$	3	160000	1.0	refer to Eqs. (51) - (57)	1.0	1.0	6

	N_1	N_2	ξ_0	ξ_1	ξ_2	Figure
Matrix $(Ti-15-3)$	10	110000	0.55	0.02	0.03	6
Fiber $(SCS-6)$	N/A	110000	0.56	N/A	0.03	6

Fig. 1: Validation of employed return criteria

Fig. 2: Variation in damage evolution for various values of λ

Fig. 3: Variation in damage evolution for various values of ξ_0

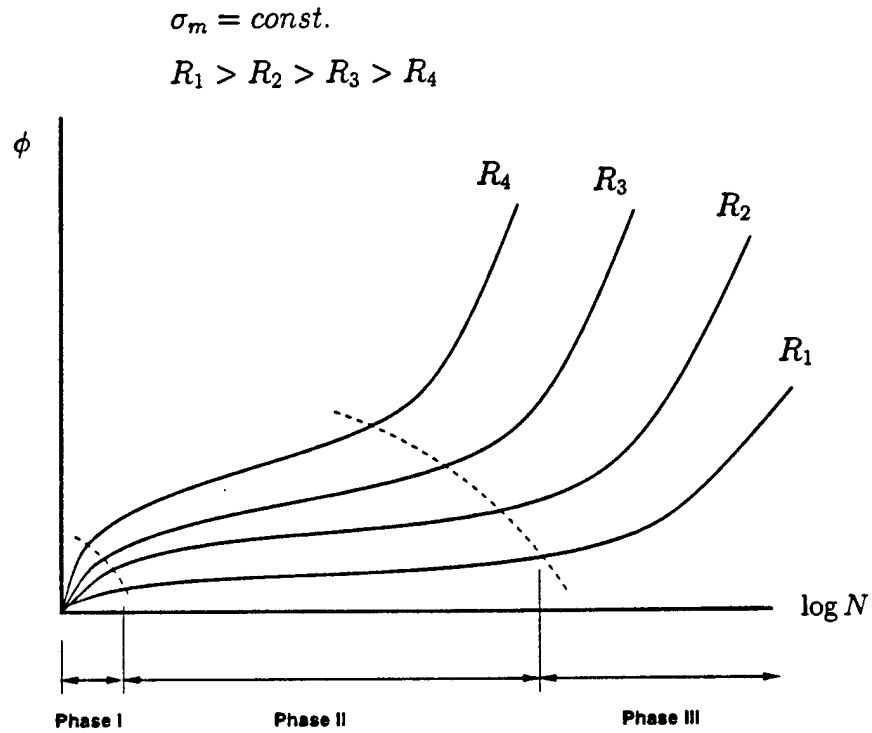Fig. 4: $\phi - N$ diagrams for determination of ξ for constant R

Fig. 5: $\phi - N$ diagrams for determination of ξ for constant σ_{mean}
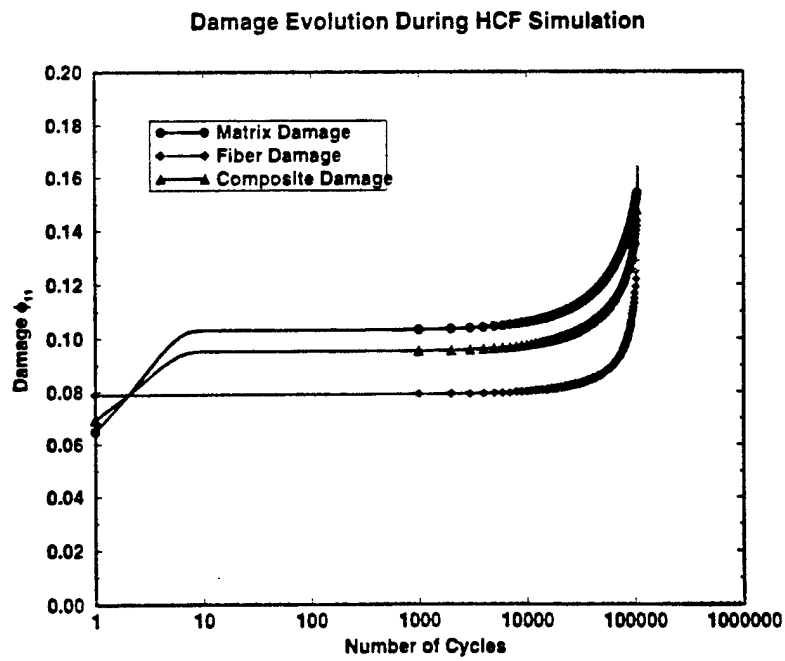
Fig. 6: Fatigue damage evolution during a complete simulation

Fig. 7: Comparison with experimental results (Johnson 1989)

Validation of Employed Return Criterion for Damage Surface g
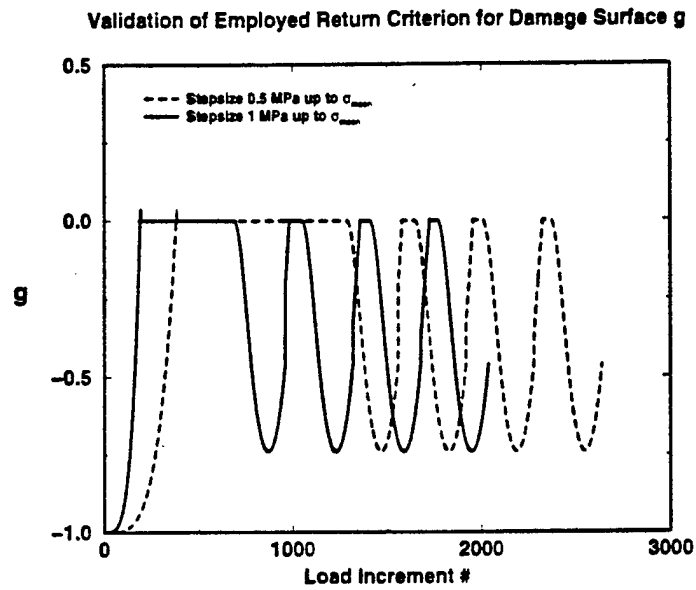
Figure 1: Validation of the employed return criterion

Influence of λ on damage evolution
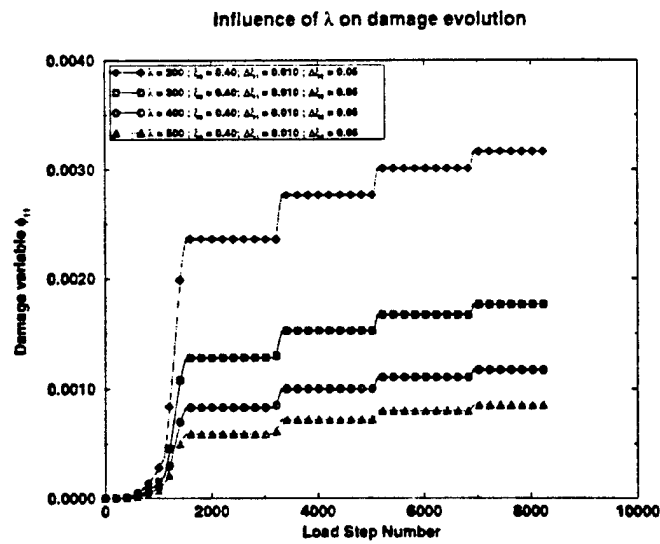
Figure 2: Variation in damage evolution for various values of λ
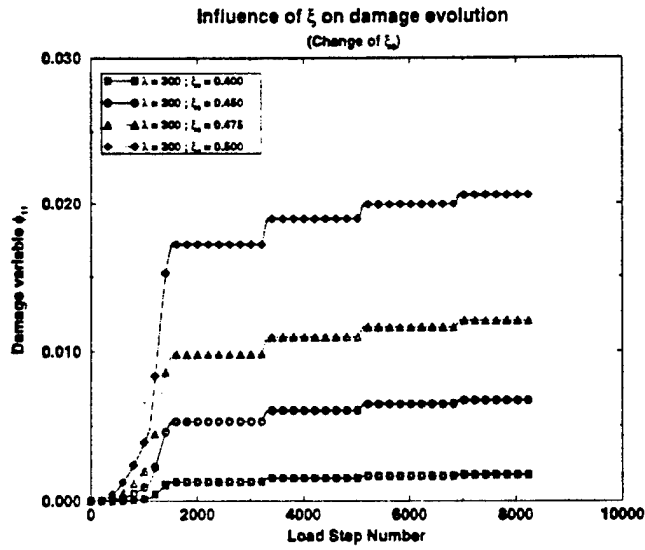
Figure 3: Variation in damage evolution for various values of ξ_0

$$R = const.$$

$$\sigma_{m_1} < \sigma_{m_2} < \sigma_{m_3} < \sigma_{m_4} < \sigma_{m_5}$$
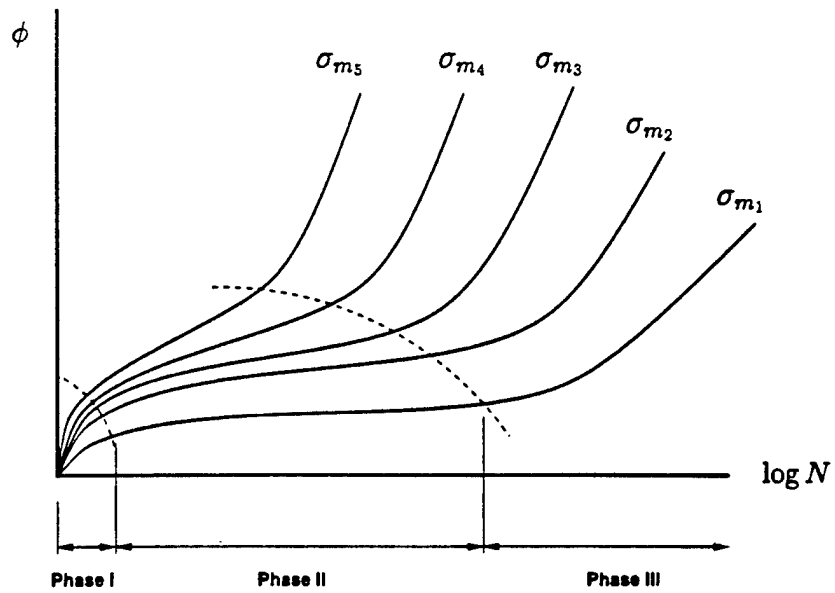
Figure 4: $\phi - N$ diagrams for determination of ξ for constant R

$$\sigma_m = const.$$

$$R_1 > R_2 > R_3 > R_4$$

Figure 5: $\phi - N$ diagrams for determination of ξ for constant σ_{mean}

Damage Evolution During HCF Simulation

Figure 6: Fatigue damage evolution during a complete simulation

Wöhler Diagram for $R = 0.1$
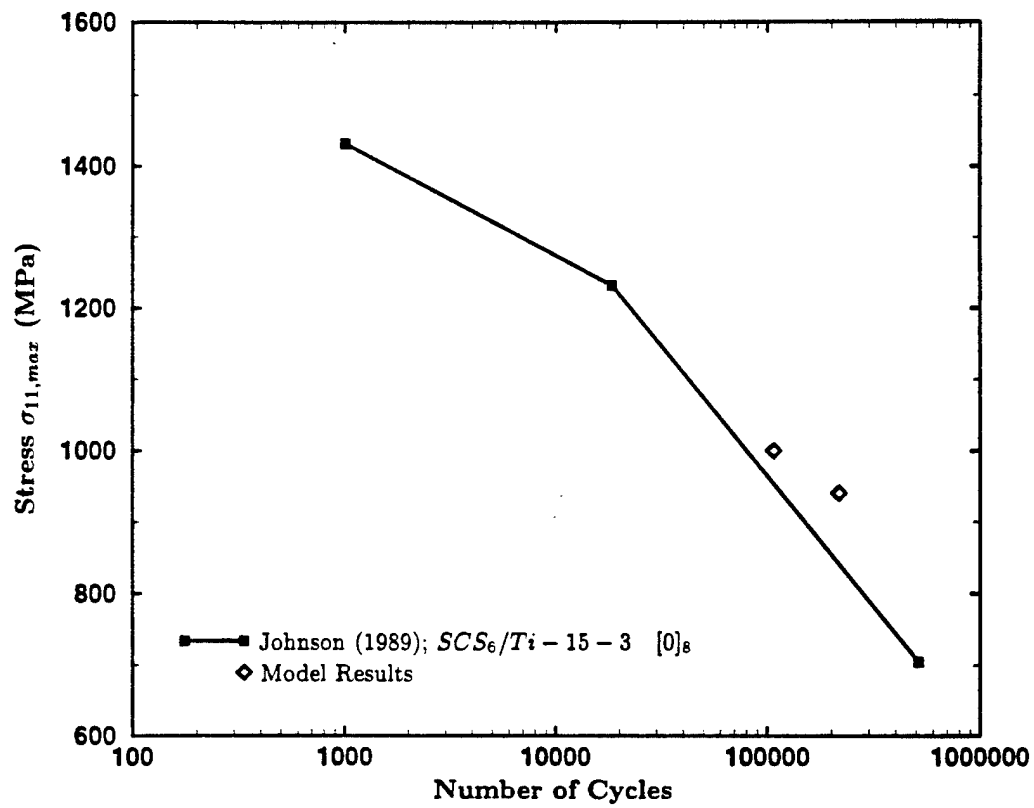
Figure 7: Comparison with experimental results (Johnson 1989)

LOCAL AND INTERFACIAL DAMAGE ANALYSIS OF METAL MATRIX COMPOSITES USING THE FINITE ELEMENT METHOD

GEORGE Z. VOYIADJIS and TAEHYO PARK

Department of Civil and Environmental Engineering, Louisiana State University, Baton Rouge, LA 70803, U.S.A.

Abstract—A micromechanical damage composite model is used here such that separate local evolution damage relations are used for each of the matrix and fiber. In addition, this is coupled with interfacial damage between the matrix and fiber exclusively. An overall response is linked to these damage relations through a certain homogenization procedure. A finite element analysis is used for quantifying each type of damage and predicting the failure loads of dog-bone shaped specimen and center-cracked laminate metal matrix composite plates. The development of damage zones and the stress–strain response are shown for two types of laminated layups, a $(0/90)_s$ layup and a $(\pm 45)_s$ layup. © 1997 Elsevier Science Ltd. All rights reserved.

INTRODUCTION

DAMAGE and plastic deformation is incorporated in the proposed model that is used for the analysis of fiber-reinforced metal matrix composite materials. The proposed micromechanical damage composite model used here is such that separate local constitutive damage relations are used for each of the matrix and fiber. This is coupled with the interfacial damage between the matrix and fiber exclusively. The damage relations are linked to the overall response through a certain homogenization procedure. Three fourth-order, damage tensors M^m, M^f and M^d are used here for the two constituents (matrix and fibers) of the composite system. The matrix damage effect tensor M^m is assumed to reflect all types of damage that the matrix material undergoes such as nucleation and coalescence of voids and microcracks. The fiber damage effect tensor M^f is considered to reflect all types of fiber damage such as fracture of fibers. An additional tensor M^d is incorporated in the overall formulation that represents interfacial damage between the matrix and fiber. An overall damage effect tensor, M, is introduced, that accounts for all these separate damage tensors M^m, M^f and M^d.

THEORETICAL PRELIMINARIES

The metal matrix composite used in this work consists of an elasto-plastic ductile metal matrix reinforced by elastic aligned continuous fibers. The composite system is restricted to small deformations with infinitesimal strains. In the initial configuration, C_o, the composite material is assumed to be undeformed and undamaged. The initial matrix and fiber subconfigurations are denoted by C_o^m and C_o^f, respectively. Due to applied loads, the composite material is assumed to undergo elasto-plastic deformation and damage, and the resulting overall configuration is denoted by C. The resulting matrix and fiber local subconfigurations are denoted by C^m and C^f, respectively. Damage is quantified using the concept proposed by Kachanov[1] whereby two kinds of fictitious configurations $\bar{C}$ and $\tilde{C}$ of the composite system are considered. $\bar{C}$ configuration is obtained from C by removing all the damages, while $\tilde{C}$ configuration is obtained from C by removing only the interfacial damage between the matrix and fiber. $\bar{C}$ is termed full effective configuration, while $\tilde{C}$ the partial effective configuration.

A coupling formulation of plastic flow and damage propagation seems to be impossible, due to the presence of the two different dissipative mechanisms that influence each other. For example, the position of slip planes affects the orientation of nucleated microcracks. One can, however, assume that the energy dissipated in the yielding and damaging processes is independent of each other and apply a phenomenological model of interaction. Use will be made of the

concept of effective stress [2]. Assuming a fictitious undamaged system, the dissipation energy due to plastic flow in this undamaged system is assumed to be equal to the dissipation energy due to plastic flow in the real damaged system.

The basic feature of the approach presented here is that local effects of damages are considered whereby these effects are described separately by the matrix, fiber and interfacial damage. It is clear the local nature of damage of this approach whereby the different damages are separately isolated. This approach can be summarized in the following three steps. First, apply the local damage effect tensors M^m and M^f to the local effective configurations $\tilde{C}^m$ and $\tilde{C}^f$, respectively. This is followed by applying the damage stress concentration factors $\tilde{B}^m$ and $\tilde{B}^f$ to the local partial effective configurations $\tilde{C}^m$ and $\tilde{C}^f$ in order to obtain the overall partial effective configuration $\tilde{C}$. Finally, one applies the interfacial damage effect tensor M^d to the overall partial effective configuration $\tilde{C}$ to obtain the overall damaged configuration C.

In the formulation of this work, quantities based on the full effective configuration, $\bar{C}$, and the partial effective configuration, $\tilde{C}$, are denoted by a superposed bar and superposed tilde, respectively. Fiber and matrix related quantities are denoted by a superscript m or f, appropriately. In addition, interfacial damage related quantities are denoted by a superscript d.

In the undamaged effective configuration $\tilde{C}$, the overall effective stress increment $d\bar{\sigma}$ can be expressed in terms of the phase effective stress increments $d\bar{\sigma}^m$ and $d\bar{\sigma}^f$ as follows:

$$d\bar{\sigma}_{ij} = \bar{c}^m \, d\bar{\sigma}_{ij}^m + \bar{c}^f \, d\bar{\sigma}_{ij}^f \qquad (1)$$

where $\bar{c}^m$ and $\bar{c}^f$ are the matrix and fiber volume fractions, respectively. The local-overall relations for the stress increments for the matrix and fibers in the fictitious local and overall configurations are given as follows:

$$d\bar{\sigma}_{ij}^r = \bar{B}_{ijkl}^r \, d\bar{\sigma}_{kl}, \quad \text{where } r = m, f, \qquad (2)$$

where $\bar{B}^r$ is the stress concentration tensor for the matrix or fibers. Similarly, the overall effective strain increment is assumed in the effective configurations such that

$$d\bar{\epsilon}_{ij} = \bar{c}^m \, d\bar{\epsilon}_{ij}^m + \bar{c}^f \, d\bar{\epsilon}_{ij}^f, \qquad (3)$$

where $d\bar{\epsilon}^m$ and $d\bar{\epsilon}^f$ are the effective matrix and fiber strain increments, respectively. The additive decomposition is assumed of the matrix and overall strain increments in $\tilde{C}^m$ and $\tilde{C}$, respectively, such that

$$d\bar{\epsilon}_{ij} = d\bar{\epsilon}_{ij}' + d\bar{\epsilon}_{ij}'' \qquad (4)$$

$$d\bar{\epsilon}_{ij}^m = d\bar{\epsilon}_{ij}^m{}' + d\bar{\epsilon}_{ij}^m{}'', \qquad (5)$$

where ' indicates the elastic and " indicates the plastic part of the increment. Equations (4) and (5) are justified in view of the assumption of small strains. The fibers are assumed to deform elastically and therefore we have

$$d\bar{\epsilon}_{ij}^f = d\bar{\epsilon}_{ij}^f{}'. \qquad (6)$$

The local-overall relations for the effective strain increments are given as follows:

$$d\bar{\epsilon}_{ij}^r = \bar{A}_{ijkl}^r \epsilon_{kl}, \quad \text{where } r = m, f, \qquad (7)$$

where $\bar{A}^r$ is the strain concentration tensor for the matrix or fibers.

The expressions for the stress and strain tensors based on the Mori–Tanaka method are given in Appendix A.

CONSTITUTIVE EQUATIONS FOR THE UNDAMAGED METAL MATRIX COMPOSITE

The constitutive relations for the matrix and fibers are given by the following relations:

$$d\bar{\sigma}_{ij}^m = \bar{D}_{ijkl}^m \, d\bar{\epsilon}_{kl}^m \qquad (8)$$

$$d\bar{\sigma}_{ij}^f = \bar{E}_{ijkl}^f \, d\bar{\epsilon}_{kl}^f, \tag{9}$$

where $\bar{D}^m$ is the elasto-plastic stiffness tensor of the matrix and $\bar{E}^f$ is the elastic stiffness tensor of the fiber. The elastic stiffnesses of the matrix and fiber are given by the following expressions

$$\bar{E}_{ijkl}^m = \bar{\lambda}^m \delta_{ij}\delta_{kl} + \bar{G}^m(\delta_{ik}\delta_{jl} + \delta_{il}\delta_{jk}) \tag{10}$$

$$\bar{E}_{ijkl}^f = \bar{\lambda}^f \delta_{ij}\delta_{kl} + \bar{G}^f(\delta_{ik}\delta_{jl} + \delta_{il}\delta_{jk}), \tag{11}$$

where $\bar{\lambda}^m$, $\bar{G}_m$, $\bar{\lambda}^f$ and $\bar{G}^f$ are Lame's constants for the matrix and fibers, respectively. Substituting for $d\bar{\sigma}^m$ and $d\bar{\sigma}^f$ from eqs (8) and (9), respectively, into eq. (1) and making use of eq. (7), one obtains the relation

$$d\bar{\sigma}_{ij} = \bar{D}_{ijpq} \, d\bar{\epsilon}_{pq}, \tag{12}$$

where

$$\bar{D}_{ijpq} = \bar{c}^m \bar{D}_{ijkl}^m \bar{A}_{klpq}^m + \bar{c}^f \bar{E}_{ijkl}^f \bar{A}_{klpq}^f. \tag{13}$$

$\bar{D}$ is the elasto-plastic stiffness of the composite in the effective undamaged configuration.

PLASTIC BEHAVIOR OF THE UNDAMAGED METAL MATRIX COMPOSITE

The elasto-plastic constitutive model for the matrix is based on the von Mises type yield function $\bar{f}^m(\bar{\sigma}_{ij}^m, \bar{\alpha}_{ij}^m)$ in the local configuration $\bar{C}^m$ such that

$$\bar{f}^m \equiv \frac{3}{2}(\bar{\sigma}_{ij}^m - \bar{\alpha}_{ij}^m)(\bar{\sigma}_{ij}^m - \bar{\alpha}_{ij}^m) - \bar{\sigma}_0^{m^2} = 0, \tag{14}$$

$\bar{\sigma}_0^m$ is a material constant denoting the uniaxial yield stress of the matrix material and $\bar{\alpha}^m$ is the backstress tensor. The plastic flow in the configuration $\bar{C}^m$ is given by the associated flow rule in the form

$$d\bar{\epsilon}_{ij}^{m\,\prime\prime} = \bar{\Lambda}_m \frac{\partial \bar{f}^m}{\partial \bar{\sigma}_{ij}^m}, \tag{15}$$

where $\bar{\Lambda}^m$ is a scalar function introduced as a Lagrangian multiplier in the constrain thermodynamic equations for the matrix material.

In order to describe kinematic hardening for the matrix, the Prager–Ziegler evolution law [3] is used here in the configuration $\bar{C}^m$, as follows:

$$d\bar{\alpha}_{ij}^m = \bar{\mu}^m(\bar{\sigma}_{ij}^m - \bar{\alpha}_{ij}^m), \tag{16}$$

where $\bar{\mu}^m$ is a scalar function given in terms of $\bar{\Lambda}_m$ as follows:

$$\bar{\mu}^m = \bar{\Lambda}^m b \frac{\dfrac{\partial \bar{f}^m}{\partial \bar{\sigma}_{ij}^m}\dfrac{\partial \bar{f}^m}{\partial \bar{\sigma}_{ij}^m}}{(\bar{\sigma}_{kl}^m - \bar{\alpha}_{kl}^m)\dfrac{\partial \bar{f}^m}{\partial \bar{\sigma}_{kl}^m}} \tag{17}$$

and b is a material parameter.

The parameter $\bar{\Lambda}^m$ is obtained from the consistency

$$d\bar{f}^m(\bar{\sigma}_{ij}^m, \bar{\alpha}_{ij}^m) = 0 \tag{18}$$

and is given by the following relation:

$$\bar{\Lambda}^m = \frac{1}{\bar{q}^m}\frac{\partial \bar{f}^m}{\partial \bar{\sigma}_{ij}^m}\bar{E}_{ijkl}^m \bar{\epsilon}_{kl}^m, \tag{19}$$

where

$$\bar{q}^m = \frac{\partial \bar{f}^m}{\partial \bar{\sigma}_{ij}^m} \bar{E}_{ijkl}^m \frac{\partial \bar{f}^m}{\partial \bar{\sigma}_{kl}^m} - \frac{\partial \bar{f}^m}{\partial \bar{\alpha}_{ij}^m}(\bar{\sigma}_{ij}^m - \bar{\alpha}_{ij}^m) \frac{\frac{\partial \bar{f}^m}{\partial \bar{\sigma}_{pq}^m} \frac{\partial \bar{f}^m}{\partial \bar{\sigma}_{pq}^m}}{(\bar{\sigma}_{kl}^m - \bar{\alpha}_{kl}^m)\frac{\partial \bar{f}^m}{\partial \bar{\sigma}_{kl}^m}} b. \tag{20}$$

The resulting elasto–plastic stiffness tensor for the matrix material in the effective undamaged configuration is given by

$$\bar{D}_{ijkl}^m = \bar{E}_{ijkl}^m - \frac{1}{\bar{q}^m} \frac{\partial \bar{f}^m}{\partial \bar{\sigma}_{pq}^m} \bar{E}_{pqij}^m \bar{E}_{klrs}^m \frac{\partial \bar{f}^m}{\partial \bar{\sigma}_{rs}^m}. \tag{21}$$

Damage effect tensors

The effective stress concept[1,4] is used in this work. Considering the overall configurations C, $\bar{C}$ and $\tilde{C}$, one can introduce an overall damage effect tensor M and a partial damage effect tensor $\tilde{M}$ for the whole composite system. These tensors are defined similarly to the definitions of M^m, M^f and M^d such that

$$\bar{\sigma}_{ij} = M_{ijkl}\sigma_{kl} \tag{22}$$

$$\bar{\sigma}_{ij} = \tilde{M}_{ijkl}\tilde{\sigma}_{kl}. \tag{23}$$

The tensor M reflects all types of damage that the composite undergoes including the damage due to the interaction between the matrix and fibers while the tensor $\tilde{M}$ reflects damage of matrix and fibers, excluding the interfacial damage. A matrix representation was explicitly derived for this fourth order tensor by expressing the stresses in vector form. The tensor M was shown to be symmetric. The symmetry property of the tensor M is used extensively in the derivation that follows. The same holds true for the tensors M^m, M^f and M^d. Similar to tensor M^d, both tensors M^m and M^f could be represented in terms of second order tensors ϕ^m and ϕ^f, respectively. The effective matrix stress and the corresponding fiber stress are defined as follows:

$$\bar{\sigma}_{ij}^m = M_{ijkl}^m \bar{\sigma}_{kl}^m \tag{24}$$

and

$$\bar{\sigma}_{ij}^f = M_{ijkl}^f \bar{\sigma}_{kl}^f, \tag{25}$$

where $\bar{\sigma}^m$ and $\bar{\sigma}^f$ are the partial effective stresses in the $\bar{C}^m$ and $\bar{C}^f$ configurations, respectively. These stresses are termed partial effective since the interfacial damage has not yet been incorporated into the formulation. The overall damage effect tensor, M, can be related to the partial damage effect tensor, $\tilde{M}$, and the local damage effect tensors such as

$$M_{ijkl} = \tilde{M}_{ijrs} M_{rskl}^d, \tag{26}$$

where

$$\tilde{M}_{ijrs} = \bar{c}^m M_{ijpq}^m B_{pqrs}^m + \bar{c}^f M_{ijpq}^f B_{pqrs}^f. \tag{27}$$

This expression defines the cumulative damage of the composite as a function of the local matrix and fiber damages M^m and M^f, respectively, as well as the interfacial damage M^d[5,6].

The expression of the fourth order local damage effect tensor M^m, M^f and M^d can be represented by a 6×6 matrix as a function of $(\delta_{ij} - \phi_{ij}^r)$ in the form

$$[M]^r = [M(\delta_{ij} - \phi_{ij}^r)], \quad r = m, f, d, \tag{28}$$

where δ_{ij} is the Kronecker delta.

In conjunction with the matrix form of M given by eq. (28), the local stress tensor σ^r is represented by a vector given by

$$[\sigma^r] = [\sigma_{11}^r, \sigma_{22}^r, \sigma_{33}^r, \sigma_{12}^r, \sigma_{23}^r, \sigma_{31}^r]^T, \quad r = m, f. \tag{29}$$

The symmetrized $\bar{\sigma}^r$ and σ used here are given by[4]

$$\bar{\sigma}_{ij}^r = \frac{1}{2}[\sigma_{ik}^r(\delta_{kj} - \phi_{kj}^r)^{-1} + (\delta_{il} - \phi_{il}^r)^{-1}\sigma_{lj}^r], \quad \text{where } r = m, f \tag{30}$$

and

$$\bar{\sigma}_{ij} = \frac{1}{2}[\sigma_{ik}(\delta_{kj} - \phi_{kj}^d)^{-1} + (\delta_{il} - \phi_{il}^d)^{-1}\sigma_{lj}]. \tag{31}$$

The stresses given by eqs (30) and (31) are frame-independent. Using the symmetrization procedure outlined by eqs (30) and (31), the corresponding 6×6 matrix form of tensor M is given by Voyiadjis and Kattan[7] as follows:

$$[M]^r = \frac{1}{2\nabla} \begin{bmatrix} 2\omega_{22}\omega_{33} - 2\phi_{23}^2 & 0 & 0 \\ 0 & 2\omega_{11}\omega_{33} - 2\phi_{13}^2 & 0 \\ 0 & 0 & 2\omega_{11}\omega_{22} - 2\phi_{12}^2 \\ \phi_{13}\phi_{23} + \phi_{12}\omega_{33} & \phi_{13}\phi_{23} + \phi_{12}\omega_{33} & 0 \\ 0 & \phi_{12}\phi_{13} + \phi_{23}\omega_{11} & \phi_{12}\phi_{13} + \phi_{23}\omega_{11} \\ \phi_{12}\phi_{23} + \phi_{13}\omega_{22} & 0 & \phi_{12}\phi_{23} + \phi_{13}\omega_{22} \end{bmatrix}$$

$$\begin{bmatrix} 2\phi_{13}\phi_{23} + 2\phi_{12}\omega_{33} & 0 & 2\phi_{12}\phi_{23} + 2\phi_{13}\omega_{22} \\ 2\phi_{13}\phi_{23} + 2\phi_{12}\omega_{33} & 2\phi_{12}\phi_{13} + 2\phi_{23}\omega_{11} & 0 \\ 0 & 2\phi_{12}\phi_{13} + 2\phi_{23}\omega_{11} & 2\phi_{12}\phi_{23} + 2\phi_{13}\omega_{22} \\ \omega_{22}\omega_{33} + \omega_{11}\omega_{33} - \phi_{23}^2 - \phi_{13}^2 & \phi_{12}\phi_{23} + \phi_{13}\omega_{22} & \phi_{12}\phi_{13} + \phi_{23}\omega_{11} \\ \phi_{12}\phi_{23} + \phi_{13}\omega_{22} & \omega_{11}\omega_{33} + \omega_{11}\omega_{22} - \phi_{13}^2 - \phi_{12}^2 & \phi_{13}\phi_{23} + \phi_{12}\omega_{33} \\ \phi_{12}\phi_{13} + \phi_{23}\omega_{11} & \phi_{13}\phi_{23} + \phi_{12}\omega_{33} & \omega_{22}\omega_{33} + \omega_{11}\omega_{22} - \phi_{23}^2 - \phi_{12}^2 \end{bmatrix}$$

$$r = m, f, d \tag{32}$$

and ∇ is given by

$$\nabla = \omega_{11}\omega_{22}\omega_{33} - \phi_{23}^2\omega_{11} - \phi_{13}^2\omega_{22} - \phi_{12}^2\omega_{33} - 2\phi_{12}\phi_{23}\phi_{13}. \tag{33}$$

ω_{ij} is used to denote $\delta_{ij} - \phi_{ij}$. ϕ_{ij} used in eqs (32) and (33) represents ϕ_{ij}^m, ϕ_{ij}^f or ϕ_{ij}^d with respect to matrix damage, fiber damage or interfacial damage, accordingly.

Damage stress and strain concentration tensors

The matrix and fiber stress concentration factors are defined as fourth-rank tensors. As composites undergo damage the stress and strain concentration factors do not remain constant. The damage stress and strain concentration tensors are given by the following relations[6]:

$$\bar{B}_{ijkl}^r = M_{ijpz}^{-1}\bar{B}_{pqrs}^r\bar{M}_{rskl}, \quad r = m, f \tag{34}$$

$$\bar{A}_{ijkl}^r = M_{ijpz}^{-1}\bar{A}_{pqrs}^r\bar{M}_{rskl}, \quad r = m, f. \tag{35}$$

ANISOTROPIC DAMAGE ANALYSIS

The damage mechanism for each of the constituents of the composite material is different from the other. The matrix undergoes ductile damage while the fiber undergoes brittle damage. The mechanism of interfacial damage is dependent on the fiber direction. It is clear that one single damage micro-mechanism cannot be considered for the three types of damages outlined above. We therefore consider each damage evolution separately.

Damage criterion

An anisotropic damage criterion is proposed in this work. In order to obtain a damage criterion for nonproportional loading, the anisotropy of damage increase (hardening) must be considered. This is accomplished by expressing the damage criterion in terms of a tensorial hardening parameter, h. The damage criterion used here is of the form suggested by Mroz[8] such that

$$g^r \equiv g^r(Y, h) = 0, \quad r = m, f, d, \tag{36}$$

where Y^r is a generalized thermodynamic force conjugate to the damage tensor ϕ^r for each of the damages associated with the matrix, fiber and debonding. Equation (36) is an isotropic function of tensors Y^r and h^r such that

$$g^r \equiv p^r_{ijkl} Y^r_{ij} Y^r_{kl} - 1 = 0, \tag{37}$$

where

$$p^r_{ijkl} = h^{-r}_{ij} h^{-r}_{kl} \tag{38}$$

and p^r_{ijkl} is equivalent to Hill's tensor for yield surfaces. The hardening tensor h^r is given by

$$h^r_{ij} = (u^r_{ik})^{1/2} \phi^r_{kl} (u^r_{lj})^{1/2} + V^r_{ij}. \tag{39}$$

Tensors u^r and V^r are here defined for orthotropic materials as follows:

$$u^r = \begin{bmatrix} \bar{\lambda}^r_1 \eta^r_1 \left(\dfrac{\kappa^r}{\bar{\lambda}^r_1}\right)^{\xi^r_1} & 0 & 0 \\ 0 & \bar{\lambda}^r_2 \eta^r_2 \left(\dfrac{\kappa^r}{\bar{\lambda}^r_2}\right)^{\xi^r_2} & 0 \\ 0 & 0 & \bar{\lambda}^r_3 \eta^r_3 \left(\dfrac{\kappa^r}{\bar{\lambda}^r_3}\right)^{\xi^r_3} \end{bmatrix} \tag{40}$$

and

$$V^r = \begin{bmatrix} \bar{\lambda}^r_1 v^2_1 & 0 & 0 \\ 0 & \bar{\lambda}^r_2 v^2_2 & 0 \\ 0 & 0 & \bar{\lambda}^r_3 v^2_3 \end{bmatrix}, \quad \text{where } r = m, f, d. \tag{41}$$

These tensors u^r and V^r are generalizations to orthotropic materials of the scalar forms for isotropic materials originally proposed by Stumvoll and Swoboda[9]. In expressions (40) and (41), the scalar quantities $\bar{\lambda}^r_1$, $\bar{\lambda}^r_2$, $\bar{\lambda}^r_3$, v^r_1, v^r_2, v^r_3, ζ^r_1, ζ^r_2, ζ^r_3, η^r_1, η^r_2 and η^r_3 are material parameters obtained by matching the theory with experimental results. The parameters $\bar{\lambda}^{r_1}$, $\bar{\lambda}^{r_2}$, $\bar{\lambda}^{r_3}$, v^r_1, v^r_2 and v^r_3 are explicitly related to the physical properties of the material[6].

In eq. (41), v^r_1, v^r_2 and v^r_3 define the initial threshold against damage for the orthotropic material. It is obtained from the constraint that the onset of damage corresponds to the stress level at which the virgin material starts exhibiting nonlinearity.

Referring to eq. (40), κ^r is a scalar hardening parameter given by

$$\kappa^r = \int_0^\phi Y^r_{ij} \, d\phi^r_{ij}, \quad \text{where } r = m, f, d. \tag{42}$$

As outlined by Stumvoll and Swoboda[9], the damaging state is any state that satisfies $g = 0$. Four states are outlined here

$$g^r < 0 \quad \text{(elastic-unloading)} \tag{43}$$

$$g^r = 0, \ \frac{\partial g^r}{\partial Y^r_{ij}} \, dY^r_{ij} < 0 \quad \text{(elastic-unloading)} \tag{44}$$

$$g' = 0, \; \frac{\partial g'}{\partial Y'_{ij}} \, dY'_{ij} = 0 \quad \text{(neutral loading)} \tag{45}$$

$$g' = 0, \; \frac{\partial g'}{\partial Y'_{ij}} \, dY'_{ij} > 0 \quad \text{(loading from a damaging state)}. \tag{46}$$

In this section, the anisotropic damage criterion g is defined by eq. (37) as well as the loading conditions outlined by eqs (43)–(46). The anisotropic damage criterion is defined through the second order tensors u' and V', and the damage tensor ϕ' for each constituent of the composite material. In this work, we assume that the matrix and the fiber are isotropic materials while the anisotropic damage criterion is used to describe the interfacial damage.

Damage evolution of the matrix

The metal matrix exhibits two energy dissipative behaviors. Although the two dissipative mechanisms of plasticity and damage influence each other, in this work, it is assumed that the energy dissipated due to plasticity and that due to damage are independent of each other. The power of dissipation for the matrix is given by

$$\bar{\Pi}^m = \bar{\Pi}^{md} + \bar{\Pi}^{mp}, \tag{47}$$

where $\bar{\Pi}^{mp}$ is the plastic dissipation and $\bar{\Pi}^{md}$ the corresponding damage dissipation. The plastic dissipation is given by

$$\bar{\Pi}^{mp} = \bar{\sigma}^m_{ij} \, d\bar{\epsilon}^{m''}_{ij}. \tag{48}$$

In this work, a small strain theory is assumed and the strain rate is assumed to be decomposed into an elastic component $\bar{\epsilon}^{m'}$ and a plastic component $\bar{\epsilon}^{m''}$, such that

$$d\bar{\epsilon}^m_{ij} = d\bar{\epsilon}^{m'}_{ij} + d\bar{\epsilon}^{m''}_{ij}. \tag{49}$$

The associated damage dissipation is given by

$$\bar{\Pi}^{md} = Y^m_{ij} \, d\phi^m_{ij}, \tag{50}$$

where Y^m is a generalized thermodynamic force conjugate to the damage tensor ϕ^m. The fictitious undamaged material is characterized by the effective stress and effective strain. Since in the full effective configuration, $\bar{C}^m$, the matrix has deformed with no additional damage, the dissipation energy in $\bar{C}^m$ is only composed of the plastic dissipation

$$\bar{\Pi}^m = \bar{\Pi}^{mp} \tag{51}$$

and therefore

$$\bar{\Pi}^m = \bar{\sigma}^m_{ij} \, d\bar{\epsilon}^{m''}_{ij}. \tag{52}$$

This is because plastic yielding is assumed to be independent of the damage process. The plastic dissipation in the damaged matrix is equal to the corresponding plastic dissipation in the full effective configuration, $\bar{C}^m$. This concludes that

$$\bar{\Pi}^{mp} = \bar{\Pi}^{mp}, \tag{53}$$

which implies that

$$\bar{\sigma}^m_{ij} \, d\bar{\epsilon}^{m''}_{ij} = \bar{\sigma}^m_{ij} \, d\bar{\epsilon}^{m''}_{ij}. \tag{54}$$

Making use of eq. (54) together with

$$\bar{\sigma}^m_{ij} = M^m_{ij} \, \bar{\sigma}^m_{kl}, \tag{55}$$

one obtains a transformation equation for the plastic strain rates such that

$$d\bar{\epsilon}_{ij}^{m''} = M_{ijkl}^{-m} \, d\bar{\epsilon}_{kl}^{m''}. \tag{56}$$

Making use of the calculus of functions of several variables, one introduces two Lagrange multipliers Λ_1^m and Λ_2^m in order to form the function Ω^m such that

$$\Omega^m = \tilde{\Pi}^m - \Lambda_1^m \tilde{f}^m - \Lambda_2^m g^m. \tag{57}$$

In eq. (57), $f^m(\bar{\sigma}^m, \bar{\alpha}^m)$ is the plastic yield function of the matrix and $\bar{\alpha}^m$ is the backstress tensor. g^m is the damage potential which is a function of Y^m. To extremize the function Ω^m, one uses the necessary conditions

$$\frac{\partial \Omega^m}{\partial \bar{\sigma}_{ij}^m} = 0 \tag{58}$$

and

$$\frac{\partial \Omega^m}{\partial Y_{ij}^m} = 0, \tag{59}$$

which give the corresponding plastic strain rate and damage rate evolution equations, respectively:

$$d\bar{\epsilon}_{ij}^{m''} = \Lambda_1^m \frac{\partial \tilde{f}^m}{\partial \bar{\sigma}_{ij}^m} \tag{60}$$

and

$$d\phi_{ij}^m = \Lambda_2^m \frac{\partial g^m}{\partial Y_{ij}^m}. \tag{61}$$

Equation (61) gives the increment of damage from the damage potential g^m. Using the consistency condition for the matrix damage g^m

$$dg^m = 0 \tag{62}$$

one obtains the parameter Λ_2^m. Equation (62) states that after an increment of damage, the volume element again must be in a damaging state. From eq. (62), one obtains

$$\Lambda_2^m = -\frac{\dfrac{\partial g^m}{\partial Y_{ij}^m} dY_{ij}^m}{\dfrac{\partial g^m}{\partial \phi_{ij}^m} \dfrac{\partial g^m}{\partial Y_{ij}^m}}. \tag{63}$$

Substituting eq. (63) into eq. (61), one obtains

$$d\phi_{ij}^m = \psi_{ijkl}^m \, dY_{ij}^m, \tag{64}$$

where ψ^m is a fourth order tensor defined as

$$\psi_{ij}^m = -\frac{\dfrac{\partial g^m}{\partial Y_{ij}^m} \dfrac{\partial g^m}{\partial Y_{ij}^m}}{\dfrac{\partial g^m}{\partial \phi_{rs}^m} \dfrac{\partial g^m}{\partial Y_{rs}^m}}. \tag{65}$$

The generalized thermodynamic force Y^m is assumed to be a function of the elastic component of the strain tensor $\bar{\epsilon}^{m'}$ and the damage tensor ϕ^m, or the stress $\bar{\sigma}^m$ and ϕ^m

$$Y_{ij}^m = Y^m(\bar{\epsilon}_{ij}^{m'}, \phi_{ij}^m) \text{ or } Y_{ij}^m = Y^m(\bar{\sigma}_{ij}^m, \phi_{ij}^m). \tag{66}$$

The evolution equation for Y^m may be expressed as follows:

$$dY_{ij}^m = \frac{\partial Y_{ij}^m}{\partial \bar{\sigma}_{kl}^m}\, d\bar{\sigma}_{kl}^m + \frac{\partial Y_{ij}^m}{\partial \phi_{kl}^m}\, d\phi_{kl}^m. \tag{67}$$

Substituting for dY^m from eq. (67) into eq. (64), one obtains the evolution equation for ϕ^m such that

$$d\phi_{kl}^m = \left(L_{ijkl}^{-m}\, \psi_{ijrs}^m\, \frac{\partial Y_{rs}^m}{\partial \bar{\sigma}_{pq}^m} \right) d\bar{\sigma}_{pq}^m \tag{68}$$

or

$$d\phi_{kl}^m = X_{klpq}^m\, d\bar{\sigma}_{pq}^m, \tag{69}$$

where

$$L_{ijkl}^m = \frac{1}{2}(\delta_{ik}\delta_{jl} + \delta_{il}\delta_{jk}) - \psi_{ijrs}^m\, \frac{\partial Y_{rs}^m}{\partial \phi_{kl}^m}. \tag{70}$$

The thermodynamic force associated with damage is obtained using the enthalpy of the damaged matrix where

$$V^m(\bar{\sigma}_{ij}^m, \phi_{ij}^m) = \frac{1}{2}\bar{\sigma}_{ij}^m\, \bar{E}_{ijkl}^{-m}(\phi^m)\bar{\sigma}_{kl}^m. \tag{71}$$

In eq. (71), $\bar{E}^m$ is the damaged elastic stiffness of the matrix. The thermodynamic force of the matrix is given by

$$Y_{ij}^m = \frac{\partial V^m}{\partial \phi_{ij}^m}. \tag{72}$$

Using the energy equivalence principle [10], one obtains a relation between the damaged elastic compliance, $\bar{E}^{-m}$, for the matrix and its corresponding undamaged elastic compliance $\bar{E}^m$ such that[11]

$$\bar{E}_{ijkl}^{-m}(\phi^m) = M_{pqij}^m(\phi^m)\bar{E}_{pqrs}^{-m}M_{rskl}^m(\phi^m). \tag{73}$$

Making use of eqs (71) and (72), the thermodynamic force for the matrix is obtained explicitly such that

$$Y_{ij}^m = \frac{1}{2}(\bar{\sigma}_{cd}^m \bar{E}_{abpq}^{-m} M_{pqkl}^m \bar{\sigma}_{kl}^m + \bar{\sigma}_{rs}^m M_{uvrs}^m \bar{E}_{uvab}^{-m} \bar{\sigma}_{cd}^m)\frac{\partial M_{abcd}^m}{\partial \phi_{ij}^m}. \tag{74}$$

Damage evolution of the fiber

The gradual degradation of the elastic stiffness of the fiber is caused only through damage and therefore no plastic dissipation occurs. We therefore have

$$\bar{\Pi}^f = \bar{\Pi}^{fd} = Y_{ij}^f\, d\phi_{ij}^d \tag{75}$$

and

$$\bar{\Pi}^f = 0. \tag{76}$$

Accordingly, the function Ω^f is given by

$$\Omega^f = \bar{\Pi}^f - \Lambda^f g^f \tag{77}$$

and

$$d\phi_{ij}^f = \Lambda^f \frac{\partial g^f}{\partial Y_{ij}^f}. \tag{78}$$

Using the consistency condition for the damage of the fiber

$$dg^f = 0 \tag{79}$$

one obtains the evolution equation for ϕ^f

$$d\phi_{ij}^f = X_{ijkl}^f \tilde{\sigma}_{kl}^f, \tag{80}$$

where X^f is a fourth order tensor similar to X^m expressed by eq. (69). Y^f is obtained in a similar approach to that of the matrix, Y^m, and has a similar form, except replacing the superscript m with f.

Interfacial damage evolution

The interfacial damage can be defined in terms of a second order symmetric tensor ϕ^d such as[6]

$$\phi_{ij}^d = \phi^d(S, \tilde{S}). \tag{81}$$

More elaborate interfacial damage expressions could be derived based on the work of Levy[12]. The corresponding power of dissipation due to interfacial damage is given by

$$\Pi^d = Y_{ij}^d \, d\phi_{ij}^d \tag{82}$$

and

$$\tilde{\Pi}^d = 0. \tag{83}$$

The function Ω^d is expressed as

$$\Omega^d = \Pi^d - \Lambda^d g^d \tag{84}$$

and

$$d\phi_{ij}^d = \Lambda^d \frac{\partial g^d}{\partial Y_{ij}^d}. \tag{85}$$

Using the consistency condition for the interfacial damage

$$dg^d = 0 \tag{86}$$

one obtains the evolution expression for ϕ^d such that

$$d\phi_{ij}^d = X_{ijkl}^d \, d\sigma_{kl}. \tag{87}$$

Similar to the procedure outlined for the other two types of damages Y^d could be easily obtained accordingly, such as

$$Y_{ij}^d = \frac{1}{2}(\sigma_{cd} \tilde{E}_{abpq}^{-1} M_{pqkl}^d \sigma_{kl} + \sigma_{rs} M_{uvrs}^d \tilde{E}_{uvab}^{-1} \sigma_{cd}) \frac{\partial M_{abcd}^d}{\partial \phi_{ij}^d}. \tag{88}$$

CONSTITUTIVE MODEL FOR THE DAMAGED MATERIAL

Derivation of the elasto-plastic constitutive model for the damaged composite system is performed in three steps. The first step involves the derivation of separate constitutive equations for the matrix and fiber in their respective damaged configurations $\bar{C}^m$ and $\bar{C}^f$. This is followed by the second step which combines the two constitutive equations into one for the overall composite system in its partial effective configuration $\bar{C}$. Finally, the interfacial damage is incorpor-

ated in order to obtain the final constitutive equation that includes all three types of damage in the damaged configuration C.

The local damaged elastic stiffness tensors $\tilde{E}^m$ and $\tilde{E}^f$ in the subconfigurations $\tilde{C}^m$ and $\tilde{C}^f$, respectively, are obtained using the hypothesis of complemental energy equivalence such that

$$\tilde{E}^m_{ijkl} = M^{-m}_{mnij} \bar{E}^m_{mnpq} M^{-m}_{pqkl} \tag{89}$$

and

$$\tilde{E}^f_{ijkl} = M^{-f}_{mnij} \bar{E}^f_{mnpq} M^{-f}_{pqkl}. \tag{90}$$

In order to obtain the damaged elasto-plastic stiffness of the matrix constituent, one needs to transform eq. (8) from the undamaged matrix configuration $\bar{C}^m$ to the damaged matrix configuration $\tilde{C}^m$. This is performed through the material time differentiation of eq. (24) together with strain rate counterpart obtained from eqs (49) and (56), such that

$$d\tilde{\epsilon}^m_{ij} = dM^{-m}_{ijkl} \bar{\epsilon}^{m'}_{kl} + M^{-m}_{ijkl} d\bar{\epsilon}^m_{kl}. \tag{91}$$

The time rate of the matrix damage tensor used in the material time differentiation of eq. (24) and its inverse used in eq. (91) may be expressed as shown below by making use of eq. (69)

$$dM^m_{ijkl} = \frac{\partial M^m_{ijkl}}{\partial \phi^m_{pq}} X^m_{pqrs} d\bar{\sigma}^m_{rs} \tag{92}$$

$$dM^{-m}_{ijkl} = \frac{\partial M^{-m}_{ijkl}}{\partial \phi^m_{pq}} X^m_{pqrs} d\bar{\sigma}^m_{rs}. \tag{93}$$

Making use of eqs (24) and (91)–(93), one obtains the resulting elasto-plastic stiffness relation for the damage matrix constituent

$$\tilde{D}^m_{ijkl} = O^{-m}_{pqij} \bar{D}^m_{pqrs} M^{-m}_{rskl}, \tag{94}$$

where

$$O^m_{ijkl} = \frac{\partial M^m_{ijkl}}{\partial \phi^m_{pq}} X^m_{pqmn} \bar{\sigma}^m_{mn} + M^m_{ijkl} - \bar{D}^m_{ijmn} \frac{\partial M^{-m}_{mnpq}}{\partial \phi^{-m}_{rs}} X^m_{rskl} \tilde{E}^{-m}_{pqab} \bar{\sigma}^m_{ab}. \tag{95}$$

The overall response of the composite system in the partial effective configuration, $\bar{C}$, is given by

$$d\bar{\sigma}_{ij} = \bar{D}_{ijkl} d\bar{\epsilon}_{kl}. \tag{96}$$

The resulting equation for $\bar{D}$ is given by[6]

$$\bar{D}_{ijkl} = \bar{C}^m \tilde{D}^m_{ijpq} \bar{A}^m_{pqkl} + \bar{C}^f \tilde{D}^f_{ijpq} \bar{A}^f_{pqkl}. \tag{97}$$

The overall damage response of the composite system is obtained from eq. (96) by applying the interfacial damage effect tensor M^d. Using the following relations

$$d\bar{\sigma}_{ij} = dM^d_{ijkl} \sigma_{kl} + M^d_{ijkl} d\sigma_{kl} \tag{98}$$

and

$$d\bar{\epsilon}_{ij} = dM^{-d}_{ijkl} \epsilon'_{kl} + M^{-d}_{ijkl} d\epsilon_{kl}, \tag{99}$$

we obtain the damage elasto-plastic constitutive relation including both the local damages, ϕ^f and ϕ^m, as well as the interfacial damage ϕ^d. Similarly, the rates of the debonding damage effect tensor used in eq. (98) and its inverse used in eq. (99) are

given as follows by making use of eq. (87)

$$dM^{d}_{ijkl} = \frac{\partial M^{d}_{ijkl}}{\partial \phi^{d}_{pq}} X^{d}_{pqrs} \, d\sigma_{rs} \tag{100}$$

and

$$dM^{-d}_{ijkl} = \frac{\partial M^{-d}_{ijkl}}{\partial \phi^{d}_{pq}} X^{d}_{pqrs} \, d\sigma_{rs}. \tag{101}$$

Finally, one obtains the damage elasto-plastic constitutive relation including both the local damages, ϕ^{f} and ϕ^{m}, as well as the interfacial damage ϕ^{d}. Making use of eqs (96)–(101) one obtains

$$d\sigma_{ij} = D_{ijkl} \, d\epsilon_{kl}, \tag{102}$$

where the damage elasto-plastic stiffness of the material is given by

$$D_{ijkl} = O^{-d}_{pqij} \bar{D}_{pqrs} M^{-d}_{rskl} \tag{103}$$

and

$$O^{d}_{ijkl} = \frac{\partial M^{d}_{ijkl}}{\partial \phi^{d}_{pq}} X^{d}_{pqmn} \sigma_{mn} + M^{d}_{ijkl} - \bar{D}_{ijmn} \frac{\partial M^{-d}_{mnpq}}{\partial \phi^{d}_{rs}} X^{d}_{rskl} E^{-1}_{pqab} \sigma_{ab}. \tag{104}$$

The elastic stiffness for the damage composite E is given such that

$$E_{ijkl} = M^{-d}_{mnij} \bar{E}_{mnpq} M^{-d}_{pqkl}, \tag{105}$$

where the elastic stiffness in the partial effective configuration $\bar{C}$ is given as follows:

$$\bar{E}_{ijkl} = \bar{c}^{m} \bar{E}^{m}_{ijpq} \bar{A}^{me}_{pqkl} + \bar{c}^{f} \bar{E}^{f}_{ijpq} \bar{A}^{fe}_{pqkl}. \tag{106}$$

COORDINATE TRANSFORMATION

The three-dimensional damage elasto-plastic constitutive equation for single lamina referring to the principal material coordinate system has been introduced in eq. (102). The general three-dimensional constitutive relation of a composite lamina referring to the off-axis coordinate system denoted by prime "'" can be obtained from eq. (102) by coordinate transformation. Here, the x–y plane coincides with the x_1–x_2 plane, and the angle between the x_1 and x axis is θ. The stress and strain vectors in those two coordinate systems are related by

$$\{d\sigma\} = [T]\{d\sigma\}'$$

$$\{d\epsilon\} = [T]\{d\epsilon\}', \tag{107}$$

where [T] is a transformation matrix given by

$$[T] = \begin{bmatrix} \cos\theta^{2} & \sin\theta^{2} & 0 & -2\cos\theta\sin\theta & 0 & 0 \\ \sin^{2}\theta & \cos^{2}\theta & 0 & 2\cos\theta\sin\theta & 0 & 0 \\ 0 & 0 & 1 & 0 & 0 & 0 \\ \cos\theta\sin\theta & -\cos\theta\sin\theta & 0 & \cos^{2}\theta - \sin^{2}\theta & 0 & 0 \\ 0 & 0 & 0 & 0 & \cos\theta & \sin\theta \\ 0 & 0 & 0 & 0 & -\sin\theta & \cos\theta \end{bmatrix}. \tag{108}$$

Substituting eq. (107) into eq. (102), we obtain the relation

$$\{d\sigma\}' = [T]^{-1}[D][T]\{d\epsilon\}'. \tag{109}$$

Thus, the damage elasto-plastic stiffness matrix referring to the off-axis coordinate x–y–z system is

$$[D]' = [T]^{-1}[D][T].$$ (110)

The constitutive equation for the plane stress problem is obtained from imposing the plane stress conditions $\sigma_{zz} = \sigma_{xz} = \sigma_{yz} = 0$ to eq. (109). The explicit expression of constitutive equation for plane stress is as follows:

$$\begin{Bmatrix} d\sigma_{xx} \\ d\sigma_{yy} \\ d\sigma_{xy} \end{Bmatrix} = \begin{bmatrix} D_{11}^* & D_{12}^* & D_{13}^* \\ D_{21}^* & D_{22}^* & D_{23}^* \\ D_{31}^* & D_{32}^* & D_{33}^* \end{bmatrix} \begin{Bmatrix} d\epsilon_{xx} \\ d\epsilon_{yy} \\ 2d\epsilon_{xy} \end{Bmatrix},$$ (111)

where

$$D_{11}^* = D_{11}' - D_{13}' \times D_{31}'/D_{33}'$$

$$D_{12}^* = D_{12}' - D_{13}' \times D_{32}'/D_{33}'$$

$$D_{21}^* = D_{21}' - D_{23}' \times D_{31}'/D_{33}'$$

$$D_{13}^* = D_{14}' - D_{13}' \times D_{36}'/D_{33}'$$

$$D_{31}^* = D_{41}' - D_{43}' \times D_{31}'/D_{33}'$$

$$D_{22}^* = D_{22}' - D_{23}' \times D_{32}'/D_{33}'$$

$$D_{23}^* = D_{24}' - D_{23}' \times D_{34}'/D_{33}'$$

$$D_{32}^* = D_{42}' - D_{43}' \times D_{32}'/D_{33}'$$

$$D_{33}^* = D_{44}' - D_{43}' \times D_{34}'/D_{33}'.$$ (112)

GROSS DAMAGE ELASTO-PLASTIC STIFFNESS

The elasto-plastic damage stiffness tensor for a single lamina in its principal material coordinate system has been presented in eq. (103). This stiffness tensor is transformed to the loading coordinate system and expressed as $[D]_k$ in matrix form. A symmetric stacking of plies is considered here such that t is the thickness of the laminate consisting of n plies and t_k is the thickness of the kth lamina. The average stress increment is expressed as follows (in vector form):

$$\{d\sigma\}_{ave} = \left[\frac{1}{t} \sum_{k=1}^{n} [D^*]_k t_k \right] \{d\epsilon\}.$$ (113)

Making use of eq. (113), one can define the gross damage elasto-plastic stiffness for the laminated composite as follows in matrix form:

$$[D_g] = \left[\frac{1}{t} \sum_{k=1}^{n} [D^*]_k t_k \right].$$ (114)

Making use of the assumption of constant strain through the laminate thickness, the stresses in each lamina are calculated as follows:

$$\{d\sigma\}_k = [\mathbf{D}^*]_k \{d\epsilon\}. \tag{115}$$

FINITE ELEMENT FORMULATION

The governing equation of the finite element method can be derived from the principle of virtual work such as

$$\int_V \sigma_{ij}\delta\epsilon_{ij}\,dV = \int_V q_i\delta u_i\,dV + \int_A t_i\delta u_i\,dA, \tag{116}$$

where δu_i is a field of virtual displacements that is compatible with applied forces and $\delta\epsilon_{ij}$ is the corresponding field of compatible virtual strains given by

$$\delta\epsilon_{ij} = \frac{1}{2}\left[\frac{\partial(\delta u_i)}{\partial x_j} + \frac{\partial(\delta u_j)}{\partial x_i}\right], \tag{117}$$

and q_i and t_i are body forces and surface tractions, respectively. For a small deformation analysis, we have

$$u_i = N_{ij}U_j \tag{118}$$

$$\delta u_i = N_{ij}(\delta U_j), \tag{119}$$

where U_j is the displacement of nodal points and N_{ij} is the displacement interpolation function or the shape function.

Substituting eqs (117) and (119) into eq. (116), one obtains the equilibrium equations as follows:

$$\int_V \sigma_{ij}\frac{\partial N_{ia}}{\partial x_j}\,dV = \int_V q_i N_{ia}\,dV + \int_A t_i N_{ia}\,dA. \tag{120}$$

One finally obtains the incremental equilibrium equations by differentiating both sides of eq. (120)

$$[\mathbf{K}]\{dU\} = \{dP\}, \tag{121}$$

where $\{dU\}$ is the unknown incremental displacement vector of the nodal points and $\{dP\}$ is the corresponding incremental nodal forces given by

$$dP_a = \int_V dq_i N_{ia}\,dV + \int dt_i N_{ia}\,dA, \tag{122}$$

where dq_i is the incremental body force and dt_i is the incremental surface traction. In eq. (121), $[\mathbf{K}]$ is the stiffness matrix which is given by

$$K_{ab} = \int_V \frac{\partial N_{ia}}{\partial x_j} D_{ijkl} \frac{\partial N_{kb}}{\partial x_\ell} \, dV. \tag{123}$$

The incremental equilibrium eq. (121) expresses the equilibrium between the internal forces $\{dF\}$ (on the left-hand-side) and the external force $\{dP\}$ (on the right-hand-side). The residual force vector $\{dR\}$ is defined by

$$\{dR\} = \{dP\} - \{dF\}. \tag{124}$$

In a damage elastic–plastic analysis, because of the nonlinear relationship between the stress and strain, the equilibrium eq. (121) is a nonlinear equation of strains, and therefore, is a nonlinear function of the nodal displacement. Iterative methods are usually employed to solve eq. (121) for displacements corresponding to a given set of external loads. Moreover, since a damage elasto-plastic constitutive relation depends on deformation history, an incremental analysis following an actual variation of external forces is used to trace the variation of displacement, strain, stress and damage along with the external forces.

In an incremental analysis, the total load $\{P\}$ acting on a structure is added in increments step by step. At the $(n + 1)$th step, the load can be expressed as

$$^{n+1}\{P\} = {}^n\{P\} + {}^{n+1}\{dP\}, \tag{125}$$

where the left superscript n indicates the nth incremental step. Assuming that the solution at the nth step, $^n\{u\}$, $^n\{\sigma\}$, $^n\{\epsilon\}$ and $^n\{\phi\}$ is known, and at the $(n + 1)$th step, one obtains the following, corresponding to the load increment $\{dP\}$,

$$^{n+1}\{u\} = {}^n\{u\} + \{du\} \tag{126}$$

$$^{n+1}\{\sigma\} = {}^n\{\sigma\} + \{d\sigma\} \tag{127}$$

$$^{n+1}\{\epsilon\} = {}^n\{\epsilon\} + \{d\epsilon\} \tag{128}$$

$$^{n+1}\{\phi\}^r = {}^n\{\phi\}^r + \{d\phi\}, \quad r = m, f, d. \tag{129}$$

SOLUTION

A full Newton–Raphson method is used in this work to solve the system of nonlinear equations that arise from the equilibrium equations. A brief description of the method is given by Voyiadjis [13]. The incremental analysis technique described in this chapter is successfully implemented into the finite element program NDA (Nonlinear Damage Analysis) using the above described iterative method. The steps involved in the process of solving are briefly described below.

(1) INCREMENT: Loop for each load increment

    (1) Calculate the load or applied displacement increment for the current incremental step or input the load/applied displacement increment.

    (2) ITERATE: Loop for full Newton–Raphson iteration:

        (1) Compute the residual load vector for this iteration subtracting the equilibrium load from the load computed for the increment.

        (2) Rotate the appropriate loads and applied displacements such that the degrees of freedom at the skew boundary (a boundary condition that is not along the global coordinate system) are normal and tangential to the skew boundary.

        (3) Assemble the stiffness matrices and find the equivalent loads for the applied incremental displacements. Since explicit integration is difficult, Gaussian points are used to evaluate the above integrals.

        (4) Solve for the incremental displacements using a linear solver.

(5) Add the solved iterative incremental displacements to the applied incremental displacements to obtain the complete iterative incremental displacements.

(6) Rotate back the complete iterative incremental displacements at the skew boundaries to the global coordinate system.

(7) Cumulate the complete iterative incremental displacements to the total incremental displacements.

(8) Find the stresses due to the iterative incremental displacements. From the iterative deformation gradient and the stresses updated, compute the updated constitutive matrix **D**. From the total incremental displacements accumulated so far and the **D** matrix, calculate the equilibrium load vector.

(9) Check if the convergence of solution is met using a particular convergence criterion. If convergence has not occurred, go back to the step ITERATE.

(10) If divergence occurs according to the convergence criterion, then reduce the load increment appropriately as specified by the user and start the iterative solution over again for that load increment.

(11) If divergence occurs for a load increment that has been reduced "*m*" times (specified by the user), then report "convergence not met" and leave the solution phase.

(12) If convergence has occurred, then perform the following operations before going for the next increment.

    (1) Update the nodal positions by adding the currently obtained incremental displacements.

    (2) Transform the quantities pertaining to the material property to the present configuration.

    (3) Print out the appropriate quantities pertaining to the converged increment according to the user's specifications.

    (4) If the total load is not reached, go back to the step INCREMENT.
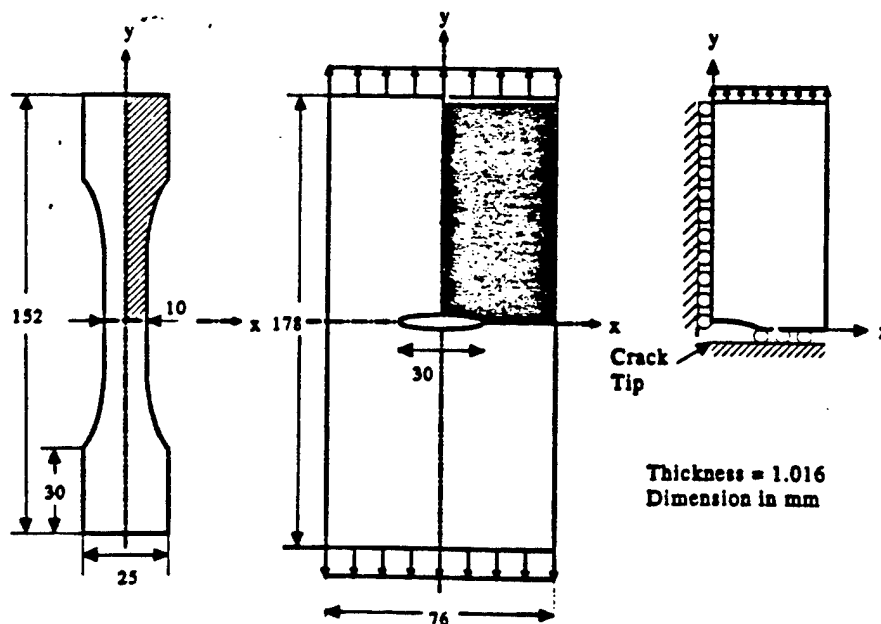
Fig. 1. Dog-bone shaped specimen and center-cracked laminate plate.
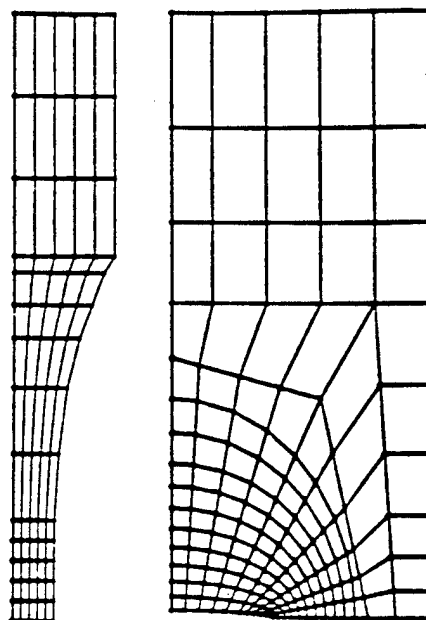
Fig. 2. Finite element meshes.

STRESS AND DAMAGE COMPUTATIONS

(1) Step 1. Retrieve σ_{ij}, σ_{ij}^r, ϕ_{ij}^r. Retrieve also the information whether the previous loading was a damage loading or not (IDAMG) and plastic loading or not (TYILD).

    (1) If IDAMG = 0 when retrieved, then evaluate the incremental elastic-predictor stress σ_{ij}^p assuming that the loading is elastic. Use the undamaged elastic stiffness matrix for the calculation ($d\sigma_{ij}^p = \bar{E}_{ijkl}\, d\epsilon_{kl}$).

    (2) If IDAMG $\neq$ 0 when retrieved, use ($d\sigma_{ij}^p = E_{ijkl}\, d\epsilon_{kl}$).

    (3) Calculate the incremental elastic-predictor stress of matrix constituent $d\sigma_{ij}^{mp}$.

    (4) Check if the predicted stress state of matrix constituent is inside the yield surface or not.

Table 1. Material properties

	Matrix (Ti–14Al–21Nb)	Fiber (SiC)
Modulus	8×10^4 MPa	41×10^4 MPa
Poisson's ratio	0.30	0.22
Initial volume fraction	0.65	0.35
Yielding stress $\bar{\sigma}_o^m$	360 MPa	
Kinematic hardening parameter b	90 MPa	

Table 2. Local damage parameters

	Matrix damage	Fiber damage	Interfacial damage
η_1	0.08	0.06	0.075
η_2	0.08	0.06	0.065
η_3	0.08	0.06	0.065
ξ_1	0.65	0.55	0.55
ξ_2	0.65	0.55	0.70
ξ_3	0.65	0.55	0.70
ν_1	0.003	0.007	0.008
ν_2	0.003	0.007	0.001
ν_3	0.003	0.007	0.001
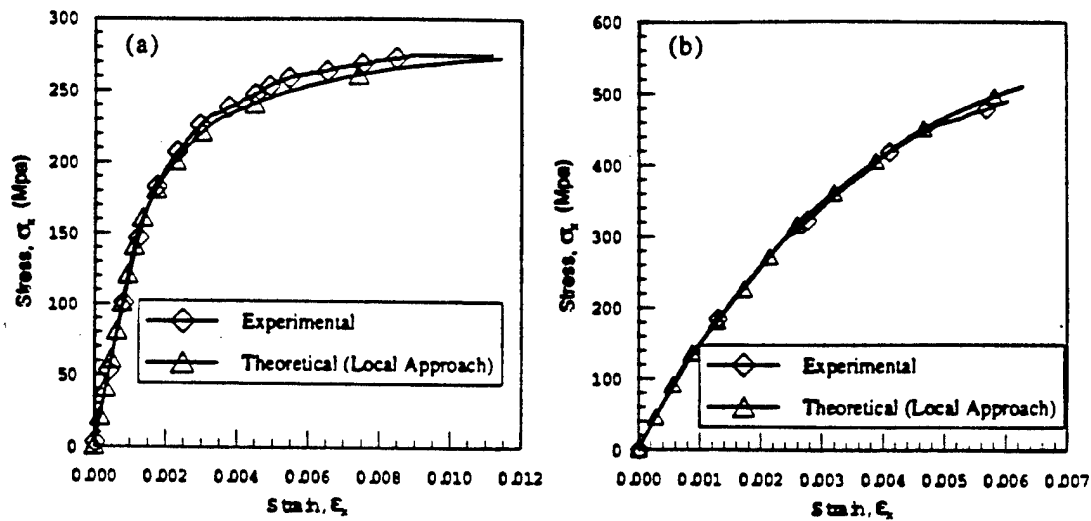
Fig. 3. (a) Stress–strain curves of [±45]s layup. (b) Stress–strain curves of [0/90]s layup.

(5) If the stress state of matrix constituent is inside the yield surface then:

    (1) Assign elastic stiffness to the constitutive stiffness and the predictor stress increment to the actual computed stress increment.

    (2) Set IYILD = 0 indicating the elastic loading has taken place.

    (3) Exit to Step 2. Otherwise, go to the next step.

    (4) Set IYILD = 1, then:

        (1) Calculate the elasto-plastic stiffness D (when IDAMG = 1) or $\bar{D}$ (when IDAMG = 0).

        (2) Update the quantities σ_{ij}, σ_{ij}^m, σ_{ij}^f, α_{ij}^m.
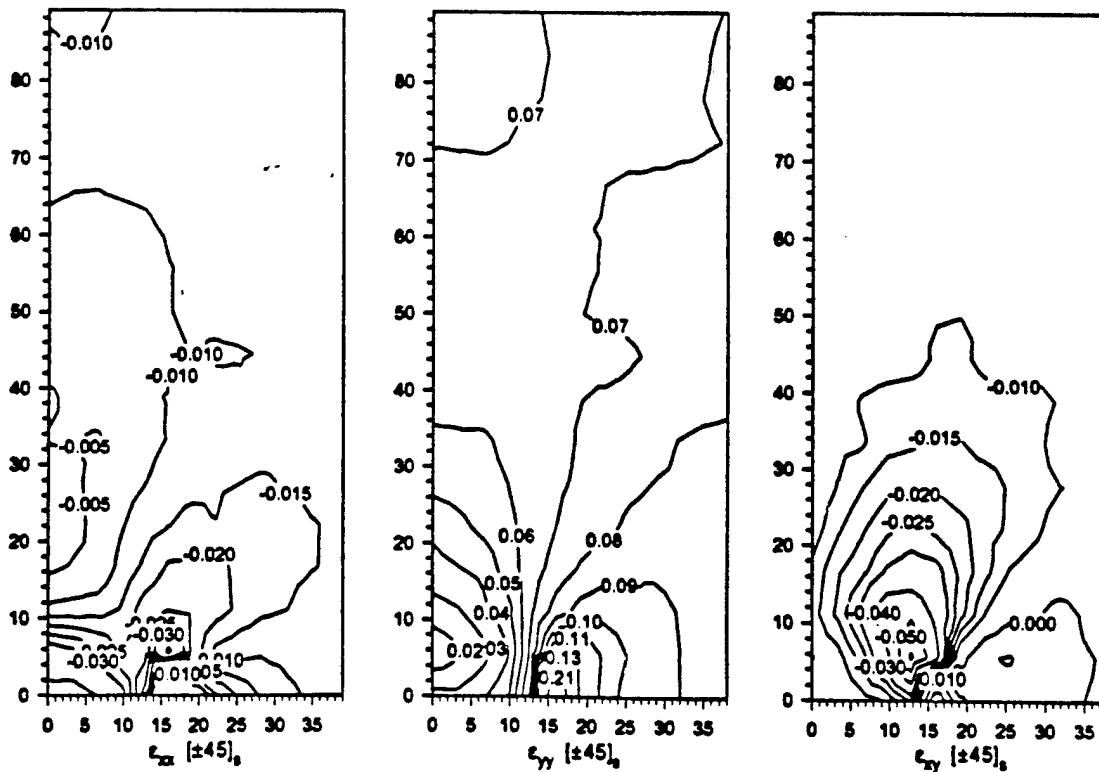
Fig. 4. Strain contours for [±45]s layup (in %).
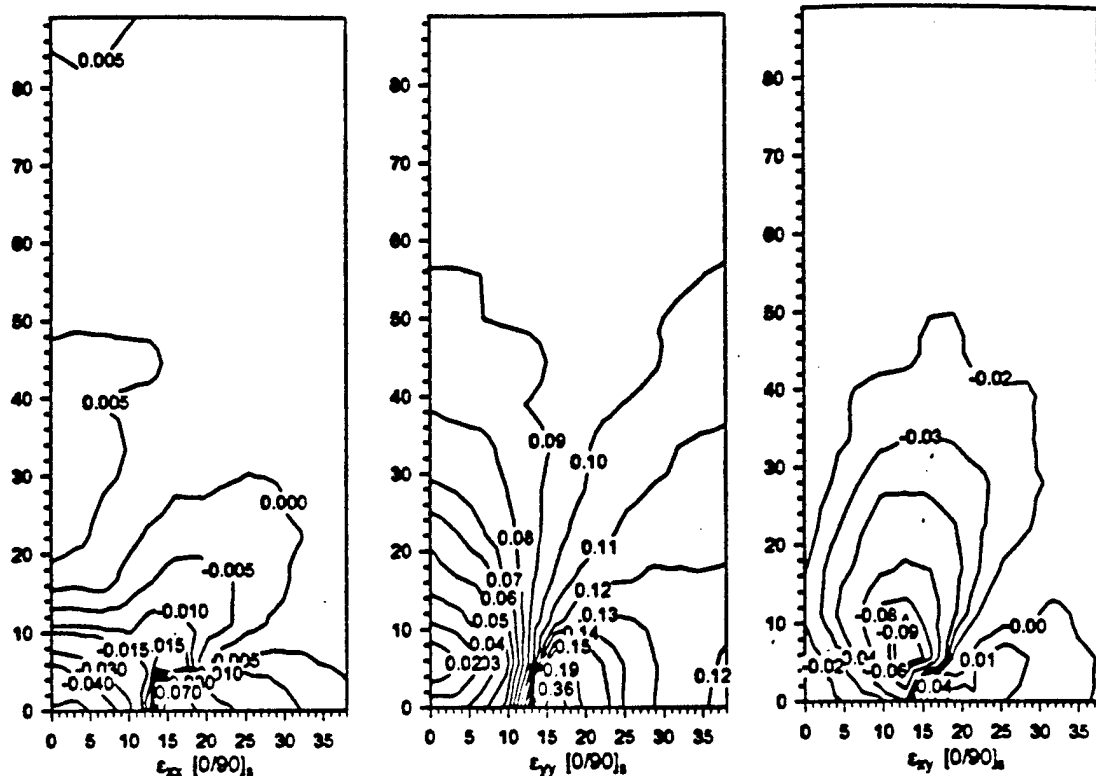
Fig. 5. Strain contours for [0/90]$_s$ layup (in %).

(2) Step 2

   (1) Check the damage criteria using the updated quantity σ_{ij}^r.

   (2) If damage criteria $g^r < 0$, then IDAMG = 0. Exit from the routines.

   (3) If damage criteria $g^r > 0$, then IDAMG = 1. Calculate the damage increment $d\phi^r$ and update damage quantity ϕ^r.

   (4) Store the updated quantities in a file.

APPLICATION TO THE DOG-BONE SHAPED SPECIMEN AND THE CENTER-CRACKED LAMINATED PLATES

The finite element method is used for solving a dog-bone shaped specimen and a center-cracked laminate plate shown in Fig. 1 that is subjected to inplane tension. Due to symmetry in geometry and loading as shown in Fig. 1, one-quarter of the plate needs to be analyzed. Two-dimensional plane stress analysis rather than three-dimensional analysis is used here since the thickness of plate is much smaller than the other dimensions. Applying the appropriate boundary conditions for the symmetry, both one-quarter of the center-cracked laminate plate and the dog-bone shaped specimen are discretized using plane stress finite elements. The finite element meshes chosen for analyzing the problems are shown in Fig. 2. The four-noded quadrilateral element is used in both finite element analyses.

Two types of laminate layups (±45)$_s$ and (0/90)$_s$ each consisting of four plies are used here. The thickness of each ply is equal to 0.254 mm. Since both layups are symmetric, no curvature is assumed. Hence, the strain through the plate thickness is assumed to be the same. The ma-
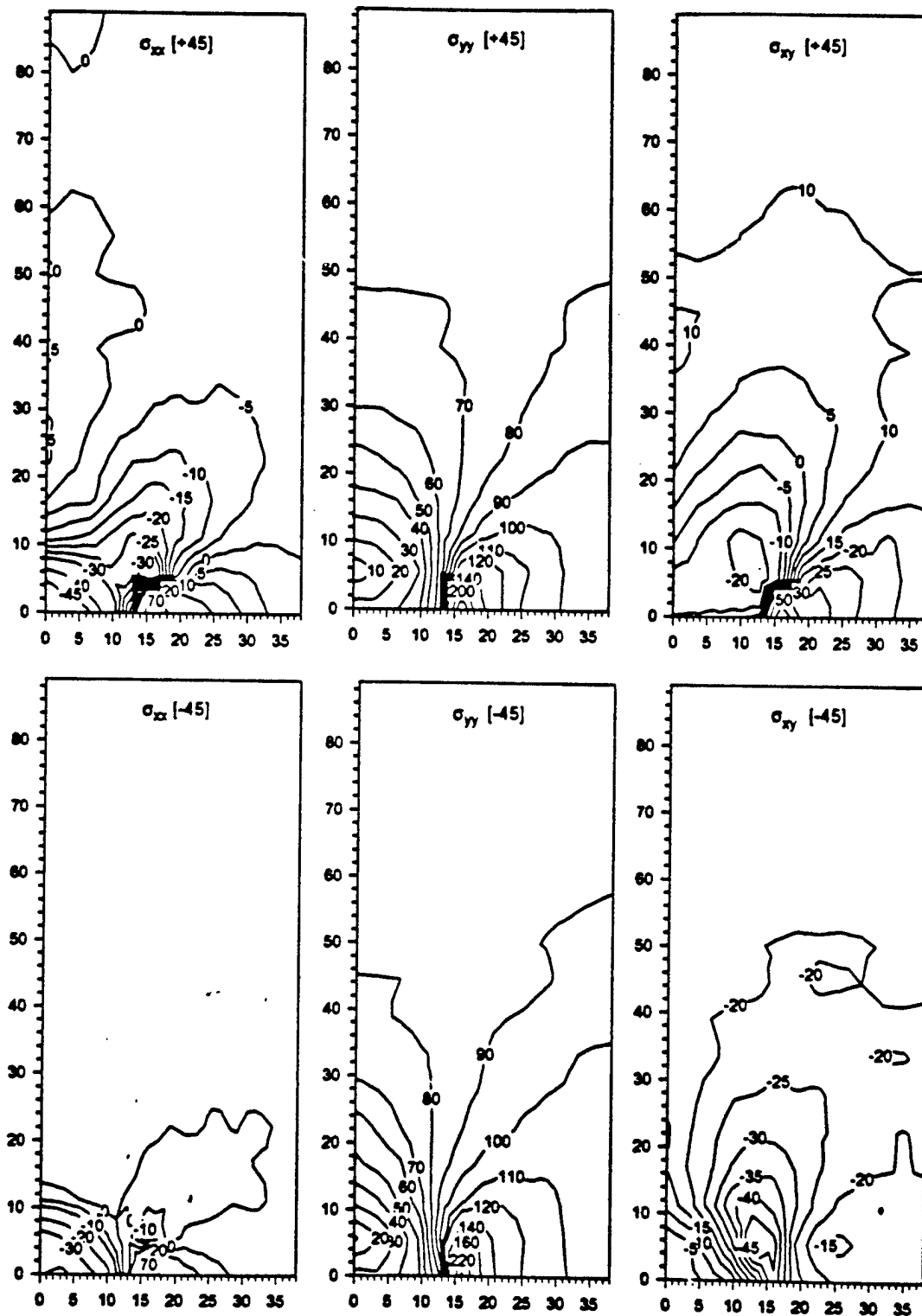
Fig. 6. Stress contours for [±45]$_s$ layup (units are in MPa).

terial properties and damage parameters using the proposed constitutive model are listed in Tables 1 and 2, respectively.

The following convergence criterion is used in this analysis which is based on the incremental internal energy for each iteration in that incremental loading[14]. It represents the amount of work done by the out-of-balance loads on the displacement increments. Comparison is made with the initial internal energy increment to determine whether or not convergence has occurred.
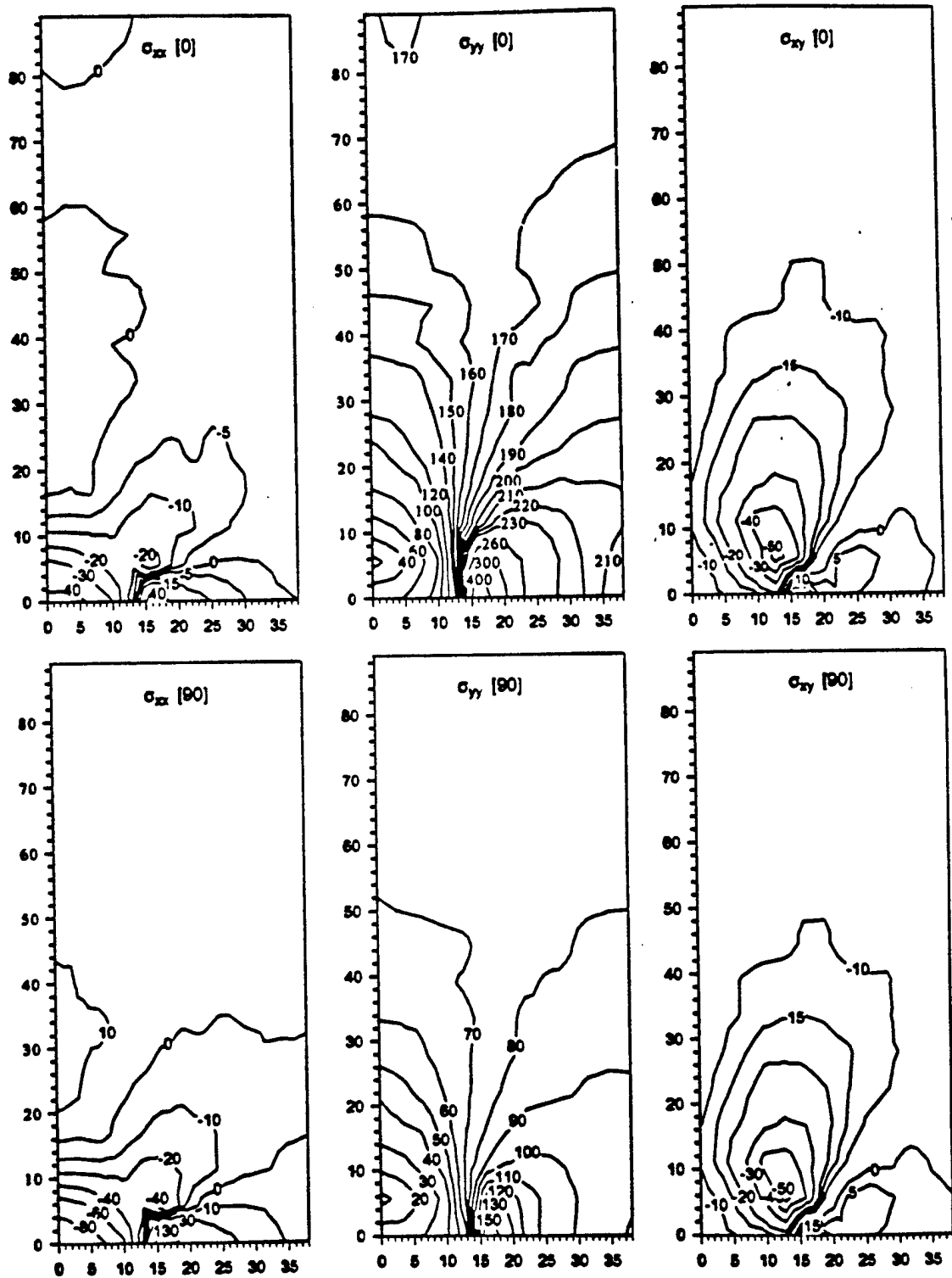
Fig. 7. Stress contours for [0/90]s layup (units are in MPa).

Convergence is assumed to occur if for an energy tolerance ϵ_E, the following condition is met:

$$\Delta U^{(i)}(^{n+1}R - {}^{n+1}F^{(i-1)}) \leq \epsilon_E(\Delta U^{(i)}(^{n+1}R - {}^nF)), \tag{130}$$

where $\Delta U^{(i)}$ is the incremental displacement residual at the (i)th iteration, $(^{n+1}R - {}^{n+1}F^{(i-1)})$ is the out-of-balance force vector at $(i-1)$ iteration and $(\Delta U^{(i)}(^{n+1}R - {}^nF))$ is the internal energy term for the (i)th iteration in the $(n+1)$th increment. Divergence is assumed to occur if the
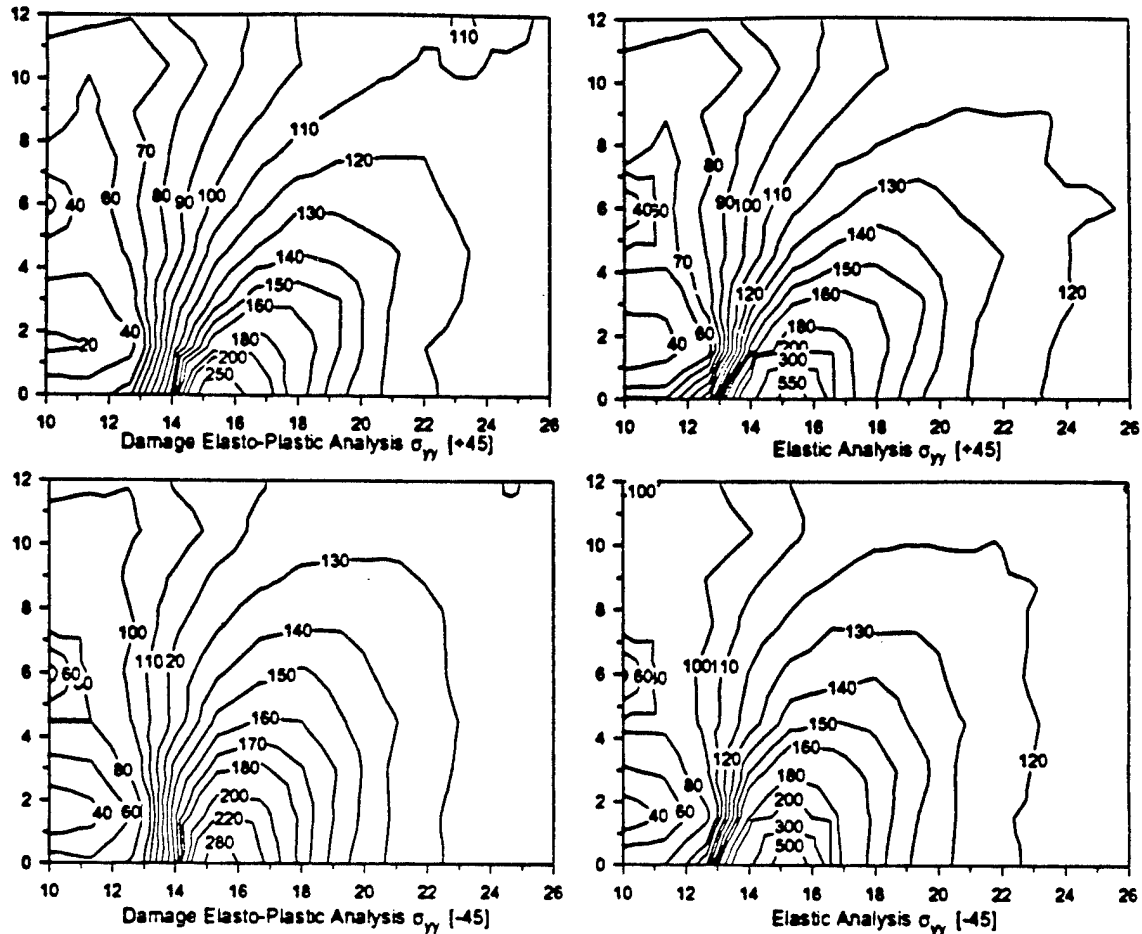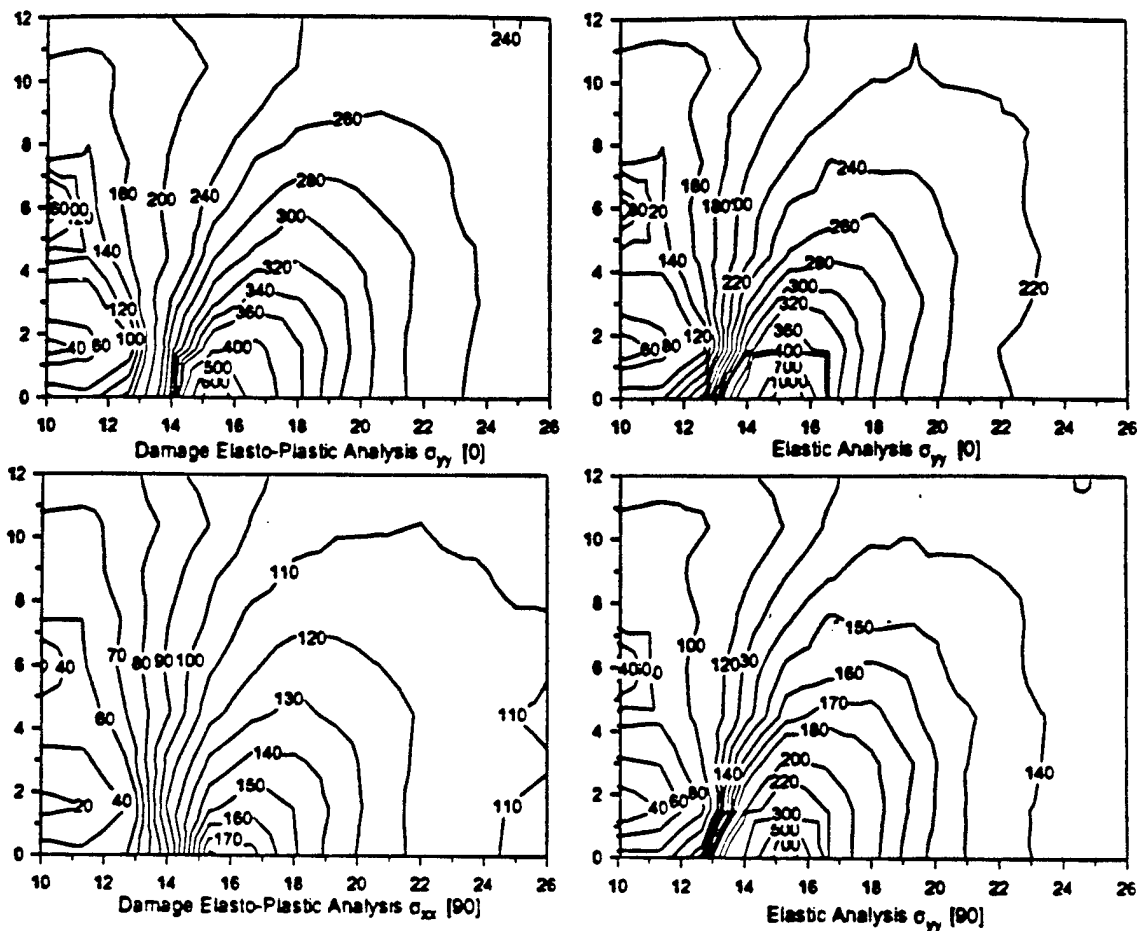
Fig. 8. Comparison of damage elasto-plastic analysis with elastic analysis of stress σ_{yy} contours around the crack tip for $(\pm 45)_S$ layup (units are in MPa).

out-of-balance internal energy for the $(i-1)$th iteration is greater than the out-of-balance internal energy for the (i)th iteration.

The load is incremented with uniform load increments of 5 MPa until the principal maximum local damage value ϕ_p^r reaches 1.0 ($\phi_p^r \geq 1.0$). The principal maximum local damage value ϕ_p^r is given by:

$$\phi_p^r = \frac{\phi_{11}^r + \phi_{22}^r}{2} + \sqrt{\left(\frac{\phi_{11}^r - \phi_{22}^r}{2}\right)^2 + \phi_{12}^{r2}}, \quad r = m, f, d. \tag{131}$$

Consequently, material failure at integration point is assumed when $\phi_p^r \geq 1$. The principal damage value of the integration point in all elements is monitored at each load increment since it is used to determine the onset of macro-crack initiation of the material.

The dog-bone shaped specimen failed when the final load of 270 MPa was reached for the $(\pm 45)_S$ layup and 480 MPa for the $(0/90)_S$ layup. These failure loads are close to the experimental failure loads 276 MPa for the $(\pm 45)_S$ layup and 483 MPa for the $(0/90)_S$ layup[15]. The material failure for the center-cracked specimen occurs at the front of the crack tip when the final load of 80 MPa is reached for the $(\pm 45)_S$ layup plate and 120 MPa for the $(0/90)_S$ layup plate.

DISCUSSION OF THE RESULTS

The stress–strain curves from both the finite element analyses and experiments of the two types of layups of the dog-bone shaped specimens are shown in Fig. 3. Good correlation is shown between the finite element analysis results and the experimental data obtained by Voyiadjis and Venson[15].

Fig. 9. Comparison of damage elasto-plastic analysis with elastic analysis of stress σ_{yy} contours around the crack tip for (0/90)$_s$ layup (units are in MPa).

Strain contours for the (±45)$_s$ layup and (0/90)$_s$ layup of the center cracked plates are shown in Figs 4 and 5, respectively. Since the two types of layups are symmetric, the strains in each laminae of the layup are the same. However, the stress and damage distributions are different for each laminae of the layup since each laminae has a different stiffness. Stress contours for each laminae are indicated in Fig. 6 for the (±45)$_s$ layup and Fig. 7 for the (0/90)$_s$ layup. In Figs 8 and 9, comparison is made between the damage analysis and the elastic analysis for the stress σ_{yy} contours around the crack tip. The damage analysis shows considerable stress reduction due to the damage around the crack tip. The stress σ_{yy} at the front of the crack tip as obtained from the elastic solution is higher than that of the material strength of the layup. However, in the damage elasto-plastic analysis, the stresses are reduced such that they are close to those of the material strength. The σ_{yy} stress reductions at the front of the crack tip are more than 50% for [±45], 40% for [0] ply and 80% for [90] ply. Stress redistributions are clearly indicated in Figs 8 and 9. Primarily due to the stress reduction around the crack tip, the stress is therefore transferred to the outer portion away from the crack tip. This is clearly indicated in Fig. 9 where the stress reduction at the 90° ply is primarily due to considerable interfacial damage.

The local damage contours around the crack tip are shown in Figs 10–13, for the failure loads in the case of [+45], [−45], [0], and [90] ply, respectively. For the [±45] layups, all types of damage such as matrix, fiber and interfacial are developed. Fiber damage is considerably more spread in the [0] ply than the interfacial damage. On the other hand, interfacial damage is more pronounced with matrix damage for the [90] ply. However, fiber damage is much less developed in the case of the [90] ply. This is in line with the experimental results obtained by Voyiadjis and Venson[15].
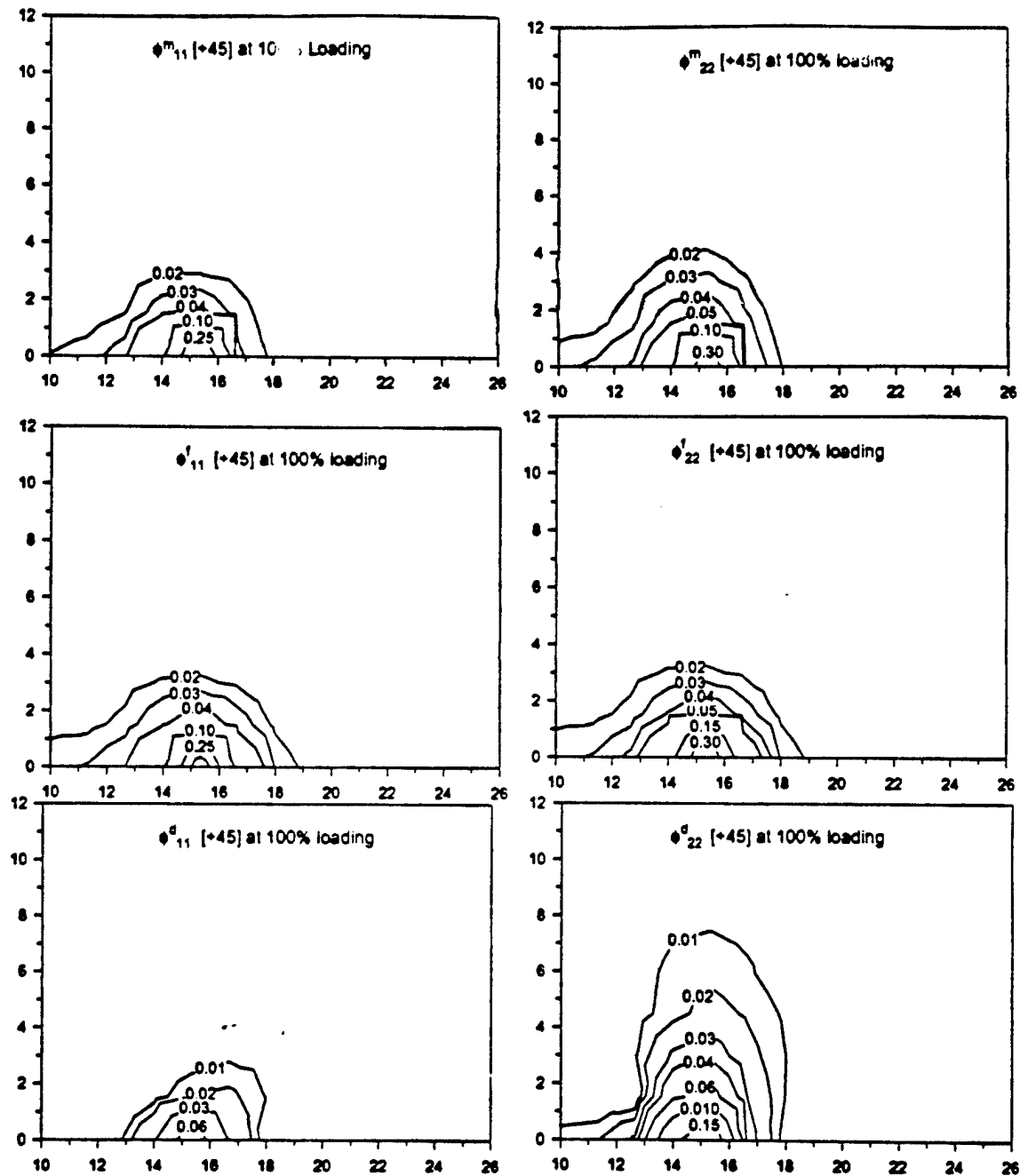
Fig. 10. Damage contours around crack tip at the failure load for [+45] lamina.

SUMMARY AND CONCLUSIONS

The proposed constitutive model is implemented numerically using the finite element method. The model is used to analyze the dog-bone shaped specimens and the center-cracked laminated plates subjected to inplane tensile forces. Very good correlations are demonstrated between the numerical results obtained using the proposed theories and the experimental results for uniaxial tension. The stress and damage contours in the case of the center cracked plate show that stress redistributions and damage are qualitatively in line with the physics of deformation. The analysis presented here allows the separate quantification of the different types of damages such as matrix, fiber or debonding.

Fig. 11. Damage contours around crack tip at the failure load for [−45] lamina.

element
-cracked
ınstrated
ıl results
ed plate
of defor-
types of
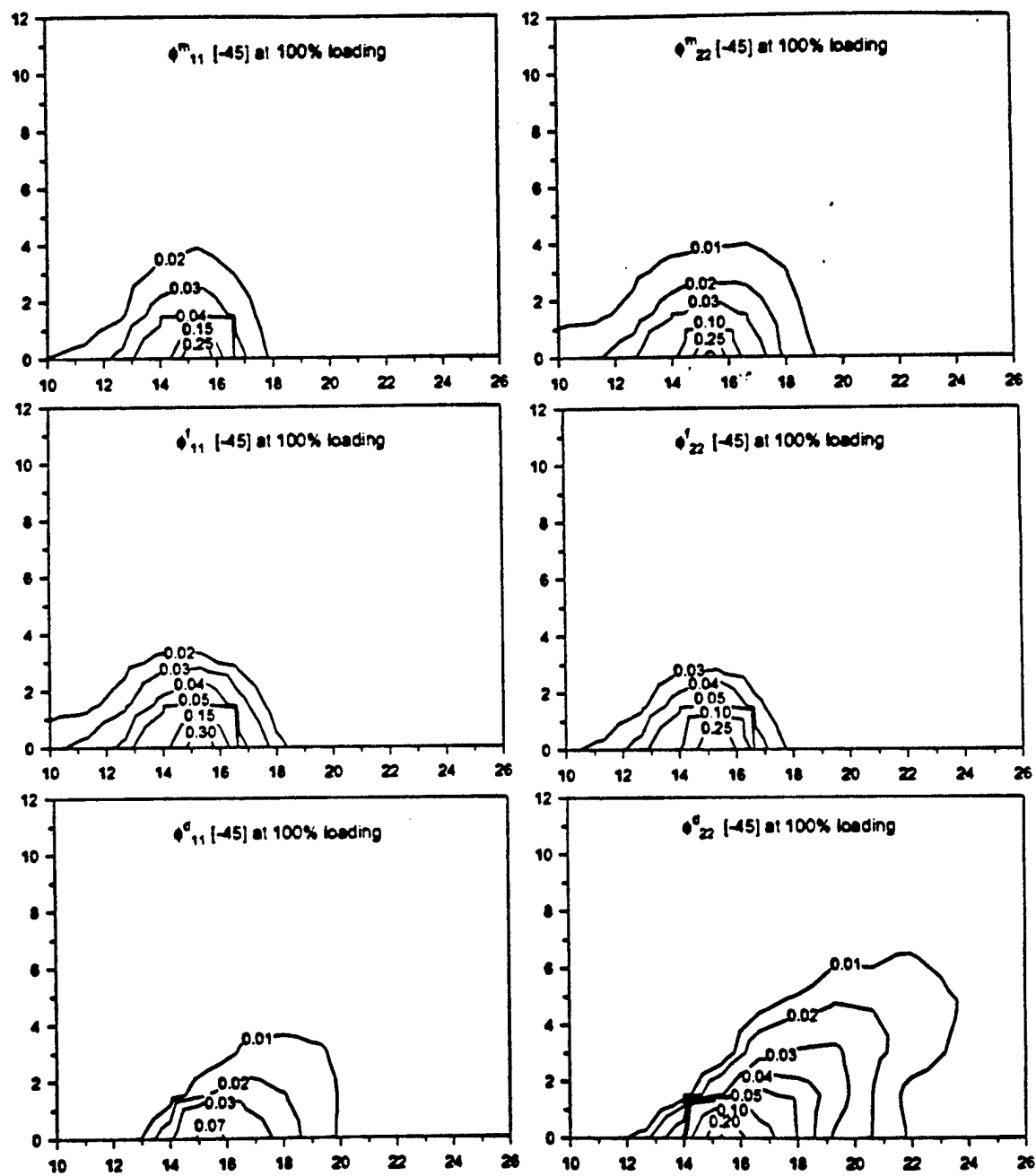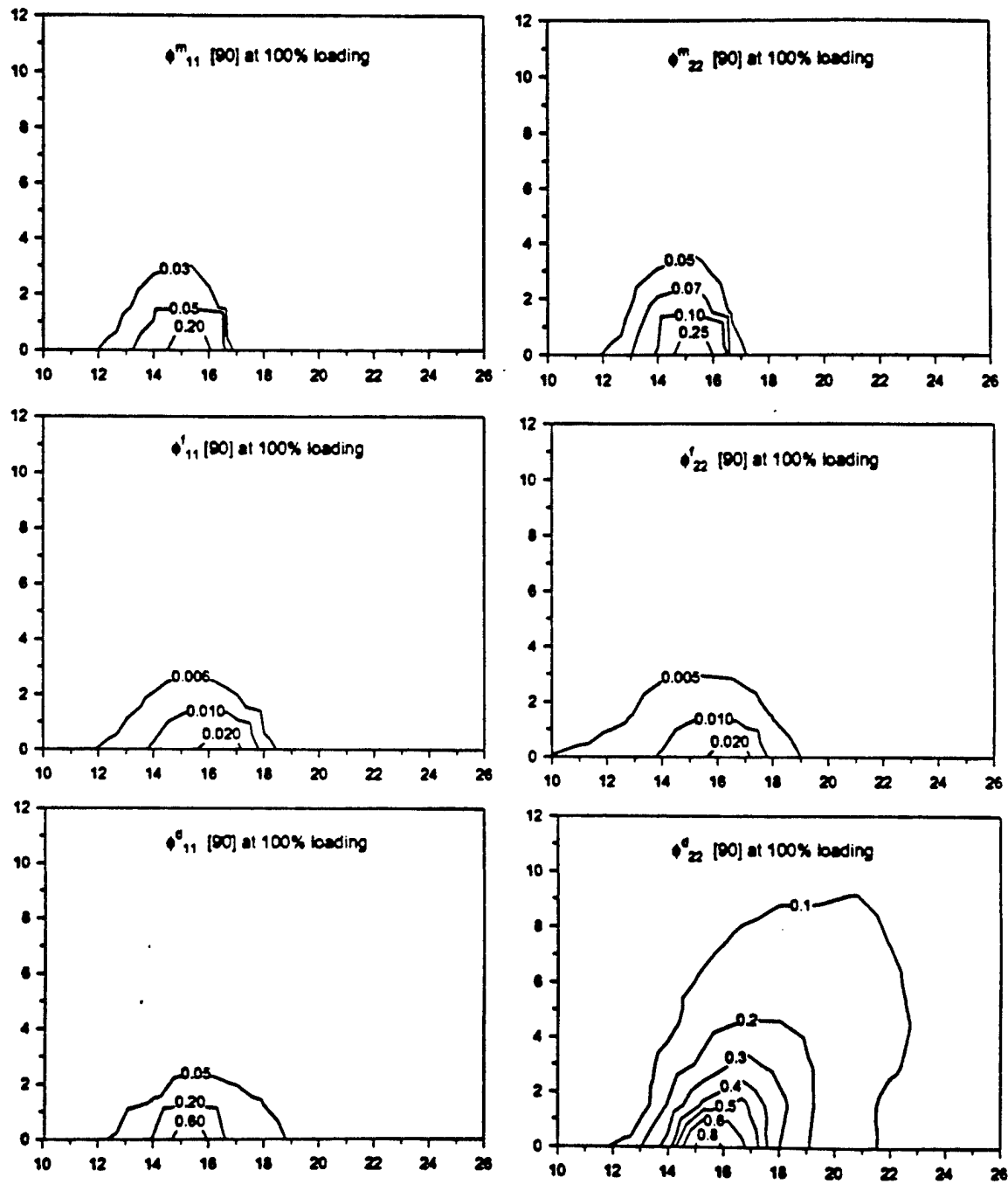
Fig. 12. Damage contours around crack tip at the failure load for [0] lamina.
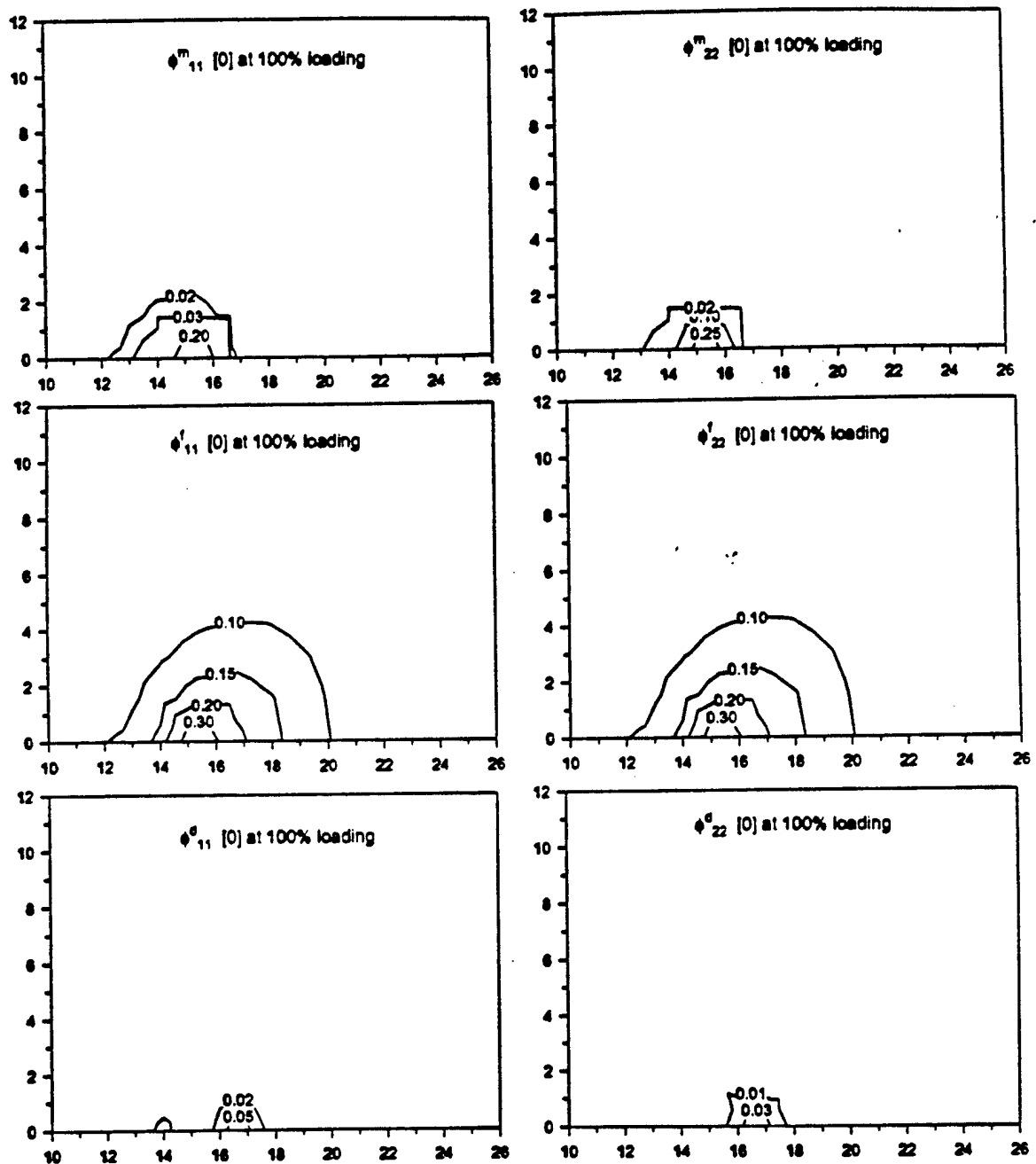
Fig. 13. Damage contours around crack tip at the failure load for [90] lamina.

The authors are currently working on damage due to delamination which will be introduced into the proposed model in future work. In order to capture delamination due to interlamina stresses, a three-dimensional, finite element analysis will be performed.

REFERENCES

1. Kachanov, L. M., On the creep fracture time. *Izv Akad. Nauk USSR Otd. Tekh.*, 1958, **8**, 26–31, in Russian.
2. Lemaitre, J., Evaluation of dissipation and damage in metals. *Proc. ICMI*, Kyoto, Japan, 1971.
3. Ziegler, H., A modification of Prager's hardening rule. *Q. appl. Math.*, 1959, **17**, 55–65.
4. Murakami, S., Mechanical modelling of material damage. *J. appl. Mech.*, 1988, **55**, 280–286.

5. Voyiadjis, G. Z. and Park, T., Anisotropic damage of fiber reinforced MMC using an overall damage analysis. *J. Engng Mech. ASCE*, 1995, 121(11), 1209–1217.

6. Voyiadjis, G. Z. and Park, T., Local and interfacial damage analysis of metal matrix composites. *Int. J. Engng Sci.*, 1995, 33(11), 1595–1621.

7. Voyiadjis, G. Z. and Kattan, P. I., A plasticity-damage theory for large deformation of solids. Part I: theoretical formulation. *Int. J. Engng Sci.*, 1992, 30, 1089–1108.

8. Mroz, Z., *Mathematical Models of Inelastic Material Behavior*. University of Waterloo, 1973, pp. 120–146.

9. Stumvoll, M. and Swoboda, G., Deformation behavior of ductile solids containing anisotropic. *J. Engng Mech., ASCE*, 1993, 119(7), 1331–1352.

10. Cordebois, J. P. and Sidoroff, F., Anisotropic damage in elasticity and plasticity. *J. de Mecanique Theorique et Applique*, 1982, 45–60.

11. Voyiadjis, G. Z. and Kattan, P. I., A continuum-micromechanics damage model for metal matrix composites. *Composite Material Technology* 1992, ASME, PD-Vol. 45, *Proceedings of the Composite Material Symposium of the Energy Technology Conference and Exposition*, Houston, Texas, 1992, pp. 83–95.

12. Levy, A. J., Decohesion at a circular interface. *Studies in Applied Mechanics*, Vol. 35, ed. G. Z. Voyiadjis, L. C. Bank and L. J. Jacobs. Elsevier, Amsterdam, 1994, pp. 173–192.

13. Voyiadjis, G. Z., Large elasto-plastic deformation of solids. Ph.D. Dissertation, Department of Civil Engineering and Engineering Mechanics, Columbia University, New York, NY, U.S.A., 1973.

14. Bathe, K., *Finite Element Procedures in Engineering Analysis*. Prentice-Hall, Englewood Cliffs, New Jersey, U.S.A., 1990.

15. Voyiadjis, G. Z. and Venson, A. R., Experimental damage investigation of a SiC–Ti aluminide metal matrix composite. *Int. J. Damage Mechanics*, 1995, 4(4), 338–361.

16. Chen, T., Dvorak, G. and Benvensite, Y., Mori–Tanaka estimates of the overall elastic moduli of certain composite materials. *J. appl. Mech.*, 1992, 59, 539–546.

APPENDIX A

Mori–Tanaka's strain and stress concentration tensors

The expressions for the elastic stress and strain concentration factors given here are based on the Mori–Tanaka method. In the recent paper by Chen *et al.*[16], the expressions for the elastic strain concentration factors $\bar{A}^r$ and the elastic stress concentration factors $\bar{B}^r$ are given by

$$\bar{A}^r_{ijkl} = \bar{A}^r_{ijpq}\bar{F}_{pqkl}, \quad r = m, f \tag{A1}$$

$$\bar{B}^r_{ijkl} = \bar{B}^r_{ijpq}\bar{G}_{pqkl}, \quad r = m, f, \tag{A2}$$

where

$$\bar{F}_{pqkl} = \bar{c}^m\bar{A}^m_{pqkl} + \bar{c}^f\bar{A}^f_{pqkl} \tag{A3}$$

$$\bar{G}_{pqkl} = \bar{c}^m\bar{B}^m_{pqkl} + \bar{c}^f\bar{B}^f_{pqkl}. \tag{A4}$$

The tensors $\bar{A}^r$ and $\bar{B}^r$ are termed the partial concentration factors for strain and stress, and are expressed in the following form:

$$\bar{A}^f_{pqkl} = [I_{pqkl} + \bar{P}_{pqrs}(\bar{E}^f_{rskl} - \bar{E}^m_{rskl})]^{-1} \tag{A5}$$

$$\bar{A}^m_{pqkl} = I_{pqkl} = \frac{1}{2}(\delta_{pk}\delta_{ql} + \delta_{pl}\delta_{qk}) \tag{A6}$$

$$\bar{B}^f_{pqkl} = [I_{pqkl} + \bar{Q}_{pqrs}(\bar{E}^{-f}_{rskl} - \bar{E}^{-m}_{rskl})]^{-1} \tag{A7}$$

$$\bar{B}^m_{pqkl} = I_{pqkl}. \tag{A8}$$

where $\bar{E}^f$ and $\bar{E}^m$ are the elastic stiffness tensors of the fiber and matrix, respectively. The tensors of $\bar{P}$ and $\bar{Q}$ depend only on the shape of the inclusion and the elastic moduli of the surrounding matrix. For example, for an inclusion in the shape of a circular cylinder in isotropic matrix, the tensor $\bar{P}$ written in matrix form (6 × 6 array) is given by

$$[\bar{P}] = \begin{bmatrix} 0 & 0 & 0 & 0 & 0 & 0 \\ 0 & \dfrac{a+4e}{8b(a+e)} & \dfrac{-a}{8b(a+e)} & 0 & 0 & 0 \\ 0 & \dfrac{-a}{8b(a+e)} & \dfrac{a+4e}{8b(a+e)} & 0 & 0 & 0 \\ 0 & 0 & 0 & \dfrac{1}{2e} & 0 & 0 \\ 0 & 0 & 0 & 0 & \dfrac{a+2e}{2b(a+e)} & 0 \\ 0 & 0 & 0 & 0 & 0 & \dfrac{1}{2e} \end{bmatrix} \tag{A9}$$

where

$$a = \frac{\bar{E}^m}{3(1-2\bar{\lambda}^m)} + \frac{\bar{G}^m}{3} \tag{A10}$$

$$e = \frac{\bar{E}^m}{2(1-\bar{\lambda}^m)}. \tag{A11}$$

where $\bar{E}^m$ is Young's modulus of the matrix, $\bar{\lambda}^m$ is the Poisson ratio of the matrix and $\bar{G}^m$ is the shear modulus of the matrix. The tensor $\bar{Q}$ in eq. (16) is given by

$$\bar{Q}_{ijkl} = \bar{E}^m_{ijkl} - \bar{E}^m_{ijpq}\bar{P}_{pqrs}\bar{E}^m_{rskl}. \tag{A12}$$

Anisotropic Damage Effect Tensors for the Symmetrization of the Effective Stress Tensor

G. Z. Voyiadjis
Boyd Professor, Mem. ASME.

T. Park
Research Associate.

Department of Civil and
Environmental Engineering,
Louisiana State University,
Baton Rouge, LA 70803

Based on the concept of the effective stress and on the description of anisotropic damage deformation within the framework of continuum damage mechanics, a fourth order damage effective tensor is properly defined. For a general state of deformation and damage, it is seen that the effective stress tensor is usually asymmetric. Its symmetrization is necessary for a continuum theory to be valid in the classical sense. In order to transform the current stress tensor to a symmetric effective stress tensor, a fourth order damage effect tensor should be defined such that it follows the rules of tensor algebra and maintains a physical description of damage. Moreover, an explicit expression of the damage effect tensor is of particular importance in order to obtain the constitutive relation in the damaged material. The damage effect tensor in this work is explicitly characterized in terms of a kinematic measure of damage through a second-order damage tensor. In this work, tensorial forms are used for the derivation of such a linear transformation tensor which is then converted to a matrix form.

Introduction

In 1958, Kachanov (Kachanov, 1958) introduced the concept of effective stress in damaged materials. This pioneering work started the subject that is now known as continuum damage mechanics. Research in this area has steadily grown and reached a stage that warrants its use in today's engineering applications. Continuum damage mechanics is now widely used in different areas including brittle (Krajcinovic, 1983; Krajcinovic and Foneska, 1981) and ductile failure (Lemaitre, 1985, 1986). In this theory, a continuous damage variable is defined and used to represent degradation of the material which reflects various types of damage at the microscale level like nucleation and growth of voids, cavities, microcrack, and other microscopic defects.

In continuum damage mechanics, the effective stress tensor is usually not symmetric. This leads to a complicated theory of damage mechanics involving micropolar media and the Cosserat continuum. Therefore, to avoid such a theory, symmetrization of the effective stress tensor is used to formulate a continuum damage theory in the classical sense. Several methods used in order to symmetrize the effective stress tensor are proposed by Lee et al. (1986) and Sidoroff (1979). A linear transformation tensor, defined as a fourth-order damage effect tensor, is proposed by Sidoroff (1979); however, no explicit form of this tensor is given. Moreover, damage tensor of higher order than two may fail to convey the physical meaning of damage. In addition, the works of Lee et al. (1986) and Sidoroff (1979) are confined to two-dimensional problems. Furthermore, no explicit expressions are derived for the fourth-order linear transformation tensors for the general anisotropic damage behavior of three-dimensional problems.

In this work, continuum damage mechanics will be reviewed based on the concept of effective stress. The effective stress is defined as the stress acting on a hypothetical undamaged configuration that produces the same elastic strain or elastic strain energy as the actual state of stress acting on the current damaged configuration based on the equivalence hypothesis. This equivalence statement is known as the hypothesis of elastic strain equivalence or the hypothesis of elastic energy equivalence. Using the definition of the effective stress and the hypothesis of elastic energy equivalence, one can solve for variable in the hypothetical undamaged configuration, such as the effective strain. However, strain in the hypothetical undamaged configuration is equal to that in the current damaged configuration under the hypothesis of elastic strain equivalence. For a detailed review of the principles of continuum damage mechanics as used in this work, the reader is referred to the works of Kachanov (1958), Lemaitre (1985, 1986), Krajcinovic (1985), Chaboche (1981, 1988a, b), Murakami (1988), Sidoroff (1979, 1980), and Voyiadjis and Kattan (1992).

In a general state of deformation and damage, the effective stress tensor $\bar{\sigma}$ is related to the stress tensor σ by the following linear transformation:

$$\bar{\sigma}_{ij} = M_{ijkl}\sigma_{kl} \qquad (1)$$

where σ is the Cauchy stress tensor and M is a fourth-order linear transformation operator called the damage effect tensor. Depending on the form used for M, it is very clear from Eq. (1) that the effective stress tensor $\bar{\sigma}$ is generally not symmetric. Using a nonsymmetric effective stress tensor as given by Eq. (1) to formulate a constitutive model will result in the introduction of the Cosserat and micropolar continua. However, the use of such complicated mechanics can be easily avoided if the proper fourth-order linear transformation tensor is formulated in order to symmetrize the effective stress tensor. Such a linear transformation tensor called the damage effect tensor is obtained in the literature (Lee et al., 1986; Sidoroff, 1979) using symmetrization methods. However, it lacks a systematic and consistent approach. It is the aim of this work to provide a solid basis for such transformation of the second-order stress tensor and its justification for the symmetrization. Three different formulations for symmetrization of the effective stress tensors proposed by Lee et al. (1986) and Sidoroff (1979) are described below. The effective stress tensor is symmetrized using the following laws:

$$\bar{\sigma}_{ij} = (\delta_{ik} - \phi_{ik})^{-1/2}\sigma_{kl}(\delta_{jl} - \phi_{jl})^{-1/2} \tag{2}$$

$$\bar{\sigma}_{ij} = \tfrac{1}{2}[\sigma_{ik}(\delta_{kj} - \phi_{kj})^{-1} + (\delta_{jk} - \phi_{jk})^{-1}\sigma_{ki}] \tag{3}$$

$$\sigma_{ij} = \tfrac{1}{2}[\bar{\sigma}_{ik}(\delta_{kj} - \phi_{kj}) + (\delta_{jk} - \phi_{jk})\bar{\sigma}_{ki}]. \tag{4}$$

Other forms for symmetrization are defined by many researchers through the fourth-order damage effect tensor such as that by Cordebois and Sidoroff (1982)

$$M_{ikjl} = (\delta_{ik} - \phi_{ik})^{-1/2}(\delta_{jl} - \phi_{jl})^{-1/2}, \tag{5}$$

by Murakami and Ohno (1980)

$$M_{ikjl} = \tfrac{1}{4}[\delta_{ij}(\delta_{kl} - \phi_{kl})^{-1} + \delta_{il}(\delta_{kj} - \phi_{kj})^{-1}$$
$$+ (\delta_{ij} - \phi_{ij})^{-1}\delta_{kl} + (\delta_{il} - \phi_{il})^{-1}\delta_{kj}], \tag{6}$$

by Betten (1983)

$$M_{ikjl} = \tfrac{1}{2}[(\delta_{ij} - \phi_{ij})^{-1}(\delta_{kl} - \phi_{kl})^{-1}$$
$$+ (\delta_{il} - \phi_{il})^{-1}(\delta_{kj} - \phi_{kj})^{-1})], \tag{7}$$

and by Lu and Chow (1990)

$$M_{ikjl} = \tfrac{1}{2}[\exp(\phi_{ij}/2)\exp(\phi_{kl}/2)$$
$$+ \exp(\phi_{il}/2)\exp(\phi_{kj}/2)]. \tag{8}$$

ϕ in the above equations is a damage tensor characterized by a second-order symmetric tensor and is given by (Murakami, 1983)

$$\phi_{ij} = \sum_{k=1}^{3} \hat{\phi}_k \hat{n}_i^k \hat{n}_j^k \quad (\text{no sum in } k) \tag{9}$$

where $\hat{n}^k$ is an eigenvector corresponding to the eigenvalue, $\hat{\phi}_k$, of the damage tensor, ϕ. Voyiadjis and Venson (1995) quantified the physical values of the eigenvalues $\hat{\phi}_k$ ($k = 1, 2, 3$) and the second-order damage tensor ϕ for the unidirectional fibrous composite by measuring the crack density with the assumption that one of the eigendirections of damage tensor coincides with the fiber direction. This introduces a distinct kinematic measure of damage which is complimentary to the deformation kinematic measure of strain. A thermodynamically consistent evolution equation for damage tensor ϕ together with a generalized thermodynamic force conjugate, Y, to the damage tensor is presented in the paper by Voyiadjis and Park (1995).

Numerous fourth-order damage effect tensors are defined by using the symmetrization laws indicated above. However, only the one by Cordebois and Sidoroff (1982) may be obtained from the symmetrization procedure given by Eq. (2). One cannot deduce explicitly the fourth-order damage effect tensor M from the remaining proposed procedures. In the case of Cordebois and Sidoroff (1982) it is impossible to get the explicit form of the square root of the second-order tensor in Eq. (5). Alternatively, the damage effect tensor using the fourth-order damage tensor ψ is defined by Chaboche (1979) as follows:

$$M_{ikjl} = (I_{ikjl} - \psi_{ikjl})^{-1} \tag{10}$$

where I_{ikjl} is a fourth-order identity tensor and is given by

$$I_{ikjl} = \tfrac{1}{2}(\delta_{ij}\delta_{kl} + \delta_{il}\delta_{kj}). \tag{11}$$

However, it is not easy to characterize physically the fourth-order damage tensor ψ_{ijkl} rather than the second-order damage tensor ϕ_{ij}. For the case of isotropic damage, the fourth-order damage tensor is defined by Ju (1990) as follows:

$$\psi_{ikjl} = d_1\delta_{ik}\delta_{jl} + d_2 I_{ikjl} \tag{12}$$

where d_1 and d_2 are scalar (dependent or independent) damage variables. Using the second-order anisotropic damage tensor ϕ_{ij}

in the damage effect tensors given by Eqs. (5), (6), (7), and (8) one may lose the physical view of the net stress tensor due to the presence of the off diagonal elements of the damage tensor ϕ_{ij}. In order to avoid this problem, the principal damage tensor rather than the second-order damage tensor is used in conjunction the damage effect tensor. However, the eigendirections of the damage tensor do not coincide with the stress tensor or eigendirection of the stress tensor. Since the damage tensor ϕ always has three orthogonal principal directions $\hat{n}^k$ ($k = 1, 2, 3$) and the three corresponding principal values $\hat{\phi}_k$ ($k = 1, 2, 3$), Eqs. (2), (3), and (4) can be expressed as follows in the coordinates that coincide with the three orthogonal principal directions of the damage tensor:

$$\hat{\sigma}_{mn} = (\delta_{mp} - \hat{\phi}_{mp})^{-1/2}\hat{\sigma}_{pq}(\delta_{nq} - \hat{\phi}_{nq})^{-1/2} \tag{13}$$

$$\hat{\sigma}_{mn} = \tfrac{1}{2}[\hat{\sigma}_{mr}(\delta_m - \hat{\phi}_m)^{-1} + (\delta_{nr} - \hat{\phi}_{nr})^{-1}\hat{\sigma}_{rm}] \tag{14}$$

$$\hat{\sigma}_{mn} = \tfrac{1}{2}[\hat{\sigma}_{mr}(\delta_m - \hat{\phi}_m) + (\delta_{nr} - \hat{\phi}_{nr})\hat{\sigma}_{rm}] \tag{15}$$

where $\hat{\phi}$ is a principle damage tensor that is given by

$$\hat{\phi}_{ij} = b_{ik}b_{jl}\phi_{kl}$$
$$= \begin{bmatrix} \hat{\phi}_1 & 0 & 0 \\ 0 & \hat{\phi}_2 & 0 \\ 0 & 0 & \hat{\phi}_3 \end{bmatrix} \tag{16}$$

and the second-order transformation tensor b is given by

$$b_{ik} = \begin{bmatrix} n_1^1 & n_2^1 & n_3^1 \\ n_1^2 & n_2^2 & n_3^2 \\ n_1^3 & n_2^3 & n_3^3 \end{bmatrix}. \tag{17}$$

This transformation tensor called the proper orthogonal tensor requires that

$$b_{ij}b_{kj} = \delta_{ik}. \tag{18}$$

The effective stress tensor in the principal damage direction coordinates system is given by

$$\hat{\bar{\sigma}}_{mn} = b_{mi}b_{nj}\bar{\sigma}_{ij}. \tag{19}$$

Similarly, the stress tensor in the principal damage direction coordinates system is given by

$$\hat{\sigma}_{pq} = b_{pk}b_{ql}\sigma_{kl}. \tag{20}$$

Using the principle damage direction coordinate system, Eq. (1) is given by

$$\hat{\bar{\sigma}}_{mn} = \hat{M}_{mpnq}\hat{\sigma}_{pq} \tag{21}$$

The fourth-order damage effect tensors given by Eqs. (5), (6), (7), and (8) should be now expressed as follows:

$$\hat{M}_{mpnq} = (\delta_{mp} - \hat{\phi}_{mp})^{-1/2}(\delta_{nq} - \hat{\phi}_{nq})^{-1/2} \tag{22}$$

$$\hat{M}_{mpnq} = \tfrac{1}{4}[\delta_{mn}(\delta_{pq} - \hat{\phi}_{pq})^{-1} + \delta_{mq}(\delta_{pn} - \hat{\phi}_{pn})^{-1}$$
$$+ (\delta_{mn} - \hat{\phi}_{mn})^{-1}\delta_{pq} + (\delta_{mq} - \hat{\phi}_{mq})^{-1}\delta_{pn}] \tag{23}$$

$$\hat{M}_{mpnq} = \tfrac{1}{2}[(\delta_{mn} - \hat{\phi}_{mn})^{-1}(\delta_{pq} - \hat{\phi}_{pq})^{-1}$$
$$+ (\delta_{mq} - \hat{\phi}_{mq})^{-1}(\delta_{pn} - \hat{\phi}_{pn})^{-1})] \tag{24}$$

$$\hat{M}_{mpnq} = \tfrac{1}{2}[\exp(\hat{\phi}_{mn}/2)\exp(\hat{\phi}_{pq}/2)$$
$$+ \exp(\hat{\phi}_{mq}/2)\exp(\hat{\phi}_{pn}/2)]. \tag{25}$$

respectively. These tensors are termed the principal damage effect tensors.

Fourth-Order Anisotropic Damage Effect Tensor

The explicit representation of the fourth-order damage effect tensor **M** using the second-order damage tensor ϕ is of particular importance in the constitutive modeling of damage mechanics. However, it is impossible to use the damage tensor ϕ rather than the principal damage tensor $\hat{\phi}$ directly in the formulation. Therefore the damage effect tensor **M** in Eq. (1) should be obtained from Eq. (21) using coordinate transformation.

Substituting Eqs. (19) and (20) into Eq. (21), one obtains the following relation:

$$\bar{\sigma}_{ij} = b_{mi}b_{nj}b_{pk}b_{ql}\hat{M}_{mpnq}\sigma_{kl}. \tag{26}$$

Therefore the fourth-order tensor **M** in Eq. (1) is given as follows:

$$[M] = \begin{bmatrix} a_{11}a_{11} & a_{12}a_{12} & a_{13}a_{13} & 2a_{11}a_{12} & 2a_{12}a_{13} & 2a_{11}a_{13} \\ a_{21}a_{21} & a_{22}a_{22} & a_{23}a_{23} & 2a_{21}a_{22} & 2a_{22}a_{23} & 2a_{21}a_{23} \\ a_{31}a_{31} & a_{32}a_{32} & a_{33}a_{33} & 2a_{31}a_{32} & 2a_{32}a_{33} & 2a_{31}a_{33} \\ a_{11}a_{21} & a_{12}a_{22} & a_{23}a_{23} & (a_{11}a_{22}+a_{12}a_{21}) & (a_{12}a_{23}+a_{13}a_{22}) & (a_{11}a_{23}+a_{13}a_{21}) \\ a_{21}a_{31} & a_{22}a_{32} & a_{23}a_{33} & (a_{21}a_{32}+a_{23}a_{31}) & (a_{22}a_{33}+a_{23}a_{32}) & (a_{21}a_{33}+a_{23}a_{31}) \\ a_{11}a_{31} & a_{12}a_{32} & a_{13}a_{33} & (a_{11}a_{32}+a_{13}a_{31}) & (a_{12}a_{33}+a_{13}a_{31}) & (a_{11}a_{33}+a_{13}a_{31}) \end{bmatrix}. \tag{36}$$

$$M_{ikjl} = b_{mi}b_{nj}b_{pk}b_{ql}\hat{M}_{mnpq}. \tag{27}$$

It is clear that the fourth-order damage effect tensors presented by Eqs. (5), (6), (7), and (8) differ from the damage effect tensor obtained by Eq. (27). Therefore the fourth-order damage effect tensor presented by the Eqs. (5), (6), (7), and (8) should be expressed in the princpal damage direction coordinate system using the principal damage tensor $\hat{\phi}$.

One of the explicit expression for the fourth-order damage effect tensors using the principal damage effect tensor given by Eq. (22) is presented here. The principal damage effect tensor given by Eq. (22) can be written as follows:

$$\hat{M}_{mpnq} = \hat{a}_{mp}\hat{a}_{nq} \tag{28}$$

where the second-order tensor $\hat{a}$ is given by

$$\hat{a}_{mp} = \begin{bmatrix} \dfrac{1}{\sqrt{1-\hat{\phi}_1}} & 0 & 0 \\[2mm] 0 & \dfrac{1}{\sqrt{1-\hat{\phi}_2}} & 0 \\[2mm] 0 & 0 & \dfrac{1}{\sqrt{1-\hat{\phi}_2}} \end{bmatrix}. \tag{29}$$

Substituting Eq. (28) into Eq. (27), one obtains the following relation:

$$M_{ikjl} = b_{mi}b_{nj}b_{pk}b_{ql}\hat{a}_{mp}\hat{a}_{nq}$$
$$= a_{ik}a_{jl}. \tag{30}$$

Using Eq. (30), a second-order tensor **a** is defined as follows:

$$a_{ik} = b_{mi}b_{pk}\hat{a}_{mp}. \tag{31}$$

The matrix form of Eq. (31) is as follows:

In order to obtain the matrix form of the damage effect tensor, the stress tensors σ_{ij} and $\bar{\sigma}_{kl}$ in Eq. (1) are converted into vector form as follows:

$$\{\sigma\} = \{\sigma_{11}\ \sigma_{22}\ \sigma_{33}\ \sigma_{12}\ \sigma_{23}\ \sigma_{13}\}^T \tag{33}$$

$$\{\bar{\sigma}\} = \{\bar{\sigma}_{11}\ \bar{\sigma}_{22}\ \bar{\sigma}_{33}\ \bar{\sigma}_{12}\ \bar{\sigma}_{23}\ \bar{\sigma}_{13}\}^T. \tag{34}$$

Using the notation of Eqs. (33) and (34), Eq. (1) is now represented in matrix notation as follows:

$$\{\bar{\sigma}\} = [M]\{\sigma\} \tag{35}$$

where $[M]$ is the 6×6 matrix representation of the fourth-order tensor **M**. The explicit form of the matrix $[M]$ is given as follows:

It is clear that the various explicit representation forms of the fourth-order damage effect tensors given by Eqs. (5), (6), (7), and (8) using the second damage tensor ϕ are violated by the tensor transformation law.

Matrix Forms of the Damage Effect Tensors for Two-Dimensional Problems

The explicit matrix forms of the damage effect tensors for two-dimensional problems are presented in this section. For the shake of simplicity, a plane state of damage, $\hat{\phi}_3 = 0$ or $\phi_{33} = \phi_{23} = \phi_{32} = \phi_{13} = \phi_{31} = 0$, is assumed for both plane stress and plane strain problems. Similar stress vector of Eqs. (33) and (34), for the two-dimensional problems are given by

$$\{\hat{\sigma}\} = \{\hat{\sigma}_{11}\ \hat{\sigma}_{22}\ \hat{\sigma}_{12}\}^T \tag{37}$$

$$\{\hat{\bar{\sigma}}\} = \{\hat{\bar{\sigma}}_{11}\ \hat{\bar{\sigma}}_{22}\ \hat{\bar{\sigma}}_{12}\}^T. \tag{38}$$

Using the notation of Eqs. (37) and (38), one obtains Eq. (21) represented in matrix notation as follows:

$$\{\hat{\bar{\sigma}}\} = [\hat{M}]\{\hat{\sigma}\} \tag{39}$$

where the 3×3 matrix, $[\hat{M}]$, termed principal damage effect matrix is given by

$$[\hat{M}] = \begin{bmatrix} \hat{M}_{1111} & \hat{M}_{1212} & \hat{M}_{1112}+\hat{M}_{1211} \\ \hat{M}_{2121} & \hat{M}_{2222} & \hat{M}_{2122}+\hat{M}_{2221} \\ \hat{M}_{1121} & \hat{M}_{1222} & \hat{M}_{1122}+\hat{M}_{1221} \end{bmatrix}. \tag{40}$$

The principal damage effect matrices corresponding to Eqs. (22), (23), (24), and (25) are as follows, respectively.

$$[a] = [b]^T[\hat{a}][b]$$

$$= \begin{bmatrix} \dfrac{b_{11}b_{11}}{\sqrt{1-\hat{\phi}_1}} + \dfrac{b_{21}b_{21}}{\sqrt{1-\hat{\phi}_2}} + \dfrac{b_{31}b_{31}}{\sqrt{1-\hat{\phi}_3}} & \dfrac{b_{11}b_{12}}{\sqrt{1-\hat{\phi}_1}} + \dfrac{b_{21}b_{22}}{\sqrt{1-\hat{\phi}_2}} + \dfrac{b_{31}b_{32}}{\sqrt{1-\hat{\phi}_3}} & \dfrac{b_{11}b_{13}}{\sqrt{1-\hat{\phi}_1}} + \dfrac{b_{21}b_{23}}{\sqrt{1-\hat{\phi}_2}} + \dfrac{b_{31}b_{33}}{\sqrt{1-\hat{\phi}_3}} \\[3mm] \dfrac{b_{12}b_{11}}{\sqrt{1-\hat{\phi}_1}} + \dfrac{b_{22}b_{21}}{\sqrt{1-\hat{\phi}_2}} + \dfrac{b_{32}b_{31}}{\sqrt{1-\hat{\phi}_3}} & \dfrac{b_{12}b_{12}}{\sqrt{1-\hat{\phi}_1}} + \dfrac{b_{22}b_{22}}{\sqrt{1-\hat{\phi}_2}} + \dfrac{b_{32}b_{32}}{\sqrt{1-\hat{\phi}_3}} & \dfrac{b_{12}b_{13}}{\sqrt{1-\hat{\phi}_1}} + \dfrac{b_{22}b_{23}}{\sqrt{1-\hat{\phi}_2}} + \dfrac{b_{32}b_{33}}{\sqrt{1-\hat{\phi}_3}} \\[3mm] \dfrac{b_{13}b_{11}}{\sqrt{1-\hat{\phi}_1}} + \dfrac{b_{23}b_{21}}{\sqrt{1-\hat{\phi}_2}} + \dfrac{b_{33}b_{31}}{\sqrt{1-\hat{\phi}_3}} & \dfrac{b_{13}b_{12}}{\sqrt{1-\hat{\phi}_1}} + \dfrac{b_{23}b_{22}}{\sqrt{1-\hat{\phi}_2}} + \dfrac{b_{33}b_{32}}{\sqrt{1-\hat{\phi}_3}} & \dfrac{b_{13}b_{13}}{\sqrt{1-\hat{\phi}_1}} + \dfrac{b_{23}b_{23}}{\sqrt{1-\hat{\phi}_2}} + \dfrac{b_{33}b_{33}}{\sqrt{1-\hat{\phi}_3}} \end{bmatrix} \tag{32}$$

$$[\hat{M}] = \begin{bmatrix} \dfrac{1}{1 - \hat{\phi}_1} & 0 & 0 \\[2ex] 0 & \dfrac{1}{1 - \hat{\phi}_2} & 0 \\[2ex] 0 & 0 & \dfrac{1}{\sqrt{(1 - \hat{\phi}_1)(1 - \hat{\phi}_2)}} \end{bmatrix} \quad (41)$$

where the transformation matrix, $[T]$, and its inverse matrix, $[T]^{-1}$ are given by

$$[T] = \begin{bmatrix} \cos^2\theta & \sin^2\theta & -2\cos\theta\sin\theta \\ \sin^2\theta & \cos^2\theta & 2\cos\theta\sin\theta \\ \cos\theta\sin\theta & -\cos\theta\sin\theta & \cos^2\theta - \sin^2\theta \end{bmatrix} \quad (49)$$

$$[\hat{M}] = \begin{bmatrix} \dfrac{1}{1 - \hat{\phi}_1} & \dfrac{1}{4}\left(\dfrac{1}{1 - \hat{\phi}_1} + \dfrac{1}{1 - \hat{\phi}_2}\right) & 0 \\[3ex] \dfrac{1}{4}\left(\dfrac{1}{1 - \hat{\phi}_1} + \dfrac{1}{1 - \hat{\phi}_2}\right) & \dfrac{1}{1 - \hat{\phi}_2} & 0 \\[3ex] 0 & 0 & \dfrac{1}{4}\left(\dfrac{1}{1 - \hat{\phi}_1} + \dfrac{1}{1 - \hat{\phi}_2}\right) \end{bmatrix} \quad (42)$$

$$[\hat{M}] = \begin{bmatrix} \dfrac{1}{(1 - \hat{\phi}_1)^2} & \dfrac{1}{2(1 - \hat{\phi}_1)(1 - \hat{\phi}_2)} & 0 \\[3ex] \dfrac{1}{2(1 - \hat{\phi}_1)(1 - \hat{\phi}_2)} & \dfrac{1}{(1 - \hat{\phi}_1)^2} & 0 \\[3ex] 0 & 0 & \dfrac{1}{2(1 - \hat{\phi}_1)(1 - \hat{\phi}_2)} \end{bmatrix} \quad (43)$$

$$[\hat{M}] = \begin{bmatrix} \exp(\hat{\phi}_1/2)\exp(\hat{\phi}_1/2) & \frac{1}{2}(\exp(\hat{\phi}_1/2)\exp(\hat{\phi}_1/2) + 1) & 2\exp(\hat{\phi}_1/2) \\ \frac{1}{2}(\exp(\hat{\phi}_1/2)\exp(\hat{\phi}_1/2) + 1) & \exp(\hat{\phi}_2/2)\exp(\hat{\phi}_2/2) & 2\exp(\hat{\phi}_2/2) \\ \exp(\hat{\phi}_1/2) & \exp(\hat{\phi}_2/2) & 2 \end{bmatrix} \quad (44)$$

where the principal damage values, $\hat{\phi}_1$ and $\hat{\phi}_2$, are given by

$$\hat{\phi}_1 = \frac{\phi_{11} + \phi_{22}}{2} + \sqrt{\left(\frac{\phi_{11} + \phi_{22}}{2}\right)^2 + \phi_{12}^2} \quad (45)$$

$$\hat{\phi}_2 = \frac{\phi_{11} + \phi_{22}}{2} - \sqrt{\left(\frac{\phi_{11} + \phi_{22}}{2}\right)^2 + \phi_{12}^2}, \quad (46)$$

respectively. Finally, the damage effect matrix can be obtained by coordinate transformation. The complete set of transformation equations for stresses in the principal damage direction coordinate system is given by

$$\{\hat{\sigma}\} = [T]\{\sigma\}. \quad (47)$$

Similarly, the effective stress vector in the principal damage direction coordinate system is given by

$$\{\dot{\hat{\sigma}}\} = [T]\{\bar{\sigma}\} \quad (48)$$

$$[T]^{-1} = \begin{bmatrix} \cos^2\theta & \sin^2\theta & 2\cos\theta\sin\theta \\ \sin^2\theta & \cos^2\theta & -2\cos\theta\sin\theta \\ -\cos\theta\sin\theta & \cos\theta\sin\theta & \cos^2\theta - \sin^2\theta \end{bmatrix} \quad (50)$$

where θ is given by

$$\theta = \frac{1}{2}\tan^{-1}\left(\frac{2\phi_{12}}{\phi_{11} - \phi_{22}}\right). \quad (51)$$

Substituting Eqs. (47) and (48) into Eq. (39), one obtains the following relation:

$$\{\bar{\sigma}\} = [T]^{-1}[\hat{M}][T]\{\sigma\}$$
$$= [M]\{\sigma\}. \quad (52)$$

The damage effect matrix $[M]$ is defined as follows:

$$[M] = [T]^{-1}[\hat{M}][T]. \quad (53)$$

Using the principal damage effect matrix given by Eq. (41), the damage effect matrix $[M]$ is given by

$$[M] = \begin{bmatrix} \dfrac{c^4}{1 - \hat{\phi}_1} + \dfrac{s^4}{1 - \hat{\phi}_2} + \dfrac{2c^2s^2}{\sqrt{(1 - \hat{\phi}_1)(1 - \hat{\phi}_2)}} & \dfrac{c^2s^2}{1 - \hat{\phi}_1} + \dfrac{c^2s^2}{1 - \hat{\phi}_2} + \dfrac{-2c^2s^2}{\sqrt{(1 - \hat{\phi}_1)(1 - \hat{\phi}_2)}} & \dfrac{-2c^3s}{1 - \hat{\phi}_1} + \dfrac{2cs^3}{1 - \hat{\phi}_2} + \dfrac{2(c^3s - cs^3)}{\sqrt{(1 - \hat{\phi}_1)(1 - \hat{\phi}_2)}} \\[3ex] \dfrac{c^2s^2}{1 - \hat{\phi}_1} + \dfrac{c^2s^2}{1 - \hat{\phi}_2} + \dfrac{-2c^3s}{\sqrt{(1 - \hat{\phi}_1)(1 - \hat{\phi}_2)}} & \dfrac{s^4}{1 - \hat{\phi}_1} + \dfrac{c^4}{1 - \hat{\phi}_2} + \dfrac{2c^2s^2}{\sqrt{(1 - \hat{\phi}_1)(1 - \hat{\phi}_2)}} & \dfrac{-2cs^3}{1 - \hat{\phi}_1} + \dfrac{2c^3s}{1 - \hat{\phi}_2} + \dfrac{-2(c^3s - cs^3)}{\sqrt{(1 - \hat{\phi}_1)(1 - \hat{\phi}_2)}} \\[3ex] \dfrac{-2c^3s}{1 - \hat{\phi}_1} + \dfrac{2cs^3}{1 - \hat{\phi}_2} + \dfrac{2(c^3s - cs^3)}{\sqrt{(1 - \hat{\phi}_1)(1 - \hat{\phi}_2)}} & \dfrac{-2cs^3}{1 - \hat{\phi}_1} + \dfrac{2c^3s}{1 - \hat{\phi}_2} + \dfrac{-2(c^3s - cs^3)}{\sqrt{(1 - \hat{\phi}_1)(1 - \hat{\phi}_2)}} & \dfrac{2c^2s^2}{1 - \hat{\phi}_1} + \dfrac{2c^2s^2}{1 - \hat{\phi}_2} + \dfrac{(c^2 - s^2)^2}{\sqrt{(1 - \hat{\phi}_1)(1 - \hat{\phi}_2)}} \end{bmatrix} \quad (54)$$

Conclusions

The fourth-order anisotropic damage effect tensor, M, using the kinematic measure for damage, expressed through the second-order damage tensor ϕ, is reviewed here in reference to the symmetrization of the effective stress tensor. This introduces for a distinct kinematic measure of damage which is complimentary to the deformation kinematic measure of strain. A thermodynamically consistent evolution equation for the damage tensor, ϕ together with a generalized thermodynamic force conjugate, Y, to the damage tensor is presented in the paper by Voyiadjis and Park (1995). It is pointed out that the principal damage tensor, $\hat{\phi}$, should be used in the formulation of the anisotropic damage effect tensor. Voyiadjis and Venson (1995) quantified the physical values of the eigenvalues, $\hat{\phi}_k (k = 1, 2, 3)$, and the second-order damage tensor, ϕ, for the unidirectional fibrous composite by measuring the crack density with the assumption that one of the eigendirections of damage tensor coincides with the fiber direction.

The fourth-order anisotropic damage effect tensor in the principal damage direction coordinate system is termed the principal damage effect tensor. By coordinate transformation, the fourth-order anisotropic damage effect tensor is obtained. This fourth-order anisotropic damage effect tensor has both physical significance and explicit form. It is therefore not a mere implicit mathematical expression to transform the current stress tensor to a symmetric effective stress tensor. Moreover, an explicit expression of the damage effect tensor is of particular importance in order to obtain the constitutive relation in the damaged material.

In this work, tensorial forms are used for the derivation of such a linear transformation tensor which is then converted to a matrix form. The explicit matrix expressions of the damage effect tensor are derived for both three-dimensional and two-dimensional problems. Especially the damage effect matrix of two-dimensional problems can be expressed by the damage variables, ϕ_{11}, ϕ_{22} and ϕ_{12}.

References

Betten, J., 1983, "Damage Tensors in Continuum Mechanics," *Journal of Mécanique Théorique et Appliquée*, Vol. 2, No. 1, pp. 13–32.

Chaboche, J. L., 1979, "Le concept de contrainte effective appliqué à l'élasticité et à la viscoplasticité en présence d'un endommagement anisotrope," *Colooque Euromech 115*, Villard de Lans, June.

Chaboche, J. L., 1988a, "Continuum Damage Mechanics ... Concepts," ASME JOURNAL OF APPLIED MECHANICS, Vol. 55, pp. 59–64.

Chaboche, J. L., 1988b, "Continuum Damage Mechanics: Part II—Damage Growth, Crack Initiation, and Crack Growth," ASME JOURNAL OF APPLIED MECHANICS, Vol. 55, pp. 65–72.

Cordebois, J. P., and Sidoroff, F., 1982, "Anisotropic Damage in Elasticity and Plasticity," *Journal de Mécanique Théorique et Appliquée*, Numéro Spécial, pp. 45–60.

Ju, J. W., 1990, "Isotropic and Anisotropic Damage Variables in Continuum Damage Mechanics," *Journal of Engineering Mechanics*, Vol. 116, No. 12, pp. 2764–2770.

Kachanov, L. M., 1958, "On the Creep Fracture Time," *Izv. Adad. Nauk. USSR Otd. Tekh.*, Vol. 8, pp. 26–31.

Krajcinovic, D., 1983, "Constitutive Equations for Damaging Materials," ASME JOURNAL OF APPLIED MECHANICS, Vol. 50, pp. 335–360.

Krajcinovic, D., 1985, "Continuous Damage Mechanics Revisited: Basic Concepts and Definitions," ASME JOURNAL OF APPLIED MECHANICS, Vol. 52, pp. 829–834.

Krajcinovic, D., and Foneska, G. U., 1981, "The Continuum Damage Theory for Brittle Materials," ASME JOURNAL OF APPLIED MECHANICS, Vol. 48, pp. 809–834.

Lee, H., Li, G., and Lee, S., 1986, "The Influence of Anisotropic Damage on the Elastic Behavior of Materials," *International Seminar on Local Approach of Fracture*, Moret-sur-Loing, France, June, pp. 79–90.

Lemaitre, J., 1985, "A Continuous Damage Mechaics Model of Ductile Fracture," ASME *Journal of Engineering Materials and Technology*, Vol. 107, No. 42, pp. 83–89.

Lemaitre, J., 1986, "Local Approach of Fracture," *Engineering Fracture Mechanics*, Vol. 25, No. 5–6, pp. 523–537.

Lu, T. J., and Chow, C. L., 1990, "On Constitutive Equations of Inelastic Solids With Anisotropic Damage," *Theoretical and Applied Fracture Mechanics*, Vol. 14, pp. 187–218.

Murakami, S., 1983, "Notion of Continuum Damage Mechanics and Its Application to Anisotropic Creep Damage Theory," *Journal of Engineering Materials and Technology*, Vol. 105, pp. 99–105.

Murakami, S., 1988, "Mechanical Modeling of Material Damage," ASME JOURNAL OF APPLIED MECHANICS, Vol. 55, pp. 280–286.

Murakami, S., and Ohno, N., 1980, "A Continuum Theory of Creep and Creep Damage," *Creep in Structures*, A. R. S. Ponter and D. R. Hayhurst, eds., IUTAM 3rd Symposium, Leichester, U.K., Sept. 8–12, Springer-Verlag, New York, pp. 422–443.

Sidoroff, F., 1979, "Description of Anisotropic Damage Application to Elasticity," *Mechanical Behavior of Anisotropic Solids* (No. 295 Comportement Mechanique Des Solides Anisotropes), J.-P. Boehler, ed., Martinus Nijhoff, Dordrecht, The Netherlands.

Sidoroff, F., 1980, "Description of Anisotropic Damage Application to Elasticity," *Physical Non-Linearities in Structural Analysis* (IUTAM Series), J. Hult and J. Lemaitre, eds., Springer-Verlag, New York, pp. 237–244.

Voyiadjis, G. Z., and Kattan, P. I., 1992, "A Plasticity-Damage Theory for Large Deformation of Solids, Part I: Theoretical Formulation," *International Journal of Engineering Science*, Vol. 30, No. 9, pp. 1089–1108.

Voyiadjis, G. Z., and Park, T., 1995, "Local and Interfacial Damage Analysis of Metal Matrix Composites," *International Journal of Engineering Science*, Vol. 33, No. 11, pp. 1595–1621.

Voyiadjis, G. Z., and Venson, A. R., 1995, "Experimental Damage Investigation of a SiC–Ti Aluminide Metal Matrix Composite," *International Journal of Damage Mechanics*, Vol. 4, No. 4, Oct., pp. 338–361.

Experimental Damage Investigation of a SiC-Ti Aluminide Metal Matrix Composite

GEORGE Z. VOYIADJIS* AND ANTHONY R. VENSON**

Department of Civil Engineering
Louisiana State University
Baton Rouge, LA 70803

ABSTRACT: Experimental investigations and procedures for the determination of damage are presented for the macro- and micro-analysis of SiC-Titanium Aluminide metal matrix composite (MMC). Uniaxial tension tests are performed on laminate specimens of two different layups. The layups are balanced symmetrically and given as (0/90), and (±45), each containing four plies. Dogbone shaped flat plate specimens are fabricated from each of the layups. Specimens for the different layups are loaded to various load levels ranging from rupture load down to 70% of the rupture load at room temperature. By loading specimens to various load levels damage evolution is experimentally evaluated through a quantitative micro-analysis technique. Micro-analysis is performed using scanning electron microscopy (SEM) on three mutually perpendicular representative cross sections of all specimens for the qualitative and quantitative determination of damage. Together these representative cross sections form a representative volume element (RVE) defined for the theoretical development of damage evolution. Results from the micro-analysis are used in evaluating the damage parameters defined in a previously developed damage theory [1]. This theory uses a second order damage tensor of which it is proposed will have non-zero off diagonal terms only if the load applied to the laminate is in a direction other than parallel to the fibers. Damage parameters are evaluated for each of the load levels below the rupture load, since damage features present at this load level are beyond the range of valid damage mechanics. Two types of damage evaluations are performed for the RVE, one for the overall quantification of damage and the other quantifying damage in the matrix and fibers separately. Damage as a result of delamination is excluded in this investigation for both types of damage evaluation, but may be included if needed. The damage curves presented show graphically a consistent evolution of damage, which validates the methods used in evaluating the damage parameter. Curves for the different laminate layups show that damage profile curves are similar for different laminate layups and orientations. The off diagonal terms of the damage tensors as evaluated by the proposed scheme are found to be significant and should be included in any constitutive damage rela-

*Professor of Civil Engineering.
**Doctoral Candidate, currently Visiting Assistant Professor, Department of Civil Engineering, University of Southwestern Louisiana, Lafayette, Louisiana.

tion. Numerical verification of these observations are to be presented in a subsequent paper.

INTRODUCTION

FIBER-REINFORCED COMPOSITE MATERIALS, specifically those with a metal matrix, are having an increasing role in consideration for the design and manufacture of composite structures. This is a result of these types of materials having the ability to attain higher stiffness/density and strength/density ratios, as compared to other materials. Along with this increased use comes the responsibility of designers to be able to understand and predict the behavior of MMC materials, especially that of damage initiation and evolution. Knowledge such as this can be obtained through experimental investigations. Although the literature contains an abundance of new developments in composite materials technology, it lacks a consistent analysis of damage mechanisms as well as damage evolution in composite materials. Much of the work in this area has taken a continuum approach to damage mechanics, such as the work by Lemaitre [2] and Chaboche [3,4]. Their work uses an anisotropic elasto-plastic damage theory that defines an effective stress based on the principle of strain equivalence. Continuum theories for damage in composite materials can produce good results; however, they do not capture the effects of damage in the fiber and matrix separately. Also, the same can be said of the stress-strain response in the constituents. Based on this, researchers have developed micro-mechanical models that determine the overall response in terms of the constituent properties. Dvorak et al. [5-7] developed such a theory for the elasto-plastic behavior of composites. Voyiadjis and Kattan [8-11] extended this theory to incorporate damage, thus yielding a complete damage theory that handles both continuum and micro-damage. This theory models damage as an overall effect such as in the continuum damage theory, as well as damage effects in the constituents. The work presented here is part of a project aimed at developing a consistent damage theory (Voyiadjis and Kattan [1]) for composite materials. This work is mainly concerned with the experimental aspects of the research.

A number of damage theories have been proposed with limited experimental investigation. These investigations are primarily confined to damage as a result of fatigue of fracture (Allix et al. [12], Poursatip [13], Ladaveze et al. [14] and Wang [15]). Each of these investigations do not present damage evolution as a function of the measured physical damage over a load history. A more recent work by Majumdar et al. [16] provides a thorough examination and explanation on the microstructural evolution of damage. However, this work has not been extended to a constitutive theory for the quantification and evolution of physical damage. Recently new experimental procedures have been introduced to quantify damage due to micro-cracks and micro-voids through X-ray diffraction, tomography, etc. (Breunig et al. [17], Baumann et al. [18] and Benci et al. [19]). Nev-

...ertheless these procedures need to be refined in order to differentiate between the different types of damages such as voids and cracks (radial, debonding, z-type). Additional experiments need to be performed in order to quantify the damage parameters as well as evaluate the proposed damage theory. Much of the work in this area has been done using a continuum approach with various schemes of measuring the damage. In each of the schemes, damage is a measure of ratio between an effective quantity and its respective damaged value. Lemaitre et al. [20] listed several methods of obtaining ratios for the damage parameter based on area of resistance, material density, and elasto-plastic modulus. Obtaining the damage parameter as a ratio of the elastic-plastic modulus and undamaged elasto-plastic moduli is most widely used because of the ease in evaluating the damaged and undamaged elasto-plastic moduli. As previously mentioned, methods such as this cannot capture or predict the effect of local components on the overall damage evolution. Within this work, a method will be outlined to experimentally evaluate different types of damage in a metal matrix composite material that can be used in conjunction with a micro-mechanical damage theory. This is outlined through an overall damage quantification as well as a local damage quantification differentiating between damage in the matrix and in the fibers. Major topics covered will be specimen design and preparation, mechanical testing (macro-analysis), SEM analysis (micro-analysis) and evaluation of damage parameters based on the results of the micro-analysis.

Specimen Design and Preparation

As previously mentioned, the material investigated is a titanium aluminide composite reinforced with continuous SiC (SCS-6) fibers. The SiC fibers are developed and produced by the manufacturer of the initial plate specimens. Typical properties of the SiC fibers, as provided by the manufacturer, are shown in Table 1. Additionally, the fibers have good wettability characteristics for metals, which should minimize the chances of voids being induced during the manufacturing process. Also, these fibers are coated with a carbon rich coating that assists in protecting the inner SiC from damage during handling.

The titanium aluminide foil is an α_2 phase material that has typical properties,

Table 1. Typical properties of silicon carbide fibers.

Diameter	0.14 mm
Density	3044 kg/mm^3
Tensile strength	3.44 GPa
Young's modulus	414 GPa
Poisson ratio	0.22
CTE	2.3×10^{-6} ppm – °C at RT

Provided by Textron Specialty Materials, Inc., Lowell, MA USA.

provided by the manufacturer, as shown in Table 2. The manufacturer also provided properties of a composite lamina for 0° and 90° orientations obtained from experimental tests conducted on manufactured specimen. These values are as reported in Table 3.

Hand layup techniques are used to fabricate two different specimen layups [i.e. $(0/90)_s$ and $(\pm45)_s$] from SCS-6 SiC fiber mats and Ti-14Al-21Nb (α_2) foils from rolled ingot material. Each of the layups contained four plies. Fibers, in the fiber mat, were held together with molybdenum wire. Consolidation is accomplished by hot-isostatic-pressing (HIP) in a steel vacuum bag at 1010°C ± 25° under 103 MPa pressure for 2 hrs. C-scans are performed on each specimen plate to evaluate the consolidation and fiber alignment of the finished product. Results indicate very good consolidation for the crossply specimen $(0/90)_s$ with some fiber misalignment along the plate edges. However, the $(\pm45)_s$ plate has generally good consolidation with significant occurrences of fiber misalignment or fiber bundling on the interior of the plate as well as the edges.

As a result of fiber misalignment and differences in coefficients of thermal expansion for the fiber and matrix, noticeable warpage is found on each of the plate specimens. Much of the warpage was confined to the edges of each plate, with a maximum relative elevation difference of 2.24 cm for the $(0/90)_s$ plate and 1.30

Table 2. Typical properties of Ti-14Al-21 Nb (α_2) matrix.

Composition:	Ti	63.4%
	Al	14.4%
	Nb	22.1%
Tensile strength		448 MPa
Young's modulus		84.1 GpA
Poisson ratio		0.30

Provided by Textron Specialty Materials, Inc., Lowell, MA USA.

Table 3. Typical properties of SiC-Ti-Al lamina.

0° tensile strength	1.38 – 1.52 GPa
90° tensile strength	103 – 206 MPa
Longitudinal modulus	199 GPa
Transverse modulus	136 GPa
Shear modulus, G_{12}	52 GPa
Poisson ratios	$\nu_{12} = 0.27$
	$\nu_{21} = 0.185$
	$\nu_{31} = 0.31$

Provided by Textron Specialty Materials, Inc., Lowell, MA USA.

Figure 1. Dogbone shaped tensile specimen.

cm for the (±45)₂ plate. Of particular concern is whether or not this warpage will induce any detectable damage during the preparation of the actual test specimens.

Nevertheless, each of the laminates is machined to produce six test specimens with shape and dimensions as indicated in Figure 1. Specimen locations are selected in order to minimize the effects of the laminate warpage on the test specimens. The locations that were selected had the minimum amount of warpage, so that the level of prestress would be negligible during testing. They also exhibit no detectable evidence of damage to the fiber or matrix. This is verified through C-scans of the individual test specimens after machining. Sample C-scans for a typical specimen for each layup are shown in Figures 2 and 3 to illustrate this fact. These are gray scale images, which are interpreted as the darker the image the better the consolidation and fiber alignment. The 3rd backwall echo represents the amplitude of the third return wave of the initial excitation frequency. Also these scans correspond to previous scans done on the initial plate specimen, which implies that machining of the test specimens did not induce any detectable damage.

The dogbone type specimen has been used successfully by previous researchers [21] to ensure specimen failure within the gage section and not the grips. These specimens had aluminum tabs arc-welded onto the ends in order to prevent the mechanical grips from damaging the specimen. Welds are made on the extreme ends, producing local damage only in the vicinity of the weld.

Mechanical Testing of Specimens

Before beginning the actual mechanical testing, much attention is given to specimen preparation, using the recommendations of Carlsson [22] and Tuttle [23], and the experimental data items sought as a guide. Quantitative information (stress and strain) is sought for use in the damage evolution model. Therefore, foil-resistance strain gages are used in obtaining the necessary strain data. Each of the dogbone type specimens has strain gages mounted on both faces, directly opposite one another. This is done to determine if eccentric loading occurs during the test, or, if the specimen contains any prestress as a result of geometrical distortion, so that adjustments can be made to the raw data for these effects. Transverse and longitudinal gages are mounted on each face to monitor transverse and longitudinal strains.

All mechanical testing is done utilizing a computer controlled testing machine with hydraulic grips. Specimens are loaded at a crosshead rate of 4.23 mm/hr to allow enough time to collect sufficient data during the test. Data is sampled continuously with all aspects of the test being controlled by a personal computer and data acquisition system once started. Calibration factors are obtained from all specimen strain gages before testing and used later during data reduction. An extensiometer was also attached to the specimen during testing with results being
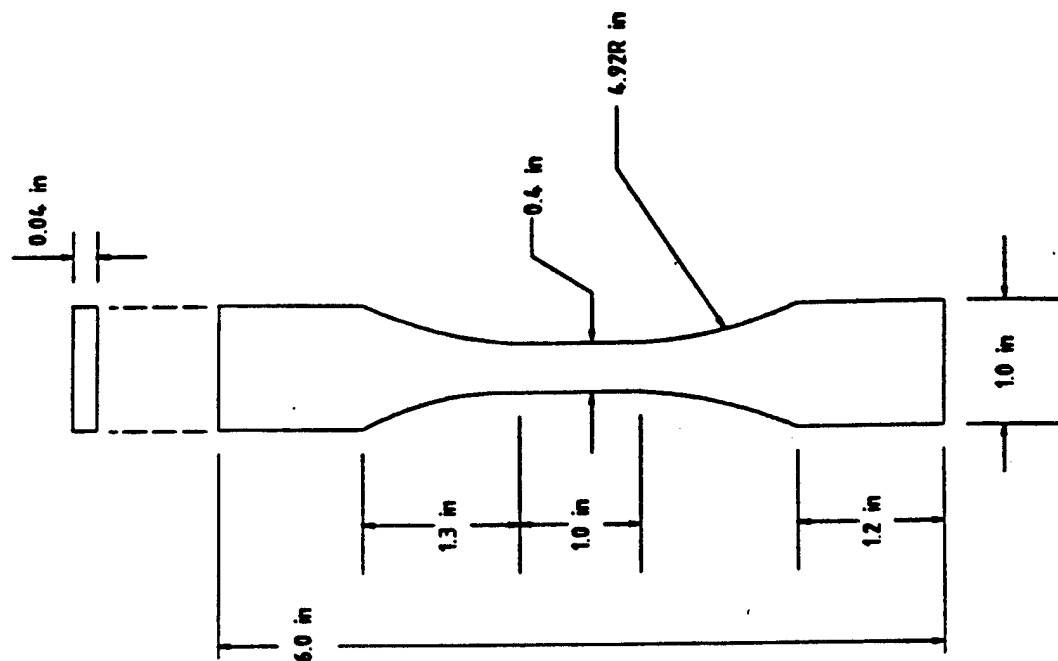
plotted on an oscilloscope for immediate feedback. Results from the extensiometer matched within ±3% the longitudinal results of the strain gages.

As a means of checking the prestress level resulting from manufacturing distortions, strain readings are taken during the process of gripping each end of the specimen in the testing machine. Strains obtained during this process from all specimens are considered negligible, with strain on the order of 120 με for the dogbone type specimens. Thus as mentioned previously, the effects of the warpage induced prestress are small and will be neglected.

Only one test specimen of each orientation of the dogbone type is loaded to rupture. The remaining five specimens are loaded at 90, 85, 80, 75 and 70% of rupture load. These five load levels are used to measure the evolution of damage in the specimens through the progression of loading. Quantification of damage for each load level is obtained by sectioning each specimen and measuring damage features on a representative cross section of the specimen. The actual process is explained fully in a subsequent section of this paper. Stress-strain curves for selected specimens of orientations (0/90)s and (±45)s are shown in Figures 4 and 5, respectively. The Nb in the matrix is added to improve ductility (Brindley [24], MacKay et al. [25]); however, it appears that ductility is also a function of

Specimen #549L-1, #549L-2, #549L-3, #549L-4
Longitudino: Stress,σ_u vs % Strain,ε_u

Figure 4. Stress-strain curves for selected (0/90)s specimens.

Ultrasonic C-Scan
Sample no. 549L-6

Amplitude of 3rd backwall echo

Figure 2. C-scan of selected (0/90)s specimen.

Ultrasonic C-Scan
Sample no. 550L-1

Amplitude of 3rd backwall echo

Figure 3. C-scan of selected (±45)s specimen.

The transverse cross section investigated is at the midpoint of the specimen gage length, and the longitudinal sections are taken normal to this section. Information within two fiber diameters of the specimen edge on transverse sections is disregarded to eliminate any possible free edge effects in the analysis. This is not done for the longitudinal cross sections since they are carefully taken from the middle of the specimen. All section surfaces are prepared by making the section cut with a low speed diamond saw, followed by grinding and polishing of the cut surface. The low speed diamond saw eliminates the possibility of introducing damage on the cross section during sectioning. In addition, the grinding and polishing further eliminates any surface defects that can be introduced by the cutting operation. In short this procedure ensures to a high degree that defects observed during the SEM analysis reflects damage as a result of the loading. Although the SEM analysis could contain radial cracks as a result of the fabrication cool down process, it is assumed that a well controlled manufacturing process is used such that the number of these cracks are low and can be neglected. Therefore, all cracks measured are attributed to loading.

The scanning electron microscope is used to scan the entire cross-sectional area of the longitudinal and transverse sections at low magnification ($<1000 \times$). Photographs are taken on an area of the cross section that is 1% of the total area and contains an average representation of damage features for the complete cross section. This area is defined as the representative cross section with three mutually perpendicular areas of this type defining the RVE that is later used to quantify damage evolution. Images are also investigated on the fracture surface of specimens loaded to rupture only as a means of qualitatively investigating the final deformation and failure mode. Results of this investigation showed fiber pull-out, with debonding occurring between the matrix and reaction zone surrounding the fiber. This implies that there is good fiber-matrix bonding. The fibers in the fiber mat are held in place with molybdenum wires to improve fiber alignment during the manufacturing process. Observations of the fracture surface showed a clean break where these wires crossed the surface. Thus, these wires tend to induce the matrix defect for loads normal to the fiber axis; otherwise, they tend to assist the matrix in transferring the load from fiber to fiber. These results also agree with the corresponding specimen stress-strain response in that information observed on the (0/90)s specimen shows very little deformation in the matrix and brittle failure of the longitudinal fibers, whereas the (±45)s specimen shows a considerable amount of matrix deformation and a ragged fracture failure of the fibers. Deformation information on these surfaces is not quantified as damage, since it is due to processes other than damage evolution and is outside the valid range of damage mechanics.

Most of the SEM photos predominantly show damage in the fibers in the form of cracks. However, there is some local damage in the matrix in the form of cracks. Figures 6 and 7 show a sample of the damage features found on all speci-
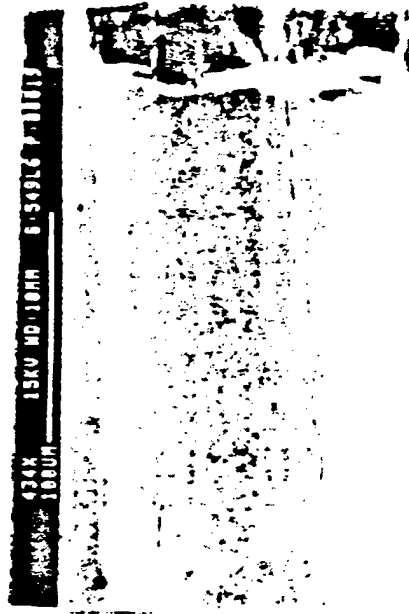

Specimen: #550L-1, #550L-2, #550L-3, #550L-4

Longitudinal Stress,σ_a vs % Strain,ε_a

LEGEND

Specimen #550L-1 Tensile load to failure (640 lbs)
Specimen #550L-3 Tensile loading to 90% ultimate (378 lbs)
Specimen #550L-4 Tensile loading to 85% ultimate (544 lbs)
Specimen #550L-2 Tensile loading to 70% ultimate (448 lbs)

Stress,σ_a (ksi)

% Strain,ε_a

Figure 5. Stress-strain curves for selected (±45)s specimens.

---

fiber orientation for constant material properties. For example, the (0/90)s specimens have a maximum total longitudinal strain less than the (±45)s specimens. A possible explanation for this observation is that there is an increased amount of mechanical interaction between the semi-ductile matrix and brittle fibers as the fiber orientation increased with respect to the loading direction. It is expected that there will be more physical damage in the matrix for the (±45)s specimens than in the (0/90)s specimens. For each of the specimen layups shown, there is a slight variability in the response curve for different specimens with the same layup. It is proposed that this variability is due to the variable nature of composite materials and not a result of the damage evolution. Although damage initiation may be different the net effect for all specimens will be the same.

SEM and Image Analysis

An SEM analysis is done on a respresentative cross section of all specimens in order to obtain a qualitative evaluation of damage in the specimens, as well as providing a means for measuring visible damage features later. Longitudinal and transverse sections are taken from all samples in the vicinity of the strain gages.

mens investigated. The predominant damage feature is a linear crack in the fiber and/or matrix. This is as expected since the low strains obtained indicate that damage features such as matrix voids will appear at a minimum. Since the predominant damage feature is a crack, a damage parameter is developed as a function of crack length only. This relationship is discussed in the following section. Specimens with (±45)₂ layups show a higher occurrence of damage features as a result of the increased fiber-matrix mechanical interaction than the (0/90)₂ specimens.

Quantification of the cracks found were obtained utilizing image analyzing equipment and software. SEM photos were scanned at a resolution of 600 dots per inch (dpi) in an attempt to yield a tag image file format (TIFF) image very close to the original photo. The scanned image was then analyzed with image analyzing software. Attempts were made to automate the process of measuring cracks on the image; however, available software was not successful in differentiating between defined damage features and noise features on the image. Therefore, a semi-automatic technique is used to measure crack lengths in that the cracks are digitized by hand before being processed with the image analyzing software. This software automatically computed the crack lengths with respect to the photo scale during digitization. Measured crack lengths were saved in a database for later processing with the damage characterization theory.
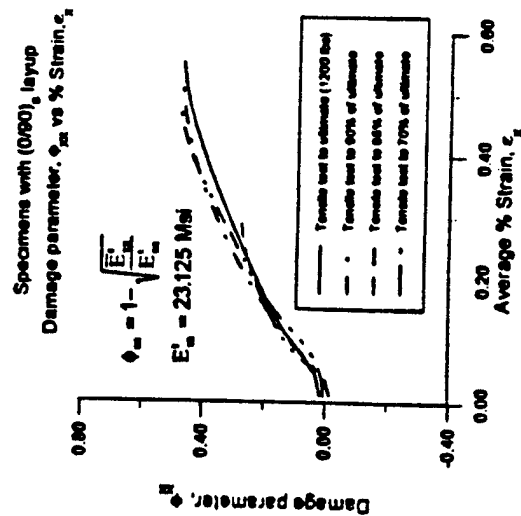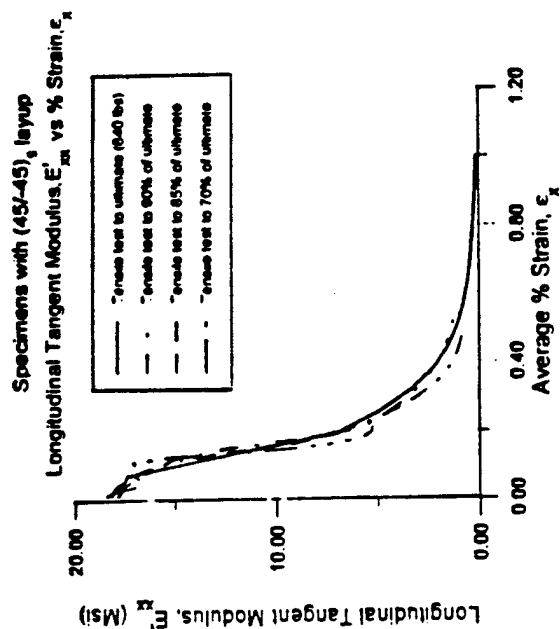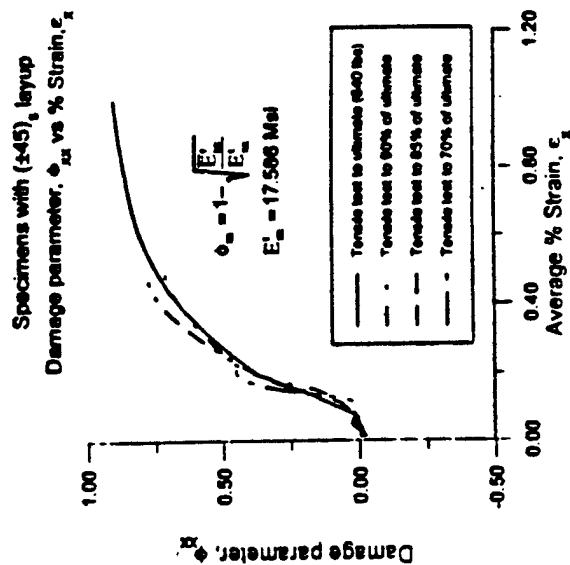
Evaluation of Damage Parameters

The damage model developed by Voyiadjis and Kattan [1] defines a second order tensorial damage parameter, ϕ, whose eigenvalues are ϕ_{ii} ($i = 1,2,3$, no sum in i). Difficulty arises in being able to determine this damage tensor. As an initial approximation, the overall continuum relationship of Kattan and Voyiadjis [26] reduced to the case of plane stress uniaxial tension with unidirectional fibers

$$\bar{E}_{xx} = E'_{xx}(1 - \phi_{xx})^2 \tag{1}$$

$$\bar{E}_{yy} = E'_{yy}(1 - \phi_{yy})^2 \tag{2}$$

is used to investigate the dogbone shaped specimens. In this expression $\bar{E}_{ii}$ ($i = x,y$, no sum in i) represents the current effective tangent modulus in the ith direction and E'_{ii} ($i = x,y$, no sum of i) represents the initial tangent modulus or the elastic modulus in the ith direction. Using the experimentally obtained stress-strain curves, the tangent modulus is obtained by numerical differentiation based on cubic spline interpolation. Tangent moduli curves with (0/90)₂ and (±45)₂ layups for selected specimens are shown in Figures 8 and 10 respectively. Damage parameter ϕ_{xx} is evaluated using Equation (1) from the results of the tangent moduli curves and are shown in Figures 9 and 11. These curves behave as they should, in that the tangent moduli curves are an inverse mirror of

Figure 6. SEM micrograph of (0/90)₃ specimen at 75% of failure load showing matrix cracking.

Figure 7. SEM micrograph of (±45)₃ specimen at 90% of failure load showing fiber cracking.

Specimens with (45/-45)$_s$ layup
Longitudinal Tangent Modulus, E^1_{xx} vs % Strain, ϵ_x

Figure 10. Tangent modulus, $E1_{xx}$ curves for (± 45)s specimens.

Specimens with (±45)$_s$ layup
Damage parameter, ϕ_{xx} vs % Strain, ϵ_x

$$\phi_{xx} = 1 - \sqrt{\frac{E^1_{xx}}{E_{xx}}}$$

$E^1_{xx} = 17.566$ Msi

Figure 11. Damage parameter, ϕ_{xx} curves for (± 45)s specimens.

Specimens with (0/90)$_s$ layup
Longitudinal Tangent Modulus, E^1_{xx} vs % Strain, ϵ_x

Figure 8. Tangent modulus, $E1_{xx}$ curves for (0/90)s specimens.

Specimens with (0/90)$_s$ layup
Damage parameter, ϕ_{xx} vs % Strain, ϵ_x

$$\phi_{xx} = 1 - \sqrt{\frac{E^1_{xx}}{E_{xx}}}$$

$E^1_{xx} = 23.125$ Msi

Figure 9. Damage parameter, ϕ_{xx} curves for (0/90)s specimens.

the corresponding stress-strain curve, as a result of the inverse relationship between the two. The damage curves also mirror the stress-strain curves. Additionally, comparison of the magnitude of the damage parameter ϕ_{zz} in Figures 9 and 11 shows that the amount of damage on the $(\pm 45)_s$ specimens is greater than that of the $(0/90)_s$ specimens. This observation is verified qualitatively and quantitatively from the SEM analysis of representative cross sections of each of the specimen layups.

Although this approximation to obtain the damage parameter ϕ_{zz} is consistent and has magnitudes within the accepted range $0 \le \phi_{zz} < 1$, further use in the theoretical development is not warranted since this expression is only valid for a pure elastic response. It is proposed to handle an elasto-plastic response [27,28] by defining the damage tensor, ϕ, as a function of crack density, ϱ, i.e. for a unidirectional laminate with uniaxial loading in the fiber direction the damage tensor becomes,

$$[\phi] = \begin{bmatrix} \bar{\varrho}_x\bar{\varrho}_x & 0 & 0 \\ 0 & \bar{\varrho}_y\bar{\varrho}_y & 0 \\ 0 & 0 & \bar{\varrho}_z\bar{\varrho}_z \end{bmatrix}$$ (3)

where vector quantity $\bar{\varrho}_i$ ($i = x,y,z$) is the normalized crack density on a cross section whose normal is along the i-axis. Damage is experimentally characterized by sectioning the uniaxial specimens perpendicular to the direction of loading and two additional plates mutually perpendicular to the loading direction. From the SEM photos the crack densities are obtained on an RVE. In the first quantification of damage (overall type) no discrimination is being made between the cracks in the matrix and fibers. The quantification of damage on the RVE for each of the representative cross sections is defined by

$$\bar{\varrho}_i = \frac{\varrho_i}{m\varrho^*}$$ (4)

$$\varrho_i = \frac{l_i}{A_i}$$ (5)

where, l_i is the total length of cracks on the ith cross-sectional area, m is a normalization factor chosen so that the values of the damage variable ϕ fall within the acceptable range $0 \le \phi_{ij} < 1$, and $\varrho^* = \sqrt{\varrho_{xx}^2 + \varrho_{yy}^2 + \varrho_{zz}^2}$. The expression for ϱ^* is selected such that it will yield a non-dimensional average value for the $\bar{\varrho}_i$. The ϱ_{max} ($i = x,y,z$) is the maximum crack density value measured of all load levels within the valid range of damage mechanics for the re-

spective representative cross-sectional area. In the case of uniaxial tension, this measured value corresponds to the crack density measured at the maximum valid load level.

In the general case for off-axis laminates, the damage tensor takes the general form,

$$[\phi] = \begin{bmatrix} \bar{\varrho}_x\bar{\varrho}_x & \bar{\varrho}_x\bar{\varrho}_y & \bar{\varrho}_x\bar{\varrho}_z \\ \bar{\varrho}_y\bar{\varrho}_x & \bar{\varrho}_y\bar{\varrho}_y & \bar{\varrho}_y\bar{\varrho}_z \\ \bar{\varrho}_z\bar{\varrho}_x & \bar{\varrho}_z\bar{\varrho}_y & \bar{\varrho}_z\bar{\varrho}_z \end{bmatrix}$$ (6)

The off diagonal terms constitute damage introduced by loads that are not parallel to the fiber direction and implies that the damage is due to the interaction of cracks on the three mutually perpendicular planes of the RVE. It also implies that shearing stresses impose this interactive damage.

Overall Quantification of Damage

For the overall quantification of damage the $\bar{\varrho}_i$ ($i = x,y,z$) represents the total crack density on the representative cross-sectional face of the RVE. In the current investigation, ϱ_i values are evaluated on specimens loaded to the five load levels below the rupture load. Crack densities are not measured for specimens loaded to rupture, since this load level produces damage features which are beyond the valid range of damage mechanics. Densities on the z-section are not measured and assumed to be one half the magnitude of those on the respective y-section. Measured values of the crack densities for each of the layups are tabulated in Tables 4 and 5. These values are the crack density values obtained directly from the image analysis process without any normalization.

Using the relationship in Equation (6), damage parameter curves for ϕ_{zz} with $(0/90)_s$ and $(\pm 45)_s$ layups are developed and shown in Figures 12 and 13 respectively and those for ϕ_{xx} are shown in Figures 14 and 15 for $(0/90)_s$ and $(\pm 45)_s$

Table 4. Overall crack densities for (0/90)s laminate.

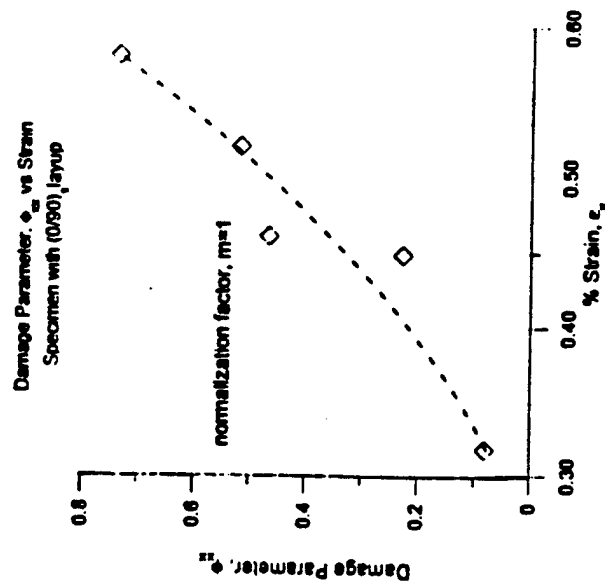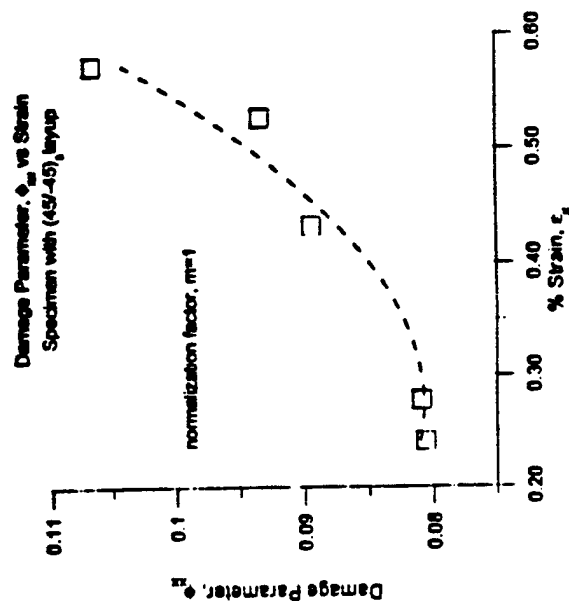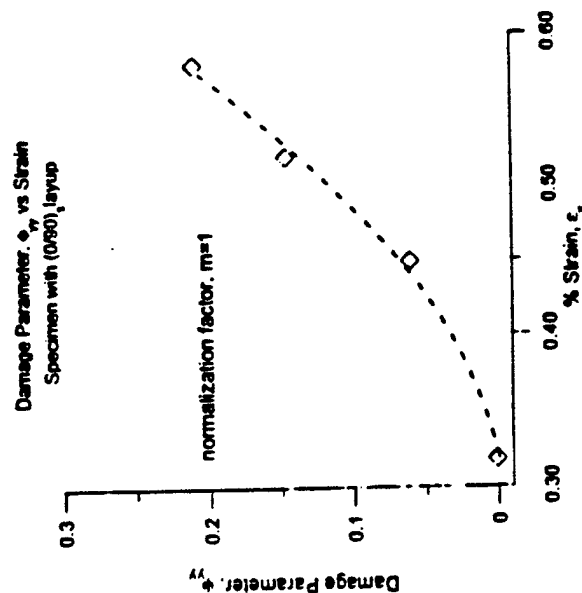| % Load	% Strain	$\varrho_x \times 10^{-4}$ mm/mm²	$\varrho_y \times 10^{-4}$ mm/mm²
70	.3182	41.82	3.41
75	.4487	70.32	36.40
80	.4611	100.77	—
85	.5202	108.24	56.43
90	.5808	126.68	67.72

Figure 13. *Experimentally measured damage parameter, ϕ_{xx} for (± 45)$_s$ laminate.*

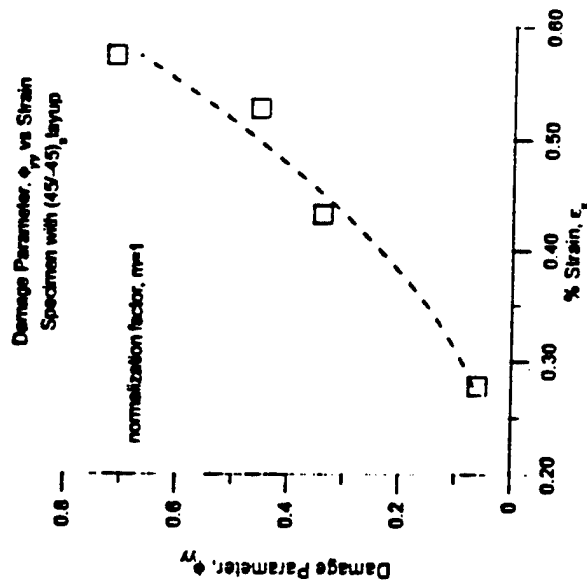Figure 14. *Experimentally measured damage parameter, ϕ_{yy} for (0/90)$_s$ laminate.*

Table 5. *Overall crack densities for (± 45)$_s$ laminate.*

% Load	% Strain	$\theta_L \times 10^{-4}$ mm/mm^2	$\theta_R \times 10^{-4}$ mm/mm^2	$\theta_R \times 10^{-4}$ mm/mm^2
70	.2414	49.23	—
75	.2779	49.32	42.44
80	.4324	51.64	101.29
85	.5268	52.99	117.01
90	.5729	56.67	146.59

layups, respectively. Each of the curves shown are second order polynomial fits of the measured data points with the normalization factor $m = 1$.

As shown in Equation (6) the damage tensor, ϕ, is fully populated for anything other than unidirectional laminates loaded in the fiber direction, as is the case for the specimens used during this investigation. Although damage parameter curves are not shown for the off diagonal damage parameters, they were computed for each laminate layup at 90% of the rupture load and given as

Figure 12. *Experimentally measured damage parameter, ϕ_{xx} for (0/90)$_s$ laminate.*

Damage Parameter, φ_yy vs Strain
Specimen with (45/-45)_s layup

normalization factor, m=1

Figure 15. Experimentally measured damage parameter, φ_yy for (±45)s laminate.

$$[\phi] = \begin{bmatrix} .73682 & .39388 & .19694 \\ & .21056 & .10528 \\ S & & .052638 \end{bmatrix}^{0.5}_{(0/90),} \tag{7}$$

$$[\phi] = \begin{bmatrix} .10679 & .27622 & .13811 \\ & .71452 & .35725 \\ S & & .17862 \end{bmatrix}^{0.5}_{(\pm45),} \tag{8}$$

Careful examination of the curve fits in Figures 12 to 15 show that the curves are consistent and well formed as compared to the theoretically generated curves of Voyiadjis and Kattan [26] for the case of a uniaxially loaded unidirectional lamina. With five data points the curve fits have an acceptable range of error; however, a much tighter fit could be obtained with more data points. The fit for the (±45)₂ layup is considerably better than that of the (0/90)₂ layup as a result of the increased amount of damage information that is offered for specimens with this layup. Further examination of these curve fits for a particular φ_ij shows that

they have very similar shapes and magnitudes. This supports the proposition made previously that damage evolution is independent of laminate layup and orientation. Additionally, as indicated by the damage tensors shown in Equations (7) and (8) for loadings not in the direction of the fiber, the off diagonal damage parameters are of a magnitude that cannot be neglected. Also, it is found that the selection for the average crack density, Q^* has an effect on the magnitude of the damage parameters. For example using $Q^* = (\sqrt{Q_{rmax}} + \sqrt{Q_{rmax}} + \sqrt{Q_{rmax}})^2$, the damage parameters shown in Equations (7) and (8) become,

$$[\phi] = \begin{bmatrix} 3.9149 & 2.0928 & 1.0464 \\ & 1.1187 & .55936 \\ S & & .27968 \end{bmatrix}^{0.5}_{(0/90),} \times 10^{-2} \tag{9}$$

$$[\phi] = \begin{bmatrix} .50804 & 1.3141 & .65708 \\ & 3.3992 & 1.6997 \\ S & & .84984 \end{bmatrix}^{0.5}_{(\pm45),} \times 10^{-2} \tag{10}$$

Comparing Equations (7) and (9) and (8) and (10), a sizeable difference is noted in the magnitude of the damage parameters. However, this difference can be nullified by redefining the normalization factor m to include this effect.

Local Quantification of Damage

For the local quantification, damage is characterized the same as for the overall quantification, with the exception that damage is separated into matrix damage and fiber damage. Fiber damage is confined to cracks within the fiber. Damage as a result of fiber-matrix debonding is classified as part of the matrix damage. Matrix damage is divided into three distinct types: radial cracks (cracks emanating from the reaction zone into the matrix), matrix cracks (within matrix only) and fiber-matrix debonding. The total damage parameter for the matrix is therefore defined as,

$$\phi_{ij} = w_1 \phi_{ij}^{rm} + w_2 \phi_{ij}^{rmm} + w_3 \phi_{ij}^{fm} \qquad (i,j = 1,2,3) \tag{11}$$

where, ϕ_{ij}^{rm} is the damage parameter resulting from radial cracks in the matrix, ϕ_{ij}^{rmm} is the damage parameter resulting from regular cracks in the matrix and ϕ_{ij}^{fm} is the damage parameter due to fiber-matrix debonding. The $w_i (i = 1,2,3)$ terms represent corresponding scalar weight functions that are determined through homogenization techniques.

Table 6. Local crack densities for (0/90)s laminate.

% Load	% Strain	$e_1^m \times 10^{-6}$ mm/mm³	$e_1^t \times 10^{-4}$ mm/mm³	$e_1^f \times 10^{-7}$ mm/mm³	$e_1^f \times 10^{-4}$ mm/mm³
70	.3182	0.00	41.82	0.00	3.41
75	.4487	0.00	70.32	0.00	36.40
80	.4611	0.00	100.77	—	—
85	.5202	0.00	106.24	0.00	56.43
90	.5808	0.00	126.68	.77	66.94

Using the same technique as for the overall quantification of damage, crack densities were computed for the composite constituents. These results are tabulated in Tables 6 and 7 for the (0/90)s and (±45)s layups respectively. As observed in Tables 6 and 7 the measurable damage in the matrix is practically nonexistent, which shows the dominant behavior of the fibers. Due to the lack of information further processing to obtain the local damage parameters is not performed. However, the information obtained agrees with the stress-strain response. The response for the (0/90)s layup is that for a specimen with high stiffness and low ductility, which implies that almost all of the load interaction with the laminate will be with the stiffer material, whereas the response for the (±45)s is that of specimen with initial high stiffness and low ductility followed by a transition into a well defined ductile plastic region.

CONCLUSION

An experimental procedure has been outlined by which micro-analysis (SEM) can be used in determining the damage tensor, ϕ, as defined by the damage model developed by Voyiadjis and Kattan [8–10,26,29]. The process of obtaining crack density is done manually at present; however, with recent developments in image processing software and tools it can be automated to yield more precise results. The degree of precision will depend to a large extent on specimen preparation and software application. Damage parameter curves are developed from

Table 7. Local crack densities for (±45)s laminate.

% Load	% Strain	$e_1^m \times 10^{-4}$ mm/mm³	$e_1^t \times 10^{-4}$ mm/mm³	$e_1^f \times 10^{-4}$ mm/mm³	$e_1^f \times 10^{-4}$ mm/mm³
70	.2414	0.00	49.23	—	—
75	.2779	0.00	49.32	0.00	42.44
80	.4324	0.00	51.84	0.00	101.29
85	.5268	0.00	52.99	0.00	117.01
90	.5729	0.00	56.67	48.98	97.61

this micro-analysis for two different laminate layups producing a graphical representation of the evolution of damage. Comparison of the curves shows that damage evolution for each of the different layups are similar and suggests that it is independent of laminate layup and orientation. It is also noted that the proposed method of evaluating damage yields significant off diagonal damage parameters for load cases other than loaded along the fiber direction. This is important in that it provides a means to capture the damage effect on all components of an anisotropic constitutive relation. These observations require further investigation as well as comparison with theoretically obtained damage parameters which is the subject of a following paper on this topic.

In addition, an attempt is made to obtain a local quantification of damage based on the individual constituents of the composite laminate. The results obtained agreed with the experimental stress-strain response; however, not enough information is available to quantify damage locally. Since, the material tested is primarily designed for high temperature application and the test was conducted at room temperature, the fibers are not allowed to display their ductile behavior. Nonetheless, applying the procedures presented allows for the quantification of damage at the overall level where all damage is lumped into a single quantity and at the local level where damage is differentiated and separated into the constituent parts.

REFERENCES

1. Voyiadjis, G. Z. and P. I. Kattan. 1993. "Micromechanical Characterization of Damage-Plastic in Metal Matrix Composites." In George Z. Voyiadjis, ed., Studies in Applied Mechanics: Damage in Composite Materials, Vol. 34, pp. 67-102, Elsevier Science.
2. Lemaire, J. 1985. "A Continuous Damage Mechanics Model for Ductile Fracture," J. Eng. Mater. Tech., January, 107:83-89.
3. Chaboche, J. L. 1988. "Continuum Damage Mechanics: Part 1—General Concepts," J. Appl. Mech., March, 55:59-64.
4. Chaboche, J. L. 1988. "Continuum Damage Mechanics: Part II—Damage Growth, Crack Initiation, and Crack Growth," J. Appl. Mech., March, 55:65-72.
5. Dvorak, G. J., Y. A. Bahei-El-Din and L. C. Bank. 1989. "Fracture of Fibrous Metal Matrix Composites—I. Experimental Results," Eng. Proc. Mech., 34(1):87-104.
6. Bahei-El-Din, Y. A., G. J. Dvorak and J.F. Wu. 1989. "Fracture of Fibrous Metal Matrix Composites—II. Modeling and Numerical Analysis," Eng. Frac. Mech., 34(1):105-123.

7. Dvorak, G. J. 1991. "Plasticity Theories for Fibrous Composite Materials," In R. K. Everett and R. J. Arsenault, eds., *Metal Matrix Composites: Mechanism and Properties*, Academic Press Limited, pp. 1–77.

8. Voyiadjis, G. Z. and P. I. Kattan. 1992. "A Continuum-Micromechanics Damage Model for Metal Matrix Composites," In D. Hui, T. J. Kozik and O. O. Ochoa, eds., *Composite Material Technology*, Vol. PD-45, ASME, PD-Vol. 45, January, pp. 83–95.

9. Voyiadjis, G. Z. and P. I. Kattan. 1991. "Ductile Fracture of Fiber-Reinforced Metal Matrix Laminates Using an Anisotropic Coupled Model of Damage and Finite-Plasticity," in L. Schwer, J. N. Reddy and A. Mal, eds., *Enhancing Analysis Techniques for Composite Materials*, Vol. NDE-10, ASME, pp. 251–259.

10. Voyiadjis, G. Z. and P. I. Kattan. 1992. "A Plasticity Damage Theory for Large Deformation of Solids, Part I: Theoretical Formulations," *Int. J. Eng. Sci.*, 30(9):1089–1108.

11. Kattan, P. I. and G. Z. Voyiadjis. 1993. "A Plasticity Damage Theory for Large Deformation on Solids, Part II: Applications to Finite Simple Shear," *Int. J. Eng. Sci.*, 31(1):183–199.

12. Allix, O., P. Ladeveze, D. Gilleta and R. Ohayon. 1989. "A Damage Prediction Method for Composite Structure," *Int. J. Num. Meth. Eng.*, 27(2):271–283.

13. Poursatip, A., M. F. Ashby and P. W. R. Beaumont. 1982. "Damage Accumulation during Fatigue of Composites," In Tsuyoshi Hayashi, Kozo Kawata and Sokichi Umekawa, eds., *Progress in Science and Engineering of Composites: Proceedings of the Fourth International Conference on Composite Materials*, Vol. 1, Japan Society for Composite Materials, pp. 693–700.

14. Ladeveze, P., M. Poss and L. Proslier. 1982. "Damage and Fracture of Tridirectional Composites," In Tsuyoshi Hayashi, Kozo Kawata and Sokichi Umekawa, eds., *Progress of Engineering of Composites: Proceedings of the Fourth International Conference on Composite Materials*, Japan Society for Composite Materials, Vol. 1, pp. 649–658.

15. Wang, S. S., H. Suemasu and E. S. M. Chim. 1987. "Analysis of Fatigue Damage Evolution and Associated Anisotropic Elastic Property Degradation in Random Short-Fiber Composites," *J. Composite Mater.*, December, 21:1084–1105.

16. Majumdar, B. S., G. M. Newaz and J. R. Ellis. 1993. "Evolution of Damage and Plasticity in Titanium-Based, Fiber-Reinforced Composites," *Metall. Trans. Ser. A.*, July, 24A:1597–1610.

17. Breunig, T. M., S. R. Stock, J. H. Kinney, A. Guvenilir and M. C. Nichols. 1991. "Impact of X-ray Tomographic Microscopy on Deformation Studies on a SiC/Al MMC. In *Material Research Society Symposium Proceedings*, Materials Research Society, pp. 135–141.

18. Baumann, K. J., W. H. Kennedy and D. L. Hebert. 1984. "Computed Tomography X-ray Scanning role of Graphite/Epoxy Coupons," *J. Composite Mater.*, 18:537–544.

19. Benci, J. E. and D. P. Pope. 1988. "Measuring Creep Damage Using Microradiography," *Metall. Trans. Ser. A.*, April, 19A:837–847.

20. Lemaitre, J. and J. Dufailly. 1987. "Damage Measurement," *Eng. Frac. Mech.*, 28(3/6):643–661.

21. Lemaitre, J. and J.-L. Chaboche. 1990. *Mech. Solids Mater.*, pp. 69–120, 346–450, Cambridge University Press.

22. Carlsson, L. A. and R. B. Pipes. 1987. *Experimental Characterization of Advanced Composites Materials*, Prentice-Hall, Inc.

23. Tuttle, M. E. and H. F. Brinson. 1984. "Resistance-Foil Strain-Gage Technology as Applied to Composite Materials," *Exp. Mech.*, March, 24(1):54–65. Errata: Vol. 26, No. 2 June 1986, 153–154.

24. Brindley, P. K. 1987. "SiC Reinforced Aluminide Composites," In N. S. Stoloff, C. C. Koch, C. T. Liu and O. Izumi, eds., *Symposia Proc: High-Temperature Ordered Intermetallic Alloys II*, Vol. 81, Materials Research Society.

25. MacKay, R. A., P. K. Brindley and F. H. Froes. 1991. "Continuous Fiber-Reinforced Titanium Aluminide Composites," *J. Miner., Metals & Mater. Soc.*, May, 43(5):23–29.

26. Voyiadjis, G. Z. and P. I. Kattan. 1993. "Damage of Fiber-Reinforced Composite Materials with Micromechanical Characterization," *Int. J. Solids Struc.*, 30(20):2757–2778.

27. Voyiadjis, G. Z., P. I. Kattan and A. R. Venson. 1993. "Evolution of a Damage Tensor for Metal Matrix Composites," In *MECAMAT 93 International Seminar on Micromechanics of Materials*, Vol. 84, pp. 406–417. Moret-sur-Loing, France, July.

28. Voyiadjis, G. Z., P. I. Kattan, A. R. Venson and T. Park. 1993. "Anisotropic Damage Mechanics Modeling in Metal Matrix Composites," Technical Report, Final Report submitted to Air Force Office of Scientific Research, 141 pages.

29. Voyiadjis, G. Z. and P. I. Kattan. 1993. "Local Approach to Damage in Elasto-Plastic Metal Matrix Composites," *Int. J. Damage Mech.*, 2(1):92–114.

Damage in MMCs Using the GMC
Part I: Theoretical Formulation

George Z. Voyiadjis and Babur Deliktas
Department of Civil and Environmental Engineering
Louisiana State University
Baton Rouge, LA 70803

1 Abstract

In this work the incorporation of damage in the material behavior is investigated. Damage is incorporated in the generalized cells model (GMC) (Paley and Aboudi, [17]) and applied to metal matrix composites (MMCs). The local incremental damage model of Voyiadjis and Park [26] is used here in order to account for damage in each subcell separately. The resulting micromechanical analysis establishes elasto-plastic constitutive equations which govern the overall behavior of the damaged composite. The elasto-plastic constitutive model is first derived in the undamaged configuration for each constituent of the metal matrix composite. The plasticity model used here is based on the existence of a yield surface and flow rule. The relations are then transformed for each constituent to the damaged configuration by applying the local incremental constituent damage tensors. The overall damaged quantities are then obtained by applying the local damage concentration factors that are obtained by employing the rate of displacement and traction continuity conditions at the interface between subcells and between neighboring repeating cells in the generalized cells model. Examples are solved numerically in order to explore the physical interpretation of the proposed theory for a unit cell composite element.

2 Introduction

In the analysis of composite materials one can fallow a continuum approach or a micromechanical approach. In the continuum approach, the composite material is treated as an orthotropic or transversely isotropic medium. The classical equations of orthotropic elasticity are used in the analysis . This approach makes no distinction between the two different phases of the matrix and the fibers. It lacks accounting for the local effects especially due to the interaction between the different phases.

For the last two decades, researchers have been using micromechanical methods in order to analyze the multiphase composite medium. Using the micromechanical approach has distinct advantages over the continuum approach

1

in the sense that the local effects can be accounted through the volume average stress and the strain increments in each of the phases. This in turn, is linked with the overall composite behavior. Different micromechanical models employ different method of achieving the local-overall relations. Hill [18, 19] employed the volume averages of stress and strain increments in the different phases and introduced concentration tensors to relate these volume averages of the local fields to the overall uniform increments. Dvorak and Bahei-El-Din [6, 7, 8] used Hill's technique to analyze the elasto-plastic behavior of the fiber reinforced composite. They considered the matrix to be elasto-plastic while the fiber is elastic. In the micromechanical analysis of elasto-plastic composites Dvorak and Bahei-El-Din [8] identified two distinct deformation modes, the matrix dominated and the fiber dominated. The first mode is prevalent for the case of stiff elastic fibers while the second mode is more treated as a general case of plastic deformation of a heterogeneous medium.

Recently, Paley and Aboudi [17] developed the generalized cells model which is capable of predicting the behavior of metal matrix periodic composites from the given properties of its constituents. The generalized cell method is developed on the basis of the method of cells model which was originally proposed by Aboudi [1]. Its applicability and reliability in the sense of composite properties such as elastic, thermo-elastic, viscoelastic response of composites, and fatigue failure curves are discussed by Aboudi [2].

Kachanov was the first pioneer who started the continuum damage mechanics. Lemaitre [15], Chaboche [3] and Krajcinovic [5] used the continuum damage mechanics to analyze different types of damage in materials ranging from brittle fracture to ductile failure. Researchers have used continuum damage model to analyze damage in composite materials by modeling the composite medium as transversely isotropic. However, the proposed continuum approach by these researchers made no distinction regarding the different phases in the analysis of deformation and damage.

In the micromechanical approach, the local damage effects are characterized separately in the sense that the damage tensors M^r are introduced for each phase of the composite system (Voyiadjis and Kattan [23]). For the two phase composite, a matrix damage tensor, M^m, is assumed to reflect all type of damages that the matrix material undergoes like nucleation and coalescence of voids and microcracks, and a fiber damage tensor ,M^f, which is considered to reflect all types of fiber damages that fiber materials undergo such as, the fracture of fiber (Voyiadjis and Park, [26]). In this research the interfacial damage effect is also expressed through the fourth order damage tensorM^d. Finally the overall damage tensor M is introduced that accounts of all those separate damages of the matrix, fiber, and interfacial effects. However, in this work the interfacial damage effect is considered as a component of the subcell itself. This can be either matrix or fiber or any other material depending on which material occupies the corresponding subcell.

2

A thermomechanical constitutive theory was recently proposed by Allen and Haris [4] to analyze the distributive damage in the elastic composite. In particular, the problem of matrix cracking has been extensively studied in the literature (Dvorak et al [10]; Dvorak and Laws [9]; Laws and Dvorak). Recently, Voyiadjis and Guelzim [22] developed an incremental damage theory for metal matrix composites based on the modified damage model outlined by Voyiadjis and Kattan [23], and Voyiadjis and Park [26].

In this work, the incremental damage model by Voyiadjis and Park [26] is incorporated into the generalized cells model of Paley and Aboudi [17] in order to analyze the damage behavior of metal matrix composites under monotonic loading conditions. An attempt is made here in order to obtain damage parameters for each subcell micromechanically based on the incremental damage model which is developed within the frame of the effective stress concept as presented by Voyiadjis and Guelzim [22]. The subcells (local) damage parameters are then related to the overall damage variables via the concentration tensors. These concentration tensors are derived in the damaged configuration in terms of the undamaged concentration and the corresponding incremental damage tensors. A damage criterion (Voyiadjis and Park, [26]) is used here for the damage evolution for each subcell. The damage evolution mechanism for each subcell is considered separately, and the extremum principle is used in order to formulate the damage evolution expression. Finally damaged constitutive relations are formulated in order. Making use of the micromechanical model (GMC) which allows one to divide the repeating volume element into many subregions together with the incremental damage model, one is able to analyze the damage at various locations and at any increment of loading. This method provides a computationally efficient approach to predict the damage by using the GMC for MMCs.

The incremental damage approach coupled with the micromechanical plasticity model is formulated here in order to analyze the damage behavior of composites in the plastic domain as well as in the elastic one. The fibers in this work are aligned and have a linear elastic behavior while the matrix is considered to be elasto-plastic material that obeys the von Mises yield criterion with an associated flow rule and a Ziegler-Prager kinematic hardening rule. However, the resulting yield condition for the damaged composite system is a combination of the generalized Ziegler Prager rule and the Phillips type rule. The motion of the yield surface is described by a kinematic hardening rule that is a linear combination of the Ziegler-Prager kinematic hardening rule, and the Phillip's hardening rule in the direction of loading. In the numerical simulation of this work, the unit cell case of the GMC model is considered such that the repeating volume element consists of an elastic fiber region together with three elasto-plastic matrix domains.

3

3 Theoretical Preliminaries

3.1 The Generalized Cells Model

The generalized cells model is the generalization of the method of cells (Aboudi, [1]) by taking any number of subcells rather than four subcells and considering the rate dependent relations of the subcell for modeling the multiphase composite materials. This generalization is particularly advantageous when dealing with elasto-plastic composites, since yielding and plastic flow of the metallic phase may take place at different locations. The GMC is able to provide a more accurate representation of the actual microstructure.

This micromechanical analysis, based on the theory of the continuum media in which equilibrium is ensured, can be summarized essentially as follows. A repeating volume element of periodic multiphase composite is first identified. This is followed by defining the macroscopic average stresses and strains from the microscopic ones. Continuity of traction and displacement rates on the average basis are then imposed at the interfacesbetween the constituents. The micro equilibrium is guaranteed by the assumption that the velocity vector is linearly expanded in terms of the local coordinates of the subcell. This forms the relation between the microscopic strains, and the macroscopic strains through the relevant concentration tensors. In the final step the overall elasto-plastic behavior of multiphase inelastic composite is determined. This is expressed as a constitutive relation between the average stress, strain, and plastic strain, in conjunction with the effective elastic stiffness tensor of the composite. In this study the same steps are followed but in addition the damage mechanics is incorporated by using the micromechanical approach in order to obtain the damaged response of each constituent as well as overall instantaneous damaged behavior of the elasto-plastic composite.

A unidirectional fibrous composite is considered here in the method of cells. It is assumed that the composite has a periodic structure in which unidirectional fibers are extended in the x_1 direction. This representative volume element is shown in Figure (1a). The representative volume element (Figure (1b)) consists of N_β by N_γ subcells such that the area of the cross section of each subcell is $h_\beta l_\gamma$ with $\beta = 1...N_\beta, \gamma = 1...N_\gamma$ and each subcell has its own local coordinate system $(x_1, x_2^{(\beta)}, x_3^{(\gamma)})$ with its origin located at the center of each subcell.

Unlike the method of cells, in this work the instantaneous behavior of the composite is considered. The displacement rate $\dot{u}_i^{(\beta\gamma)}$ (dot denotes time derivative) is expanded linearly in terms of the distance from the center of the subcell (Paley and Aboudi, [17]). This leads the following first order expression

$$\dot{u}_i^{(\beta\gamma)} = \dot{w}_i^{(\beta\gamma)} + \bar{x}_2^{(\beta)}\dot{\theta}_i^{(\beta\gamma)} + \bar{x}_3^{(\gamma)}\dot{\psi}_i^{(\beta\gamma)} \tag{1}$$

where, $\dot{w}_i^{(\beta\gamma)}$ is the rate tensor of the displacement components at the center of the subcell, and $\dot{\theta}_i^{(\beta\gamma)}, \dot{\psi}_i^{(\beta\gamma)}$ are microvariables rates that characterize the linear dependence of the displacement rates on the local coordinates $\bar{x}_2^{(\beta)}, \bar{x}_3^{(\gamma)}$.

The small strain rate tensor and the constitutive law for the material that occupies the subcell $(\beta\gamma)$ are given by the following expressions respectively

$$\dot{\bar{\epsilon}}_{ij}^{(\beta\gamma)} = \frac{1}{2}\left(\frac{\partial \dot{\bar{u}}_i^{(\beta\gamma)}}{\partial \bar{x}_j} + \frac{\partial \dot{\bar{u}}_j^{(\beta\gamma)}}{\partial \bar{x}_i}\right) \tag{2}$$

$$\dot{\bar{\sigma}}_{ij}^{(\beta\gamma)} = \bar{D}_{ijkl}^{(\beta\gamma)}\dot{\bar{\epsilon}}_{ij}^{(\beta\gamma)} \tag{3}$$

The instantaneous stiffness tensor, $\bar{D}^{(\beta\gamma)}$. depends on the deformation history, loading path and applied loading rate. In this study for elasto-plastic materials, the von Mises yield criterion with an associated flow rule and the Ziegler-Prager kinematic hardening rule are used. This elasto-plastic tensor in the undamaged material is given by the following relation

$$\bar{D}_{ijkl}^{(\beta\gamma)} = \bar{E}_{ijkl}^{(\beta\gamma)} - \frac{1}{\bar{Q}}\frac{\partial \bar{f}^{(\beta\gamma)}}{\partial \bar{\sigma}_{pq}^{(\beta\gamma)}}\bar{E}_{pqij}^{(\beta\gamma)}\bar{E}_{klrs}^{(\beta\gamma)}\frac{\partial \bar{f}^{(\beta\gamma)}}{\partial \bar{\sigma}_{rs}^{(\beta\gamma)}} \tag{4}$$

where $\bar{Q}$ is given by

$$\bar{Q} = \frac{\partial \bar{f}^{(\beta\gamma)}}{\partial \bar{\sigma}_{ij}^{(\beta\gamma)}}\bar{E}_{ijkl}^{(\beta\gamma)}\frac{\partial \bar{f}^{(\beta\gamma)}}{\partial \bar{\sigma}_{kl}^{(\beta\gamma)}} - \frac{\partial \bar{f}^{(\beta\gamma)}}{\partial \bar{\alpha}_{ij}^{(\beta\gamma)}}(\bar{\sigma}_{ij}^{(\beta\gamma)} - \bar{\alpha}_{ij}^{(\beta\gamma)})\frac{\frac{\partial \bar{f}^{(\beta\gamma)}}{\partial \bar{\sigma}_{pq}^{(\beta\gamma)}}\frac{\partial \bar{f}^{(\beta\gamma)}}{\partial \bar{\sigma}_{pq}^{(\beta\gamma)}}}{(\bar{\sigma}_{ij}^{(\beta\gamma)} - \bar{\alpha}_{ij}^{(\beta\gamma)})\frac{\partial \bar{f}^{(\beta\gamma)}}{\partial \bar{\sigma}_{kl}^{(\beta\gamma)}}}b^{(\beta\gamma)} \tag{5}$$

In equation (5), $\bar{f}^{(\beta,\gamma)}$ is the von Mises yield criterion with kinematic hardening expressed in terms of the backstress tensor $\bar{\alpha}^{(\beta,\gamma)}$. The material parameter $b^{(\beta,\gamma)}$ pertains to the evolution behavior of the back stress (Voyiadjis and Kattan, [23]). In the special case of perfectly elastic materials $\bar{D}^{(\beta\gamma)}$ is replaced by the standard elastic stiffness tensor $\bar{E}^{(\beta\gamma)}$ which characterizes the behavior of elastic materials in the subcells. More elaborate plasticity models for the in-situ characterization of metal matrix composites is given by the first author in other works(Voyiadjis and Ganesh, [24]) . However, in this work a simple model is used.

The objective of the work outlined by Paley and Aboudi [17] is to solve the microvariables given in equation (1). This equation is substituted into the small strain tensor by employing the rate of displacement and traction continuity conditions at the interfaces between the subcells and between neighboring repeating cells in order to obtain the relation between the average subcell strain rate components and the average overall strain rate components via strain concentration tensors. The first step is to write a set of continuum equations in terms of the microvariables. These interface conditions are shown in Figures 2 and 3. Since it is ensured that at any instant the component of displacement rates should be continuous at the interfaces, the following relations can be obtained in terms of

5

the micro variable rates using the continuity conditions of displacement rates at the interfaces between the subcells and the neighboring cell and these relations are given by

$$\dot{w}_i^{(\beta\gamma)} + \frac{1}{2}h_\beta \dot{\theta}_i^{(\beta\gamma)} = \dot{w}_i^{(\hat{\beta}\gamma)} - \frac{1}{2}h_{\hat{\beta}}\dot{\theta}_i^{(\hat{\beta}\gamma)} \tag{6}$$

and

$$\dot{w}_i^{(\beta\gamma)} + \frac{1}{2}\ell_\gamma \dot{\psi}_i^{(\beta\gamma)} = \dot{w}_i^{(\beta\hat{\gamma})} - \frac{1}{2}\ell_{\hat{\gamma}}\dot{\psi}_i^{(\beta\hat{\gamma})} \tag{7}$$

All the field variables in equations (6) and (7) are evaluated at the centerline $x_2^{(\beta)}$ for the subcell $(\beta\gamma)$ and $x_2^{(\hat{\beta})}$ for the subcell $(\hat{\beta}\gamma)$. As indicated in Figure 2(b) since the interface is along the x_3 direction one has $x_3^{(\gamma)}$ for the subcell $(\beta\gamma)$ and $x_3^{(\hat{\gamma})}$ for the subcell $(\beta\hat{\gamma})$ and the interface is along the x_2 direction. This relation can be expressed by

$$x_2^{(\beta)} = x^{(I)} - h_\beta/2 \quad \text{or} \quad x_2^{(\hat{\beta})} = x^{(I)} + h_{\hat{\beta}} \tag{8}$$

and

$$x_3^{(\gamma)} = x^{(I)} - \ell_\gamma/2 \quad \text{or} \quad x_3^{(\hat{\gamma})} = x^{(I)} + \ell_{\hat{\gamma}}/2 \tag{9}$$

By employing a Taylor expansion of field variables in equation (6) together with equation (8) and omitting second and higher order terms, one obtains

$$\dot{w}_i^{(\beta\gamma)} - \frac{1}{2}h_{(\beta)}\left(\frac{\partial}{\partial x_2}\dot{w}_i^{(\beta\gamma)} - \dot{\theta}_i^{(\beta\gamma)}\right) = \dot{w}_i^{(\beta\gamma)} + \frac{1}{2}h_{(\hat{\beta})}\left(\frac{\partial}{\partial x_2}\dot{w}_i^{(\beta\gamma)} - \dot{\theta}_i^{(\hat{\beta}\gamma)}\right) \tag{10}$$

A similar expression can obtained by using equation (7) in equation (9) for the interface conditions along x_3 direction such that

$$\dot{w}_i^{(\beta\gamma)} - \frac{1}{2}\ell_{(\gamma)}\left(\frac{\partial}{\partial x_2}\dot{w}_i^{(\beta\gamma)} - \dot{\psi}_i^{(\beta\gamma)}\right) = \dot{w}_i^{(\beta\hat{\gamma})} + \frac{1}{2}\ell_{\hat{\gamma})}\left(\frac{\partial}{\partial x_2}\dot{w}_i^{\beta\hat{\gamma}} - \dot{\psi}_i^{(\beta\hat{\gamma})}\right) \tag{11}$$

These equations are valid in the equivalent continuum medium in which the repeating volume element can be defined by a point P. This mapping procedure of repeating volume elements at P within the equivalent homogeneous medium eliminates the discrete structure of the composite. Since a composite is subjected to homogeneous boundary conditions, the behavior of all repeating cells are identical, and a uniform field exits at the equivalent homogeneous medium. The governing constitutive laws of this equivalent continuum medium can be established by the generalized cells model.

From equations (10) and (11) the $N_\beta + N_\gamma$ continuum relations can be written in terms of the microvariables $\dot{\theta}_i^{(\beta\gamma)}$ and $\dot{\psi}_i^{(\beta\gamma)}$, and their explicit expression can be

found in reference [17]. The composite standard average strain rate $\bar{\dot{\epsilon}}^{(\beta\gamma)}$ is given by

$$\bar{\dot{\epsilon}}_{ij} = \frac{1}{hl} \sum_{\beta=1}^{N\beta} \sum_{\gamma=1}^{N\gamma} h_\beta \, \ell_\gamma \bar{\dot{\epsilon}}_{ij}^{(\beta\gamma)} \tag{12}$$

It is possible to derive a $2(N_\beta + N_\gamma) + N_\beta N_\gamma + 1$ system of continuum relations expressed in terms of the subcell strain rate tensors $\dot{\epsilon}_{ij}^{(\beta\gamma)}$ by using the previous $N_\beta + N_\gamma$ continuum equations together with expression (12). After tedious mathematical manipulations, these relation can be given as follow

$$\bar{\dot{\epsilon}}_{11} = \bar{\dot{\epsilon}}_{11}^{(\beta\gamma)} \qquad\qquad \beta, \gamma = 1 \cdots, N_\beta, N_\gamma \quad (N_\beta N_\gamma \quad \text{relations}) \tag{13}$$

$$\bar{\dot{\epsilon}}_{22} = \frac{1}{h} \sum_{\beta=1}^{N\beta} h_\beta \bar{\dot{\epsilon}}_{22}^{(\beta\gamma)} \qquad\qquad \gamma = 1 \cdots, N_\gamma \quad (N_\gamma \quad \text{relations}) \tag{14}$$

$$\bar{\dot{\epsilon}}_{33} = \frac{1}{\ell} \sum_{\gamma=1}^{N\gamma} \ell_\gamma \bar{\dot{\epsilon}}_{33}^{(\beta\gamma)} \qquad\qquad \beta = 1 \cdots, N_\beta \quad (N_\beta \quad \text{relations}) \tag{15}$$

$$2\bar{\dot{\epsilon}}_{23} = \frac{1}{h\ell} \sum_{\beta=1}^{N\beta} \sum_{\gamma=1}^{N\gamma} h_\beta \, \ell_\gamma \bar{\dot{\epsilon}}_{23}^{(\beta\gamma)} \qquad (\text{one relation}) \tag{16}$$

$$2\bar{\dot{\epsilon}}_{13} = \frac{1}{\ell} \sum_{\gamma=1}^{N\gamma} \ell_\gamma \bar{\dot{\epsilon}}_{13}^{(\beta\gamma)} \qquad\qquad \beta = 1 \cdots, N_\beta \quad (N_\beta \quad \text{relations}) \tag{17}$$

$$2\bar{\dot{\epsilon}}_{12} = \frac{1}{h} \sum_{\beta=1}^{N\beta} h_\beta \bar{\dot{\epsilon}}_{12}^{(\beta\gamma)} \qquad\qquad \gamma = 1 \cdots, N_\gamma \quad (N_\gamma \quad \text{relations}) \tag{18}$$

The above $2(N_\beta + N_\gamma) + N_\beta N_\gamma + 1$ continuum relations are expressed in matrix form by Paley and Aboudi [17] as follows

$$A_G \dot{\bar{\epsilon}}_s = J\dot{\bar{\epsilon}} \tag{19}$$

where the 6-order average strain-rate vector is of the form

$$[\dot{\bar{\epsilon}}] = [\dot{\bar{\epsilon}}_{11}, \dot{\bar{\epsilon}}_{22}, \dot{\bar{\epsilon}}_{33}, \dot{\bar{\epsilon}}_{23}, \dot{\bar{\epsilon}}_{13}, \dot{\bar{\epsilon}}_{12}] \tag{20}$$

and the $6N_\beta N_\gamma$ order subcells strain-rate vector is defined as follows

$$[\dot{\bar{\epsilon}}] = [\dot{\bar{\epsilon}}^{(11)}, \dot{\bar{\epsilon}}^{(12)}, \dot{\bar{\epsilon}}^{(21)} \cdots \dot{\bar{\epsilon}}^{(\beta\gamma)}] \tag{21}$$

7

The A_G is $2(N_\beta + N_\gamma) + N_\beta N_\gamma + 1$ by $6N_\beta N_\gamma$ matrix and involves the geometrical properties of the repeating cells while J is a $2(N_\beta + N_\gamma) + N_\beta N_\gamma + 1$ by 6 matrix .

One now needs $5N_\beta N_\gamma - 2(N_\beta + N_\gamma) - 1$ continuum relations to complete the $6\ N_\beta N_\gamma$ set of continuum equations. They can be obtained by imposing the continuity of the rates of traction at the interfaces between the subcells and between neighboring repeating cells. The continuity of average stress rates at the interfaces can be expressed by the following relations

$$\dot{\bar{\sigma}}_{2j}^{(\beta\gamma)} = \dot{\bar{\sigma}}_{2j}^{(\beta\gamma)}, j = 1, 2, 3 \qquad (22)$$

and

$$\dot{\bar{\sigma}}_{3j}^{(\beta\gamma)} = \dot{\bar{\sigma}}_{3j}^{(\beta\gamma)}, j = 1, 2, 3 \qquad (23)$$

One can express the average stress rate $\dot{\bar{\sigma}}_{ij}^{(\beta\gamma)}$ in the subcells in terms of the average strain rate $\dot{\bar{\epsilon}}_{ij}^{(\beta\gamma)}$ by using the constitutive law of the material (equation (3)) in the subcells. Using equation (22) and (23) the remaining continuum equations which can be written in the matrix form as follow

$$A_m \dot{\bar{\epsilon}}_s = 0 \qquad (24)$$

A_m is $5N_\beta N_\gamma - 2(N_\beta + N_\gamma) - 1$ by $6N_\beta N_\gamma$ matrix. A_m involves the instantaneous properties of the material in the various subcells. The $6N_\beta\ N_\gamma$ continuum equation can be written in the following matrix form by combining equations (19) and (24)

$$A_m^* \dot{\bar{\epsilon}}_s = K \dot{\bar{\epsilon}} \qquad (25)$$

where the $6N_\beta\ N_\gamma$ order square matrix A_m^* is given in the form

$$A_m^* = \begin{bmatrix} A_m \\ A_G \end{bmatrix} \quad \text{and} \quad K = \begin{bmatrix} 0 \\ J \end{bmatrix} \qquad (26)$$

One can now solve the linear system of equations (25) in order to obtain the following expression

$$\dot{\bar{\epsilon}}_s = A_c \dot{\bar{\epsilon}} \qquad (27)$$

where

$$A_c = \left[A_m^* \right]^{-1} K \qquad (28)$$

A_c is the instantaneous strain concentration tensor that relates the average strain-rate tensor in the subcell to the average overall strain-rate tensor. The matrix A_c can be partitioned into a number of $N_\beta\ N_\gamma$ by 6x6 matrices as shown below

$$A_c = \begin{bmatrix} A_c^{(11)} \\ \vdots \\ A_c^{(N_\beta N_\gamma)} \end{bmatrix} \qquad (29)$$

8

$A_c^{(\beta\gamma)}$ is the instantaneous strain concentration tensor for the subcell which relates the average strain rate tensor in the subcell $(\beta\gamma)$ to the average total strain rate tensor. One can now obtain the overall effective instantaneous stiffness tensor of the composite by using the strain concentration tensor of the subcell along with its respective subcell constitutive equations (Paley and Aboudi, 1992).

3.2 Incremental Damage Model

In this study, the incremental damage model is used in order to characterize the damage using the fourth order incremental damage tensor $m^{(\beta\gamma)}$ where $(\beta\gamma)$ designates the subcell . The concept of effective stress as generalized by Murakami [16] is used here in order to introduce the damage for the $(N_\beta$ by $N_\gamma)$ constituents of the composite system. The $m^{(\beta\gamma)}$ is assumed to reflect all types of damages that corresponding subcells undergo such as nucleation and coalescence of voids, and microcracks. This local damage response is linked to the overall damage response of the composite medium through the stress and strain concentration tensors. The elasto-plastic stiffness tensor is derived for the damaged composite using the subcell incremental damage tensors in the generalized cells model, and the relation between the subcell incremental damage tensor $m^{(\beta\gamma)}$ and the incremental overall damage tensor m.

Kachanov [12] introduced a simple scalar damage model for isotropic materials by using the concept of the effective stress. The incremental damage model was further developed subsequently on the base of the effective stress concept for anisotropic materials by Voyiadjis and Park [26] and Voyiadjis and Guelzim [22] In its formulation three configurations are assumed namely the initial undeformed and undamaged configuration C_0 , the deformed and damaged configuration C, and the state of the body after it has only deformed without damage $\bar{C}$, (Voyiadjis and Kattan [23]) as indicated in Figure 4.

By considering the equality of forces between the damaged, C, and the undamaged fictitious configuration ,$\bar{C}$, the following linear transformation can be written between the Cauchy stress in the configuration C, and the effective Cauchy stress in the configuration $\bar{C}$

$$\bar{\sigma}\bar{A} = \sigma A \quad \text{or} \quad \bar{\sigma} = (1 - \phi)^{-1} \tag{30}$$

where

$$\phi = \frac{A - \bar{A}}{A} \tag{31}$$

and ϕ is a scalar (Kachanov [12]). In the above equations A and $\bar{A}$ are the areas of the crossections of the axially loaded bar in the C, and $\bar{C}$ configurations respectively. The term ϕ is a measure of damage. The concept of effective stress

9

as generalized by Murakami [16] is given through the generalization of equation (30) such that

$$\bar{\sigma} = M : \sigma \qquad (32)$$

where M is a fourth-order damage effect tensor and is a function of the second order symmetric tensor ϕ. The effective Cauchy stress tensor $\bar{\sigma}$ need not be symmetric or frame invariant. However, the symmetrized effective Cauchy stress tensor $\bar{\sigma}$ used here is given by (Lee et al. [13])

$$\bar{\sigma}_{ij} = \frac{1}{2}[\sigma_{ik}(\delta_{kj} - \phi_{kj})^{-1} + (\delta_{il} - \phi_{il})^{-1}\sigma_{lj}] \qquad (33)$$

ϕ is a second rank tensorial generalization of the scalar function ϕ given by equation (30). The stress given by equation (32) is frame independent. Utilizing the symmetrization procedure outlined by equation (33), a 6 by 6 matrix form of tensor M is derived by Voyiadjis and Kattan [23]. However, the fourth order tensorial form of M is utilized in this work.

In order to find the incremental damage tensor m, one can use equation (32). The rate (incremental) expression of this equation can be written as follows

$$\dot{\bar{\sigma}} = M : \dot{\sigma} + \dot{M} : \sigma \qquad (34)$$

The superposed dot implies the material time differentiation. In order for equation (34) to be homogeneous in time of order one (i.e stress-rate independent) $\dot{M}$ should be a linear function of $\dot{\sigma}$. This is demonstrated by the following expression

$$\dot{\phi} = X : \dot{\sigma} \qquad (35)$$

Since $\dot{M}$ is a function of ϕ, one obtains therefore

$$\dot{M}_{ijkl} = \frac{\partial M_{ijkl}}{\partial \phi_{pq}} \dot{\phi}_{pq} \qquad (36)$$

Consequently by substituting equations (35) and (36) into equation (34), the following relation may be written in the form

$$\dot{\bar{\sigma}} = m : \dot{\sigma} \qquad (37)$$

where m represent the fourth order incremental damage tensor and is given by Voyiadjis and Guelzim [22]

$$m_{ijkl} = M_{ijkl} + G_{ijpqkl}\sigma_{pq} \qquad (38)$$

where

$$G_{ijpqrs} = \frac{\partial M_{ijkl}}{\partial \phi_{pq}} X_{pqrs} \qquad (39)$$

The explicit expression for the fourth order tensor X in equation (39) is given in Section 4.4. The proposed damage model was used successfully for both monotonic and cyclic loads Vojiadjis and Ganesh [25]

10

4 Theoretical Formulation

4.1 Basic Assumptions

In this work, C_0 denotes the initial undeformed and undamaged configuration of a single laminate while $C_0^{(\beta\gamma)}$ is the initial undeformed and undamaged subcell sub-configuration of a single laminate. The composite material is assumed to undergo elasto-plastic deformation and damage due to the applied loads. The resulting overall configuration for a single laminate is denoted by C. Damage is expressed by generalizing the concept proposed by Kachanov [12]. The fictitious configurations $\bar{C}^{(\beta\gamma)}$ is obtained from $C^{(\beta\gamma)}$ by removing the different types of damages that the corresponding subcell $(\beta\gamma)$ has undergone due to the applied stresses. The total or incremental subcell stress at configuration $C^{(\beta\gamma)}$ is converted to the respective total or incremental stress at the fictitious configuration $\bar{C}^{(\beta\gamma)}$ through the damage tensor $M^{(\beta\gamma)}$ or $m^{(\beta\gamma)}$ respectively. The incremental damage tensor $m^{(\beta\gamma)}$ reflects the damage related that subcell only. Following this local damage description, local-overall relations are used to transfer the local damage effect to the whole composite system in configuration C. This is accomplished through the stress and strain concentration tensors of the subcells.

The coupled formulation of plastic flow and damage propagation is quite complex due to the presence of the two different dissipative mechanisms that influence each other. This could be indicated by the fact that the position of the slip planes affect the orientation of nucleated microcracks. A phenemological model of interaction can then be applied. In this work use is made of the concept of the effective stress (Lemaitre) [14]. Making use of a fictitious undamaged system, the dissipation energy due to plastic flow in this undamaged system is assumed to be equal to the dissipation energy due to plastic flow in the damaged system. The damages at the single laminate level are described separately by the damage in the subcells according to the material in the subcells. The subcell incremental damage tensors, $m^{(\beta\gamma)}$, is better suited for use in the formulation of the constitutive equation of the damaged material behavior due to the incremental nature of plasticity.

In this work, direct tensor notation is employed whenever possible. The tensors are denoted by the bold face letters. The following notation wherever possible for tensor operation is followed throughout the paper for the second-rank tensors U and V and the for the fourth-rank tensors C and D. The following notation is used in this work $U : V = U_{ij}V_{ij}, U.V = U_{ij}V_{kl}, C : U = C_{ijkl}U_{kl}, U.C = U_{ij}C_{ijkl}$ and $C : D = C_{ijmn}D_{mnkl}$. I_2 and I_4 are respectively the second-rank and fourth-rank identity tensors: $I_2 = \delta_{ij}$ and $I_4 = \frac{1}{2}(\delta_{ik}\delta_{jl} + \delta_{il}\delta_{jk})$ where δ_{ij} is known as the Kronecker delta. The transpose and inverse of tensors are denoted by the superscript "T" and "-1" respectively.

11

4.2 Local-Overall Relations of The Damage Tensors

In this section the relations between incremental damage tensor $m^{(\beta\gamma)}$ of subcells $(\beta\gamma)$ and overall incremental damage tensor m of the composite medium are derived by using the fact that the average damaged stress rates $\dot{\sigma}$ can be obtained as the average sum of the the damaged stress rates $\dot{\sigma}^{(\beta\gamma)}$ of the subcells in the damaged configuration $C^{(\beta\gamma)}$ and is given by the following relation

$$\dot{\sigma} = \frac{1}{V} \sum_{\beta=1}^{N_\beta} \sum_{\gamma=1}^{N_\gamma} v_{\beta\gamma} \dot{\sigma}^{(\beta\gamma)} \tag{40}$$

In equation (40) V is the total area of the representative volume element while $v_{\beta\gamma}$ is the area of the individual subcell in the damaged configuration. Subcell incremental damage tensor $m^{(\beta\gamma)}$ can be introduced in a similar form to equation (37) such that

$$\dot{\bar{\sigma}}^{(\beta\gamma)} = m^{(\beta\gamma)} : \dot{\sigma}^{(\beta\gamma)} \tag{41}$$

where $m^{(\beta\gamma)}$ encompasses all the pertinent damages that the corresponding subcell undergoes. The effective subcell Cauchy stress rate $\dot{\bar{\sigma}}^{(\beta\gamma)}$ is related to the overall effective stress rate $\dot{\bar{\sigma}}$ in the composite through the stress concentration tensor $\bar{B}^{(\beta\gamma)}$ as follows

$$\dot{\bar{\sigma}}^{(\beta\gamma)} = \bar{B}^{(\beta\gamma)} : \dot{\bar{\sigma}} \tag{42}$$

where the effective stress concentration tensor $\bar{B}^{(\beta\gamma)}$ is given in the following expression by Paley and Aboudi [17]

$$\bar{B}^{(\beta\gamma)} = \bar{C}^{(\beta\gamma)} : \bar{A}^{(\beta\gamma)} : [\bar{C}]^{-1} \tag{43}$$

where $\bar{C}^{(\beta\gamma)}$ is the effective stiffness tensor for the subcell, $\bar{A}^{(\beta\gamma)}$ is the undamaged strain concentration tensor for the subcell and the $\bar{C}$ is the overall undamaged effective stiffness tensor for the composite. One can solve $\dot{\sigma}^{(\beta\gamma)}$ from equation (41) such that

$$\dot{\sigma}^{(\beta\gamma)} = [m^{(\beta\gamma)}]^{-1} : \dot{\bar{\sigma}}^{(\beta\gamma)} \tag{44}$$

Making use of relations (42) and (44) in (40), one obtains the following expression

$$\dot{\sigma} = \frac{1}{V} \sum_{\beta=1}^{N_\beta} \sum_{\gamma=1}^{N_\gamma} v_{\beta\gamma} [m^{(\beta\gamma)}]^{-1} : \bar{B}^{(\beta\gamma)} : \dot{\bar{\sigma}} \tag{45}$$

This equation can be easily written in a similar form to equation (37) where m represents the overall incremental damage tensor which reflects all types of damages

12

that the composite undergoes including that due to the interaction between the subcells. The resulting expression is given by

$$m = \left[\frac{1}{V}\sum_{\beta=1}^{N_\beta}\sum_{\gamma=1}^{N_\gamma} v_{\beta\gamma}[m^{(\beta\gamma)}]^{-1} : \bar{B}^{(\beta\gamma)}\right]^{-1} \tag{46}$$

This expression defines the cumulative incremental damage of the composite as a function of its subcell components.However, m may be expressed in terms of the fiber damage m^f, the matrix damage m^m, and the damage due to debonding m^d(Voyiadjis and Park, [26]).

4.3 Damaged Strain and Stress Concentration Tensors

Concentration tensors do not remain constant as the composite undergoes damage. However, they are constant in the undamaged elastic domain. In this work undamaged concentration factors are modified for the incremental damage model in conjunction with the hypothesis of the equivalence of elastic strain energy [20]. The effective elastic strain and stress concentration tensors are obtained by using the generalized cells model. The subcell strain rate tensors can be related to the overall strain rate tensor in the following way

$$\dot{\bar{\epsilon}}^{(\beta\gamma)} = \bar{A}^{(\beta\gamma)} : \dot{\bar{\epsilon}} \tag{47}$$

where fourth order tensor, $\bar{A}^{(\beta\gamma)}$ is the instantaneous strain concentration tensor for the subcell $(\beta\gamma)$ and is given by equation (29). The undamaged stress concentration tensors $\bar{B}^{(\beta\gamma)}$ of the subcells are already defined in the previous section and their relations are given by equations (42) and (43).

The damaged concentration tensors can be obtained in terms of the undamaged concentration factors and incremental damage tensors in connection with the elastic energy equivalence, given by

$$d\bar{U}^{(\beta\gamma)} = dU^{(\beta\gamma)} \tag{48}$$

or

$$\frac{1}{2}d\dot{\bar{\sigma}}^{(\beta\gamma)} : d\dot{\bar{\epsilon}}^{(\beta\gamma)} = \frac{1}{2}d\dot{\sigma}^{(\beta\gamma)} : d\dot{\epsilon}^{(\beta\gamma)} \tag{49}$$

Substituting equation (41) into equation (49), one obtains the following relation

$$\dot{\bar{\epsilon}}^{(\beta\gamma)} = [m^{(\beta\gamma)}]^{-1} : \dot{\epsilon}^{(\beta\gamma)} \tag{50}$$

The above equation can be written for the overall behavior in similar form as shown below

$$\dot{\bar{\epsilon}} = [m]^{-1} : \dot{\epsilon} \tag{51}$$

Consequently by combining equations (50) and (51) with equation (47), the relation between the damaged strain rate $\dot{\bar{\epsilon}}^{(\beta\gamma)}$ of the subcell and the damaged strain rate $\dot{\bar{\epsilon}}$ can be obtained in the form shown below

$$\dot{\bar{\epsilon}}^{(\beta\gamma)} = A^{(\beta\gamma)} : \dot{\bar{\epsilon}} \tag{52}$$

where $A^{(\beta\gamma)}$ is the damaged stress concentration tensor for subcell $(\beta\gamma)$ and its expression is given by

$$A^{(\beta\gamma)} = m^{(\beta\gamma)} : \bar{A}^{(\beta\gamma)} : [m]^{-1} \tag{53}$$

Similarly by using equations (37) and (41) with (42), the damaged stress concentration tensor for the subcell can be given as follows

$$\dot{\bar{\sigma}}^{(\beta\gamma)} = B^{(\beta\gamma)} : \dot{\bar{\sigma}} \tag{54}$$

where $B^{(\beta\gamma)}$ is the damaged stress concentration tensor for subcell $(\beta\gamma)$ and its expression is given by

$$B^{(\beta\gamma)} = [m^{(\beta\gamma)}]^{-1} : \bar{B}^{(\beta\gamma)} : m \tag{55}$$

4.4 Damage Criterion

In order to study the evolution of damage in composite materials, one first needs to investigate the damage criterion. The anisotropic damage criterion used here is expressed in term of a tensorial parameter h (Voyiadjis and Park, [26]). It is clear that the damage mechanism for each subcell of the composite materials should be accounted separately since each subcell can be occupied by a different type of material in addition their boundary and geometric conditions can be different for each subcell. Therefore one single damage mechanism cannot be considered for all subcells in the multiphase composite medium. The anisotropic damage criterion based on the Mroz theory [27] is generalized by Voyiadjis and Park [26] as follows

$$g^{(\beta\gamma)} \equiv g^{(\beta\gamma)}(Y, \kappa) = 0 \tag{56}$$

or

$$g^{(\beta\gamma)} \equiv Y_{ij}^{(\beta\gamma)} P_{ijkl}^{(\beta\gamma)} Y_{kl}^{(\beta\gamma)} - 1 = 0 \tag{57}$$

14

where

$$P_{ijkl}^{(\beta\gamma)} = h_{ij}^{-(\beta\gamma)} h_{kl}^{-(\beta\gamma)} \tag{58}$$

$Y^{(\beta\gamma)}$ is the generalized thermodynamic force conjugate to the damage tensor $\phi^{(\beta\gamma)}$. The hardening tensor $h^{(\beta\gamma)}$ is expressed as follows

$$h_{ij}^{(\beta\gamma)} = U_{ij}^{(\beta\gamma)} + V_{ij}^{(\beta\gamma)} \tag{59}$$

where tensors $U^{(\beta\gamma)}$ and $V^{(\beta\gamma)}$ are defined for orthotropic materials in terms of the generalized Lame constant $\lambda_1^{(\beta\gamma)}, \lambda_2^{(\beta\gamma)}, \lambda_3^{(\beta\gamma)}$ and the material parameters $\nu_1^{(\beta\gamma)}, \nu_2^{(\beta\gamma)}, \nu_3^{(\beta\gamma)}, \xi_1^{(\beta\gamma)}, \xi_2^{(\beta\gamma)}, \xi_3^{(\beta\gamma)},$ and $\eta_1^{(\beta\gamma)}, \eta_2^{(\beta\gamma)}, \eta_3^{(\beta\gamma)}$ which are obtained by matching the theory with the experimental results. Voyiadjis and Park [26] used the following expressions for $U_{ij}^{(\beta\gamma)}$ and $V_{ij}^{(\beta\gamma)}$.

$$U_{ij}^{(\beta\gamma)} = \begin{pmatrix} \lambda_1\eta_1\left(\frac{\kappa}{\lambda_1}\right)^{\xi_1} & 0 & 0 \\ 0 & \lambda_2\eta_2\left(\frac{\kappa}{\lambda_2}\right)^{\xi_2} & 0 \\ 0 & 0 & \lambda_3\eta_3\left(\frac{\kappa}{\lambda_3}\right)^{\xi_3} \end{pmatrix}^{(\beta\gamma)} \tag{60}$$

and

$$V_{ij}^{(\beta\gamma)} = \begin{pmatrix} \lambda_1\nu_1^2 & 0 & 0 \\ 0 & \lambda_2\nu_2^2 & 0 \\ 0 & 0 & \lambda_3\nu_3^2 \end{pmatrix}^{(\beta\gamma)} \tag{61}$$

$\kappa^{(\beta\gamma)}$ is the scalar representing the total damage energy and is given by the following relation

$$\kappa^{(\beta\gamma)} = \int_0^t Y^{(\beta\gamma)} : \dot{\phi}^{(\beta\gamma)} dt \tag{62}$$

or

$$\dot{\kappa}^{(\beta\gamma)} = Y^{(\beta\gamma)} : \dot{\phi}^{(\beta\gamma)} \tag{63}$$

The generalized Lame constants are defined as follow (Voyiadjis and Park, [26]).

$$\lambda_i^{(\beta\gamma)} = \bar{E}_i^{(\beta\gamma)}(1 - \phi_i^{(\beta\gamma)})^2 \tag{64}$$

$\bar{E}_i^{(\beta\gamma)}$ are the magnitudes of the effective moduli of elasticity along the principle axes defined along the direction of the fiber and transversely to them. In order to check the damaging state of the material, the following four steps are outlined

below by (Stumvoll and Swoboda [21])

$$g^{(\beta\gamma)} < 0, \qquad \text{(elastic unloading)} \qquad (65)$$

$$g^{(\beta\gamma)} = 0, \qquad \frac{\partial g^{(\beta\gamma)}}{\partial Y^{(\beta\gamma)}} : \dot{Y}^{(\beta\gamma)} < 0, \quad \text{(elastic unloading)} \qquad (66)$$

$$g^{(\beta\gamma)} = 0, \qquad \frac{\partial g^{(\beta\gamma)}}{\partial Y^{(\beta\gamma)}} : \dot{Y}^{(\beta\gamma)} = 0, \quad \text{(neutral loading)} \qquad (67)$$

$$g^{(\beta\gamma)} = 0 \qquad \frac{\partial g^{(\beta\gamma)}}{\partial Y^{(\beta\gamma)}} : \dot{Y}^{(\beta\gamma)} > 0, \quad \text{(loading from a damaging state)} \qquad (68)$$

The case corresponding to loading or unloading from an elastic state is given by relation (65). For elastic unloading it is represented by relation (66). In the case of neutral loading it is represented by relation (67). Finally for the loading case it is given by relation (68) from a damaging state. It is clear from the above outlined steps that, the damage criterion ($g^{(\beta\gamma)} \equiv 0$) should be satisfied for the state of damage to occur. As mentioned before for the damage evolution of materials , different types of micro-mechanics damage are considered for each subcell depending on the material properties within the subcell. In this work, for an elasto-plastic matrix, the subcell is assumed to undergo ductile damage while the elastic fiber in the subcell undergoes brittle damage and their total energy dissipation is different from each other. For the elasto-plastic matrix, two energy dissipative mechanisms of damage and plasticity are exhibited. Although the two energy dissipative behaviors are not independent from each other, in this work it is assumed that energy dissipative due to plasticity and energy dissipative due to damage are not coupled with each other. The power of dissipation of the matrix material can be written in the following form

$$\Pi^{(\beta\gamma)} = \Pi^{(\beta\gamma)d} + \Pi^{(\beta\gamma)p} \qquad (69)$$

where $\Pi^{(\beta\gamma)d}$ is the damage dissipation and $\Pi^{(\beta\gamma)p}$ is the plastic dissipation. It is assumed that plastic yielding is independent of the damage process, and therefore the later term can be replaced by its undamaged configuration and it can be expressed as follows

$$\bar{\Pi}^{(\beta\gamma)p} = \bar{\sigma}^{(\beta\gamma)} : \dot{\bar{\epsilon}}^{(\beta\gamma)} + \dot{\bar{\beta}}^{(\beta\gamma)} : \bar{\alpha}^{(\beta\gamma)} \qquad (70)$$

where the term $\dot{\bar{\beta}}^{(\beta\gamma)} : \bar{\alpha}^{(\beta\gamma)}$ is associated with kinematic hardening. The associated damage dissipation is given by

$$\Pi^{(\beta\gamma)d} = Y^{(\beta\gamma)} : \dot{\phi}^{(\beta\gamma)} + K^{(\beta\gamma)} \dot{\kappa}^{(\beta\gamma)} \qquad (71)$$

16

The term $K^{(\beta\gamma)}\dot{\kappa}^{(\beta\gamma)}$ is associated with isotropic damage hardening. The first author has also introduced [22] a coupled incremental damage and plasticity theory for metal matrix composites. One can use the calculus of the function of several variables in order to introduce two Lagrange multipliers $\dot{\Lambda}_1^{(\beta\gamma)}$ and $\dot{\Lambda}_2^{(\beta\gamma)}$ to form the function $\Omega^{(\beta\gamma)}$ in the following form

$$\Omega^{(\beta\gamma)} = \Pi^{(\beta\gamma)} - \dot{\Lambda}_1^{(\beta\gamma)} \bar{f}^{(\beta\gamma)} - \dot{\Lambda}_2^{(\beta\gamma)} g^{(\beta\gamma)} \tag{72}$$

In this equation, $\bar{f}^{(\beta\gamma)}(\bar{\sigma}, \bar{\alpha})$ is the plastic yield function of the elasto-plastic matrix and $\bar{\alpha}^{(\beta\gamma)}$ is the back stress tensor. The term $g^{(\beta\gamma)}$ is the damage potential which is a function of the thermo-dynamic force tensor $Y^{(\beta\gamma)}$ and the damage hardening parameter $\dot{\kappa}^{(\beta\gamma)}$. One can extremize the function $\Omega^{(\beta\gamma)}$ to solve for the Lagrange multipliers $\dot{\Lambda}_1^{(\beta\gamma)}$ and $\dot{\Lambda}_2^{(\beta\gamma)}$. These necessary conditions are given in the following form respectively

$$\frac{\partial \Omega^{(\beta\gamma)}}{\partial \bar{\sigma}^{(\beta\gamma)}} = 0 \quad \text{and} \quad \frac{\partial \Omega^{(\beta\gamma)}}{\partial Y^{(\beta\gamma)}} = 0 \tag{73}$$

Making use of equations (70), (71) in equation (69) and using the calculus of functions, one can use the extremum relations in equations (73) to obtain the following expressions

$$\dot{\bar{\epsilon}}^{(\beta\gamma)} - \dot{\Lambda}_1^{(\beta\gamma)} \frac{\partial \bar{f}^{(\beta\gamma)}}{\partial \bar{\sigma}^{(\beta\gamma)}} = 0 \tag{74}$$

and

$$\dot{\phi}^{(\beta\gamma)} - \dot{\Lambda}_2^{(\beta\gamma)} \frac{\partial g^{(\beta\gamma)}}{\partial Y^{(\beta\gamma)}} = 0 \tag{75}$$

The Lagrange multiplier $\dot{\Lambda}_1^{(\beta\gamma)}$ in equation (74) can be obtained by using the consistency condition for the yield function for the elasto-plastic matrix in conjunction with the Ziegler-Prager kinematic hardening rule. The corresponding yield function is given by

$$\bar{f}^{(\beta\gamma)} = \frac{3}{2}(\bar{\sigma} - \bar{\alpha})^{(\beta\gamma)} : (\bar{\sigma} - \bar{\alpha})^{(\beta\gamma)} - \bar{\sigma}_o^2 \tag{76}$$

where $\alpha^{(\beta\gamma)}$ is given by

$$\dot{\bar{\alpha}}^{(\beta\gamma)} = \dot{\bar{\mu}}^{(\beta\gamma)} (\bar{\sigma} - \bar{\alpha})^{(\beta\gamma)} \tag{77}$$

and $\dot{\bar{\mu}}^{(\beta\gamma)}$ is defined such that

$$\dot{\bar{\mu}}^{(\beta\gamma)} = 3b^{(\beta\gamma)} \dot{\Lambda}_1^{(\beta\gamma)} \tag{78}$$

17

In equation (78) $b^{(\beta\gamma)}$ is the kinematic hardening parameter for the elasto-plastic subcells. The consistency condition of the yield function in equation (76) can be written in the following form

$$\dot{\bar{f}}^{(\beta\gamma)} \equiv 0 \tag{79}$$

or

$$\frac{\partial \bar{f}^{(\beta\gamma)}}{\partial \bar{\sigma}^{(\beta\gamma)}} : \dot{\bar{\sigma}}^{(\beta\gamma)} + \frac{\partial \bar{f}^{(\beta\gamma)}}{\partial \dot{\bar{\alpha}}^{(\beta\gamma)}} : \dot{\bar{\alpha}}^{(\beta\gamma)} = 0 \tag{80}$$

This condition assures that in a plastic loading process the subsequent stress and deformation state remains on the subsequent yield surface. One can use this consistency condition together with the equations (77) and (78) in order to obtain $\dot{\Lambda}_1^{(\beta\gamma)}$ in the following form

$$\dot{\Lambda}_1^{(\beta\gamma)} = \frac{1}{H^{(\beta\gamma)}} \frac{\partial \bar{f}^{(\beta\gamma)}}{\partial \bar{\sigma}^{(\beta\gamma)}} \dot{\bar{\sigma}}^{(\beta\gamma)} \tag{81}$$

where the scalar quantity H is given by

$$H^{(\beta\gamma)} = 3b^{(\beta\gamma)} \frac{\partial \bar{f}^{(\beta\gamma)}}{\partial \bar{\alpha}^{(\beta\gamma)}} : (\bar{\sigma}^{(\beta\gamma)} - \bar{\alpha}^{(\beta\gamma)}) \tag{82}$$

Equation (75) gives the incremental relation of the damage variable for each subcell. Similarly using the consistency condition of the damage potential $g^{(\beta\gamma)}$, one can obtain the parameter $\dot{\Lambda}_2^{(\beta\gamma)}$. The corresponding damage consistency relation can be given as follows

$$\dot{g}^{(\beta\gamma)} \equiv 0 \tag{83}$$

where $g^{(\beta\gamma)}$ can be defined as a function of $g^{(\beta\gamma)} \equiv g^{(\beta\gamma)}(Y, \kappa)$ or $g^{(\beta\gamma)} \equiv g^{(\beta\gamma)}(\sigma, \phi, \kappa)$. Equation (83) can be written as follows

$$\frac{\partial g^{(\beta\gamma)}}{\partial \sigma^{(\beta\gamma)}} : \dot{\sigma}^{(\beta\gamma)} + \frac{\partial g^{(\beta\gamma)}}{\partial \phi^{(\beta\gamma)}} : \dot{\phi}^{(\beta\gamma)} + \frac{\partial g^{(\beta\gamma)}}{\partial \kappa^{(\beta\gamma)}} \dot{\kappa}^{(\beta\gamma)} = 0 \tag{84}$$

By substituting equation (63) and (75) into (84), the above equation can be expressed in terms of the parameter $\dot{\Lambda}_2^{(\beta\gamma)}$ where

$$\frac{\partial g^{(\beta\gamma)}}{\partial \sigma^{(\beta\gamma)}} : \dot{\sigma}^{(\beta\gamma)} + \Lambda_2^{(\beta\gamma)} \frac{\partial g^{(\beta\gamma)}}{\partial \phi^{(\beta\gamma)}} : \frac{\partial g^{(\beta\gamma)}}{\partial Y^{(\beta\gamma)}} + \frac{\partial g^{(\beta\gamma)}}{\partial \kappa^{(\beta\gamma)}} Y^{(\beta\gamma)} : \dot{\phi}^{(\beta\gamma)} = 0 \tag{85}$$

One can solve for the parameter $\dot{\Lambda}_2^{(\beta\gamma)}$ from equation (85) such that

$$\Lambda_2^{(\beta\gamma)} = \frac{\frac{\partial g^{(\beta\gamma)}}{\partial \sigma^{(\beta\gamma)}} : \dot{\sigma}^{(\beta\gamma)}}{\frac{\partial g^{(\beta\gamma)}}{\partial \phi^{(\beta\gamma)}} : \frac{\partial g^{(\beta\gamma)}}{\partial Y^{(\beta\gamma)}} + \frac{\partial g^{(\beta\gamma)}}{\partial \kappa^{(\beta\gamma)}} Y^{(\beta\gamma)} : \frac{\partial g^{(\beta\gamma)}}{\partial Y^{(\beta\gamma)}}} \tag{86}$$

Using relation (86) with (75) , the incremental damage evolution equation for the subcell $(\beta\gamma)$ can be obtained in the following form

$$\dot{\phi}^{(\beta\gamma)} = X^{(\beta\gamma)} : \dot{\sigma}^{(\beta\gamma)} \tag{87}$$

where $X^{(\beta\gamma)}$ is the fourth order tensor such that

$$X^{(\beta\gamma)} = \frac{\frac{\partial g^{(\beta\gamma)}}{\partial Y^{(\beta\gamma)}} \frac{\partial g^{(\beta\gamma)}}{\partial \sigma^{(\beta\gamma)}}}{\frac{\partial g^{(\beta\gamma)}}{\partial \phi^{(\beta\gamma)}} : \frac{\partial g^{(\beta\gamma)}}{\partial Y^{(\beta\gamma)}} + \frac{\partial g^{(\beta\gamma)}}{\partial \kappa^{(\beta\gamma)}} Y^{(\beta\gamma)} : \frac{\partial g^{(\beta\gamma)}}{\partial Y^{(\beta\gamma)}}} \tag{88}$$

The thermodynamic force tensor $Y^{(\beta\gamma)}$ associated with damage can be obtained by using the enthalpy of the damaged materials. This energy equation is given by

$$V^{(\beta\gamma)}(\sigma,\phi) = \frac{1}{2}\sigma^{(\beta\gamma)} : E^{-(\beta\gamma)}(\phi) : \sigma^{(\beta\gamma)} - \Phi^{(\beta\gamma)}(\alpha) \tag{89}$$

where $\Phi^{(\beta\gamma)}$ is the specific energy due to kinematic hardening. $E^{-(\beta\gamma)}$ is the damaged elastic compliance tensor for the subcell. It can be expressed in terms of the undamaged compliance tensor $\bar{E}^{(\beta\gamma)}$ and the damage tensor $M^{(\beta\gamma)}$ such that

$$E^{-(\beta\gamma)} = M^{(\beta\gamma)} : \bar{E}^{-(\beta\gamma)} : M^{(\beta\gamma)} \tag{90}$$

The thermodynamic force $Y^{(\beta\gamma)}$ of the subcell $(\beta\gamma)$ is given as the partial derivative of enthalpy of the damaged material equation (89) with respect to the second order damage tensor $\phi^{(\beta\gamma)}$ in the following expression

$$Y^{(\beta\gamma)} = \frac{\partial V^{(\beta\gamma)}}{\partial \phi^{(\beta\gamma)}} \tag{91}$$

Making use of equations (89) and (90) in equation (91), one can write the thermodynamic force $Y^{(\beta\gamma)}$ explicitly (Voyiadjis and Park) [26] as follows

$$Y_{ij}^{(\beta\gamma)} = \frac{1}{2}(\sigma_{cd}^{(\beta\gamma)} \bar{E}_{abpq}^{(\beta\gamma)} M_{pqkl}^{(\beta\gamma)} \sigma_{kl}^{(\beta\gamma)} + \sigma_{rs}^{(\beta\gamma)} M_{uvrs}^{(\beta\gamma)} \bar{E}_{uvab}^{(\beta\gamma)} \sigma_{cd}^{(\beta\gamma)}) \frac{\partial M_{abcd}^{(\beta\gamma)}}{\partial \phi_{ij}^{(\beta\gamma)}} \tag{92}$$

If the material in the subcell $(\beta\gamma)$ is elastic, one can easily see that the gradual degradation of the elastic material in the corresponding subcell is caused only through damage and consequently no plastic dissipation occurs in the material, that is $\Pi^d = 0$ in equation (69). A similar procedure is followed as outlined before to investigate the damage evolution for elastic materials.

19

4.5 Overall Damaged Stiffness Tensor for the Model

In this section, the elasto-plastic constitutive model for the damaged multiphase composite medium is obtained. The procedure can be outlined by the following steps. First one obtains the subcell (local) damage quantities in their respective damaged configuration $C^{(\beta\gamma)}$ from their undamaged relations such as, stress, strain concentration tensors, and undamaged effective stiffness of composite. These quantities can be obtained through the generalized cells model. This is followed by combining the (N_β by N_γ) subcell constitutive relations by using equation (40) in conjunction with the concentration factors in the damaged configuration $C^{(\beta\gamma)}$ in order to obtain the constitutive relation of the overall composite system in the damaged configuration C.

One can start with by substituting equation (44) in equation (40). The following relation is then obtained.

$$\dot{\sigma} = \frac{1}{V} \sum_{\beta=1}^{N_\beta} \sum_{\gamma=1}^{N_\gamma} v_{\beta\gamma} [m^{(\beta\gamma)}]^{-1} : \dot{\bar{\sigma}}^{(\beta\gamma)} \tag{93}$$

The term $\dot{\bar{\sigma}}^{(\beta\gamma)}$ in equation (93) is replaced with the relation in equation (3), where the fourth order effective tensor $\bar{C}^{(\beta\gamma)}$ in the effective configuration is to be replaced by the corresponding stiffness tensor depending on the properties of the material in the respective subcells. The resulting expression is written as follows

$$\dot{\sigma} = \frac{1}{V} \sum_{\beta=1}^{N_\beta} \sum_{\gamma=1}^{N_\gamma} v_{\beta\gamma} [m^{(\beta\gamma)}]^{-1} : \bar{C}^{(\beta\gamma)} : \dot{\bar{\epsilon}}^{(\beta\gamma)} \tag{94}$$

By substituting equation (50) and (52) into (94), finally one can obtain the following relation

$$\dot{\sigma} = \frac{1}{V} \sum_{\beta=1}^{N_\beta} \sum_{\gamma=1}^{N_\gamma} v_{\beta\gamma} \left\{ [m^{(\beta\gamma)}]^{-1} : \bar{C}^{(\beta\gamma)} : [m^{(\beta\gamma)}]^{-1} \right\} : A^{(\beta\gamma)} : \dot{\epsilon} \tag{95}$$

or

$$\dot{\sigma} = C : \dot{\epsilon} \tag{96}$$

where C represents the instantaneous overall stiffness tensor of the multiphase composite medium in the damaged configuration C, and is given by

$$C = \frac{1}{V} \sum_{\beta=1}^{N_\beta} \sum_{\gamma=1}^{N_\gamma} v_{\beta\gamma} [m^{(\beta\gamma)}]^{-1} : \bar{C}^{(\beta\gamma)} : [m^{(\beta\gamma)}]^{-1} : A^{(\beta\gamma)} \tag{97}$$

From equation (97), one concludes that the overall stiffness tensor in the damaged configuration C can be expressed through its subcell (local) stiffness tensors and strain concentration factors in the damaged configuration $C^{(\beta\gamma)}$.

5 Numerical Simulation of the Model

The numerical implementation of the proposed model is done for the special case of the unit cell model. The applicability of the incremental damage model is assessed herein by using the unidirectional metal matrix composite material. The damaged response of the subcells as well as for the overall composite system is obtained.

The unit cell model used here assumes that the unidirectional array of fibers(SiC) extending in the X_1 direction is elastic and isotropic while the matrix (Ti-14A1-21Nb) is elasto-plastic work-hardening material and constitutes the three subcell regions around the fiber. Table 1 gives the material properties of this composite. The loading is assumed applied incrementally along the fiber direction and damage is checked only for the elastic region. Plastic deformations are ignored in this example and is the topic of the companion paper by Voyiadjis and Deliktas, (1997) .The representative unit cell used here can be described using non-dimensional quantities and the subcell volume fractions can be given as a function of its non-dimensional quantities (h_1, h_2, ℓ_1, ℓ_2 and h, ℓ) such that

$$c^{(11)} = \frac{h_1 \ell_1}{h\ell} \qquad , \qquad c^{(12)} = \frac{h_1 \ell_2}{h\ell} \tag{98}$$

$$c^{(21)} = \frac{h_2 \ell_1}{h\ell} \qquad , \qquad c^{(22)} = \frac{h_2 \ell_2}{h\ell} \tag{99}$$

These non dimensional quantities can be related to the volume fractions of the fiber and matrix as follows

$$c^f = \frac{h_1 \ell_1}{h\ell} \qquad c^m = \frac{h_1 \ell_2 + h_2 \ell_1 + h_2 \ell_2}{h\ell} \tag{100}$$

The relations between h_1 and ℓ_1 , h and ℓ are known. The above non-dimensional quantities can be easily calculated from the phase volume fractions.

In this work for simplicity, the fiber and the unit cell are assumed square i.e $h_1 = \ell_1$ and $h = \ell$. From this assumption one can find the non-dimensional quantities in terms of the phase volume fractions as follows

$$h_1 = \sqrt{c^f} \qquad h_2 = 1 - \sqrt{c^f} \tag{101}$$

Once the non-dimensional quantities are determined, the next step is to follow the procedure outlined in section (3.1) in order to obtain the strain concentration tensor $\bar{A}^{(\beta\gamma)}$ of the subcells and the corresponding overall effective stiffness tensor $\bar{C}$ in the undamaged configuration. One can easily observe that in equation (27), the strain vector $\bar{\epsilon}_s$ is reduced from ($N_\beta N_\gamma$ by 1) to a (24 by 1) vector form. The matrix A_c becomes a (24 by 6) matrix and can be partitioned into four, (6 by 6)

21

matrices where each one of them represents the strain concentration matrix of the corresponding subcell. This matrix is given as follows

$$\bar{A}^{(\beta\gamma)} = \begin{bmatrix} 1 & 0 & 0 & 0 & 0 & 0 \\ A_{21} & A_{22} & A_{33} & 0 & 0 & 0 \\ A_{31} & A_{32} & A_{33} & 0 & 0 & 0 \\ 0 & 0 & 0 & A_{44} & 0 & 0 \\ 0 & 0 & 0 & 0 & A_{55} & 0 \\ 0 & 0 & 0 & 0 & 0 & A_{66} \end{bmatrix}^{(\beta\gamma)} \tag{102}$$

More elaborate information about the strain concentration matrix can be found in references [1, 17].

The damage evolution for the subcell of the proposed model is performed by following the formulation in section(4.4). The tensorial manipulation is preferred in the numerical solution in order to get more elaborate and consistent results. In the damage analysis of materials, the main objective is to satisfy the consistency condition ($g \equiv 0$) at any state of damage. This phenomenon can be explained as follows. Loading of the material by an increment of stress in the damaged state causes the stress tensor to move to the subsequent damage surface, which defines the boundary of the current undamaged region and can be expressed by equation (77). A this state g is only a function of the three variables σ, ϕ and κ. If the stress point lies within the undamaged region, no damage takes places. i.e. $\phi = 0$ and $\kappa = 0$. On the other hand if the state of stress at this point is increased by an increment of stress, the current state of stress will not be in equilibrium such that $g(\sigma + d\sigma, \phi, \kappa) > 0$ which would mean that the current stress point has left the damage surface, which is impossible.

In order to bring the stress point back on the damage surface, an increment of damage $d\phi$ and $d\kappa$ are induced by equation (63) and (87) respectively. The current damage surface $g(\sigma + d\sigma, \phi + d\phi, \kappa + d\kappa) = 0$ will then be satisfied.

The numerical solution investigates the damage evolution for each subcell separately by using different damage parameters for different constituents of the metal matrix composite. Small stress increments are applied along the fiber direction. These damage parameters for the matrix and fiber are given in Table 2.

In this work, three subsequent configurations, the initial undeformed/undamaged C_o, the damaged C and undamaged/deformed $\bar{C}$ are shown in Figure 4. In the one dimensional state of stress, the relation between the scalar value of the overall damage and the subcell damage can be obtained by assuming that the volume fractions of the material in the initial configuration configuration C_o and in the damaged configuration C to be the same. The volume fractions for these three configurations are given as follows

$$c_o = \frac{A_o^{(\beta\gamma)}}{A_o} \qquad c = \frac{A^{(\beta\gamma)}}{A} \qquad \bar{c} = \frac{\bar{A}^{(\beta\gamma)}}{\bar{A}} \tag{103}$$

22

where $c_o = c$ is assumed. One can express the total area of each configuration as a sum of the areas of the subcells such that

$$A_o = \sum_{\beta,\gamma=1}^{2} A_o \qquad A = \sum_{\beta,\gamma=1}^{2} A \qquad \bar{A} = \sum_{\beta,\gamma=1}^{2} \bar{A} \qquad (104)$$

Making use of equation (31) in (104), one can obtain the following relation

$$(1-\phi)A = \sum_{\beta,\gamma=1}^{2} (1-\phi^{(\beta\gamma)})A^{(\beta\gamma)} \qquad (105)$$

By dividing both sides of above equation by A and simplifying, the following expression is obtained

$$\phi = \sum_{\beta,\gamma=1}^{2} \frac{A^{(\beta\gamma)}}{A}\phi^{(\beta\gamma)} \qquad (106)$$

if the term $\frac{A^{(\beta\gamma)}}{A}$ is replaced by the initial volume fraction c_o, the above equation yields the following expression

$$\phi = \sum_{\beta,\gamma=1}^{2} c_o{}^{(\beta\gamma)}\phi^{(\beta\gamma)} \qquad (107)$$

The program output gives the damage response of the material in each subcell as well as the overall. In Figure 5, different values for the parameter ν are used to plot the damage criterion, g, versus the stress in order to study the sensitivity and robustness of this parameter. For the range of values used here $1.8X10^{-3}$ to $8X10^{-4}$ the behavior of the parameter is quite robust. In Figure 6 different values for the parameter ν are used in order to plot the damage variable ϕ versus σ for the subcells (12) and (22). These subcells are chosen in order show how the damage can vary in each subcell even though both cells may have the same material properties. This implies that the boundary and geometry conditions are effective in analyzing the damage of the subcells.

In Figures 7 and 8 the variation of parameters η and ξ is studied by plotting the damage versus the stress. It is observed that a 0.2 change between the different values of η is more sensitive to the damage behavior of the material than a difference in ξ values of 0.05. The corresponding parameters η and ξ are evaluated for the fiber in subcell (11). It is observed that for η values between 0.1 and 0.06 and for ξ values between 0.48 and 0.52, the material is quite sensitive to damage, which is indicated in Figures 9 and 10 respectively.

In Figure 11 the damage versus the stress is plotted for the different subcells together with the overall damage in order to study the local versus the overall relation. The model gives the expected results such that the overall damage behavior is the average of the local ones.

23

Finally, the stress strain curves for the subcells and for the overall composite are plotted and compared with their undamaged curves in Figure 12. It is clear that there is a reduction in the stiffnesses of the material with an accompanying non linear behavior after the damage is initiated in the material.

6 Summary and Conclusions

The main objectives of this work is to incorporate damage in the generalized cells model in order to predict the elasto-plastic damaged behavior of the metal matrix composites, and also to investigate the applicability and reliability of both the generalized cells model and the incremental damage model. The example solved in the previous section demonstrates the ability to properly interpret damage through the proposed approach.

The proposed study can be summarized as follows. The undamaged constitutive relations are obtained using the generalized cells model. This model imposes the continuity of the displacement and traction rates at the interfaces on the average basis. For elasto-plastic materials within the subcell, a von Mises yield criterion with an associated Ziegler Prager kinematic hardening rule is used here in order to obtain the undamaged elasto-plastic stiffness of the material in the corresponding subcell. The fourth order damage tensor M and the incremental damage tensor m are introduced for each subcell separately (rather than a two phase). The undamaged quantities are then transformed in to the corresponding damaged ones by using the damage tensors.

The anisotropic damage criterion is used here and the damage evolution of each subcell is considered separately. The challenging part of this work is to evaluate the eighth order damage tensor. Another important part in this work is to to satisfy the consistency condition at any increment of loading in the damage state. In this work, the eighth order tensor is calculated correctly by using MAPLE. The consistency condition is satisfied by using the numerical solution procedure outlined previously Finally the overall damaged stiffness tensor for the model is obtained in terms of its subcell damaged constitutive relations.

The numerical solution is performed for the case of a unit cell in the elastic domain by applying a monotonic increment of load. The proposed work is computationally efficient in predicting the damaged behavior of the material. The applicability and reliability of the incremental damage model has been established. Using the generalized cell model allows one to predict more accurately the damage in the subregions as well as in the overall composite.

In this work an example pertaining to the elastic analysis of a single lamina is presented. In Part II of the companion paper of this work (Voyiadjis and Babur, [11]), the proposed model is used for the elasto-plastic analysis with damage for both a single lamina and laminated plates. The numerical results are also

Table 1: Material Properties

	Matrix(Ti-14A1-21Nb)	Fiber(SiC)
Modulus	$8 X 10^4$ Mpa	$41 X 10^4$ Mpa
Poisson's Ratio	0.30	0.22
Initial Volume Fraction	0.65	0.35

Table 2: Local Damage Parameters

	Matrix Damage	Fiber Damage
η_1	0.08	0.06
η_2	0.08	0.06
η_3	0.08	0.06
ξ_1	0.55	0.52
ξ_2	0.55	0.52
ξ_3	0.55	0.52
ν_1	0.0013	0.001
ν_2	0.0013	0.001
ν_3	0.0013	0.001

compared with experimental data.

References

[1] J. Aboudi. Micromechanical Analysis of Composites by the Method of Cells. *Apply. Mech, Rev.*, 42:193–221, 1989.

[2] J. Aboudi. Mechanics of Composite Materials - A Unified Micromechanical Approach. *Elsevier, Amsterdam*, 1991.

[3] J.L. Chaboche. Continuum damage mechanics. *J.Apply.Mech.*, 55:59–64, 1988.

[4] D.H.Allen and C.E.Harris. A thermomechanical Constitutive theory for elastic composites with distributed damage.Theoretical formulation. *Int.J.Solids Structure*, 23:1301–1318, 1987.

[5] D.Krajcinovic. Constitutive equations for the damaging materials. *J.Apply.Mech.*, 50:355–360, 1983.

[6] G.J.Dvorak and Y.A Bahei-El-Din. Elastic-plastic behavior of fibrous composites. *J.Mech.Phys.Solids*, 27:51–72, 1979.

[7] G.J.Dvorak and Y.A Bahei-El-Din. Plasticity analysis of fibrous composites. *J.Apply.Mech.*, 49:327–335, 1982.

[8] G.J.Dvorak and Y.A Bahei-El-Din. A bimodal plasticity theory of fibrous composite materials. *Acta.Mech.*, pages 219–241, 1987.

[9] G.J.Dvorak and N. Laws. Analysis of progressive matrix cracking in composite laminates- II. First ply failure. *J.Comps.Mater.*, 29:309–329, 1987.

[10] G.J.Dvorak, N. Laws, and M.Hejazi. Analysis of progressive matrix cracking in composite laminates. I. Thermoelastic properties of crack with a ply. *J.Comps.Mater.*, pages 216–234, 1985.

[11] G.Z.Voyiadjis and B.Deliktas. Damage in MMCs Using the GCM Part II: Numerical Implamentation. *(to be submited)*, 1997.

[12] L. M. Kachanov. On the Creep Fracture Time. *Izv akad. Nauk USSR Otd. Tech.*, 8:26–31, 1958.

[13] H. Lao, K. Peng, and J. Wang. An Anisotropic Damage Criterion for Deformation Instability and it's Application to Forming Limit Analysis of Metal Plates. *Engineering Fracture Mechanics*, 21:1031–, 1985.

[14] J. Lemaitre. Evaluation of Dissipation and Damage in Metals. *Proc. ICMI, Kyoto, Japan*, 1971.

[15] J. Lemaitre. A Continuous Damage Mechanics Model For Ductile Fracture. *Journal of Engineering Materials and Technology*, 107:83–89, 1985.

[16] S. Murakami. Mechanical Modeling of Material Damage. *Journal of Applied Mechanics*, 55:280–286, 1988.

[17] M. Paley and J. Aboudi. Micromechanical Analysis of Composites by the Generalized Cells Model. *Mechanics of Materials*, 14:127–139, 1992.

[18] R.Hill. A self-consistent mechanics of composite material. *J.Mech.Phys.Solids*, 13:213–222, 1965.

[19] R.Hill. On constitutive micro-variables of heterogeneous solids at finite strain. *Proc.Roy.Soc.Lond.*, A326:131–147, 1972.

[20] F. Sidoroff. Description of Anisotropic Damage Application to Elasticity. *IUTAM Colloquium on Physical Nonlinearities in Structural Analysis*, pages 237–244, 1981.

[21] Stumvoll and Swoboda. . *J.Engng.Mech..*, ASCE119:1331, 1993.

[22] G. Z. Voyiadjis and Guelzim. A Coupled Incremental Damage and Plasticity Theory, for Metal Matrix Composites. *Journal of the Mechanical Behavior of Materials*, 6:193–219, 1996.

[23] G. Z. Voyiadjis and P. I. Kattan. A Plasticity-Damage Theory for large Deformations of Solids, Part I: Theoretical Formulation. *International Journal of Engineering Science*, 30:1089–1108, 1992.

[24] G. Z. Voyiadjis and G. Thiagarajan. An Anisotropic Yield surface Model fo rDirectionally Metal MatrixComposites. *International Journal of Plasticity*, 11:867–894, 1995.

[25] G. Z. Voyiadjis and G. Thiagarajan. A Cyclic Anisotropic-Plasticity Model for Metal Matrix Composites. *International Journal of Plasticity*, 12:69–91, 1996.

[26] G. Z. Voyiadjis and T.Park. Local and Interfacial Analysis Damage of, Metal Matrix Composites. *International Journal of Engineering Science*, 33:1595–1613, 1995.

[27] Z.Mroz. mathematical models of inelastic material behavior. *Univ. of Waterloo.*, pages 120–146, 1973.

List of Figures

List of Figures

b)

a)

Figure 1

29

Figure 2(a)

Interface (I)
between two neighboring cells

Figure 2(b)

Interface (I)
between two subcells

x_2

L

h

x_3
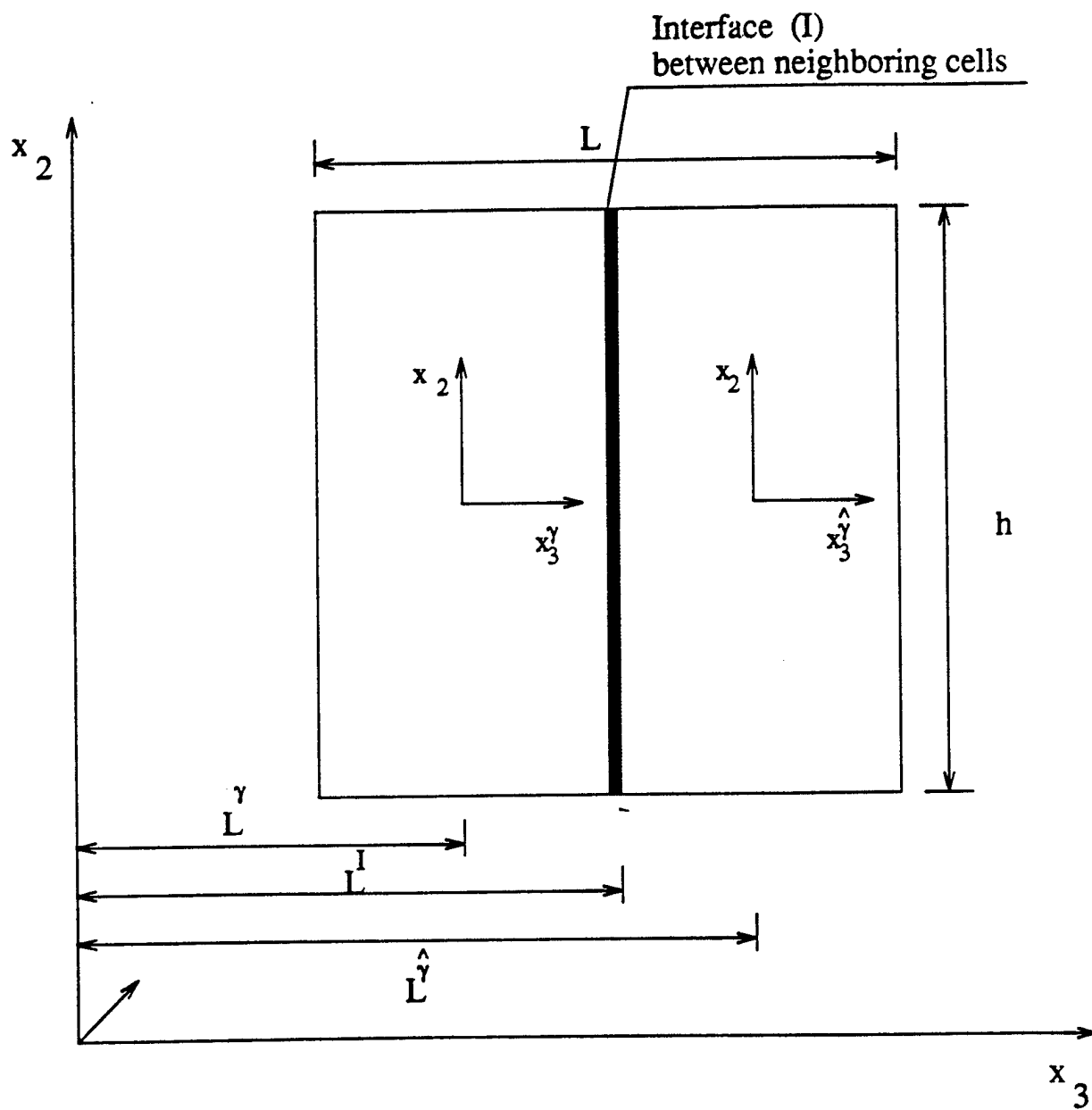
x_2 x_2

x_3^γ x_3^γ

L^r

L^I
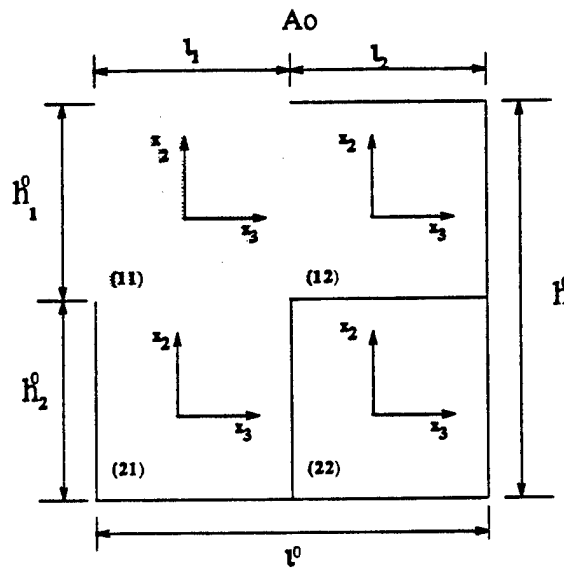
$L^{(r+1)}$

x_3

31

Figure 3(a)

Figure 3(b)

(a) Initial State, C_o

(b) Damaged State, C
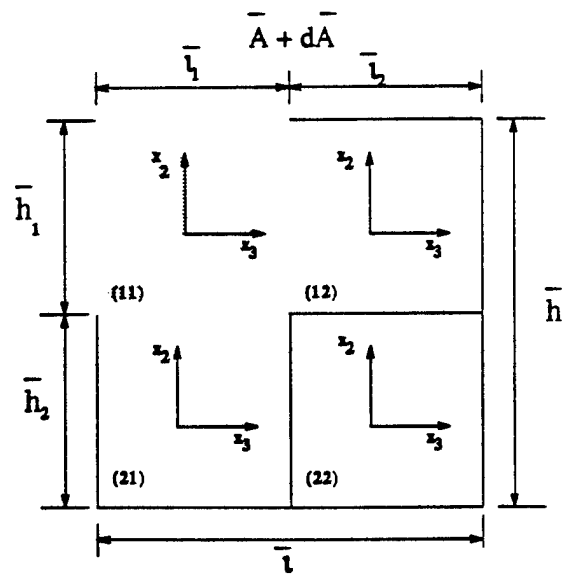
(c) Fictitious Undamaged State, $\tilde{C}$

33

Figure 4

Figure 5

Damage Criterion for Different Damage Parameters
Subcell (12)
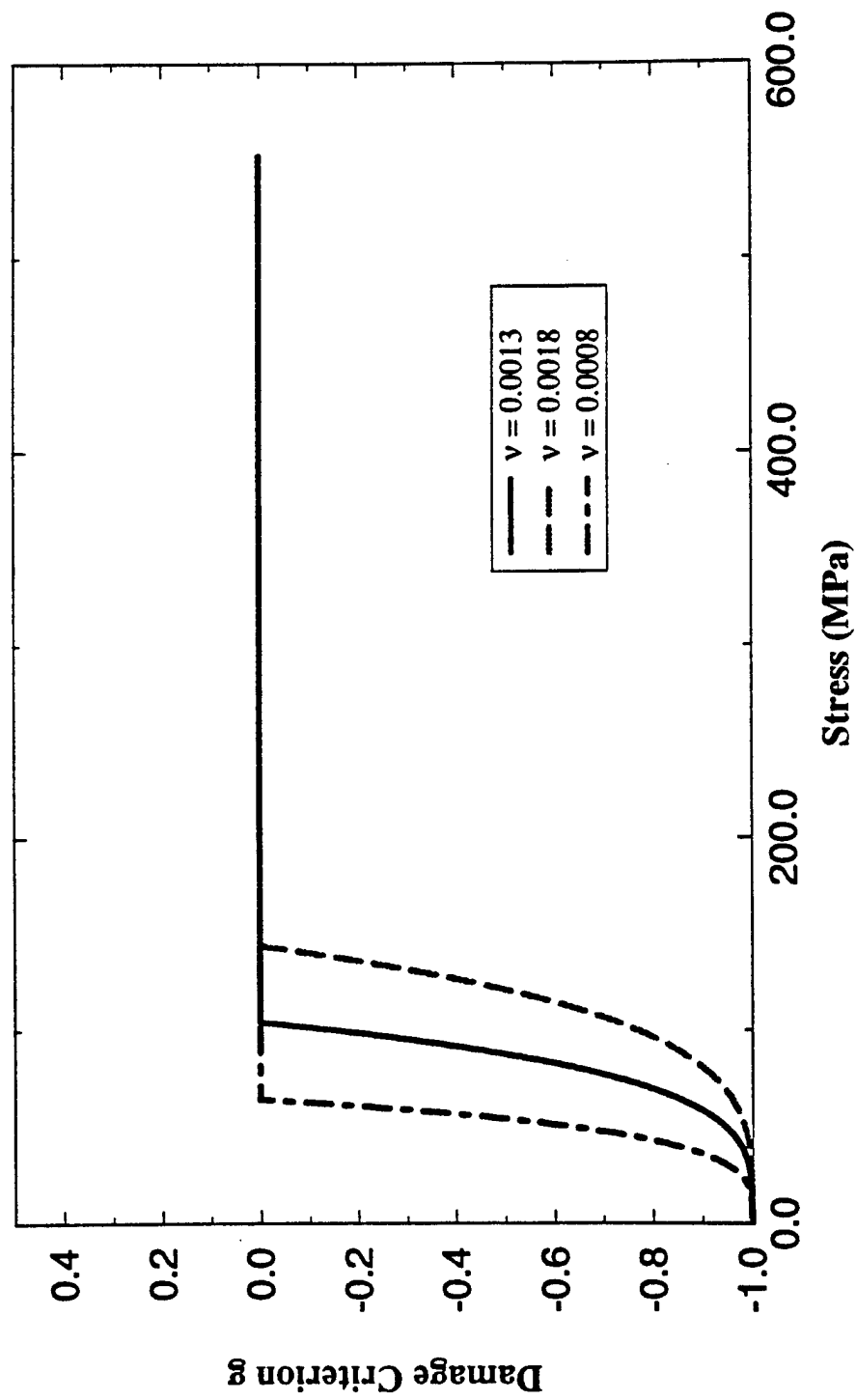
Damage Evaluation for Diffrent Damage Paremeters
Subcell (12) & (22)
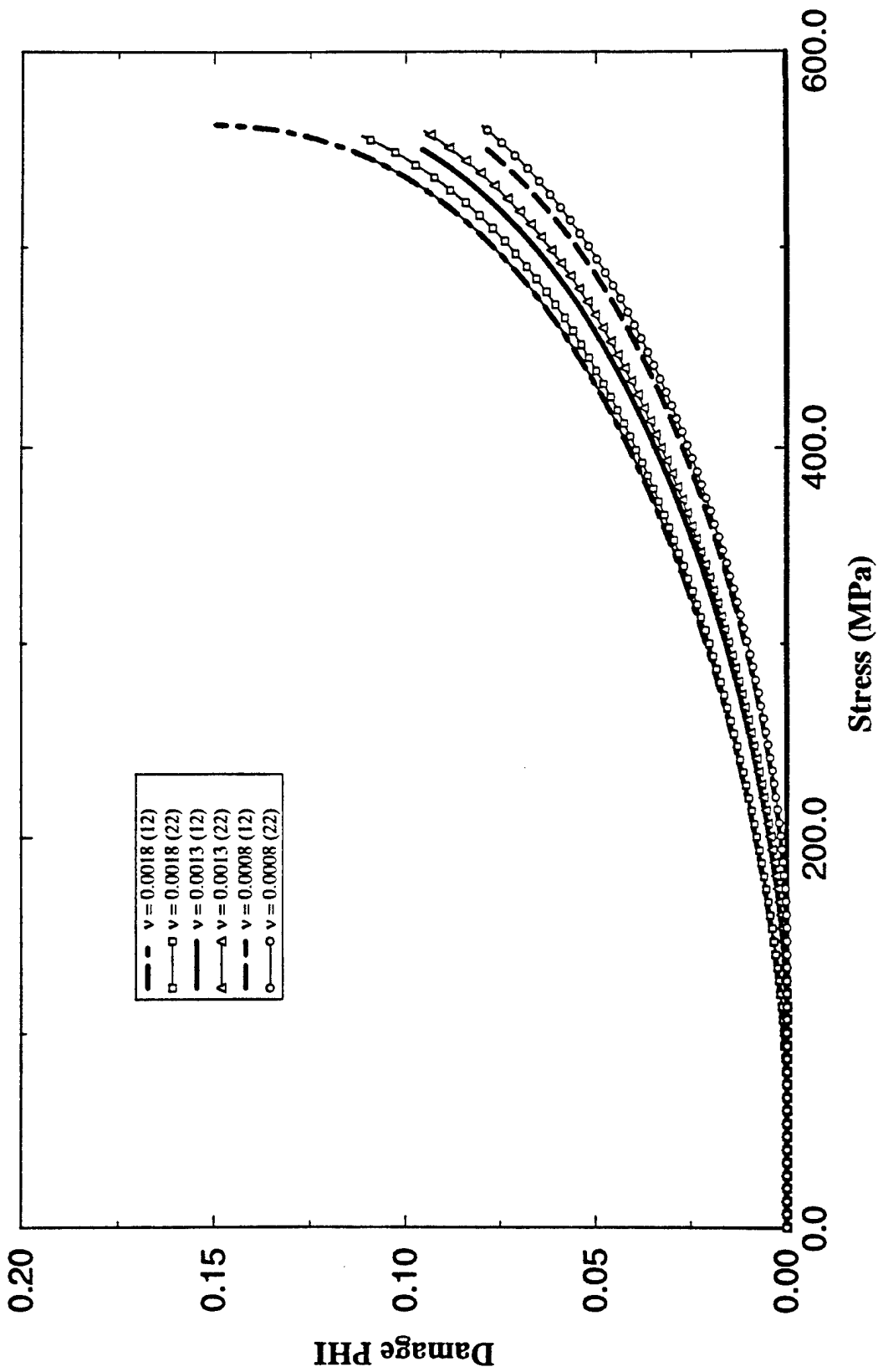
Figure 6

Damage Evaluation for Different Damage Parameters Subcell (12) & (22)

Figure 7

Damage Evolution For Different Damage Prameters
Subcell (12)
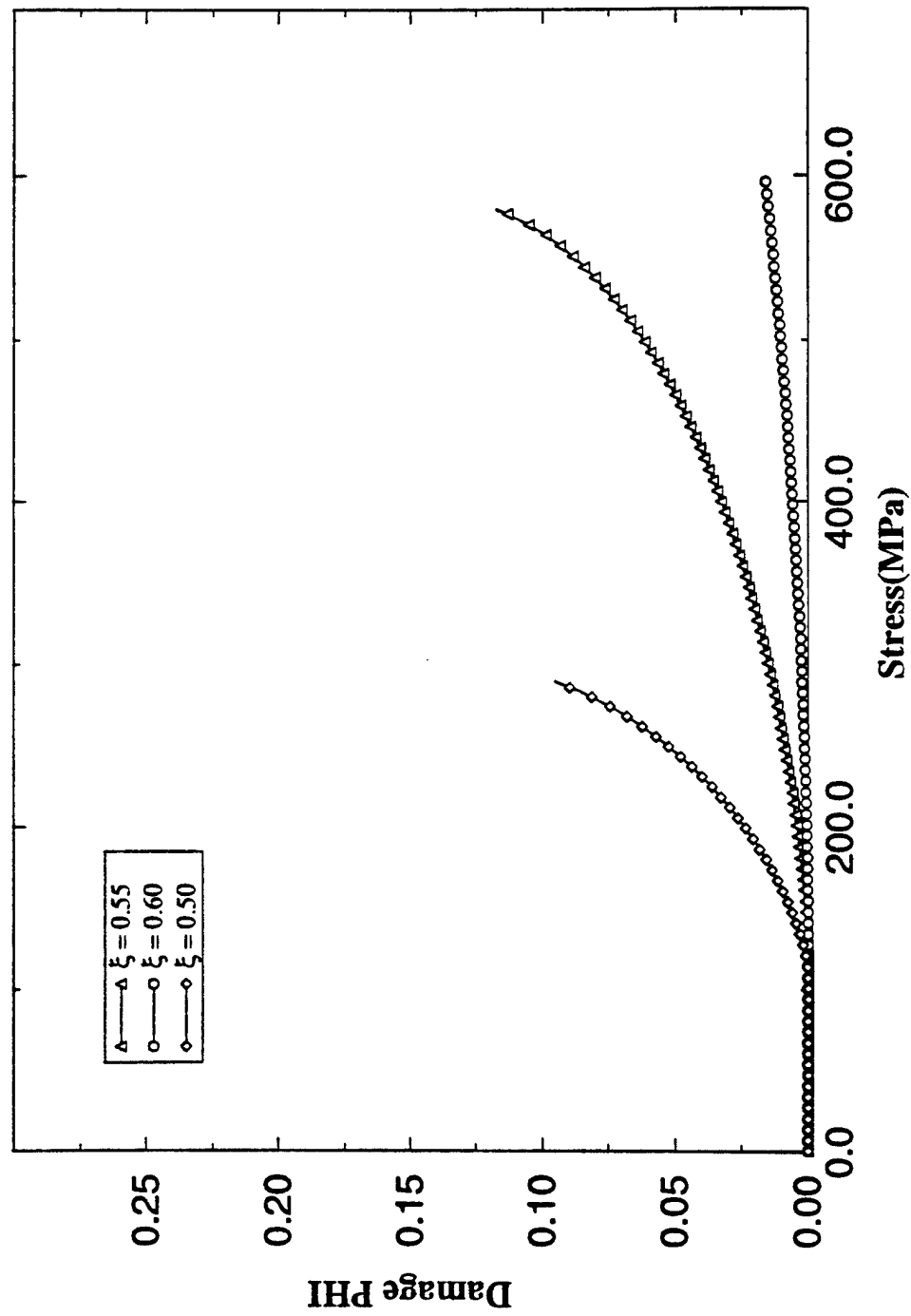
Figure 8

Damage Evolution for Different Parameters

Subcell 11 (Fiber)

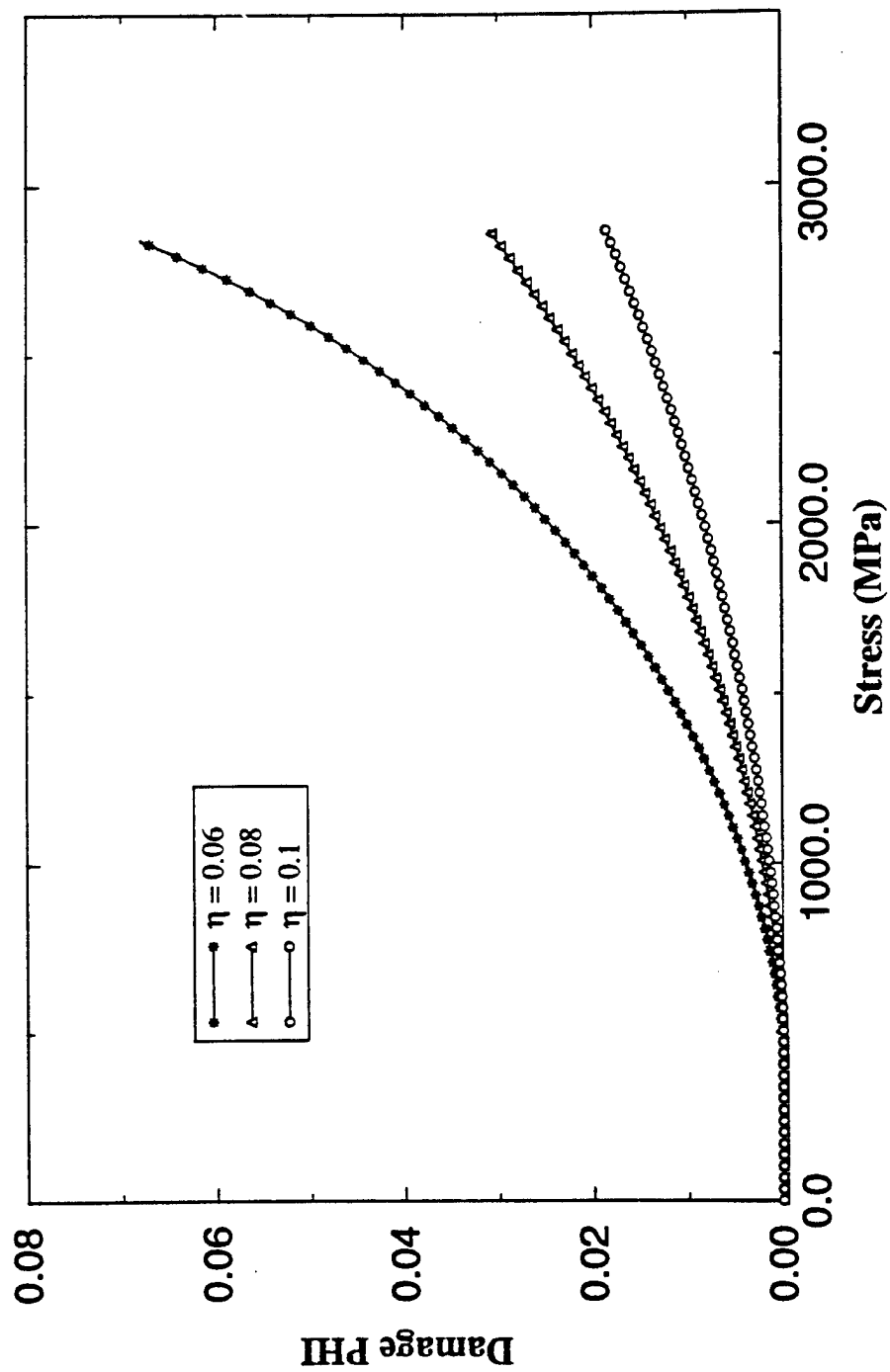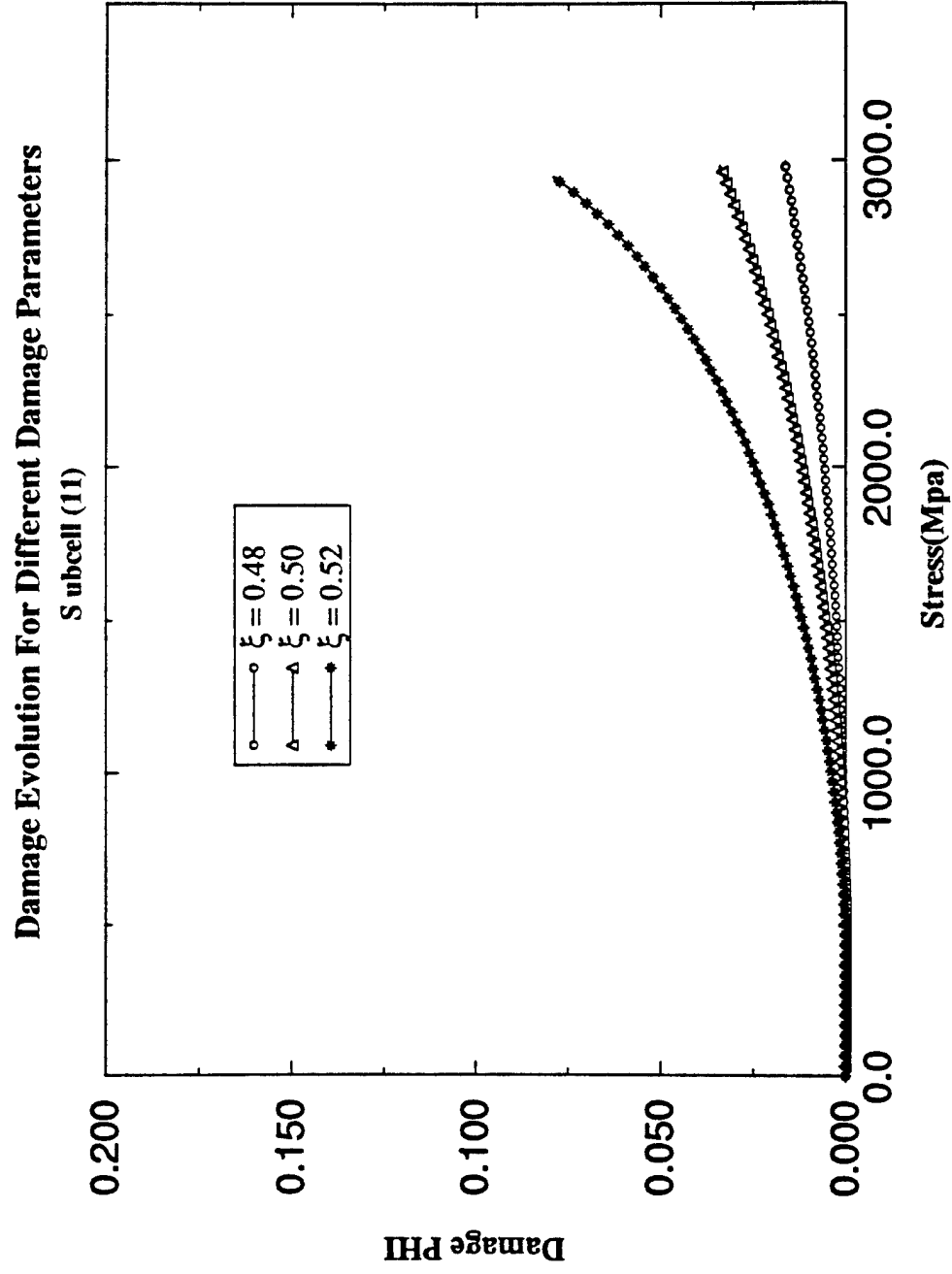Figure 9

Damage Evolution For Different Damage Parameters
Subcell (11)

$\xi = 0.48$
$\xi = 0.50$
$\xi = 0.52$

Damage PHI

Stress(Mpa)

Figure 10

Damage Evolution for Unit Cell Element

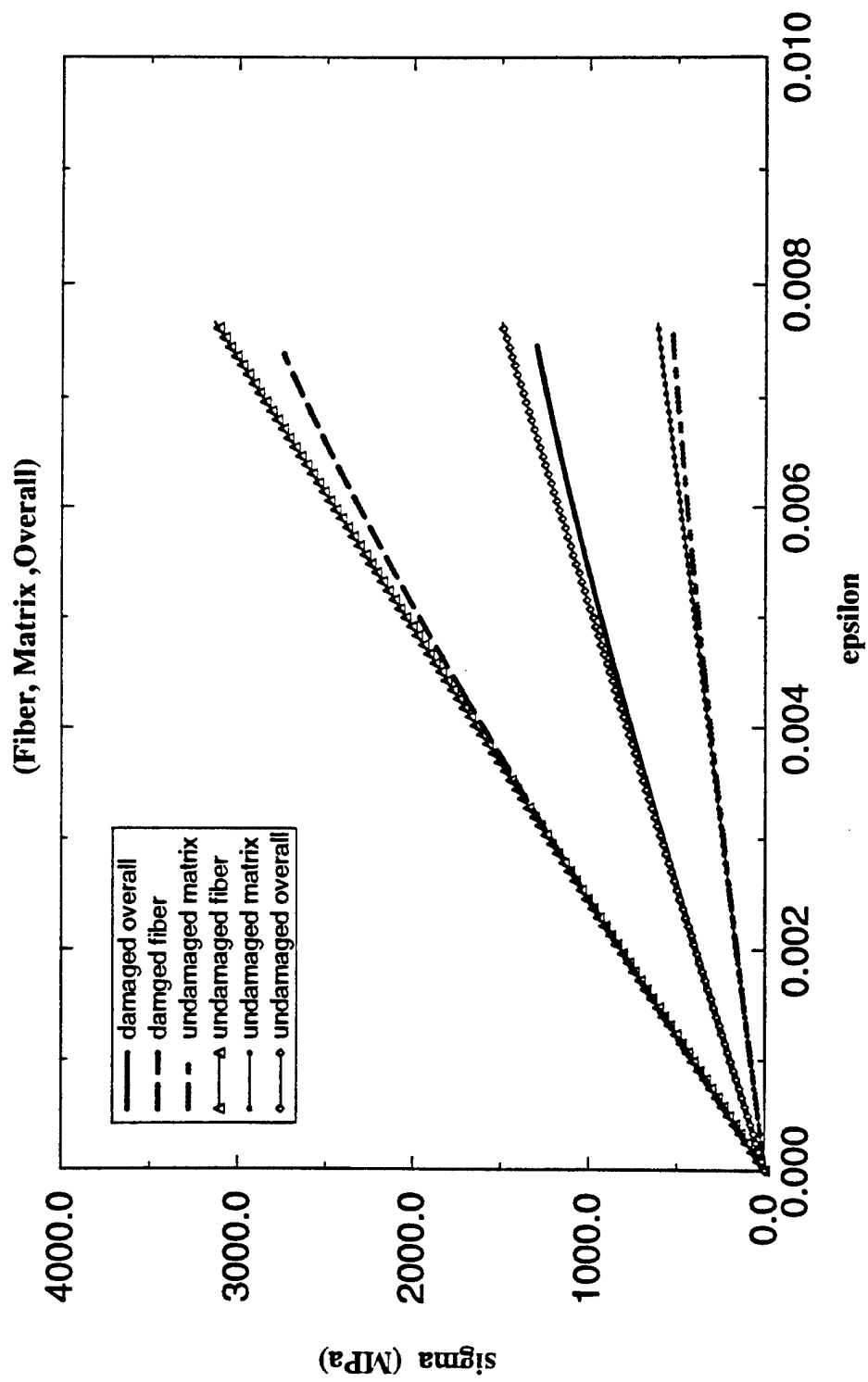(Subcells (11), (12) , (22)) and (Overall-1)
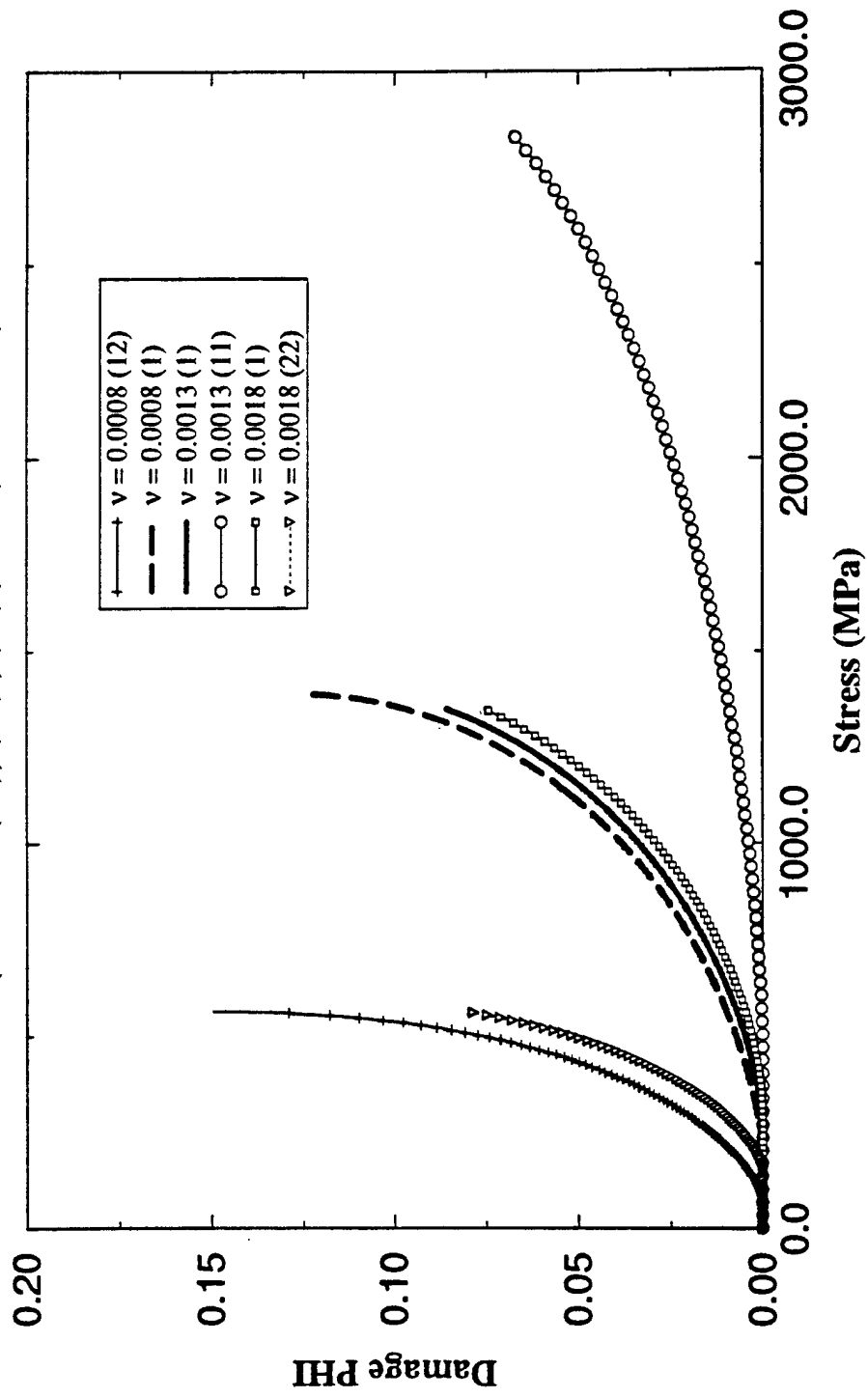
Figure 11

Stress Strain Curves

(Fiber, Matrix ,Overall)

Figure 12